



UNIVERSITÀ DEGLI STUDI DI MILANO

*Scuola di Dottorato in Scienze Biologiche e Molecolari*

*XXIX Ciclo*

**RNA in DNA: from structure  
to genome instability**

**Alice Meroni**

PhD Thesis

**Scientific tutor: Federico Lazzaro**

Academic year: 2017-2018



SSD: BIO/11

Thesis performed at Department of Biosciences,  
University of Milan,  
Milano 20133, Italy

# Table of Contents

<b>Part I</b>	<b>1</b>
<b>Abstract</b>	<b>1</b>
<b>State Of The Art</b>	<b>2</b>
Nucleic acids (DNA and RNA)	2
Genome Duplication	6
The Cell cycle	6
DNA Replication	8
DNA Polymerase Fidelity	12
Genome Instability	15
DNA Repair Mechanisms	15
Base Excision Repair (BER)	16
Nucleotide Excision Repair (NER)	16
Mismatch Repair (MMR)	17
Double Strand Break (DSB) Repair	18
DNA Damage Response	18
Post-Replication Repair	20
Template Switching (TS)	23
Translesion Synthesis (TLS)	24
Polymerase $\eta$	29
Polymerase $\kappa$ and $\iota$	33
Rev1	34
Polymerase $\zeta$	36
Ribonucleotides in DNA	38
Ribonucleotides Incorporation In The Genome	38
Ribonucleotides Removal From DNA	44
RNases H and Ribonucleotide Excision Repair	45
Top1 processing	48
Other processing	51
Negative <i>In Vivo</i> Consequences Of Ribonucleotides Incorporation	54
Replication Stress	54
Genome Instability	56
RNase H2 and diseases	57
Ribonucleotides Effects on DNA structure	58
Positive <i>In Vivo</i> Consequences Of Ribonucleotides	61

<b>Aim of the projects</b>	<b>64</b>
Aim I - Determine how ribonucleotides influence DNA structure	64
Aim II - Unravelling a new activity of yeast Pol $\eta$ in dealing with ribonucleotides	65
<b>Results and Conclusions</b>	<b>66</b>
I - The incorporation of ribonucleotides induces structural and conformational changes in DNA	66
I - Characterization of structural and configurational properties of DNA by Atomic Force Microscopy	69
II - Measuring the levels of ribonucleotides embedded in genomic DNA	70
II - Yeast DNA Polymerase $\eta$ is involved in genome replication under low deoxyribonucleotides pools conditions	71
<b>Discussion</b>	<b>72</b>
<b>References</b>	<b>73</b>
<b>Part II</b>	<b>110</b>
Published Paper I	111
The incorporation of ribonucleotides induces structural and conformational changes in DNA	
Published Paper II	134
Characterization of structural and configurational properties of DNA by Atomic Force Microscopy	
Published Paper III	152
Measuring the levels of ribonucleotides embedded in genomic DNA	
<b>Part III</b>	<b>162</b>
Manuscript in Preparation	163
Yeast DNA Polymerase $\eta$ is involved in genome replication under low deoxyribonucleotides pools situations	

# Part I

# Abstract

The presence of RNA in the genome of living cells is one of the emerging topics of the last two decades and has been implicated in many biological processes. I focused my attention on ribonucleotides (rNMPs) embedded into DNA during genome duplication, as a threat to its integrity. In fact, rNMPs have been classified as the most frequent non-canonical nucleotides introduced during genome duplication by DNA polymerases. Such high incorporation frequency has been related to a physiological role in mismatch repair, but it can be easily turned into a source of genomic instability if rNMPs are not removed from DNA. This task is performed by RNase H activities that enable error-free repair of embedded single and multiple ribonucleotides.

I first approached the issue of ribonucleotides incorporation into DNA from a physical point of view. Utilizing Atomic Force Microscopy I studied how ribonucleotides intrusions impact on DNA structure. The results obtained provided new insights on the structural changes imposed by ribonucleotides persistence into DNA. The other part of my Ph.D. project concerned the study of rNMPs incorporation *in vivo*, using the budding yeast *S. cerevisiae* as a model organism. The second aim was to unravel the function of the Translesion Synthesis polymerase  $\eta$  (Pol  $\eta$ ) when the genome contains residual ribonucleotides and when deoxyribonucleotides (dNTPs) pools are depleted. We found that DNA polymerase  $\eta$  is responsible for the cell lethality observed when dNTPs are scarce and RNase H activities are defective. Therefore, I explored and characterized this unexpected toxic activity. We propose a model where Pol  $\eta$  supports cell survival in low dNTPs conditions by promoting DNA replication using ribonucleotides. While this activity is normally beneficial to wild type cells, it is highly toxic to cells defective for RNase H activities.

# State Of The Art

## Nucleic acids (DNA and RNA)

---

Nucleic acids are polymeric macromolecules essential for every form of life. They play a role both in storage and expression of genetic information and, together with proteins, are the most important biological macromolecules (Alberts B, Johnson A, Lewis J, Raff M, 2002). They were discovered in 1869, by Friederich Miescher who found an unknown substance in the nucleus of leukocytes, and called it *nuclein*. He noticed that *nuclein* was full of phosphorous and later he confirmed that it was a characteristic component of all cells nuclei (reviewed in (Dahm, 2008)).

In living organisms, there are basically two main types of nucleic acids: DNA, deoxyribonucleic acid, and RNA, ribonucleic acid. Nucleic acids are constituted by monomers called nucleotides. Nucleotides are organic molecules composed of a pentose sugar, one or more phosphate group, and a nitrogenous base. Chemically they are phosphate esters of a pentose with a nitrogenous base covalently linked to the C1 carbon of the sugar. The monomeric units of RNA are ribonucleotides, in which the sugar is the D-ribose, whereas DNA is made up of deoxyribonucleotides, with 2'-deoxy-D-ribose as sugar unit (Figure 1). The nitrogenous bases are mainly derivatives of purines or pyrimidines, planar molecules containing nitrogen atoms. *In vivo*, the most abundant purines are adenine (A) and guanine (G), while pyrimidines are cytosine (C), uracil (U) and thymine (T). They are linked to the pentose sugar through a glycosidic bond with the C1 atom, while on the opposite side the phosphate group is connected with the C5 atom. DNA and RNA have the same bases on their nucleotides, except for uracil that is used only in RNA in place of thymine. Nucleotides are joined together through a phosphodiester bond, between the phosphate group and the two adjacent pentoses, resulting in linear polymeric chains.

Additionally, one polynucleotide chain can interact with another one through the formation of hydrogen bonds between complementary bases: adenine always pairs with thymine or uracil through two hydrogen bonds, while guanine pairs with cytosine through three hydrogen bonds (**Chargaff, 1950**). In cells, the synthesis of nucleotides can occur either *de novo* or by recycling pathways linked to other degradative processes (**Voet & Voet, 2010**).

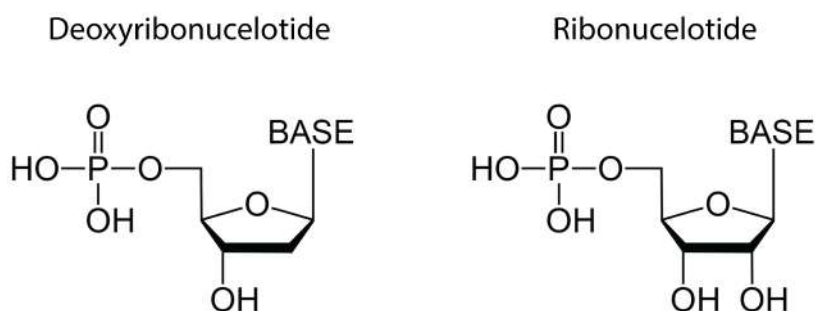


Figure 1. Chemical structures of deoxy- and ribonucleotides.

RNA is a biopolymer constituted of ribonucleotides (rNMPs) that plays a fundamental role in many processes as transcription, translation, and regulation of gene expression. Compared to DNA, RNA molecules are usually shorter and generally exist as single stranded molecules; nevertheless, ssRNAs can be highly structured because of the formation of intra-strand pairing between complementary bases. The overall structure of RNAs can be very intricate, it comprises many secondary structures as stem-loops, which together assume a three-dimensional structure that reflects the function of the molecule (**Tinoco & Bustamante, 1999**). RNA is synthesized by RNA polymerase(s) during the transcription process, using one DNA strand as a template and adding ribonucleotides with respect of the base pairs complementarity (**Ochoa, 1961**). In this way, the genetic information contained in DNA can be transferred to a specific RNA, called messenger RNA or mRNA, and later such information can be translated into proteins (**F. Crick, 1970**). The translation process requires specific RNA molecules as well, known as transfer RNA or tRNAs and ribosomal rRNAs (**Sharp, Schaack, Cooley, Burke, & Soil, 1985**). More recently, a large number of other kinds of RNAs have been discovered, playing

important roles in RNA processing, regulation of gene expression and signaling (**Carthew & Sontheimer, 2009; Matzke & Matzke, 2004**). It is broadly assumed that RNA was the first primordial nucleic acid molecule, superintending the so-called RNA world (**Gilbert, 1986**). Then DNA was evolutionarily selected over RNA, given its ability to long-term store the genetic information and its increase stability to hydrolysis (**Larralde, Robertson, & Miller, 1995**).

DNA is a linear polymer of deoxyribonucleotides (dNMPs), which generally exist as a double stranded molecule with two helices of opposite polarity. The revolutionary discovery of DNA structure in 1953 by James Watson and Francis Crick was the most noteworthy turning point of the molecular biology; they indeed proposed for the first time a double helical model, with an external backbone of alternating sugars and phosphate groups with the base pairs located inside the helix (**F. H. C. Crick & Watson, 1954; Watson & Crick, 1953**). Double-stranded DNA molecules assume a typical conformation in physiological conditions, called B-form. The B-form is well characterized by a series of parameters (**A. H. Wang et al., 1979**) (**Wing et al., 1980**) that together explain its particular stability in aqueous solutions and its suitability for the storage of biological information. DNA can also assume other conformations, as the A-form or the Z-form, depending on its hydration level, sequence, chemical modifications or proteins bound (**Dickerson et al., 1982**). In particular, the A-form is a wide and compact structure, also adopted by dsRNA molecules.

The succession of the four bases along the DNA backbone encodes the genetic information, which is duplicated exploiting the two strands complementarity. Indeed, hydrogen bonds between the bases inside the helix can be easily broken and rejoined like a zipper, and this represents on the base of the DNA replication process. Besides DNA replication, numerous biological processes need helix opening, which consequently induces the formation of supercoils (**Alberts B, Johnson A, Lewis J, Raff M, 2002**). The topological state of DNA is hence under a tight control since it can interfere and affect

important processes such as duplication or gene expression. A special type of enzymes, called DNA topoisomerases, modulate and control the topology of DNA in living cells (**Champoux, 2001**). Genomic DNA is densely packaged into a very small volume, it is first wrapped around specific proteins called histones, and then it is coiled again many times to achieve the well-known shape of chromosomes (**Kornberg, 1974**). This highly condensed structure serves other important roles, such as controlling the DNA accessibility by protein factors (**G. Li & Reinberg, 2011**).

## Genome Duplication

---

Duplication of genetic information is a key event during the life cycle of a cell, and for this reason, it is carried out with high accuracy and carefulness. This chapter describes the main events of the cell cycle, with a particular focus on DNA replication and the fidelity of this important process.

### The Cell cycle

The cell cycle comprises the series of events occurring during the lifetime of a eukaryotic cell, leading to cell division. Once cellular components are doubled and the genome is accurately duplicated, cells are ready to equally distribute the materials into two identical daughter cells. The cell cycle is organized in consecutive and discrete phases, interphase (G<sub>1</sub>, S and G<sub>2</sub> phases) and mitosis (M) (Figure 2) (Masai, Matsumoto, You, Yoshizawa-Sugata, & Oda, 2010). DNA replication occurs once and only once during the Synthesis phase (S), then chromosomes are segregated during Mitosis (M) followed by cytokinesis. These phases are temporarily spaced by two Gap phases, G<sub>1</sub> between M and S and G<sub>2</sub> between S and M. In the course of these Gaps cells grow, accumulate nutrients, energy and get ready for chromosomes segregation (Masai et al., 2010). The progression through the cell cycle is driven by the cyclin-CDK kinase complexes, which phosphorylate specific targets regulating the passage from one phase to another (Nigg, 1995). Moreover, cell cycle progression is firmly controlled at specific points by checkpoint mechanisms, assessing that the requirements needed for the entrance into a specific phase have been met (Sible, Tyson, & Novák, 2002). In conclusion, the transition from one phase to another is dependent on the proper completion of the previous one.

The concept of *checkpoint* was introduced for the first time in 1989 by Hartwell and Weinert, proving that an incomplete cell cycle phase inhibits the entrance in the next one (L. H Hartwell & Weinert, 1989). There are three main checkpoints acting at the boundary of G<sub>1</sub>/S and G<sub>2</sub>/M phases and during M phase (Longhese, Foiani, Muzi-Falconi, Lucchini, & Plevani, 1998). They mainly ensure that cells have reached a critical size and amount of biosynthetic

material to fully replicate DNA ( $G_1/S$  checkpoint or START), that no damages are present on DNA ( $G_2/M$  and intra-S checkpoint) and the spindle is correctly formed and chromosomes are properly attached to it (M checkpoint or metaphase checkpoint). In the case of issues, checkpoint mechanisms both coordinate the action of repair mechanisms and stop or slow down the cell cycle until those problems are solved (Barnum & O'Connell, 2014; L. H Hartwell & Weinert, 1989; Murray, 1992; Sible et al., 2002).

In particular conditions, such as nutrient deficiency, cells exit from the cell cycle and enter into a quiescent phase called  $G_0$  phase, which in turn can be later reverted when favorable conditions are met. In the case of terminally differentiated cells, as neurons, the  $G_0$  state can be a permanent state genetically and epigenetically programmed (Masai et al., 2010).

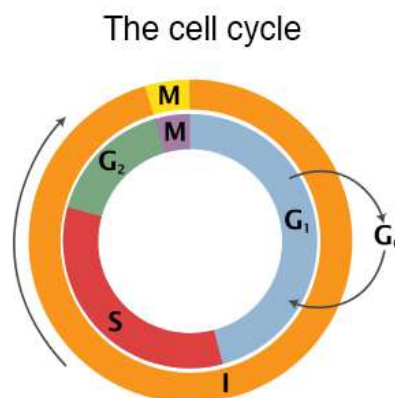


Figure 2. Scheme of the cell cycle.

Budding yeast *S. cerevisiae* was used extensively as the model organism to study the cell cycle and its regulation (Leland H Hartwell, 1974). Since it grows by budding, it is easy to follow and distinguish between the different stages of cell cycle, just by looking at the morphology of cells under the optical microscope. The bud emerges at the end of the  $G_1$  phase and grows continuously during S phase until it reaches a size slightly smaller than the mother cell. For this reason, bud size is a useful marker of cell-cycle position. Different genetic or chemical methods have been developed to block and synchronize yeast cells at a specific position of the cell cycle, reversibly or

irreversibly (**Rosebrock, 2017**). The most widely chemical methods involve the use of: alpha-factor mating pheromone, which blocks cells at the end of G<sub>1</sub> phase; hydroxyurea (HU), which arrest cells at the beginning of S phase, by dNTPs pool depletion; nocodazole, which interferes with microtubules polymerization preventing mitotic spindle assembly in M phase.

## **DNA Replication**

*It has not escaped our notice that the specific pairing we have postulated immediately suggests a possible copying mechanism for genetic material.* It was 1953, and with this sentence, Watson and Crick concluded their paper about the structure of the double helix (**Watson & Crick, 1953**). The intrinsic nature of DNA invokes a copying mechanism, in which the two strands are used as templates to synthesize the complementary ones. A few years later, Meselson and Stahl elegantly demonstrated that DNA replication is a semi-conservative process: parental helices are opened and copied following the complementarity of base pairs (**Meselson & Stahl, 1958**). The net result of this mechanism is two identical DNA molecules in which one strand is the parental one and the other is newly synthesized.

DNA duplication in eukaryotes is a very complicated and regulated process that involves a large number of proteins (**Leman & Noguchi, 2013**). It occurs once and only once per cell cycle, during S phase. As for the cell cycle, much about this process was learned from the budding yeast *S. cerevisiae*. To start DNA replication, precise conditions need to be satisfied, as the right amount of nutrients, nucleotides, positive environmental factors and so on (**P. M. J. Burgers & Kunkel, 2017**). Eukaryotes genomes are composed of linear dsDNA organized in chromosomes and replication starts from specific positions, named replication origins. Yeast origins were identified as sequences that enable replication and maintenance when introduced in a plasmid, so they were named autonomously replicating sequences (ARS) (**Stinchcomb, Struhl, & Davis, 1979**). In the yeast genome there are around 400 ARSs, and they are not fired at the same time, but rather following an established order that

correlates with the transcriptional activities of the surrounding genes (**Dhar, Sehgal, & Kaul, 2012; Vujcic, Miller, & Kowalski, 1999**); early and highly efficient origins are often associated with active genes, while inefficient and late origins are associated with silent genes (**Raghuraman et al., 2001; Vujcic et al., 1999**). ARSs sequences are rich in A-T to facilitate dsDNA double helix opening and contain a very short consensus sequence of 11 bp, essential for replication initiation (**Newlon & Theis, 2002; Theis & Newlon, 1997**). In G<sub>1</sub> phase, the Origin Recognition Complex (ORC) binds this consensus sequence, and a pre-replicative complex (pre-RC) is assembled on each ARS, a process known as licensing (**Diffley, 1995**). Subsequently Cdc6 and Ctd1 proteins are recruited and they cooperate to load the MCM complex, which has helicase activity, forming a licensed pre-RC. The pre-RC has to be activated to start DNA synthesis at the onset of S phase; the CDK and DDK kinases are the ones that promote the activation of the pre-RC, by triggering a rapid degradation of Cdc6 (**Drury, Perkins, & Diffley, 2000**) and stimulating MCM helicase activity (**Sheu & Stillman, 2006**), respectively; these are crucial events in precluding ARS re-replication. Then the DDK, together with the CDK, recruit Cdc45, a key step for the formation of the activated initiation complex (**Tercero, Labib, & Diffley, 2000**). Indeed, Cdc45 loading onto DNA is critical for the successive loading of the protein machinery required for DNA synthesis, as DNA polymerase  $\alpha$ , DNA polymerases  $\delta$  and  $\epsilon$ , replication protein A (RPA) and proliferating cell nuclear antigen (PCNA) (**Walter & Newport, 2000; Zou & Stillman, 2000**). As a result, the DNA around the ARS is locally unwound by the MCM complex, and the whole replicative machinery (replisome) is assembled on the two separated DNA strands (**Takisawa, Mimura, & Kubota, 2000**).

The unlocked replication origin proceeds in a bidirectional way, in fact two replisomes are assembled at each branch point of the replication bubble, region known as replication fork, where many proteins act in concert to allow its progression (Figure 3). The main players are undoubtedly the DNA polymerases, enzymes that catalyze *ex novo* nucleotides polymerization using a

single stranded template and a 3'-OH primer junction (**P. Kannouche et al., 2001**)(**Lehman, Bessman, Simms, & Kornberg, 1958**). The incoming nucleotide is selected with very high fidelity by replicative DNA polymerases, by proving its ability to form a Watson-Crick pairs with the one in the template (**Thomas A Kunkel, 2004**). The Pol  $\alpha$ -primase complex provides the 3'-OH primer to replicative polymerases by synthesizing *de novo* RNA primers of ~10 nucleotides, using DNA as a template. The Pol  $\alpha$ -primase has also the peculiar capability to switch its polymerization activity from RNA to DNA and, after the synthesis of ~10 rNMPs, it proceeds with ~30-40 dNMPs (**Lehman & Kaguni, 1989; Plevani & Chang, 1977**). Despite the unique directionality of DNA polymerases (5'→3') and the opposite polarity of the two DNA strands, replication proceeds simultaneously on both directions. This apparent incongruence was solved in 1968 by Okazaki, who proposed the semi-discontinuous model of replication (**Okazaki, Okazaki, Sakabe, Sugimoto, & Sugino, 1968**). One DNA strand (*leading* strand) is replicated in the fork direction by the DNA polymerase  $\epsilon$ , while the other (*lagging* strand), is copied discontinuously by the DNA polymerase  $\delta$  (**Thomas A. Kunkel & Burgers, 2008**). Here the replication proceeds in the fork direction by synthesizing 100-200 bp discontinuous fragments (Okazaki fragments), that are subsequently joined together by the DNA ligase (**A. Johnson & O'Donnell, 2005**). Clearly the replication of the lagging strand requires multiple priming events, while for leading strand initiation, ideally only one priming event is sufficient. The Pol  $\alpha$ -primase complex serves its function by exhibiting only moderate processivity and low fidelity (**T A Kunkel, Hamatake, Motto-Fox, Fitzgerald, & Sugino, 1989**); on the contrary, replicative DNA polymerases are highly processive enzymes (**Fortune et al., 2005; Shcherbakova et al., 2003**), and their task is assisted by the proliferating cell nuclear antigen (PCNA) (**P. M. Burgers, 1991; Chilkova et al., 2007; Lee, Pan, Kwong, Burgers, & Hurwitz, 1991**). PCNA is a homotrimeric sliding clamp that forms a closed ring around DNA, it is essential for DNA replication and interacts with numerous components of the replisome (**Moldovan, Pfander, & Jentsch, 2007**). PCNA hence coordinates

the polymerase switch on the lagging strand between Pol  $\alpha$  and Pol  $\delta$ , but also between replicative and specialized Translesion DNA polymerases when the replication fork is being blocked by a DNA lesion (explained in detail below) (Essers et al., 2005).

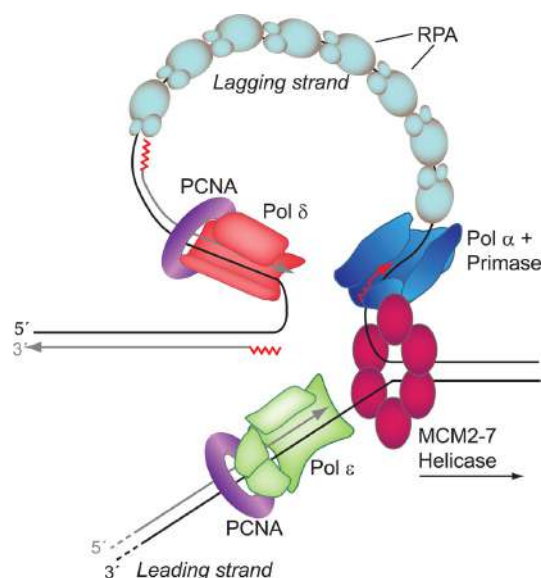


Figure 3. Simplified model of replication fork (McCulloch & Kunkel, 2008)

The RNA primers used by replicative polymerases need to be removed from the genome because they will cause instability if left unresolved (Zheng & Shen, 2011). The Okazaki fragments maturation serves this purpose, leading to the primers removal concurrent with the lagging strand synthesis. When Pol  $\delta$  reaches the 5' end of the downstream Okazaki fragment, it continues DNA synthesis displacing the RNA-DNA primer faced and generating a flap of varying lengths. In the case of short flaps, the removal is achieved either by an iterative cycle with direct cleavage by the flap endonuclease 1 (Rad27/FEN<sub>1</sub>) (Garg, Stith, Sabouri, Johansson, & Burgers, 2004) or by multiple incisions by RNase H<sub>2</sub> (or RNase H<sub>1</sub>) that can occur up to the final ribonucleotide of the RNA primer, that is finally removed by FEN<sub>1</sub> (Qiu, Qian, Frank, Wintersberger, & Shen, 1999). If the flap becomes longer than 30 nucleotides, it is immediately covered by RPA and the DNA $\alpha$  helicase/nuclease cleaves it (Levikova & Cejka, 2015). Once a DNA-DNA nick is accomplished, the DNA ligase I terminates the process linking the two free ends with a phosphodiester

bond. This cycle is made processive by PCNA, that again coordinates the proteins involved and makes tight the complex (**Zheng & Shen, 2011**). Okazaki fragment maturation is completed in a short time and nucleosomes are assembled at the fork junction, both in leading and lagging strand, indicating that the DNA close to the branch is already fully ligated (**Sogo, Lopes, & Foiani, 2002**).

Beyond helicases, that can unwind DNA duplex, topoisomerases regulate the DNA topology by adding or removing supercoils formed during the replication process. Type I topoisomerases remove supercoils, i.e. relax DNA, by nicking and closing one strand of dsDNA; type II topoisomerases change DNA topology by breaking and rejoining dsDNA, introducing or removing supercoils. A moving replication fork generates positive supercoils, therefore these enzymes are very important to solve genomic torsional stresses (**Champoux, 2001**).

### **DNA Polymerase Fidelity**

Genome duplication is carried out with high fidelity thanks to the accuracy of replicative DNA polymerases and the backup control by the Mismatch Repair Mechanism (MMR); together they ensure an *in vivo* error rate of 1 every  $10^9$  nucleotide insertions. Uncorrected errors can result in dangerous mutations; nevertheless, a low mutation rate contributes to the sequence variability on which natural selection is based on.

The bulk of replication is committed to three B-family polymerases, Pol  $\epsilon$ , Pol  $\delta$  and Pol  $\alpha$ , while the A-family Pol  $\gamma$  is responsible for the mitochondrial DNA replication (**Bebenek & Kunkel, 2004**). Replication fidelity is mostly guaranteed by the capacity of replicative DNA polymerase to select the correct incoming nucleotide and this high selectivity is dependent on the ability to form correct hydrogen bonds between the template and the incoming nucleotides bases (**Kool, 2002**). The free energy difference between a correct and a mispaired pair of nucleotides is high enough to make the latter very unfavorable (**Petruska et al., 1988**). However, the difference value of free energy is too low to be used as the only selection parameter. The base pair

geometry contributes as well to the discrimination, indeed only geometrically equivalent A-T and G-C pairs fit perfectly in the active site of polymerases, where there is no available space for other molecules as water (**Beard & Wilson, 2003**). Thanks to the steric hindrance, DNA Pols bind correct dNTPs with 10 to  $10^3$  fold higher affinity respect to the incorrect ones (**S. S. Patel, Wong, & Johnson, 1991; Wong, Patel, & Johnson, 1991**). The binding of incorrect nucleotides would delay enzyme's conformational changes needed for catalysis and, as a consequence, reduce the rate of phosphodiester bond formation (**M F Goodman, 1997; S. J. Johnson & Beese, 2004**).

Mismatched termini are hence more difficult to extend, and the resulting delay induces a fray that moves it to the 3'-exonuclease site of the enzyme (**Myron F. Goodman, Creighton, Bloom, Petruska, & Kunkel, 1993**). As a matter of fact the two principal DNA polymerases  $\epsilon$  and  $\delta$  own a proofreading domain (**A. Morrison & Sugino, 1994; a Morrison, Johnson, Johnston, & Sugino, 1993; Pavlov, Maki, Maki, & Kunkel, 2004; Vanderstraeten, Van den Brûle, Hu, & Foury, 1998**) to excise mismatched nucleotides, and this increase fidelity up to  $10^3$  fold (Table 1) (**T A Kunkel & Bebenek, 2000**).

DNA polymerases can also generate small insertions or deletions (indels), when one or few bases in the template DNA are unpaired and then realign improperly (**Garcia-Diaz & Kunkel, 2006**). As for base substitutions, indels rates vary depending on the polymerase but are strongly challenged by the sequence context, i.e. repetitive sequences (**Garcia-Diaz & Kunkel, 2006**). In Table 1 are reported the error rates of base substitutions and indels, calculated for the major yeast replicative DNA polymerases.

Table 1. Error rates of Replicative DNA polymerases.

<i>S. cerevisiae</i> Polymerase		Single Base Substitution ( $\times 10^{-5}$ )	Single Base Indel ( $\times 10^{-5}$ )	Reference
Exonuclease proficient	$\delta$	$\leq 1.3$	1.3	(Fortune et al., 2005)
	$\epsilon$	$\leq 0.2$	$\leq 0.05$	(Shcherbakova et al., 2003)
Exonuclease deficient	$\delta$	1.3	5.7	(Fortune et al., 2005)
	$\epsilon$	24	5.6	(Shcherbakova et al., 2003)
	$\alpha$	9.6	3.1	(T A Kunkel et al., 1989)

## Genome Instability

---

Cells are constantly threatened by chemical and physical agents that challenge the integrity of the genome. In human cells, nearly  $10^4$ - $10^5$  lesions occur on DNA every day, and all have to be repaired, indicating how the maintenance of genome integrity is crucial during the cell cycle (Lindahl & Barnes, 2000). The failure of repair DNA damages results in DNA replication or transcription blockage, as well as impairment of DNA functions *per se*; genome instability is the condition in which cells accumulate different genetic alterations, from point mutations to gross chromosomal rearrangements (Aguilera & Gómez-González, 2008). In higher eukaryotes, the loss of function of genes responding to DNA damage often results in genetic syndromes and cancer predisposition (J. H. J. Hoeijmakers, 2001; Negrini, Gorgoulis, & Halazonetis, 2010; Pikor, Thu, Vucic, & Lam, 2013; Z. Shen, 2011).

The DNA Damage Response (DDR) is the complicated network, which includes multiple repair mechanisms, damage tolerance pathways and cell cycle checkpoints that guarantee genome integrity. Genomic insults arise from various sources that directly hit the DNA; these can be exogenous, as UV light, IR, and chemicals, or endogenous, as reactive oxygen species (ROS) and spontaneous hydrolysis of nucleotide residues. DNA replication process contributes actively to genome instability, with mismatches, indels and ribonucleotides incorporation.

In this section, the main repair mechanisms are briefly described with the exception of the Ribonucleotide-Excision Repair (RER) that is detailed in the next section. The main focus of this chapter is the DNA Damage Tolerance (DDT), also called Post-Replication Repair (PRR).

### DNA Repair Mechanisms

Cells have evolved a plethora of DNA repair mechanisms, each one specialized in a particular type of damage, able to specifically recognize and efficiently resolve the lesion.

### **Base Excision Repair (BER)**

Chemically damaged bases that do not strongly disturb DNA structures are repaired by Base Excision Repair (BER) (Almeida & Sobol, 2007). These lesions include deaminated, oxidized and alkylated bases that are recognized and cleaved by specific DNA glycosylases. These enzymes remove the damaged base from the nucleotide, leaving an abasic site (AP) that is subsequently incised by AP-endonucleases, resulting in a single-nucleotide gap. Finally, the gap is filled by the specialized DNA polymerase  $\beta$  and sealed by the XRCC1/Ligase III complex. BER is also specialized in repair of single strand breaks with dirty ends (Hegde, Hazra, & Mitra, 2008) that require the action of end-processing enzymes such as Aprataxin (Gueven et al., 2004) and TDP1 (tyrosyl-DNA-phosphodiesterase) to create ligatable DNA ends (Caldecott, 2007).

### **Nucleotide Excision Repair (NER)**

Nucleotide Excision Repair (NER) acts on a large variety of DNA lesions that induce local distortions of the DNA double helix (J. H. Hoeijmakers, 1993). The most important and studied NER substrates are pyrimidine dimers and 6-4 photoproducts, generated by UV light, and DNA intra- and inter-strand crosslinks (Sertic, Pizzi, Lazzaro, Plevani, & Muzi-Falconi, 2012).

Eukaryotic cells possess two different NER sub-pathways: transcription-coupled NER (TC-NER), which removes transcription-stalling lesions on actively transcribed genes, and global genome NER (GG-NER), which eliminates lesions anywhere along the genome (Dijk, Typas, Mullenders, & Pines, 2014). The initial recognition of the damage is different in TC-NER and GG-NER, in one case the lesion is sensed by the stalling of the RNA polymerase, while in the other, two specific complexes detect the distortion of the DNA helix. After lesion detection, TC- and GG-NER converge into a common mechanism in which the transcription factor TFIIH complex is recruited (Compe & Egly, 2016) and its helicase activities unwind DNA of approximately 30 nucleotides, allowing the assembly of other NER factors to process the

lesion. The DNA bubble is stabilized by Rad14/XPA and RPA, and two specific endonucleases (Rad2/XPG and Rad1-Rad10/ERCC1-XPF) cut at the 3' and at the 5' of the damage, thus excising the DNA fragment including the damage. The gap is then filled by replicative DNA polymerases or the human TLS Pol  $\kappa$  (Tomoo Ogi et al., 2010) and sealed by DNA ligases I or III.

### **Mismatch Repair (MMR)**

The MMR machinery moves along with the replication forks and it is responsible for the repair of mismatched nucleotides, insertions or deletions introduced during genome duplication (Z. Li, Pearlman, & Hsieh, 2016). Prokaryotic and eukaryotic MMR are very similar both in protein structures and mechanisms. Briefly, the mismatch is recognized and bound by specific proteins (MutS $\alpha$ -MutS $\beta$ ) that in turn trigger the recruitment of MutL $\alpha$ , MutL $\beta$  and MutL $\gamma$  heterodimers and ultimately of the Exonuclease 1 (Exo1). Exo1 is specifically localized on the newly synthesized strand, where it degrades the DNA containing the error, producing a gap (Kolodner & Marsischky, 1999; Thomas A. Kunkel & Erie, 2005). Lastly, the DNA polymerases fill the gap and the DNA ligase I seals the nick.

It is crucial that the MMR repair distinguishes between the parental and the neo-synthesis strand. In bacteria, the transient hemi-methylation allows to discriminate between the two strands whereas in eukaryotes the mechanism is less clear. Surely nicks present in the lagging strand provide frequent entry points for Exo1, while in the leading strand, the continuity could be interrupted by nicks generated at ribonucleotides sites by the RNase H2. As the MMR acts concomitantly with replication, PCNA is responsible to coordinate the process, driving the machinery in the correct direction by specific and oriented protein-protein interactions (Ghodgaonkar et al., 2013; Lujan, Williams, Clausen, Clark, & Kunkel, 2013).

## **Double Strand Break (DSB) Repair**

All the mechanisms described above rely on the presence of one correct strand, which is used as a faithful template to restore integrity. However, both the strands could be damaged at the same time, as for DNA double strand breaks (DSBs) and inter-strand cross-links (ISCLs). These lesions are the most dangerous for cells because they are more difficult to repair, as there is none backup copy to use. DSBs are repaired by two main pathways: homologous recombination (HR) (**San Filippo, Sung, & Klein, 2008**) and non-homologous end-joining (NHEJ) (**Lieber, 2010**), according to the phase of the cell cycle. Homologous recombination is predominant in S and G<sub>2</sub> phases since it exploits the undamaged sequence of the homologous sister chromatid (**Longhese, Bonetti, Manfrini, & Clerici, 2010**). In brief, once a DSBs occurs, ends are held together and resected in 5'-3' direction, generating 3'-overhangs that are cooperatively covered by RPA and then by Rad51 protein (**Mimitou & Symington, 2011**). The nucleo-protein filament drives the strand invasion into the homologous sister chromatid, where strands are temporarily exchanged. Therefore the strand invasion provides a template to accurately repair the DSB. During G<sub>1</sub> phase, DSBs are prevalently repaired by NHEJ (**Huertas, 2010**); as for HR, ends are tethered together, then resection occurs and the two ends are rapidly sealed. During NHEJ, loss or changes of a few nucleotides may occur, indeed it is considered an error-prone process (**Lieber, 2010; San Filippo et al., 2008**).

## **DNA Damage Response**

As mentioned before, cells are constantly exposed to DNA damages and they possess plenty of lesion-specific DNA repair pathways to deal with. Besides the specificity to different DNA lesions, all these pathways activate a common checkpoint known as DNA Damage Response (DDR) (**T A Weinert & Hartwell, 1988**). The DNA damage checkpoints arrest the cell cycle to provide the time and the means to carry out DNA repair (**Lazzaro et al., 2009; Rao & Johnson, 1970; T A Weinert & Hartwell, 1988**). Then, when repair is

completed, the checkpoint signal is turned off and cells can re-enter the cell cycle. In yeast, the cell cycle is controlled by three (Nyberg, Michelson, Putnam, & Weinert, 2002) main checkpoints that respond to DNA damage accordingly to the phase in which is experienced (Nyberg et al., 2002). The G<sub>1</sub>/S checkpoint prevents replication of damaged DNA (Siede, Friedberg, Dianova, & Friedberg, 1994); the intra-S checkpoint slows down S-phase and stabilizes the stalled replication forks (Paulovich & Hartwell, 1995); the G<sub>2</sub>/M checkpoint prevents the segregation of damaged chromosomes arresting cells prior to anaphase (Ted A. Weinert, Kiser, & Hartwell, 1994). Basically, checkpoints are conserved signal transduction cascades, mainly based on phosphorylation events, which convey the signal from damage sensors to DDR effectors. The DNA damage checkpoint cascade is conventionally described by grouping the factors involved in DNA damage sensors, adapters, transducers, and finally effector (Nyberg et al., 2002).

Although cells have to deal with a huge diversity of DNA damages, all DNA repair pathways activate the same checkpoint, and that is possible by the generation of a common intermediate during lesion processing. The common intermediate that activates the DDR is the ssDNA covered by RPA (Zou, 2003). Indeed, ssDNA is generated during every lesion processing, from NER (Giannattasio, Lazzaro, Longhese, Plevani, & Muzi-Falconi, 2004) to DSBs (Sugawara & Haber, 1992) or replication fork stalling (Branzei & Foiani, 2005). The exposed ssDNA is detected by the sensor kinase Mec1 and its partner Ddc2, which together trigger the checkpoint cascade (Feng, 2016). Essentially, there are two apical checkpoint kinases, Mec1 and Tel1 in yeast, that correspond to ATR and ATM in human; in yeast, Mec1 is the main kinase while Tel1 is redundant and has only marginal roles (Usui, Ogawa, & Petrini, 2001), while in human they are equally important, with ATR responding to ssDNA exposing lesions and ATM directly responding to DSBs (Abraham, 2001). An important role in checkpoint activation is played by the 9-1-1 complex (Rad17/Mec3/Ddc1) (Bonilla, Melo, & Toczyski, 2008), a PCNA-like complex that is loaded on the ssDNA-dsDNA junction and help in the recruitment of Mec1 substrates (Majka, Binz, Wold, & Burgers, 2006). Indeed, activated

Mec1 phosphorylates a series of factors, in particular two key kinases known as Rad53/CHK2 and Chk1/CHK1 (Harrison & Haber, 2006); while Rad53 is absolutely required for checkpoint activation in every cell cycle phase, Chk1 is strictly involved in activation of G2/M phase checkpoint (Sanchez et al., 1999). Adaptor proteins help the activation of the transducer kinases, and among them, the most important in *S. cerevisiae* is Rad9 (Pellicioli & Foiani, 2005). Once phosphorylated, Rad53 is active and starts to phosphorylate itself and the downstream targets (Sun, Hsiao, Fay, & Stern, 1998). Since Rad53 phosphorylation level correlates with its kinase activity and thus with the extent of damages, Rad53 phosphorylation is generally used as a marker of the checkpoint activation in budding yeast (Pellicioli et al., 1999). Therefore, both Rad53 and Chk1 kinases transduce the checkpoint signal by phosphorylating a series of effectors, accordingly to the cell cycle phase.

Among the effectors, the most noticeable are Pds1 and Dun1. Pds1 is the yeast securin, which prevents the separase from cleaving cohesins to release the sister chromatids into anaphase (Cohen-Fix & Koshland, 1997); Dun1 mainly controls intracellular dNTPs levels by regulating the RNR enzyme, specifically by increasing the dNTPs pool in the case of damage and checkpoint activation (X Zhao, Chabes, Domkin, Thelander, & Rothstein, 2001; Xiaolan Zhao & Rothstein, 2002). Overall, checkpoint mechanisms are clearly important for cell survival, indeed, mutations in checkpoint genes are responsible for many diseases and malignant cancers (Lengauer, Kinzler, & Vogelstein, 1998).

### **Post-Replication Repair**

Although cells are able to constantly deal with thousands of lesions per day, some lesions could escape from the DNA repair mechanisms. Unrepaired lesions become dangerous during the next S phase when DNA polymerases have to replicate over them. Replicative DNA polymerases are so accurate in copying DNA that they cannot accommodate any kind of lesions, as bulky adducts or distortion in the helix structure; thus, in the case they come across damaged nucleotides, they actually stall. Prolonged stalling of replication forks

leads to the formation of secondary breaks, incomplete replication, forks collapse and ultimately genome instability. Therefore, cells have evolved an additional resource to survive and overcome replication fork stalling, named DNA Damage Tolerance (DDT) or Post-Replication Repair (PRR). DDT or PRR is acting on a remarkable set of lesions, in which the surrounding DNA is single-stranded so it cannot be simply excised; thus cells choose to leave the damage unaltered while preferring to promote the completion of replication. In a second time, a specific repair mechanism, acting on double-stranded DNA, would subsequently repair the lesion.

PRR comprises two pathways that allow to progress through the lesion in an error-prone or error-free manner, the Translesion Synthesis (TLS) and Template Switching (TS), respectively (Figure 4)(**Chang & Cimprich, 2009; Y. Gao, Mutter-Rottmayer, Zlatanou, Vaziri, & Yang, 2017; Ghosal & Chen, 2013**).

These two pathways are tightly regulated and coordinated by PCNA, the maestro of replication forks (**Moldovan et al., 2007**). Besides tethering replicative DNA polymerases, it acts as a platform for the most of the factors involved in replication and repair (**Moldovan et al., 2007**), and moreover, it can be modified by Ubiquitin or SUMO groups, generating extra surfaces to interact with other specific proteins. PCNA post-translational modifications are essential to deal with fork stalling and initiate Post-Replication Repair (**Hoege, Pfander, Moldovan, Pyrowolakis, & Jentsch, 2002; Moldovan et al., 2007; Stelter & Ulrich, 2003**).

During replication, DNA polymerases movement is generally uncoupled from the MCM helicase activity, which unwinds DNA in front of the forks. In the case of fork stalling, the MCM helicase continues unwinding of DNA, thereby generating ssDNA, that is immediately protected by RPA and triggers the DNA replication checkpoint activation (**Byun, Pacek, Yee, Walter, & Cimprich, 2005**). RPA-coated DNA recruits Rad18 and then Rad6 (**Davies, Huttner, Daigaku, Chen, & Ulrich, 2008; Huttner & Ulrich, 2008; Tsuji et al., 2008**), an E3 ubiquitin ligase and E2 ubiquitin-conjugating enzymes respectively, that together attach a single ubiquitin chain at the K164 residue of

PCNA (Hoege et al., 2002; Stelter & Ulrich, 2003). PCNA mono-ubiquitination is the activation signal for the error-prone TLS pathway, which involves the use of low-fidelity DNA polymerases to bypass the lesion and allow the downstream restart of replication fork (Freudenthal, Gakhar, Ramaswamy, & Washington, 2010; P. L. Kannouche, Wing, & Lehmann, 2004). The recruitment of Rad18 at the site of damage is strictly dependent upon RPA coating of ssDNA, but it can be modulated by several factors. The TLS polymerase  $\eta$ , is able to bind both Rad18 and PCNA, thus promoting their interaction and enhancing PCNA ubiquitination (Durando, Tateishi, & Vaziri, 2013); furthermore, NBS1 member of the MRN complex and BRCA1 are involved in facilitating Rad18 recruitment to the lesion (Tian et al., 2013; Yanagihara et al., 2011). However, in higher eukaryotes, Rad18 could be not the only E3 Ub-ligase for PCNA, indeed PCNA-ubiquitination is observed even in absence of Rad18, suggesting there could be other back-up E3 enzymes for this important ubiquitination (Shimizu, Tateishi, Tanoue, Azuma, & Ohmori, 2017; Simpson et al., 2006).

The mono-ubiquitination of PCNA is hence the signal for the activation of the TLS pathway, whereas its extension with additional ubiquitin peptides triggers the Template Switching pathway (Figure 4)(Lajos Haracska, Torres-Ramos, Johnson, Prakash, & Prakash, 2004). Rad5 is the E3 Ub-ligase that extends the K164 mono-ubiquitination on its K63, in coordination with the E2 ubiquitin-conjugating complex Ubc13-Mms2 (Hoege et al., 2002).

PCNA is also SUMOylated both during normal cell cycle and in the case of replication stress (Gali et al., 2012); the function of such modification is still debated but there are evidence that PCNA-SUMO prevents DNA repair through homologous recombination in S phase (Schiestl, Prakash, & Prakash, 1990). PCNA-SUMO interacts with Srs2, the helicase that displaces Rad51 from DNA, thus inhibiting HR and pushing towards PRR pathways (Krejci et al., 2003; Papouli et al., 2005; Pfander, Moldovan, Sacher, Hoege, & Jentsch, 2005).

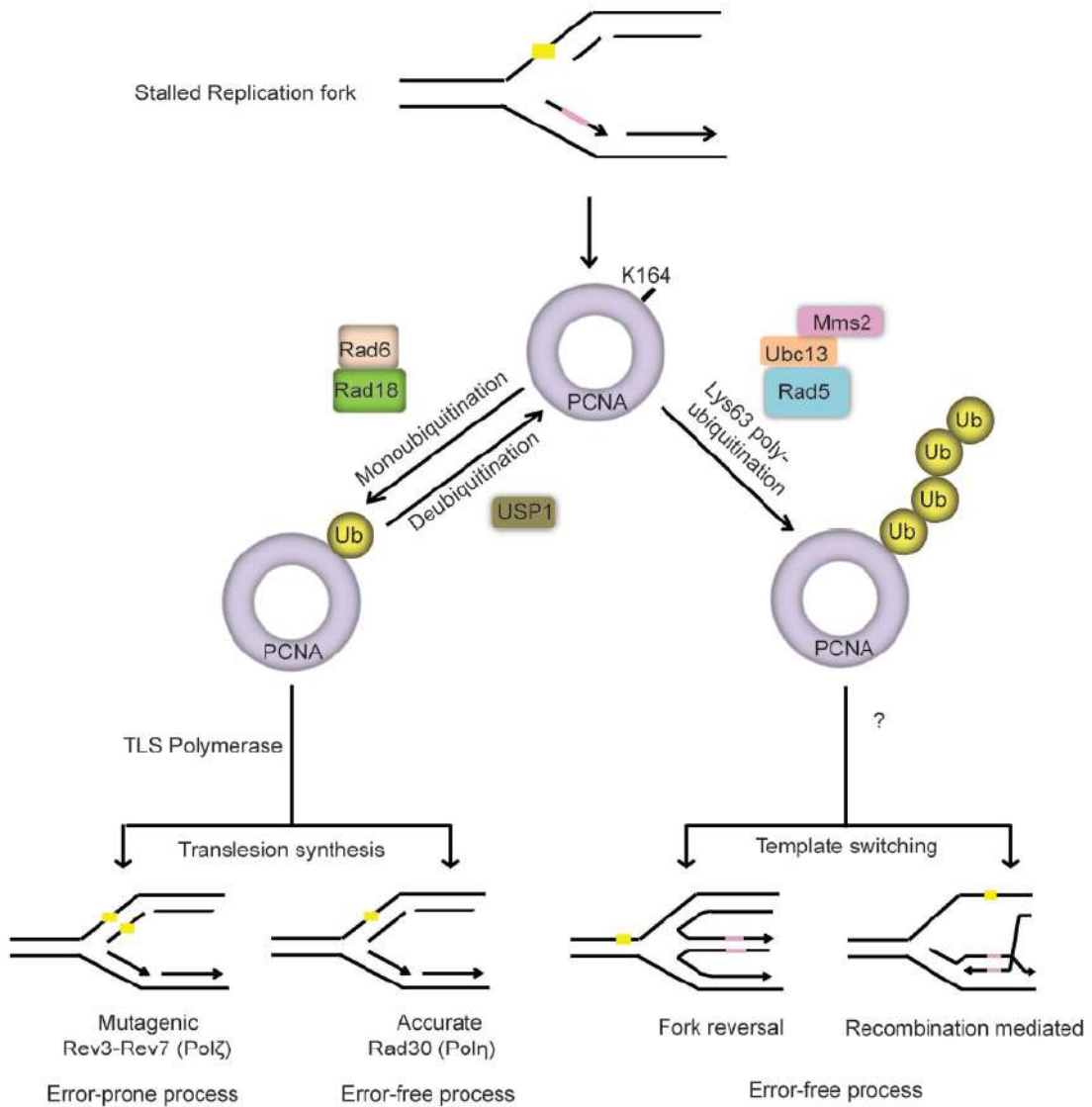


Figure 4. Post-Replication Repair Pathways. (Ghosal & Chen, 2013)

### Template Switching (TS)

The template switching is thus triggered by the poly-ubiquitination of the DNA clamp PCNA. This mechanism allows cells to bypass the lesion in an error-free manner, by using the newly synthesized strand of the opposite filament as a template (Figure 4). When the replication fork stalls, PCNA can be either mono- or poly-ubiquitinated, in the case of poly-ubiquitin chain addition by Rad5 (Minca & Kowalski, 2010; Xiao, Chow, Broomfield, & Hanna, 2000) and the Ubc13-Mms2 complex (Broomfield, Chow, & Xiao, 1998; Hofmann & Pickart, 1999), the newly synthesized strand is re-annealed with the newly

synthesized strand of the opposite filament, by using a subset of Rad52 epistasis group (**Gangavarapu, Prakash, & Prakash, 2007**) and Rad51 (**Branzei, Vanoli, & Foiani, 2008**). Here, the Pol  $\delta$  extends the DNA by using the daughter newly synthesized as a template (**Torres-Ramos, Prakash, & Prakash, 1997**) and the recombination-like structures formed are resolved by Sgs1-Top3-Rim1 complex (**Giannattasio et al., 2014**). Therefore, this pathway overcomes the lesion by a recombination event between partially replicated sister strands (**Branzei et al., 2008; Giannattasio et al., 2014; H. Zhang & Lawrence, 2005**). The poly-ubiquitination of PCNA is the crucial event to trigger TS, even if its function is not completely clear; on the other hand, the SUMOylation of PCNA strongly inhibits TS by keeping Srs2 next to the fork in a way that it displaces Rad51, that is necessary for strand invasion in TS (**Branzei et al., 2008**). As for Rad18, there could be sort of backup E3-ligase to poly-ubiquitinate PCNA; in mammals Rad5 has two orthologous, SHPRH (**Unk et al., 2006**) and HTLF (**Unk et al., 2008**), and mouse embryonic cells lacking both these factors still retain the ability to poly-ubiquitinate PCNA (**Krijger et al., 2011**).

### **Translesion Synthesis (TLS)**

Translesion Synthesis is indeed triggered by the mono-ubiquitination of PCNA by Rad18, and it involves the action of specialized DNA polymerases able to replicate over a distorted or damaged template. These TLS polymerases transiently replace the replicative ones, synthesizing DNA over and beyond the lesion for a short tract (**Sale, Lehmann, & Woodgate, 2012**). This mechanism could involve one or two TLS polymerases; in the first case the TLS Pol replicate over the lesion and then extend DNA, in the latter the first step is carried out by one TLS Pol that is replaced with another that extend the damaged junction (**Shachar et al., 2009; Woodgate, 2001**). An open active site that can accommodate damaged and biased bases characterize TLS polymerases, but at the same time, it makes them more prone to introduce errors (**Vaisman & Woodgate, 2017**). In addition, they lack an exonuclease domain, so they are not able to proofread possible uncorrected nucleotides

(Prakash, Johnson, & Prakash, 2005). TLS is hence sometimes accompanied by unwanted mutagenesis, consequently it should be tightly regulated, especially impeding the access of TLS Pols to normal proceeding replication forks (Sale et al., 2012). Accordingly, the usage of TLS Pols could reduce replication accuracy but ensures its progression and completion. However, even if TLS could be potentially mutagenic, it could also be error-free in the case the correct specialized TLS Pol is recruited to bypass the damage. In this way, TLS could contribute to DNA Damage Tolerance without compromising genome instability.

In yeast there are three TLS polymerases, Pol  $\eta$  and Rev1 that belong to the Y-family DNA polymerases and Pol  $\zeta$ , a B-family polymerase; in humans there are four Y-family TLS polymerases, Pol  $\eta$ , Pol  $\kappa$ , Pol  $\iota$  and Rev1, and eight are required for TLS and other repair mechanisms, Pol  $\zeta$ , Pol  $\beta$ , Pol  $\lambda$ , Pol  $\mu$ , TdT, Pol  $\nu$ , Pol  $\theta$  and PrimPol (Prakash et al., 2005). In general, Y-family DNA polymerases possess an open and spacious active site that can accommodate DNA lesions (Pata, 2010), that site is solvent exposed thereby allowing a competition between water molecules and bases in forming hydrogen bonds; however, in this way they lose fidelity in selecting the correct incoming nucleotides (Ling, Boudsocq, Woodgate, & Yang, 2001; J Trincão et al., 2001). The catalytic site is composed of three domains, the fingers, palm and thumb that resemble the typical open right-hand structure found in the most other families (J Trincão et al., 2001; Zhou, Pata, & Steitz, 2001). The catalysis reaction requires two Mg<sup>2+</sup> ions, that additionally help in the substrate positioning within the active site and balance opposite charges (Castro et al., 2007; Jäger & Pata, 1999; Wei Yang, Lee, & Nowotny, 2006). Respect to the B-family polymerases, they also present an additional unique domain called *little finger* or Polymerase Associated Domain (PAD) (Jose Trincão et al., 2001), with low sequence conservation (Wilson, Jackson, & Pata, 2013; W. Yang & Woodgate, 2007); crystallographic studies showed clearly that the substrate DNA is positioned between the thumb and PAD (Prakash et al., 2005). In general, TLS polymerases do not present any 3'-5'

exonuclease domain (**Reha-Krantz, 2010**), have low processivity and catalytic efficiency and show higher error rates on undamaged DNA (**Wei Yang, 2014**).

Since TLS has to be strictly controlled, Y-family Pols present different regulatory regions that control their access to the forks (Figure 5). The PCNA Interacting Peptide (PIP) interacts with PCNA, specifically with the Inter-Domain Connecting Loop (ICDL) on PCNA itself; the Ubiquitin-Binding Module (UBM) and Ubiquitin-Binding Zinc Domain (UBZ) bind ubiquitin in a non-covalent manner and induce conformational changes that prevent subsequent interactions with other ubiquitin molecules (**Bienko et al., 2005; Pata, 2010**). Both PIP and UBZ or UBM domains regulate the direct interaction between TLS Pols and PCNA or mono-ubiquitinated PCNA (**Bienko et al., 2005; C. Guo et al., 2006; Plosky et al., 2006**), nevertheless they show high affinity for the latter (**P. L. Kannouche & Lehmann, 2004; P. L. Kannouche et al., 2004**) and this could prompt the displacement of replicative polymerases in the instance of fork stalling and PRR activation (**Zhuang et al., 2008**). Interestingly, the ubiquitinated residue K164 of PCNA is not on its IDCL (**Gulbis, Kelman, Hurwitz, O'Donnell, & Kuriyan, 1996**), but it is located on the back face of PCNA, as to establish distinct interactions with TLS and replicative polymerases, that contact the front PCNA surface (**Freudenthal et al., 2010**). Another important domain is the Rev1-Interacting Region (RIR), which mediates the interaction with Rev1 that function also as a scaffold for other TLS Pols (**Prakash et al., 2005**).

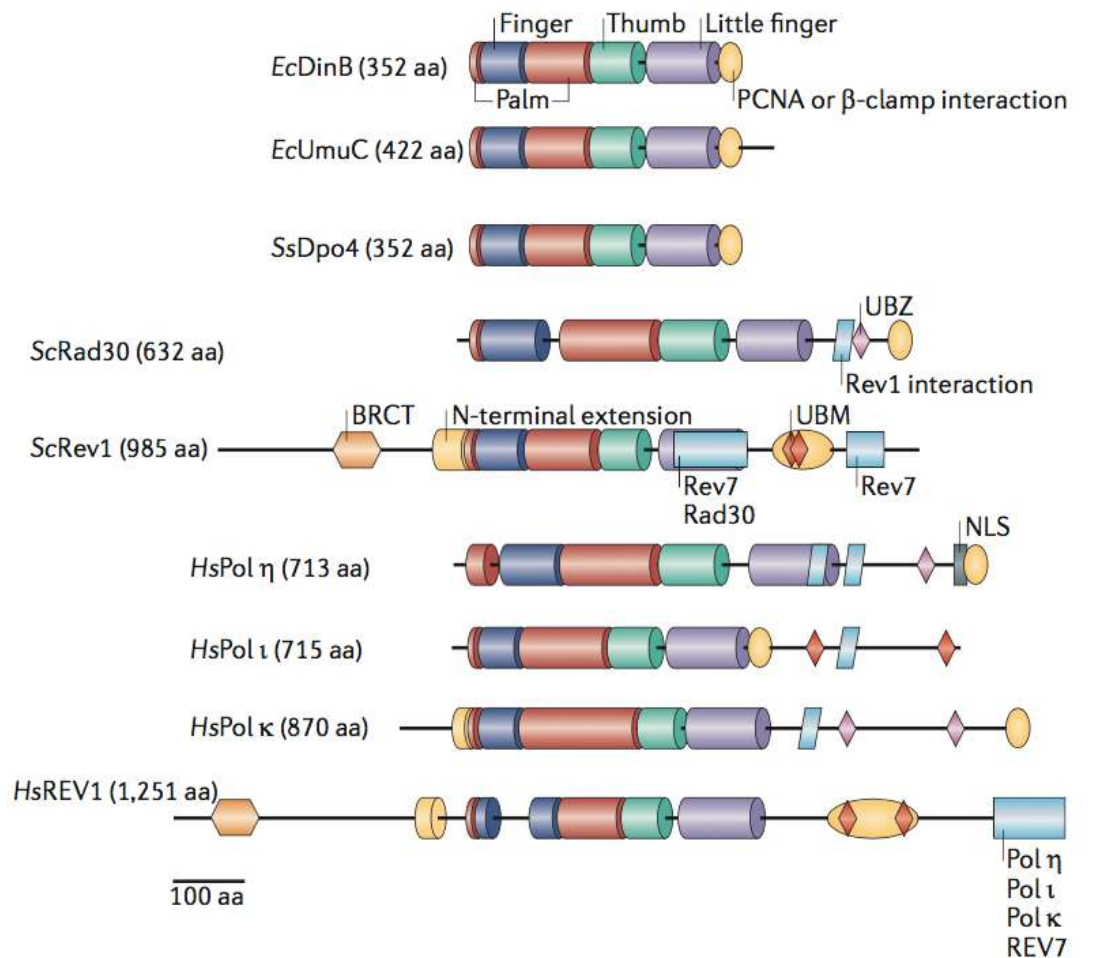


Figure 5. Domains of TLS Polymerases. (Sale et al., 2012)

Currently, there are two models for TLS-mediated lesion bypass that are not mutually exclusive: the polymerase-switching model and the gap-filling model (Figure 6) (Lehmann, 2006; Lehmann et al., 2007; Lehmann & Fuchs, 2006; L S Waters et al., 2009). In the polymerase-switching model, TLS is performed during active DNA replication, when a moving replication fork stalls. Here, the replicative DNA polymerase is temporarily exchanged with the TLS Pol that specifically bypasses the lesion. Then, another TLS polymerase could join the process by extending the mispaired terminus generated by the first TLS Pol. Lastly, a second switch restores the replicative DNA polymerase at the fork, thus enabling resumption of processive and accurate DNA synthesis. Conversely, the gap-filling model is performed in late S phase, G<sub>2</sub>/M or G<sub>1</sub>, in absence of actively replicating forks. In the case of replication forks stalling, DNA synthesis could be reprimed downstream of the lesion, thereby leaving a ssDNA gaps behind it. This repriming event could occur both in the lagging

strand, by initiating a new Okazaki fragment, or in the leading strand. Thus, TLS are recruited later to manage with the lesion, which is bypassed and then DNA is subsequently sealed.

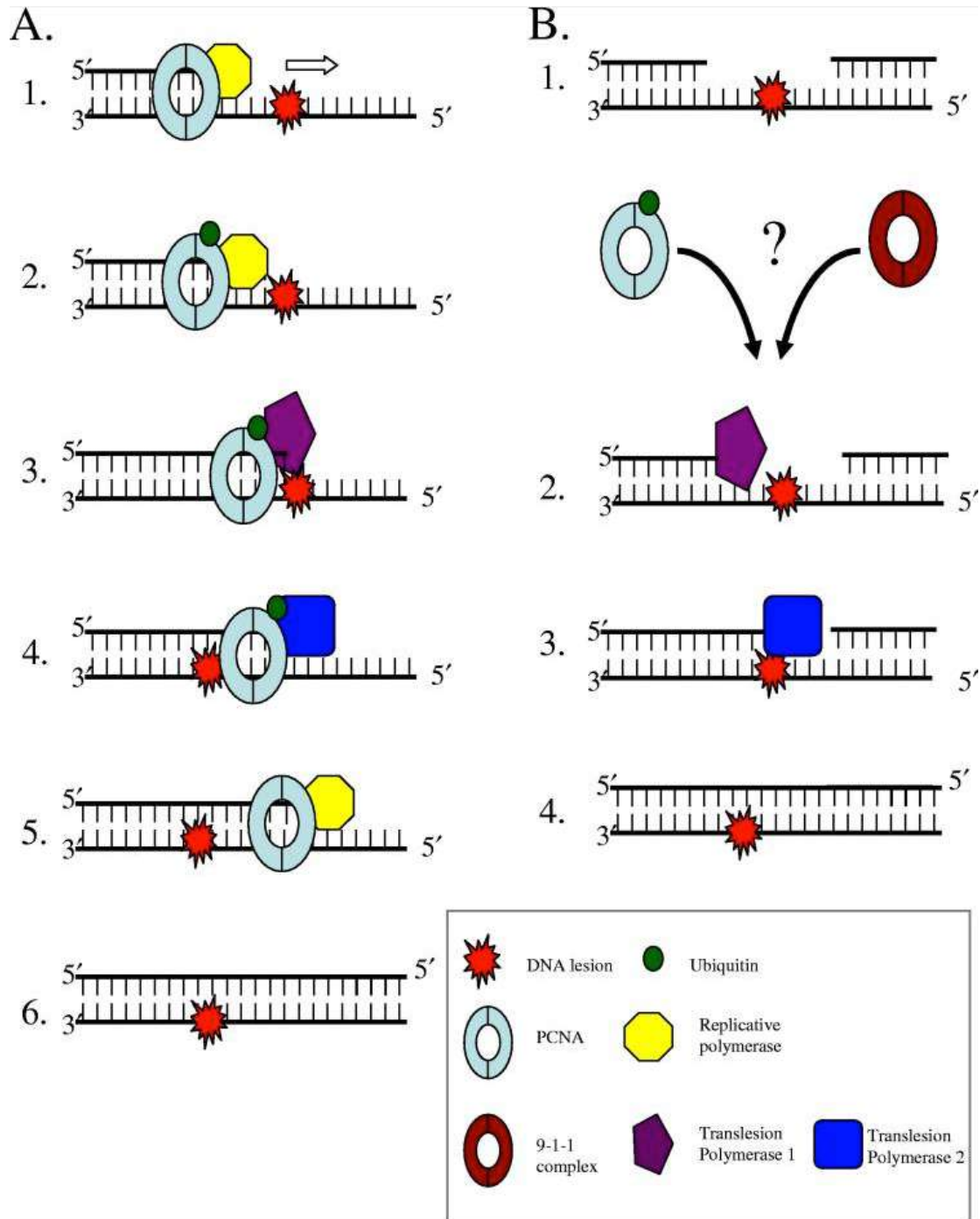


Figure 6. Models of TLS (L S Waters et al., 2009)

## Polymerase $\eta$

Yeast *RAD30* gene codes for the yeast TLS polymerase  $\eta$ , a Y-family polymerase specialized in the bypass of UV-induced lesions, as cyclobutane pyrimidine dimers (CPDs) (R E Johnson, Prakash, & Prakash, 1999). *RAD30* was identified in yeast as an ortholog of *E.coli* UmuC and DinB, proteins involved in bypass and error-free repair of UV-induced damages (McDonald, Levine, & Woodgate, 1997; Roush, Suarez, Friedberg, Radman, & Siede, 1998) and the first human and mouse orthologs were discovered few years later (R E Johnson, Kondratich, Prakash, & Prakash, 1999; Chikahide Masutani et al., 1999; Matsuda et al., 2001); interestingly, Pol  $\eta$  is the only TLS whose deficiency is associated with diseases. Indeed, defects in hPol  $\eta$  (*POLH*) lead to the onset of the *xeroderma pigmentosum* variant (XP-V) genetic syndrome (Chikahide Masutani et al., 1999), characterized by high incidence of skin cancer and sunlight sensitivity, due to the inability to deal with UV lesions sun-induced (Gratchev, Strein, Utikal, & Sergij, 2003). Other orthologs of yeast *RAD30* in human and mice are the DNA polymerase  $\kappa$  and  $\iota$  (Gerlach et al., 1999; McDonald et al., 1999; T Ogi, Kato, Kato, & Ohmori, 1999; A Tissier, McDonald, Frank, & Woodgate, 2000).

Pol  $\eta$  belongs to the Y-family polymerases, the catalytic core is located at the N-terminus of the protein, while in the C-terminus are the regulatory regions, PIP, UBZ, RIR and a NLS for higher eukaryotes. Pol  $\eta$  is known for its excellent ability to accommodate and bypass many different DNA lesions, CPD *in primis* (R E Johnson, Prakash, et al., 1999), but also 7,8-dihydro-8-oxoguanine (L Haracska, Prakash, & Prakash, 2000), abasic site (Lajos Haracska, Washington, Prakash, & Prakash, 2001), 1,2-intrastrand d(GpG)-cisplatin crosslink (Biertümpfel et al., 2010), (+)-trans-anti-benzo[a]pyrene-N<sub>2</sub>-dG (Y. Zhang, Yuan, Wu, Rechkoblit, et al., 2000), acetylaminofluorene-adducted guanine (Yuan et al., 2000), 6-O-methylguanine (L Haracska et al., 2000), thymine glycol (Kusumoto, Masutani, Iwai, & Hanaoka, 2002) and adducts derived from cisplatin and ozaliplatin (Vaisman, Masutani, Hanaoka, & Chaney, 2000); whereas it is blocked by 6-4 photoproducts (C. Masutani, Kusumoto, Iwai, & Hanaoka, 2000), BPDE-dG (Chiapperino et al., 2002),

butadiene epoxide (Minko, Washington, Prakash, Prakash, & Lloyd, 2001),  $\gamma$ -HOPdG (Minko et al., 2003) and N6-etheno-deoxyadenosine (Levine et al., 2001). In particular, Pol  $\eta$  has a major role in accurate and non-mutagenic bypass of CPDs and 7,8-dihydro-8-oxoguanine; in its absence, other TLS polymerases are thought to bypass the lesions although with low fidelity and introducing mutations (Lehmann, 2005; Y. Wang et al., 2007).

*In vitro*, Pol  $\eta$  copies damaged DNA more efficiently than undamaged DNA (R E Johnson, Prakash, et al., 1999), thus the TLS process can be considered error-free in most of the cases; in addition, it dissociates from DNA as soon as the lesion has been bypassed, in order to prevent low fidelity replication of the undamaged DNA (Biertümpfel et al., 2010). The mechanism of accurate CPDs bypass was elucidated by crystallographic and biochemical studies, in which it was demonstrated the molecular splinting strategy adopted by Pol  $\eta$  (Biertümpfel et al., 2010). The open active site accommodates both the thymines of a CPD, stabilizing the adduct and splinting it with the surrounding DNA to assume the B-form. In this way the two consecutive thymines can be read and replicated accurately forming the correct hydrogen bonds between base pairs (Biertümpfel et al., 2010). When the CPD is replicated, it subsequently exits from the active site, one more nucleotide is added and steric clashes occurs with the polymerase, that dissociates from DNA (Kusumoto, Masutani, Shimmyo, Iwai, & Hanaoka, 2004; McCulloch et al., 2004). Therefore Pol  $\eta$  precisely bypass the lesion but it is also displaced to avoid inaccurate DNA synthesis on undamaged bases. On the other hand, this inaccuracy on undamaged DNA is used from B-cells during somatic hypermutation process, to generate antibodies diversity (Faili et al., 2004; X. Zeng et al., 2001). In particular, during class switch recombination, Pol  $\eta$  introduces errors preferentially in front of A/T bases (Faili et al., 2004; X. Zeng et al., 2001) by misincorporating dGTP and efficiently extend the yet created mismatch to complete the mutagenesis (Y. Zhao et al., 2013).

Recently Pol  $\eta$  has been implicated also in genome stability maintenance in unperturbed conditions, rather than translesion synthesis on damaged DNA. In fact, depletion of human Pol  $\eta$  slightly affects cell cycle progression and

particularly reduces the stability of common fragile sites (CFSs), triggering the activation of DNA damage checkpoint ATM-mediated (**Rey et al., 2009**). Pol  $\eta$  is actually found on CFSs, where the replicative polymerases possibly stall, thereby preventing cells to enter mitosis with under-replicated DNA (**Bergoglio et al., 2013**). *In vitro* studies demonstrated that Pol  $\eta$ , and also Pol  $\kappa$ , are able to exchange with Pol  $\delta$  at CFSs and then to efficiently replicate the non-B-DNA CFS structures (**Barnes, Hile, Lee, & Eckert, 2017**).

A less investigated role of Pol  $\eta$  is the D-loop extension during homologous recombination (HR) in chicken DT40 cells (**Rattray & Strathern, 2005**). It has been shown that Pol  $\eta$  co-immunoprecipitates with Rad51 and extends the 3'-OH terminus generated after strand invasion, a structure known as D-loop (**Kawamoto et al., 2005; McIlwraith et al., 2005**). However this aspect need further investigation since it has been described only *in vitro* and in one particular cell type.

Pol  $\eta$  presents a PIP and an Ubiquitin-Binding motif on its C-terminus, whose roles are still debated. Indeed, the interaction with mono-ubiquitinated PCNA is crucial but not essential for Pol  $\eta$ -mediated TLS. When replication forks stall, Rad18 is generally recruited to mono-ubiquitinated PCNA, and this modification shifts its binding preference towards TLS Pols, respect to replicative Pols. *In vitro*, PCNA stimulates Pol  $\eta$  activity (**L Haracska, Johnson, et al., 2001**) but mono-ubiquitinated PCNA is not required for its access of replication forks, but it enhances the interaction with PCNA by itself (**Lajos Haracska, Kondratik, Unk, Prakash, & Prakash, 2001**). Actually, PCNA is mono-ubiquitinated on its back face, so the interaction of Pol  $\eta$  does not interfere with Pol  $\delta$ , that is contacting the front face of PCNA (**Freudenthal et al., 2010**); on the other hand, Pol  $\eta$  shows the same affinity for PCNA or Ub-PCNA *in vitro* (**Hedglin, Pandey, & Benkovic, 2016**). It is also true that Pol  $\eta$  interacts with both Rad18 and PCNA on its C-ter, thereby facilitating their interaction and enhancing PCNA ubiquitination (**Durando et al., 2013**). In mouse, Pol  $\eta$  co-purifies with Rad18, Rad6 and Rev1 (**Stary, Kannouche, Lehmann, & Sarasin, 2003**) and it co-localizes in DNA damage-dependent foci with Rad18 (**Watanabe et al., 2004**). In human cells, Pol  $\eta$

forms foci with mono-ubiquitinated PCNA upon DNA damage (P. L. Kannouche et al., 2004), and the localization in foci is dependent on mono-ubiquitinated PCNA (Watanabe et al., 2004). The UBZ domain is required to bypass UV lesions both in yeast and mammals (Bienko et al., 2005; Parker, Bielen, Dikic, & Ulrich, 2007); while the PIP domain seems not essential to perform TLS, and Pol  $\eta$  PIP mutants hence complement UV-sensitivity of cell lacking Pol  $\eta$  (Narottam Acharya et al., 2008; Narottam Acharya, Yoon, Hurwitz, Prakash, & Prakash, 2010; Gueranger et al., 2008).

In general, Pol  $\eta$  forms foci in cells treated exposed to DNA damage as UV and MMS (P. Kannouche et al., 2001) or exposed to replication stress with hydroxyurea (de Feraudy et al., 2007), but there is also a small portion of cells where Pol  $\eta$  forms spontaneous foci, either damage-independent or Rad18/PCNA-independent (Watanabe et al., 2004). In any case, the association with the chromatin is highly dynamic, Pol  $\eta$  shows a residence time in nuclear foci that is less than one second (Sabbioneda et al., 2008).

The interaction with Rev1, through the RIR domain (Xie, Yang, Xu, & Jiang, 2012), is confirmed in vertebrates and flies even if its biological significance is still understood (Kosarek et al., 2008; Agnès Tissier et al., 2004).

Pol  $\eta$  is regulated at the transcriptional level in yeast, specifically upon UV treatment its transcript is three-fold induced (McDonald et al., 1997), while in mouse there is no induction upon UV irradiation but during cell proliferation (Yamada, Masutani, Iwai, & Hanaoka, 2000). Pol  $\eta$  post-translational modifications have been detected only in higher eukaryotes, thereby suggesting a more complicated regulation. As a response to UV damages, Pol  $\eta$  is phosphorylated by ATR (Göhler, Sabbioneda, Green, & Lehmann, 2011), while it is ubiquitinated at the C-ter by the E3 ubiquitin-ligase PIRH2 to possibly regulate its access to replication forks (Jung, Hakem, Hakem, & Chen, 2011). The ubiquitin moiety attached directly to Pol  $\eta$  interacts with its UBZ domain, keeping it occupied from any interaction with other ubiquitin molecules, as the one of the Ub-PCNA (Jung et al., 2011). However, it is not still fully known how the ubiquitination regulates Pol  $\eta$  function, it clearly inhibits the interaction with PCNA (Jung et al., 2011) and it is dependent on

the UBZ domain but is not responsive to DNA damage (**Parker et al., 2007**). In yeast, Pol  $\eta$  is a short-lived protein that is stabilized upon DNA damage, this regulation is accomplished by proteasomal degradation, thereby suggesting that some post-translational modifications could occur (**Skoneczna, McIntyre, Skoneczny, Policinska, & Sledziewska-Gojska, 2007**).

### **Polymerase $\kappa$ and $\iota$**

The DNA polymerase  $\kappa$  is present only in higher eukaryotes and it is evolutionary related to Pol  $\eta$ . The structure of Pol  $\kappa$  comprises the conserved motifs at the N-ter of the protein, which retains the catalytic activity, while the PAD domain is located on the C-ter of the protein (**Uljon et al., 2004**); as Pol  $\eta$ , it has also a RIR domain that binds the C-ter of Rev1 (**Xie et al., 2012**). Indeed, Pol  $\kappa$  differs from the other Y-family polymerases because of the position of the PAD domain, that is not required for the catalysis (**Uljon et al., 2004**). Pol  $\kappa$  is the most faithful Y-family polymerases, with error rates from  $10^{-3}$  to  $10^{-4}$  and play its role as a proficient extender of mismatched primer termini (**Washington, Johnson, Prakash, & Prakash, 2002**). It extends a mismatched primer after the lesion bypass of another TLS Pol, even if it shows the tendency to generate single nucleotides deletion. The ability to proficiently extend mispaired termini is due to the fact that the PAD domain establishes few contacts with DNA. On the other hand, it has a very poor capability to bypass DNA damage as CPDs, 6-4-photoproduct or abasic sites (**Lajos Haracska, Unk, et al., 2002; Lajos Haracska, Prakash, & Prakash, 2002a**). Pol  $\kappa$  is diffused in the nucleus and forms DNA damage-dependent foci, through the interactions stabilized by the PIP and the UBM domains (**Caixia Guo, Tang, Bienko, Dikic, & Friedberg, 2008; Tomoo Ogi, Kannouche, & Lehmann, 2005**). Interestingly, Pol  $\kappa$  deficient mouse are UV sensitive (**Tomoo Ogi, Shinkai, Tanaka, & Ohmori, 2002**).

As Pol  $\kappa$ , Pol  $\iota$  is homolog of Pol  $\eta$  and it is present only in higher eukaryotes. The structure is similar to the other Y-family polymerases (**Nair, Johnson, Prakash, Prakash, & Aggarwal, 2004**), the unique feature of Pol  $\iota$  is that it imposes Hoogsteen base pairing in its active site, rather than Watson-Crick

pairing (Nair et al., 2004). The fidelity of Pol  $\iota$  synthesis varies depending on the template, in general it is more faithful and efficient on purine templates (L. Haracska, Johnson, et al., 2001; Agnès Tissier, McDonald, Frank, & Woodgate, 2000; Washington, Johnson, Prakash, & Prakash, 2004; Y. Zhang, Yuan, Wu, & Wang, 2000). It is not able to bypass CPDs, but it replicates over abasic sites, 6-4 photoproducts and N<sub>2</sub>-adducted guanines (Washington, Minko, et al., 2004) but it bypasses 8-oxoguanine and 2-Acetylaminofluorene (AAF) adducted guanine by frequently incorporating a cytosine (Y. Zhang, Yuan, Wu, Taylor, & Wang, 2001)

### **Rev1**

Rev1 gene was identified in yeast as its deletion causes a *REVersioneless* phenotype (Larimer, Perry, & Hardigree, 1989), that means reduction of either spontaneous or induced mutagenesis; indeed Rev1, together with Pol  $\zeta$ , it is responsible for mutagenic repair of UV-induced DNA damage from yeast to humans (P. E. Gibbs et al., 2000; Christopher W. Lawrence & Christensen, 1978). It is technically a deoxycytidil transferase, which incorporates dCTP preferentially on G template or abasic sites (Lajos Haracska, Prakash, & Prakash, 2002b; John R. Nelson, Lawrence, & Hinkle, 1996). To accomplish this specific activity, Rev1 selects the incoming dCTP by forming hydrogen bonds with an Arginine residue in the active site, rather than with the template DNA (Nair, Johnson, Prakash, Prakash, & Aggarwal, 2005). Besides, Rev1 shows very low processivity, by adding 2 nucleotides per DNA-binding event (Lajos Haracska, Prakash, et al., 2002b). Even though Rev1 is necessary for the most of base substitution mutations induced by UV light, its catalytic activity seems to have no role in UV mutagenesis (L. Haracska, Unk, et al., 2001; Ross, Simpson, & Sale, 2005). In fact, the incorporation of dCTP is an unlikely event opposite UV-induced lesions (P. E. M. Gibbs, Borden, & Lawrence, 1995; L. Haracska, Unk, et al., 2001) but the presence of Rev1 is necessary to bypass 6-4 photoproduct and for mutagenesis that occurs following TLS through abasic sites (L. Haracska, Unk, et al., 2001). In

conclusion, although the dCMP transferase activity of Rev1 is conserved from yeast to humans, it is not required for *in vivo* bypass of many lesions (**Lin et al., 1999; John R. Nelson et al., 1996**).

Actually, Rev1 have more structural and regulatory functions rather than catalytic ones. It has the capability to interact with different partners via its BRCT (BRCA1 C-terminal) domain, the C-terminal ~100 amino acids, the PAD, and the ubiquitin-binding motifs (UBMs). The role of Rev1 in survival and mutagenesis is hence to coordinate the recruitment of other factors at the damaged site (**C. Guo, 2003; L. Haracska, Unk, et al., 2001**).

The BRCT domain is found in many proteins associated with cell cycle regulation and DNA damage (**Callebaut & Mornon, 1997**), and mutations in Rev1's BRCT lead to decreased viability and mutagenesis after DNA damage (**Jansen et al., 2005; Lemontt et al., 1971; Ross et al., 2005**). The BRCT domain interacts with PCNA to localize Rev1 at replication foci (**Caixia Guo et al., 2006**); intriguingly Rev1 does not have any PIP domain, suggesting it makes distinct contact with PCNA respect to the other TLS polymerases. Additionally, Rev1 binds Pol  $\zeta$  by contacting the Rev7 accessory subunit through its C terminus and BRCT domain (**D'Souza & Walker, 2006**). In general, TLS polymerases interact in turn with Rev1 through the RIR domain. Specifically, Pol  $\zeta$ , Pol  $\eta$ , Pol  $\iota$  and Pol  $\kappa$  could gain the access to replication forks by interacting with Rev1 C-terminus (**C. Guo, 2003; Murakumo et al., 2001; Ohashi et al., 2004; Agnès Tissier et al., 2004**); the fact that all TLS Pols contact the same region on Rev1 might ensure that only one of them could gains the full access to the stalled fork and perform TLS at a time. The C-terminus is so fundamental to accomplish lesion bypass that Rev1 truncated proteins, lacking the C-ter region, do not complement a *rev1* $\Delta$  strain (**D'Souza, Waters, & Walker, 2008; Kosarek et al., 2008; Ross et al., 2005**). Furthermore, the PAD domain interacts *in vitro* with both Pol  $\zeta$  and Pol  $\eta$  (**N. Acharya et al., 2005; Narottam Acharya, Haracska, Prakash, & Prakash, 2007**). In mouse, Rev1 localizes at DNA damage-induced foci binding ubiquitinated PCNA through a non-canonical UBM domain (**C. Guo et al., 2006**). In conclusion, Rev1 is a scaffold that coordinates at the molecular level

first the action of TLS polymerases that bypass the lesion, and then the primer extension by Pol  $\zeta$  (Masuda, Ohmae, Masuda, & Kamiya, 2003; Murakumo et al., 2001). The expression of Rev1 is cell cycle regulated, with the highest expression in G<sub>2</sub>/M phases (Lauren S Waters & Walker, 2006), suggesting a role in post-replication gap filling rather than lesion bypass at stalled forks during replication. It is also phosphorylated in a cell cycle-dependent manner and in response to DNA damage, but it is unknown how this phosphorylation regulates Rev1 function (Sabbioneda, Bortolomai, Giannattasio, Plevani, & Muzi-Falconi, 2007). Besides, Rev1 and Pol  $\zeta$  are targeted also to mitochondria and contributes to mtDNA mutagenesis in yeast *S. cerevisiae* (Rasmussen, Chatterjee, Rasmussen, & Singh, 2003; H. Zhang, Chatterjee, & Singh, 2006).

### Polymerase $\zeta$

The polymerase  $\zeta$  differs from the other TLS since it belongs to the B-family polymerases, as the replicative ones. It is a heterodimer composed by the catalytic subunit (Rev3) (Lemontt et al., 1971) and the accessory subunit (Rev7) (Christopher W. Lawrence, Das, & Christensen, 1985; J R Nelson, Lawrence, & Hinkle, 1996). Even though Pol  $\zeta$  is a B-family polymerase, it lacks the proofreading activity and its error rate on undamaged DNA is  $\sim 10^{-4}$  (Robert E. Johnson, Washington, Haracska, Prakash, & Prakash, 2000; Christopher W. Lawrence, 2004). In yeast, the deletion of *REV3* or *REV7* genes does not affect cell viability but results in reduced spontaneous and damage induced mutagenesis (Christopher W. Lawrence, 2004); while in mice, the knock-out of *REV3* results in embryonic lethality, suggesting its crucial role in rapidly proliferating cells (Bemark, Khamlichi, Davies, & Neuberger, 2000; Esposito et al., 2000; Wittschieben, Reshmi, Gollin, & Wood, 2006).

Pol  $\zeta$  is the most proficient polymerase in extending a wide range of mispaired termini as CPDs (Robert E. Johnson et al., 2000), abasic sites (L. Haracska, Unk, et al., 2001) and 8-oxo G (Lajos Haracska, Prakash, & Prakash, 2003). With its extender role, Pol  $\zeta$  largely contributes to UV-induced

mutagenesis (C W Lawrence, Nisson, & Christensen, 1985; C W Lawrence, O'Brien, & Bond, 1984) and abasic site mutagenesis (R. E. Johnson et al., 1998). On the other hand, it is nearly completely blocked and inhibited in front of the majority of DNA lesions (Robert E. Johnson et al., 2000) with the particular exception of ribonucleotides. Pol  $\zeta$  is actually designated to bypass embedded ribonucleotides during replication, thus enabling fork progression especially in low dNTPs conditions (Lazzaro et al., 2012).

Finally, Pol  $\zeta$  extensively interacts with Rev 1, contributing to the bulk of mutagenesis in eukaryotes (Cheung et al., 2006; P. E. Gibbs, McGregor, Maher, Nisson, & Lawrence, 1998; Lemontt et al., 1971; McNally, Neal, McManus, McCormick, & Maher, 2008). The accessory subunit Rev3 contacts Rev1 C-terminal, enhancing Rev7 polymerase activity (N. Acharya, Johnson, Prakash, & Prakash, 2006; D. Guo, Xie, Shen, Zhao, & Wang, 2004), while Rev7 as well interacts with Rev1, which triggers its recruitment at lesion sites (C. Guo, 2003; Murakumo et al., 2001; Ohashi et al., 2004). Therefore, the cellular levels of Pol  $\zeta$  are strictly controlled, specifically its abundance is kept low mainly to avoid extra mutagenesis (Christopher W. Lawrence, 2004).

## Ribonucleotides in DNA

---

Thirty years ago was firstly hypothesized the theory of the RNA-world by Gilbert, who proposed the existence of a primordial world based on RNA to store, read and transmit the genetic information (**Gilbert, 1986**). DNA is more stable respect to RNA because the 2'-OH hydroxyl group of the sugar moiety is highly reactive and sensitive to spontaneous hydrolysis (**Y. Li & Breaker, 1999**); this advantaged DNA-based organisms over the RNA-based ones (**Cech, 2012**).

Therefore the presence of RNA in DNA genomes could potentially affect its structure or influence DNA transaction and alter the stored information. It has been fully demonstrated and proved that ribonucleotides are frequently incorporated during genome duplication from bacteria (**McDonald, Vaisman, Kuban, Goodman, & Woodgate, 2012; Y. Shen, Koh, Weiss, & Storici, 2012**) to mammalian cells (**Hiller et al., 2012; Pizzi et al., 2015; M. A. M. Reijns et al., 2012**), and their persistence has been associated with instability. In the following paragraphs are discussed in detail the mechanisms of RNA incorporation, the removal and the positive and negative outcomes of this phenomenon.

### Ribonucleotides Incorporation In The Genome

The major source of genomic ribonucleotides is provided by the DNA polymerase  $\alpha$ , which synthesizes short RNA primers during replication (**Kuchta & Stengel, 2010**). Thus the RNA primer synthesis, especially in the lagging strand, represents undoubtedly the principal source of RNA in the genome. However the RNA primers are efficiently and rapidly removed during Okazaki fragments maturation, so their presence is just temporarily (**Yeeles, Poli, Mariani, & Pasero, 2013**). Moreover, consecutive RNA tracts as mRNA (**Pomerantz & O'Donnell, 2008**) or primers synthesized by the PrimPol

(García-Gómez et al., 2013) are also used to restart stalled replication forks (Yeeles et al., 2013).

Early studies showed that DNA polymerases can be forced to introduce ribonucleotides and behave as a weak RNA polymerase (T. Chen & Romesberg, 2014; G. Gao, Orlova, Georgiadis, Hendrickson, & Goff, 1997; P. H. Patel & Loeb, 2000). Besides the selection of the correct base, DNA polymerases have evolved a sugar selectivity to discriminate between deoxyribonucleotides (dNTPs) and ribonucleotides (NTPs) (Joyce, 1997). The discrimination is mainly achieved by a steric clash of the 2'-OH group with conserved residues of the polymerase's steric gate (Joyce, 1997; W. Wang, Wu, Hellinga, & Beese, 2012). Usually, in the steric gate, there is a bulky residue that serves as a bottleneck to prevent ribonucleotides incorporation (P. H. Patel, Kawate, Adman, Ashbach, & Loeb, 2001; P. H. Patel & Loeb, 2000). A-family polymerases use a Glu amino acid, while the others, B-, X-, Y- and retrotranscriptase, use Tyr or Phe residues (Brown & Suo, 2011); Pol  $\beta$  and pol  $\lambda$ , members of the X-family use a peptide backbone portion to exclude rNTPs (Brown et al., 2010). Clearly, the steric gate plays a crucial role in discriminating the correct base among the four dNTPs (W. Wang et al., 2012). Indeed, mutations in the conserved Tyr residue (Y645) of yeast Pol  $\epsilon$  results in cell lethality (Pavlov, Shcherbakova, & Kunkel, 2001) but, in spite of that, the adjacent residue M644 can be mutated without affecting viability (S. A. Nick McElhinny, Kumar, et al., 2010). In particular, when Gly replaces M644, the sugar discrimination is strongly impaired resulting in huge ribonucleotides incorporation, on the other hand, a substitution with Leu has the opposite outcome, increasing sugar selectivity (S. A. Nick McElhinny, Watts, et al., 2010). Also, translesion DNA polymerases use the steric gate to control sugar selectivity, F35 and Y39 are respectively the conserved residues in Pol  $\eta$  (Donigan et al., 2015) and Pol  $\iota$  (Donigan, McLenigan, Yang, Goodman, & Woodgate, 2014) that have been shown to increase rNTPs incorporation when mutated.

Replicative DNA polymerases have a 3'-exonuclease proofreading activity to excise mispaired bases (Pavlov et al., 2004), but this is not so proficient at

removing ribonucleotides (Clausen, Zhang, Burgers, Lee, & Kunkel, 2013; T.-C. Lin, Chun Xia Wang, Catherine M. Joyce, & Konigsberg\*, 2001; Williams et al., 2012). Once an rNTP has been introduced in the place of a dNTP, the subsequent nucleotide incorporation would proceed slowly, possibly facilitating its transfer to the exonuclease domain (Brown & Suo, 2011).

Deoxyribonucleotides are produced in cells by the enzymatic reduction of ribonucleotide substrates, specifically by replacing the 2'-OH group with a hydrogen atom. The ribonucleotide reductase enzyme (RNR) catalyzes this reaction (Herrick & Sclavi, 2007), and this is considered to be the rate limiting step of dNTPs production *in vivo*. RNR is indeed stimulated during S phase, when cells actually need dNTPs for DNA duplication (Lowdon & Vitols, 1973). RNR activity is controlled by free dNTPs concentration and also by cellular ATP, through a feedback mechanism ensuring a stringent control on the dNTPs production (Chabes et al., 2003). Thus, the dNTPs pool varies during the cell cycle, and it specifically increases during S phase (Reichard, 1985). However, the rNTPs pool is always several folds higher than the dNTPs one (Traut, 1994), and this difference varies depending on the considered organism and nucleotide species (S. A. Nick McElhinny, Watts, et al., 2010) (Table 2). In conclusion, during genome duplication, these high ribonucleotides concentration strongly challenges DNA polymerases activity.

Table 2. Nucleotides pool in *S. cerevisiae* (S. A. Nick McElhinny, Watts, et al., 2010)

dNTPs	Concentration ( $\mu\text{M}$ )	rNTPs	Concentration ( $\mu\text{M}$ )
dA	16	rA	3000
dC	14	rC	500
dG	12	rG	700
dT	30	rT	1700

McElhinny and colleagues measured the ability of DNA polymerases to discriminate between the two sugar moieties, by using an *in vitro* primer

extension assay followed by alkaline treatment (**S. A. Nick McElhinny, Watts, et al., 2010**). In reactions with physiological rNTPs and dNTPs concentration, yeast Pol  $\alpha$ , Pol  $\delta$ , and Pol  $\epsilon$  stably incorporate one ribonucleotide every 625, 5000 or 1250 deoxyribonucleotides, respectively (**S. A. Nick McElhinny, Watts, et al., 2010**). Considering these values as physiological, more than 13000 ribonucleotides would be introduced in a single yeast genome duplication. Later, Sparks and colleagues obtained different incorporation rates, by using a slightly different assay, and by adding accessory proteins as RPA, PCNA and the RFC complex (**Sparks et al., 2012**). It was found that rNTPs incorporation reduces the processivity of replication of ~40%, and the insertion frequency was calculated to be 1 rNTP every 720 dNTPs for Pol  $\delta$  and 1 every 640 for Pol  $\epsilon$  (**Sparks et al., 2012**). Such a difference can be likely ascribed to the presence of the accessory factors, which cooperatively ensure a processive mode of replication.

Given that human Pol  $\delta$  (**Clausen, Zhang, et al., 2013**) and Pol  $\epsilon$  (**Göksenin et al., 2012**) have ribonucleotide incorporation propensities similar to their corresponding yeast homologous, and the genomic ribonucleotides incorporation has been assessed both in human and mouse (**Hiller et al., 2012; Pizzi et al., 2015; M. A. M. Reijns et al., 2012**), the amount of rNMPs introduced in a complete mammalian genome duplication would exceed three million. Altogether, these data suggest that ribonucleotides are the most non-canonical nucleotides introduced into the genome (**S. A. Nick McElhinny, Watts, et al., 2010**), especially in the leading strand filament that is synthesized by the DNA Pol  $\epsilon$  (**Thomas A. Kunkel & Burgers, 2008**) (Figure 7). Further evidence of ribonucleotide incorporation comes from studies on the mitochondrial genome replication, where the DNA polymerase  $\gamma$  has been shown to be able to incorporate rNTPs *in vitro* (**Kasiviswanathan & Copeland, 2011**) as well as the principal bacterial replicative DNA polymerase III (**Yao, Schroeder, Yurieva, Simmons, & O'Donnell, 2013**).

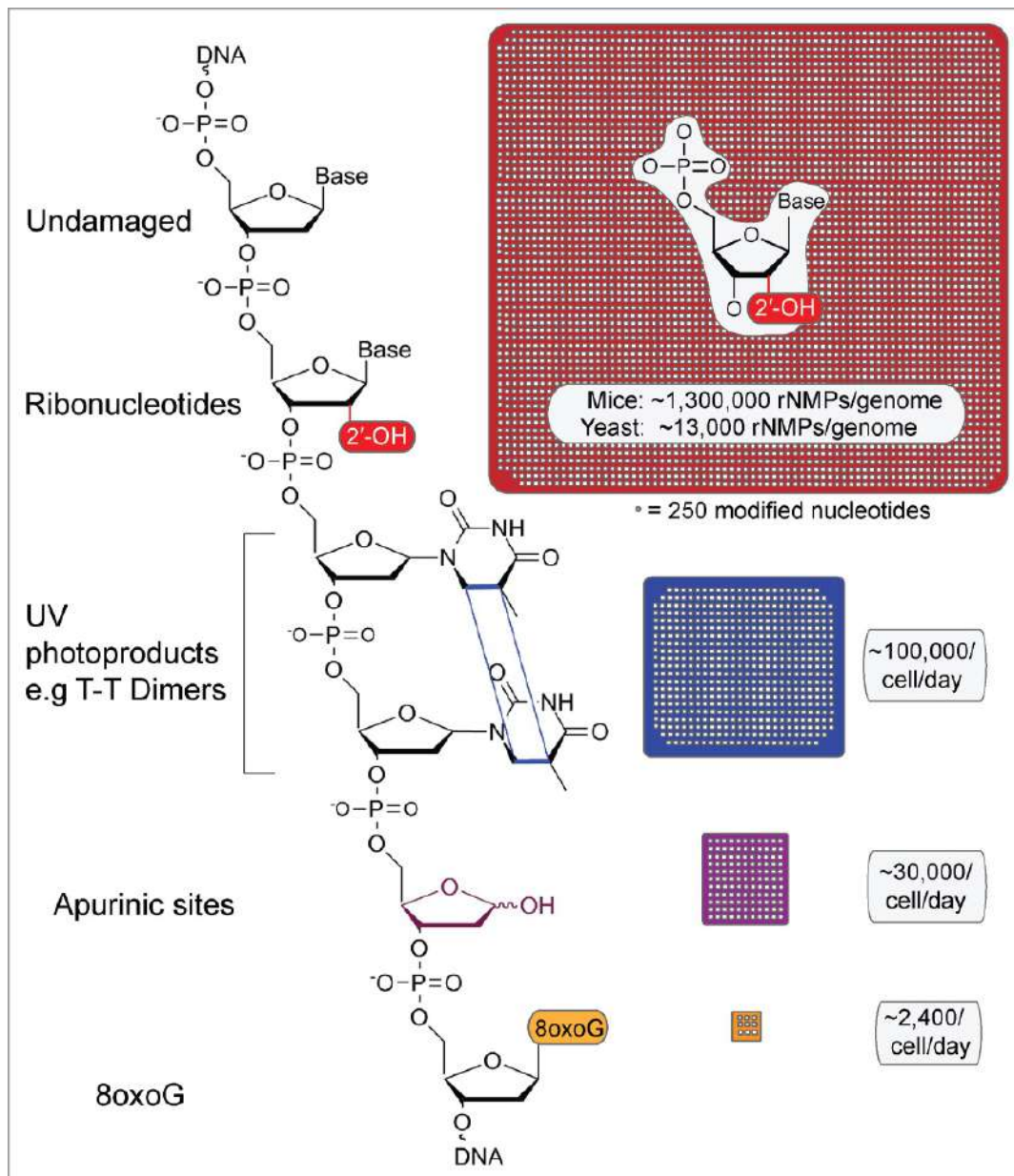


Figure 7. Ribonucleotides are an abundant form of DNA damage. (Wallace & Williams, 2014)

Replicative DNA polymerases are not the only ones that place ribonucleotides into the genome. DNA polymerase  $\mu$  is involved in double-strand breaks DNA repair through the non-homologous end joining (NHEJ) pathway, where it participates by filling small gaps preferentially with ribonucleotides (S. A. Nick McElhinny & Ramsden, 2003; Zhu & Shuman, 2008). NHEJ is prevalent in G<sub>1</sub> phase when dNTPs concentrations are particularly low, and this could partially explain the use of ribonucleotides by Pol  $\mu$  in the gap-filling synthesis step. The Terminal deoxynucleotidyl

Transferase (TdT) is an atypical polymerase implicated in NHEJ during the V(D)J recombination process, it adds random nucleotides without requiring a DNA template. It has been demonstrated that even TdT could incorporate rNTPs during its action (**Boulé, Rougeon, & Papanicolaou, 2001**). In addition, also the Tetrahymena telomerase (**Collins & Greider, 1995**) and by *E. coli* Pol V, which participates in translesion synthesis (**Vaisman et al., 2012**) insert ribonucleotides. By contrast, in *Schizosaccharomyces pombe* and *Schizosaccharomyces japonicas*, two adjacent ribonucleotides are incorporated into a specific position in the mating-type locus by Pol  $\alpha$ . These two embedded rNTPs constitute an imprinting phenomenon and designate cells for mating-type switching (**Vengrova & Dalgaard, 2006; C. Yu, Bonaduce, & Klar, 2012**).

Recently, four different groups mapped the position of embedded ribonucleotides in a genome-wide manner (**Jinks-Robertson & Klein, 2015**). They used different but related methodologies to deep sequencing *S. cerevisiae* (**Clausen et al., 2015; Koh, Balachander, Hesselberth, & Storici, 2015; M. A. M. Reijns et al., 2015**) and *S. pombe* (**Daigaku et al., 2015**) genomes, where ribonucleotides sites were previously marked. They showed that ribonucleotides are scattered into the genome but not randomly distributed, with many loci showing no reads and some with more than 1000 reads. Accordingly, there are hotspots of incorporation, especially in correspondence of sequences present in multiple copies, like mitochondrial DNA, rDNA and Ty transposons; noteworthy, in those regions RNA:DNA hybrids as well were found to be enriched (**El Hage, Webb, Kerr, Tollervey, & Andujar, 2014**). Furthermore, ribonucleotides are more abundant into the leading strand, with rCTP and rGTP preferential incorporation, suggesting a sequence context dependency. Altogether they also provided further evidence of the division of labor at the replication fork, confirming Pol  $\epsilon$  and Pol  $\delta$  as the major leading and lagging strand polymerase, respectively.

Ultimately, R-loops are considered another source of ribonucleotides but different from the ones described so far. Primarily, R-loops are structures composed of an RNA:DNA hybrid and a ssDNA, formed during the transcription process. Thus, the RNA part of the hybrid is the mRNA

transcribed by the RNA polymerase and the DNA part is the coding DNA sequence; whereas the ssDNA is the strand that has been displaced to allow transcription. In this particular case, the RNA is not embedded into DNA and there are no RNA-DNA junctions. R-loops are rare events but when they form are very stable structures, which could threaten genome instability but also be tolerated to accomplish biological functions (Aguilera & García-Muse, 2012; Skourti-Stathaki & Proudfoot, 2014). R-loops biology is an emerging topic of the last years and as for embedded ribonucleotides, there are available techniques to genome-wide map their locations, both in yeast and human cells (Chan et al., 2014; Ginno, Lott, Christensen, Korf, & Chédin, 2012).

### **Ribonucleotides Removal From DNA**

Ribonucleotides presence into the genome is essentially transient and there is more than one pathway responsible for their removal. As mentioned before, RNA primers are removed in multiple ways during Okazaki fragment maturation and are not considered for the discussion in the following paragraphs. Ribonucleases H are the enzymes deputed to hydrolyze the RNA moiety of RNA:DNA hybrid molecules (Cerritelli & Crouch, 2009). They were first described in 1969, by Peter Hausen, that identified them in calf thymus extracts (Stein & Hausen, 1969). In the following years, it was established that there are two types of RNase H, named RNase H1 and RNase H2 in eukaryotes or RNase HI and RNase HII in prokaryotes. Type 1 and 2 differs greatly in protein structure, but they are partially redundant in substrate specificity (Cerritelli & Crouch, 2009).

Thus, in addition to the low proofreading activity of replicative DNA polymerases, embedded ribonucleotides are removed mainly by a RNase H-based pathway (Ribonucleotide Excision Repair, RER) and alternatively by a Top1-dependent mechanism.

## **RNases H and Ribonucleotide Excision Repair**

The RNase H<sub>1</sub> is a monomeric enzyme whose catalytic activity requires an RNA:DNA hybrid containing at least four consecutive ribonucleotides as substrate (Eder, Walder, & Walder, 1993). The hybrid is thus cleaved by the RNase H<sub>1</sub>, which leaves the last ribonucleotides attached to DNA. Mammalian RNase H<sub>1</sub> is found both in the nucleus and in the mitochondria, where it is targeted by a specific sequence (Suzuki et al., 2010); it has been shown to be essential for mitochondrial DNA replication during mouse embryogenesis (Cerritelli et al., 2003). The nuclear function of the RNase H<sub>1</sub> has not yet been defined, possible substrates are the RNA primers of the lagging strand or stretches of ribonucleotides introduced during replication, whereas known targets are the R-loops formed during transcription (El Hage et al., 2014; W. Shen et al., 2017) and the TERRA-telomeric hybrids (Arora et al., 2014).

RNase H<sub>2</sub> is the major source of nuclear RNase H activity in mammalian and yeast cells (Arudchandran et al., 2000). It is a heterotrimeric complex composed of the RNASEH<sub>2</sub>A, RNASEH<sub>2</sub>B and RNASEH<sub>2</sub>C subunits, Rnh201, Rnh202, and Rnh203, respectively, in yeast (Chon et al., 2009; Jeong, Backlund, Chen, Karavanov, & Crouch, 2004). The RNASEH<sub>2</sub>A/Rnh201 subunit retains the catalytic activity and can cleave processively both rNMPs stretches or single embedded ribonucleotides (Eder et al., 1993; Pileur, Toulme, & Cazenave, 2000; Rychlik et al., 2010). The complex is active only when all the subunits are assembled together, both in *S. cerevisiae* (Nguyen et al., 2011) and in mammalian cells (Chon et al., 2009). In the former, the two structural subunits form a sub-complex, then the catalytic subunit binds the heterodimer and the complex become active (Nguyen et al., 2011); human RNase H<sub>2</sub> complex is assembled in the cytosol, then it is imported into the nucleus in a manner dependent on RNASEH<sub>2</sub>B subunit (Kind et al., 2014). The role of these accessory subunits has to be fully clarified, but they likely provide a platform for the assembly of the entire complex, increasing its stability and processivity.

Human RNase H<sub>2</sub> interacts with PCNA through the PIP domain, located in the C-terminus of the B subunit. The interaction with PCNA is important to

localize the complex at replication foci and in repair sites (**Bubeck et al., 2011; Kind et al., 2014**), nevertheless there are evidence of PCNA-independent recruitment (**Kind et al., 2014**). In any case, the interaction with PCNA ensures that RNase H2 is the leading RNase H activity during genome duplication. As a secondary role during replication, both RNase H1 and H2 resolve R-loops structures (**Amon & Koshland, 2016**) and act as a backup mechanism in Okazaki fragment maturation (**Murante, Henricksen, & Bambara, 1998; Turchi, Huang, Murante, Kim, & Bambara, 1994**); indeed, the RNase H1 is not able to remove the last ribonucleotide attached to DNA and RNase H2 cleaves only at the 5' of it, thus the participation in Okazaki fragment maturation could be only an additional function in the case of need.

The first indication of the existence of a ribonucleotides-removal pathway came in 2002, when a DNA substrate with embedded ribonucleotides was incubated with *S. cerevisiae* protein extract. The ribonucleotide-containing DNA (RC-DNA) was nicked at 5' of the ribonucleotide with a subsequent cut at its 3', releasing the ribonucleotide monophosphate (**Rydberg & Game, 2002**). Further incubations with extracts from cells lacking either RNase H2, FEN1 or both leads to the conclusion that the RC-DNA was firstly nick at ribonucleotide's site by the RNase H2 and FEN1 endonuclease was involved the second cut (**Rydberg & Game, 2002**).

Other subsequent studies validated the model and stated the removal of ribonucleotides as a new repair pathway called Ribonucleotide-Excision Repair (RER) (**Sparks et al., 2012**). During RER, the RNase H2 recognizes single embedded rNMPs and cleaves at the 5' of the ribose, generating a nick whose ends have a 3'-OH and a 5'-RNA-DNA junction (Figure 8). Then, the DNA Pol  $\delta$  carries out a strand-displacement synthesis from RNase H2 incision, in collaboration with PCNA and the RFC clamp loader; this step could be performed also by the DNA Pol  $\epsilon$  but with less efficiency respect to Pol  $\delta$  (**Sparks et al., 2012**). The yet generated 5'-flap is substrate of the endonuclease FEN1 and the resulting nick is sealed by the DNA ligase I (Figure 8). FEN1 drives the processing of short flaps in Okazaki fragment maturation, but it can be partially substituted with the nuclease Exo1 (**Tishkoff et al., 1997**); as expected,

Exo1 can substitute FEN1 in RER reaction *in vitro*, although at a slower rate, on the contrary, Dna2 seems not involved in RER (Sparks et al., 2012). The enzymes involved in the RER pathway are highly conserved in all three kingdoms of life, from Archea to bacteria, yeast, plants and mammals (Heider, Burkhart, Santangelo, & Gardner, 2017; Vaisman et al., 2014).

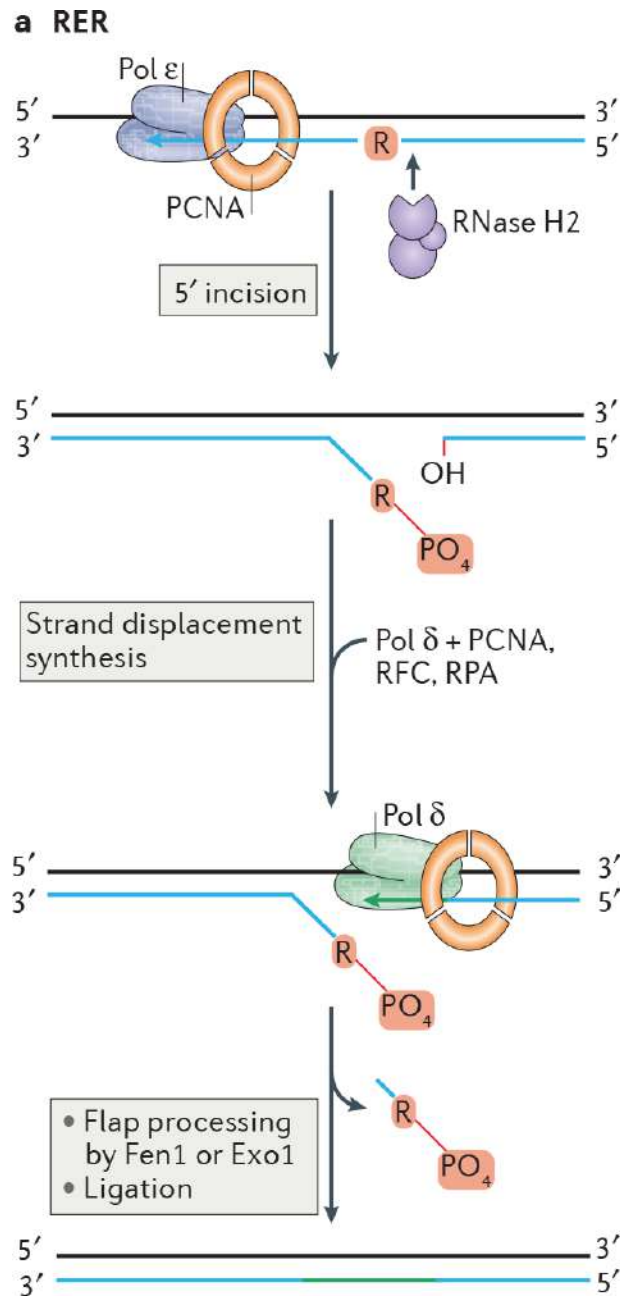


Figure 8. Ribonucleotide-excision Repair. (Williams, Lujan, & Kunkel, 2016)

The discovery of abundant alkali-sensitive sites in genomic DNA extracted from yeast cells lacking RNase H2 (*rnh201Δ*) was a strong indication that the removal pathway was almost completely RNase H2-dependent also *in vivo* (**S. A. Nick McElhinny, Kumar, et al., 2010**). In particular, RER mechanism is likely to take place during replication, as all its components possess a PCNA-interacting domain (PIP). *In vitro*, PCNA greatly stimulates ribonucleotide excision repair, probably keeping together the complex but, on the other side, *in vitro* reconstructed RER does not seem to require the PIP motif of RNase H2 (**Sparks et al., 2012**). For what concerns the expression of the RNase H2 complex, in *S. cerevisiae* the mRNA levels fluctuate within the cell cycle (**Arudchandran et al., 2000**), peaking during S and G<sub>2</sub>/M phases, while in HeLa cells, all three RNase H2 subunits are constantly present throughout the cell cycle (**M. A. M. Reijns et al., 2012**).

### **Top1 processing**

The Topoisomerase 1 (Top1) is known to resolve DNA supercoils generated during transcription and replication; in fact, it solves the torsional stresses by incising and resealing one DNA strand after the stress has been released. The first evidence of Top1 ribonuclease activity came from biochemical studies, where it was demonstrated that Top1 is able to cleave at rNMPs positions in a DNA duplex. The Top1 cleavage leaves a 5'-OH on one end and a 3'-P on the other, which in turn reacts with the 2'-OH group of the ribose, generating an unligatable 2'-3' cyclic phosphate (**Sekiguchi & Shuman, 1997**) (Figure 9). Interestingly, yeast cells lacking RNase H2 are viable despite the presence of rNMPs in the genome and, moreover, they exhibit a peculiar phenotype of 2-5 bp deletions in short repetitive sequences (**S. A. Nick McElhinny, Kumar, et al., 2010**). This characteristic deletion pattern was associated with Top1 (**Kim et al., 2011**) that, in absence of RNase H2, gain the access to embedded rNMPs. However, the 2'-3' cyclic phosphate generated by Top1 cleavage cannot be directly sealed and need further processing prior to ligation; this can basically occur in an error-free or error-prone manner (Figure 9) (**J.-E. Cho, Kim, Li, &**

**Jinks-Robertson, 2013**). The current model involves a second Top1 cleavage upstream the nick that would release a short DNA oligo containing the 2'-3' cyclic phosphate and would leave a gap of few nucleotides (**Shar-Yin Naomi Huang, Ghosh, & Pommier, 2015; Sparks & Burgers, 2015**). Such gap is subsequently filled by the coordinate action of Srs2, Exo1, and Pol  $\delta$ , which together restore the correct DNA sequence without losing any information (**Potenski, Niu, Sung, & Klein, 2014; Sparks & Burgers, 2015**). Conversely, especially in short tandem repeats, the DNA strand in front of the gap could realign, bringing close the two ends that are re-ligated by Top1 itself (**J.-E. Cho et al., 2013**). As a result, a short-bp deletion is generated, as the ones observed in RNase H2 deficient yeast cells (**S. A. Nick McElhinny, Kumar, et al., 2010**). It is curious that RER-defective cells present ribonucleotides in their genomes, despite the presence of proficient Top1 (**S. A. Nick McElhinny, Kumar, et al., 2010; Pizzi et al., 2015; M. A. M. Reijns et al., 2012**) and moreover, this Top1 activity on ribonucleotides turns out to be detectable only in absence of RNase H2. Altogether, these observations lead to the conclusion that Top1 is active only on a subset of embedded rNMPs and, during normal DNA replication, RER pathway removes ribonucleotides before Top1 can get to them. Indeed, the deletion of *TOP1* in *rnh201 $\Delta$*  yeast strain abolishes the accumulation of 2-5 bp deletions while leaving unprocessed ribonucleotides in the genome (**Williams et al., 2013**). Lastly, the alternative activity of Top1 has been associated with other severe consequences, as the formation of DSBs in the case the second cleavage occurs in the opposite DNA strand (**Shar-Yin N Huang, Williams, Arana, Kunkel, & Pommier, 2016**).

The unexpected activity of Top1 points out a new role of the RNase H2 in resolving issues related to the accumulation of torsional stress. In fact, ribonucleotides are more frequently incorporated in the leading strand of replication (**Clausen et al., 2015; Koh et al., 2015; M. A. M. Reijns et al., 2015**), where supercoiling form and have to be relaxed (**H. Yu & Dröge, 2014**). The nick generated by the RNase H2 could help in the elimination of leading strand supercoils; in its absence, Top1 is required to supply such activity.

Accordingly, Top1 activity on ribonucleotides was found to be specific of the leading strand in *S. cerevisiae* (Williams et al., 2015).

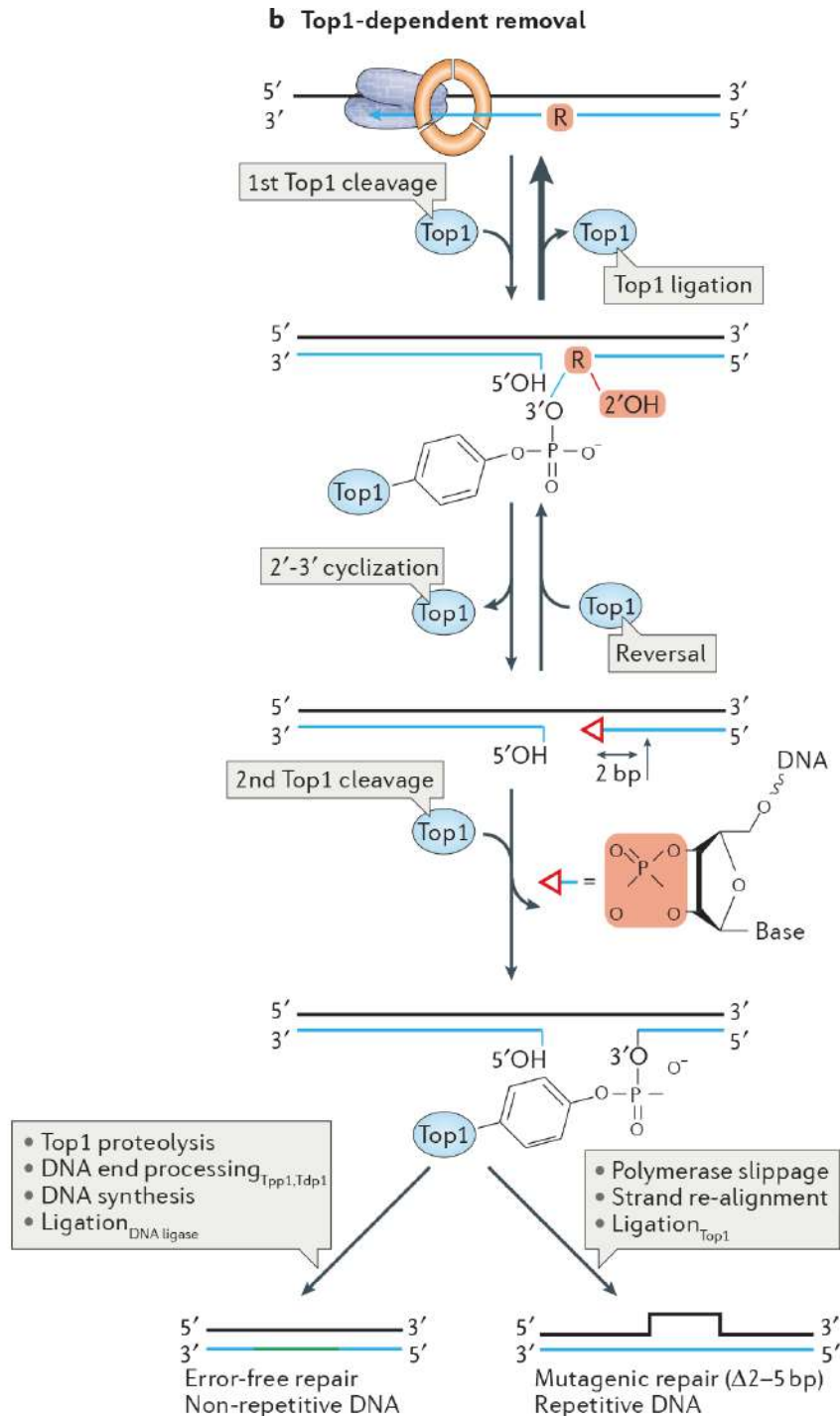


Figure 9. Top1- processing of ribonucleotides. (Williams et al., 2016)

## **Other processing**

There are other ancillary ways in which ribonucleotides could be processed, and they surely need further investigations (Figure 10). For instance, a delay in RER processing could lead to a premature attempt to ligate the nick generated by RNase H2, resulting in an adenylated 5'-RNA-DNA junction (**Tumbale, Williams, Schellenberg, Kunkel, & Williams, 2013**). Eukaryotic cells possess ATP-dependent DNA ligases to seal nicks generated during replication or repair; the catalytic mechanism involved the adenylation of the enzyme active site, then the adenylate is transferred to the 5'-phosphate group of DNA that is sealed with the release of AMP (**Lehman, 1974**). In the specific case of nicks generated by RNase H2, DNA ligases could accidentally try to seal them, without succeeding in correct ligation. The attempt to ligate a RNA-DNA junction triggers the premature release of the enzyme, resulting in adenylated DNA (**Ahel et al., 2006; Harris et al., 2009; Tumbale et al., 2011**). In that rare case, DNA ligase would exacerbate a pre-existing damage, but aprataxin (APTX) is capable to restore adenylated DNA even if contains a ribonucleotide. When this sort of ligation proofreading occurs, RER can process the substrate and any negative outcomes would be avoided (**Tumbale et al., 2013**).

In addition to the important role of the Topoisomerase 1, also the eukaryotic Topoisomerases 2 are involved in ribonucleotides processing. Top2a and Top2b regulate DNA topology by breaking and re-ligating both DNA strands after stress release (**Nitiss, 2009a, 2009b**). The presence of ribonucleotides stimulates both the Top2a and Top2b activity, resulting in the generation of a covalent adduct between the enzymes and the RNA-DNA tract (**R. Gao et al., 2014; Y. Wang, Knudsen, Bjergbaek, Westergaard, & Andersen, 1999**). As a consequence, these adducts could hamper transcription and replication processes (**Pommier, 2013**) but are promptly repaired by Tdp2 (**Gómez-Herreros et al., 2013; Z. Zeng, Cortés-Ledesma, El Khamisy, & Caldecott, 2011**), that directly reverses the covalent linkage (**R. Gao et al., 2014**). The Top2-dependent pathway has been described only in human cells and mouse, but it is absent in lower eukaryotes as yeast.

In *E. coli* cells, ribonucleotides are efficiently recognized as DNA-distorting lesions by Nucleotide Excision Repair (NER), which acts as a backup mechanism in absence of RER pathway (**McDonald et al., 2012**). *In vitro* reconstituted bacterial NER is active on substrates containing up to five ribonucleotides, and it is stimulated by the presence of mismatches (**Vaisman et al., 2013**). However, this is not conserved in eukaryotes, neither in yeast or in human cells NER targets embedded rNMPs (**Lindsey-Boltz, Kemp, Hu, & Sancar, 2015**). There are only a few evidence that also the Mismatch Repair (MMR) is partially used as a backup pathway in absence of RER both in *E. coli* and *S. cerevisiae* (**Y. Shen et al., 2012**) but all these findings need further investigation to be fully assessed.

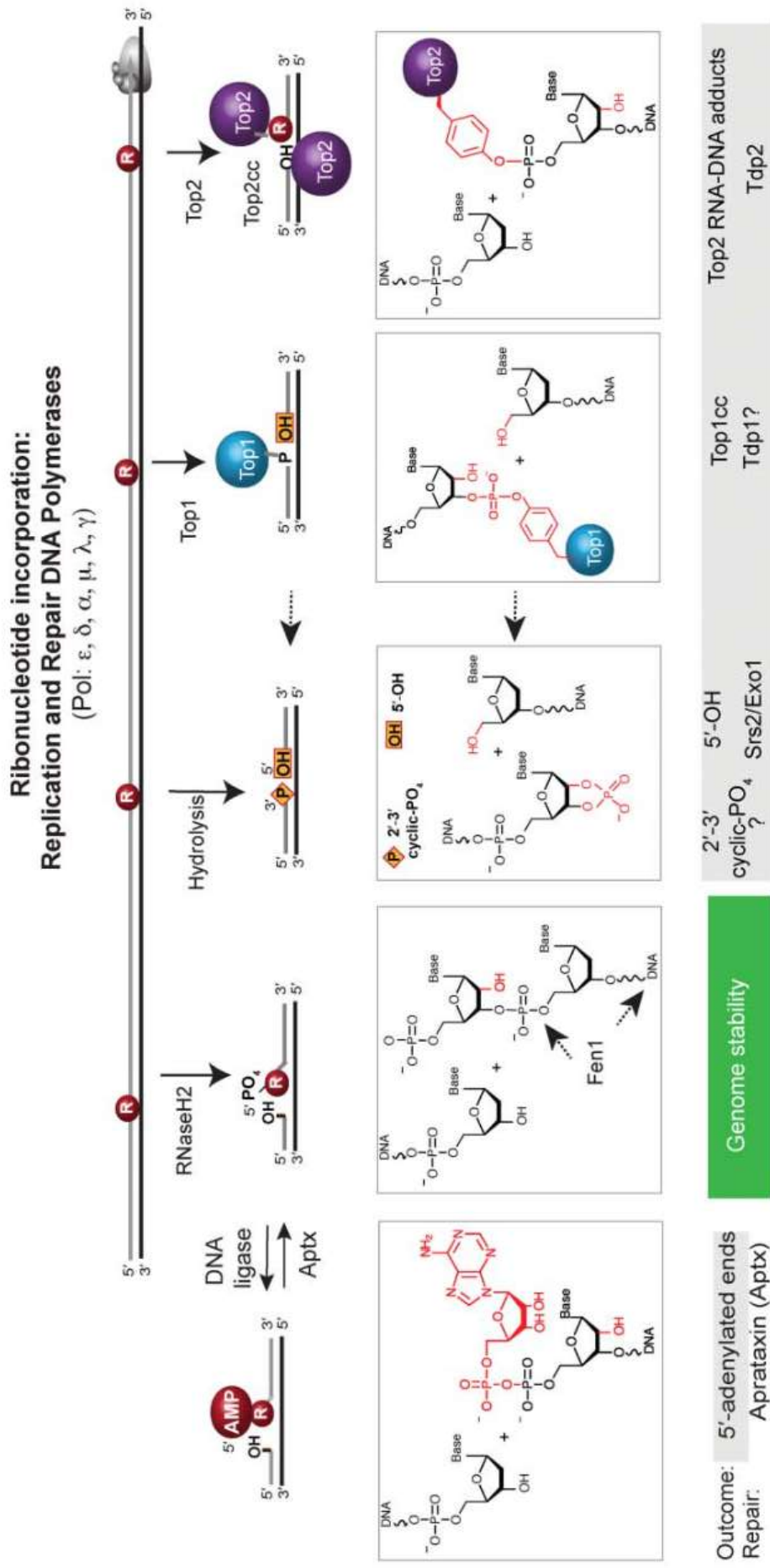


Figure 10. Overview of ribonucleotides-processing mechanisms. (Wallace & Williams, 2014)

## Negative *In Vivo* Consequences Of Ribonucleotides Incorporation

Negative consequences of ribonucleotides incorporation are principally due to failure of removal or improper processing. The molecular details come from several studies done with yeast mutants, which showed that cells accumulating ribonucleotides essentially exhibit replication stress and genome instability.

### Replication Stress

Yeast cells lacking RNase H2 activity and carrying the Pol  $\epsilon$  allele with increased ribonucleotide incorporation frequency (*pol2-M644G*) have been characterized to better understand phenotypes linked to rNMPs persistence in the genome (S. A. Nick McElhinny, Kumar, et al., 2010). They display typical replication stress phenotypes: slow growth, accumulation in S phase, activation of the S phase checkpoint, slightly elevated dNTP pools and sensitivity to the replication stress agent hydroxyurea (HU) (S. A. Nick McElhinny, Kumar, et al., 2010). On the other hand, cells carrying allele *pol2-M644L*, with decreased rNMPs incorporation, do not show these phenotypes, suggesting that they are due to rNMPs introduced during genome duplication (S. A. Nick McElhinny, Kumar, et al., 2010). The additional deletion of *TOP1* gene alleviates these consequences, implying that they are partially due to the error-prone processing mediated by the Topoisomerase 1 (Williams et al., 2013). In mouse, knocking down the RNase H2 results in embryonic lethality and the *RNase H2*<sup>-/-</sup> embryos grow very slowly (Hiller et al., 2012; M. A. M. Reijns et al., 2012). Moreover, mouse cells depleted by the RNase H2 activity contain a huge amount of ribonucleotides in the genome, proliferate slowly, activate the p53-dependent checkpoint, display high p21 and cyclin G1 levels, histone H2AX foci and genome instability (Hiller et al., 2012; M. A. M. Reijns et al., 2012). The same is observed for human cells depleted for RNase H2, they indeed show impaired cell proliferation, chronic activation of the PRR, sensitivity to HU, 53BP1 foci accumulation and micronuclei formation (Pizzi et al., 2015).

These detrimental outcomes could be due to the encounter of an unresolved nick by a moving replication fork, thus leading to a DSB, as well as

ribonucleotides in the template strand, which stall DNA polymerases. Indeed, the presence of ribonucleotides induce stalling of the polymerases *in vitro*; the Pol  $\delta$  and Pol  $\epsilon$  actually bypass single rNMPs with 69% and 66% of efficiency, respectively (Clausen, Murray, Passer, Pedersen, & Kunkel, 2013; Watt, Johansson, Burgers, & Kunkel, 2011). Furthermore, stalling increases with the number of consecutive embedded ribonucleotides, mostly for Pol  $\epsilon$ , that is completely unable to bypass four adjacent rNMPs (Clausen, Murray, et al., 2013). Therefore, these non-canonical nucleotides are barely replicated, likely because they do not fit correctly in the dNTPs-binding site. In fact, structural studies revealed that stalling is associated with the displacement of the conserved tyrosine (Y645) present in that pocket (Clausen, Murray, et al., 2013), which is considered the most important residue in the discrimination mechanism (Joyce, 1997). Interestingly, the B-family TLS polymerase  $\zeta$  is able to efficiently bypass even four consecutive ribonucleotides in the DNA template (Lazzaro et al., 2012). This capability becomes relevant in cells lacking both RNase H1 and H2 (*rnh1 $\Delta$  rnh201 $\Delta$* ) when exposed to replication stress with hydroxyurea (HU). As the aforementioned rNMPs accumulating cells, *rnh1 $\Delta$  rnh201 $\Delta$*  cells exhibit replication stress phenotypes and are sensitive to HU (Lazzaro et al., 2012). In hydroxyurea stress these cells rely on the two PRR mechanisms, template switching or TLS, to deal with embedded ribonucleotides. In particular, the TLS Pol  $\zeta$  is fundamental during replication to bypass embedded ribonucleotides encountered in the DNA template (Lazzaro et al., 2012). Since these effects are proper of cells lacking both the RNases H, and replicative polymerases show only reduce rates in front of single rNMPs, they are likely to be caused by stretches of rNMPs, that can be overcome by Pol  $\zeta$  or the template switching (Lazzaro et al., 2012).

R-loops contribute as well to replication stress in *rnh1 $\Delta$  rnh201 $\Delta$*  cells, which lose the capability to degrade RNA:DNA hybrids formed during transcription. Unresolved R-loops induce stalling of replication forks and activate the S phase checkpoint (Bermejo, Lai, & Foiani, 2012; El Hage, French, Beyer, & Tollervey, 2010). Accordingly, the combination of *rnh1 $\Delta$  rnh201 $\Delta$*  deletions with *pol2-M644G* results in cell lethality, probably because of both rNMPs and

R-loops accumulation, which together could provide a great number of substrates for Top1-dependent error-prone removal (**Lazzaro et al., 2012; Williams et al., 2013**). Importantly, R-loops contribute to the observed replication stress but they are not the principal cause. For instance, the HU sensitivity of *rnh1Δ rnh201Δ* cells is not attributable to R-loops accumulation (**Lazzaro et al., 2012**). Additionally, a separation-of-function mutant of the RNase H2 (*rnh201Δ-RED*) helped to distinguish at least between the action on single and multiple ribonucleotides (**Williams, Gehle, & Kunkel, 2017**). Indeed, the *rnh201Δ-RED* mutant, which repairs only stretches of rNMPs, behaves as the *rnh201Δ* strain, displaying replication stress, checkpoint activation and the characteristic 2-5 bp deletions of the Topoisomerase 1 (**Williams et al., 2017**). Altogether, these results confirm single embedded rNMPs during replication as the first source of replication stress and the collateral aforementioned effects.

### **Genome Instability**

The persistence of ribonucleotides into the genome leads to various processing, which could be potentially mutagenic. As discussed above, RNase H lacking cells have increased levels of mutagenesis, in particular 2-5 bp deletions caused by Top1-alternative processing (**J. Z. Chen, Qiu, Shen, & Holmquist, 2000; J. E. Cho, Kim, & Jinks-Robertson, 2015**), especially in the leading strand (**Williams et al., 2013, 2015**) or under conditions of high transcription (**Clark, Lujan, Kissling, & Kunkel, 2011**). In absence of the RNase H2, highly transcribed sequences accumulate also complex mutation templated by quasi-palindromes, independently from Top1 (**Kim, Cho, Li, & Jinks-Robertson, 2013**). These complex mutations arise from DNA re-primed synthesis on realigned quasi-palindrome sequences and are dependent on the direction of DNA replication and TLS (**Kim et al., 2013**).

The lack of RNase H activities is furthermore associated with large-scale genome instability. In yeast, whole-genome studies described gross chromosomal rearrangements (GCRs) (**Allen-Soltero, Martinez, Putnam, &**

**Kolodner, 2014; Wahba, Amon, Koshland, & Vuica-Ross, 2011**), increased loss of heterozygosity (LOH), translocations and copy number variation in diploid cells (**Conover et al., 2015; O'Connell, Jinks-Robertson, & Petes, 2015**). These findings are supported by the use of polymerase mutants that increase or decrease ribonucleotides incorporation, and respectively increase and decrease the described genome instability phenotypes (**Conover et al., 2015**) and are mainly observed in absence of RNase H2 (**Zimmer & Koshland, 2016**). Even mouse embryonic fibroblasts, defective in RNase H2, exhibit chromosomal rearrangements in metaphase chromosomes, inter-chromosomal translocations, and contain increased levels of micronuclei (**M. A. M. Reijns et al., 2012**), that are also observed in human cells depleted of RNase H2 (**Pizzi et al., 2015**).

Defects in RNase H2 affects also the expression of several yeast genes associated with response to oxidative and osmotic stress, heat shock, changes in pH and exposure to heavy metals and xenobiotics (**Arana et al., 2012**).

### **RNase H2 and diseases**

Accurate processing of ribonucleotides is a relevant aspect for different human pathologies (**M. A. M. Reijns & Jackson, 2014**). The first important link between ribonucleotides and diseases came in 2006 by Crow and its group, when they found mutations in all the three RNase H2 subunits in patients suffering from the Aicardi-Goutières syndrome (**Crow, Leitch, et al., 2006**). Aicardi-Goutières syndrome (AGS) is a rare autosomal recessive encephalopathy whose clinical features mimic a congenital viral infection (**G. Rice et al., 2007**); patients are characterized by high levels of type 1 interferon (IFN $\alpha$ ) that drives an auto-inflammatory response perhaps triggered by the accumulation of exogenous or endogenous promiscuous nucleic acids. Moreover, AGS syndrome can be caused by different mutations in other genes, all involved in processing of cellular nucleic acids: TREX1, a 3'-5' ssDNA exonuclease (**Crow, Hayward, et al., 2006; Stetson, Ko, Heidmann, & Medzhitov, 2008; Y. G. Yang, Lindahl, & Barnes, 2007**), SAMHD1, a

triphosphohydrolase (G. I. Rice et al., 2009), ADAR<sub>1</sub>, an adenosine deaminase specific for dsRNA (G. I. Rice et al., 2012) and the most recent IFIH<sub>1</sub>, a dsRNA sensor (G. I. Rice et al., 2014). Mutations in RNase H<sub>2</sub> genes are the most abundant in AGS patients and they affect the complex catalytic activity, stability, abundance and cellular localization (Figiel et al., 2011; M. A. M. M. Reijns et al., 2011).

The most severe mutation leads to a non-conservative missense substitution (G37S), in the A subunit, close to the catalytic site, that indeed affects the enzymatic activity of the complex (Crow, Leitch, et al., 2006), resulting in more unprocessed ribonucleotides into the genome (Pizzi et al., 2015). Intriguingly, the majority of mutations, rather than lead to loss of function, disturb complex stability or interactions and are found in RNase H<sub>2</sub>B and H<sub>2</sub>C subunits. The A177T is hence the most common substitution found in patients, and it is a missense mutation that replaces a conserved residue of the structural B subunit (Crow, Leitch, et al., 2006). Additionally, mutations in RNase H<sub>2</sub> are related to the autoimmune disorder systemic lupus erythematosus (SLE) (Günther et al., 2015), a pathology that shares many features in common with AGS, as the increased level of INF<sub>1</sub> in response to nucleic acids (Aicardi & Goutières, 2000).

Since the discovery of aprataxin (*APTX*) capability to act on adenylated DNA-RNA, ribonucleotides have been associated also to the neurological disease AOA<sub>1</sub> (Ataxia with Oculomotor Apraxia Type 1) (Coutinho & Barbot, 1993; Schellenberg, Tumbale, & Williams, 2015). Biochemical studies indeed proved that the mutations in *APTX* gene found in AOA<sub>1</sub> patients impair its ability to resolve RNA-DNA junctions (Schellenberg et al., 2015).

### **Ribonucleotides Effects on DNA structure**

Going down to a smaller scale, it is important to consider which kind of influence embedded ribonucleotides exert on DNA structure; this would hence provide molecular insights on the *in vivo* consequences described above. As mentioned above, the only difference between DNA and RNA is the presence of

the 2' hydroxyl group on the ribose sugar, and this causes very profound differences on the overall structure of these two nucleic acids. In fact, double stranded RNA molecules have a typical A-conformation, characterized by a wider and more compressed structure than dsDNA. The base pairs are more inclined with respect to the perpendicular plane of the axis and there are 11 bp per turn respect to 10 bp of DNA. Few studies in the literature address the issue on Ribonucleotide-containing DNA (RC-DNA) structure, and moreover, some data are conflicting to each other. Generally, it is a common way to think that the presence of one or more ribonucleotides into a DNA duplex disturbs its canonical structure.

During the nineties were crystallized the first chimeras, very short self-complementary oligos with embedded ribonucleotides. X-ray diffraction analysis suggested that the presence of ribonucleotides induces a complete change towards the A-conformation, both when they are in the middle or at the ends of the molecule (**Ban, Ramakrishnan, & Sundaralingam, 1994; Egli, Usman, & Rich, 1993**). The duplex displayed the typical residues per turn of A-form, the bases are inclined respect to the axis and the topology of the major and minor groove are reversed (**Ban et al., 1994; Egli et al., 1993**). The 2'-OH group points outside of the helix, lying close to the surface of the shallow groove, suggesting that can be easily probed by side chains of proteins (**Egli et al., 1993; Wahl & Sundaralingam, 2000**). Therefore, it looks like that the presence of just one ribonucleotide can induce a conformational change from a B- to A-DNA structure. They also pointed out the non-uniform character of the crystals, in which the molecule showed local deviations from B-conformation rather than a pure A-conformation; this was effectively confirmed by CD spectroscopy, which underlines the mixed presence of A and B conformations (**Egli et al., 1993**). It is possible that the 2'-OH dictates intra-molecular interactions that stabilize the A-form. It is important to note that in those kinds of studies molecules are immobilized as a crystal, in conditions far away from the physiological ones. In the same years, in solution NMR experiments with RC-oligos (Ribonucleotide-Containing) revealed that the overall structure was not changed but the conformational transition was limited around the

rNMP insertion (**Chou, Flynn, Wang, & Reid, 1991; Jaishree, van der Marel, van Boom, & Wang, 1993; Nishizaki et al., 1996**). It was figured out that the perturbation was more subtle respect to the one measured with X-ray crystallography. The general idea was that the ribonucleotide influence is propagated only towards the adjacent nucleotides; the reason why they observed just localized distortions of the B-DNA structure. Indeed, CD spectra went in the same direction, exhibiting a mixed A- and B-type absorption bands (**Chou et al., 1991**). Seems so that RNA and DNA conformations could coexist in the same molecule. The situation was the same when more than one ribonucleotide were inserted, molecules indeed displayed a mixed conformation depending on the chemical nature of the sugar (**Nishizaki et al., 1996**).

This issue became biologically relevant a few years ago when ribonucleotides were found to be the most non-canonical nucleotides present in cell genomes (**S. A. Nick McElhinny, Watts, et al., 2010**). Since that discovery, new works were done on the RC-DNAs structure. It was solved a Dickerson dodecamer structure containing a single nucleotides (**DeRose, Perera, Murray, Kunkel, & London, 2012**); the NMR analysis confirmed the previous conclusion on the partial B to A transition and MD simulations suggested that even 50% of ribonucleotide substitutions would not fully convert the B-DNA into A-DNA. Certainly, there were local perturbations, caused by the ribose but there was not a global transition to the A-form (**DeRose et al., 2012**). In addition, Atomic Force Microscopy measurements on short RC-DNAs showed that ribonucleotides perturb also the backbone elasticity (**Chiu et al., 2014**). Another recent Atomic Force Microscopy study (presented in this Ph.D. Thesis) performed on very long (hundreds-of-base pair) RC-DNA molecules highlighted the effects on the overall molecule structure. Indeed, it was shown that the incorporation of ribonucleotides induces a shortening of the molecules length and makes them more flexible respect their DNA counterpart (**Meroni et al., 2017**).

In conclusion, the structural influence of ribonucleotides is evident. A possible explanation for the discrepancy between pioneer solid and in solution

studies is that lattice-packaging constraints may favor a conformational regularity. Therefore, less symmetric forms found in solution does not crystallize well, and the crystal selection would be between more regular A and B conformations. Taken together these data strongly suggest that the main incentive for such conformational changes is the 2' hydroxyl group of the ribose. A global or local conformational change may occur also in the cellular environment with strong impacts on many biological processes and/or it might be recognized as a structural signal.

### **Positive *In Vivo* Consequences Of Ribonucleotides**

The high frequency of ribonucleotides misincorporation suggests that could be physiologically relevant as a signal, rather than be only a mere error of DNA polymerases. Therefore incorporation and removal should be carefully balanced, especially if ribonucleotides may influence cellular processes.

For instance, in yeast, ribonucleotides have a role as strand-discrimination signals to guide the MMR machinery on DNA (**Lujan et al., 2013**). In bacteria, DNA is generally methylated on GATC sequences and, during replication, the newly synthesized strand is easily distinguishable because of the temporary lack of methylation (**Cooper, Lahue, & Modrich, 1993**). Bacterial MMR takes advantage of the absence of methylation in the newly synthesized strand to resolve mismatches and restore the correct sequence as it is in the parental strand (**Cooper et al., 1993**). Conversely, strand discrimination in eukaryotes is less clear because there is no similar signaling system. One open question is how the MMR repair could distinguish between the two strands and accomplish a proper repair. One hypothesis is that the transient ends of Okazaki fragments may be the signals for lagging strand MMR (**S. a Nick McElhinny, Kissling, & Kunkel, 2010**), while the signals for the more continuously replicated leading strand are uncertain. Ribonucleotides could hence serve this purpose, and genetic and biochemical data proved that the nicks generated by the RNase H2 could serve as entry point for the MMR machinery (**Ghodgaonkar et al., 2013; Lujan et al., 2013**). This would be

consistent with the higher levels of ribonucleotides inserted in the leading strand by Pol  $\epsilon$ . Therefore, ribonucleotides mark the nascent leading strand making it clearly distinguishable from the parental one and their incision is used by the leading MMR to repair mismatches (**Lujan et al., 2013**). The discovery of the mutant version of Pol  $\epsilon$  that introduce less ribonucleotides (*pol2-M644L*) together with the fact that it is not found *in vivo*, could be interpreted as an evolutionary choice to keep the one that inserts more but not too many ribonucleotides during replication. However, it has also been reported that MMR is active on mismatches that comprise ribonucleotides *in vitro* (**Cilli, Minoprio, Bossa, Bignami, & Mazzei, 2015**).

In *Schizosaccharomyces pombe* (**Vengrova & Dalgaard, 2006**) and *Schizosaccharomyces japonicas* (**C. Yu et al., 2012**) the switching between the two mating types occurs via homologous recombination induced by ribonucleotides (**Sayrac, Vengrova, Godfrey, & Dalgaard, 2011**). Two ribonucleotides are inserted by the DNA polymerase  $\alpha$  in a specific position of the mating locus and, for unclear reasons, they escape from RER. Thus, the ribonucleotides imprint persists till the next replication cycle and induces the stalling of the DNA Pol  $\epsilon$ , thereby triggering homologous recombination to switch between the mating type loci (**Vengrova & Dalgaard, 2006**).

When deoxyribonucleotides are not available or critically low, ribonucleotides could be used to fill this shortfall. For instance, in G<sub>1</sub> phase of the cell cycle dNTPs level are quite low, and the DNA polymerase  $\mu$  carries out the gap-filling step of DSB repair via non-homologous end joining (NHEJ) pathway by using ribonucleotides (**S. A. Nick McElhinny & Ramsden, 2003; Zhu & Shuman, 2008**).

An emerging function of RNases H is the telomere maintenance and length regulation through the processing of telomeric repeat-containing RNA (TERRA) (**T. Y. Yu et al., 2014**). TERRA are transcribed from telomeres, where they are stabilized as R-loops structures and are implicated in telomere stability and regulation of telomerase (**Rippe & Luke, 2015**). In yeast and humans, TERRA R-loops render telomeres prone to form DSBs and then to proceed with homology-directed repair (HDR) to elongate critically short telomeres and

escape senescence (**Arora et al., 2014; Balk et al., 2013; Chu et al., 2017**). In yeast, RNase H1 and H2 are recruited specifically to long telomeres to degrade TERRAs, thus preventing accumulation of RNA:DNA hybrids (**Arora et al., 2014; Graf et al., 2017**), whereas at short telomeres their recruitments is diminished, to hence increase TERRA presence at telomere and trigger HDR to elongate telomeres and avoid senescence (**Graf et al., 2017**).

# Aim of the projects

During my PhD fellowship I worked mainly on two projects, both related to the process of ribonucleotides incorporation in DNA and its consequences, both *in vivo* and *in vitro*. I will dedicate a distinct paragraph to describe the aims of each project.

## **Aim I - Determine how ribonucleotides influence DNA structure**

---

The purpose of the Aim I is to investigate the impact of ribonucleotides incorporation on the DNA structure. The structural effects of ribonucleotides embedded in DNA have been described in the past, by using simulations or looking at very short DNA oligos, trapped in unphysiological conditions.

The goal of this project was to find a reproducible method that allows the production of long RC-DNA molecules with elevated yield; this was done with the attempt to describe rNMPs-induced structural effects in conditions more close to the environmental ones. Moreover, the choice to conduct the analysis by means of Atomic Force Microscopy (AFM) permitted to obtain robust data, which underline average population behaviors rather than a single molecule evidence. The tapping operation mode of AFM allowed detecting molecules as they equilibrate on the substrate, avoiding any sample deformation due to the imaging method. Finally, the traces of the molecules were digitalized, and by the implementation of several MATLAB routines, it was possible to extrapolate structural parameters and describe the changes due to the ribonucleotides incorporation.

## Aim II - Unravelling a new activity of yeast Pol $\eta$ in dealing with ribonucleotides

---

The second Aim was to unravel the function of the TLS polymerase  $\eta$  when the genome is ribonucleotides-enriched and the dNTPs pool is depleted.

Unprocessed genomic ribonucleotides lead to severe consequences as replication stress and genome instability; furthermore, yeast cells lacking both RNaseH1 and RNaseH2 (*rnh1 $\Delta$  rnh201 $\Delta$* ) are sensitive to treatment with low doses of HU or MMS (Lazzaro et al., 2012). In particular, only when subjected to hydroxyurea stress, cells use Pol  $\zeta$ -mediated TLS and/or the TS pathway to overcome rNMPs that stall DNA replication. Indeed, the simultaneous removal of Pol  $\zeta$  (*rev3 $\Delta$  rev7 $\Delta$* ) and the template switching (*mms2 $\Delta$* ) results in *rnh1 $\Delta$  rnh201 $\Delta$*  cells death, when exposed to low doses of hydroxyurea (Lazzaro et al., 2012). Surprisingly, by deleting all the yeast TLS polymerases, Rev1, Pol  $\zeta$  and Pol  $\eta$  (*rev1 $\Delta$  rev3 $\Delta$  rev7 $\Delta$  rad30 $\Delta$* ) in the *rnh1 $\Delta$  rnh201 $\Delta$*  genetic background, almost completely restore cell viability in HU. Moreover, by looking at the single contribution of each TLS Pol, the recovery has been fully recapitulated only by the deletion of *RAD30* gene, encoding for the Pol  $\eta$ . It is important to note that these genetic dependencies are specifically associated with the HU stress response and not to other treatments, as MMS. Hydroxyurea affects DNA synthesis by decreasing the dNTPs pool, so it would be relevant in cells defective for ribonucleotides removal. Furthermore, the strong effect of viability recovery by deletion of *RAD30* is observed also in presence of the TS pathway and/or Pol  $\zeta$ . Altogether, these genetic data suggest that Pol  $\eta$  is acting in a somehow toxic manner, causing the sensitivity to HU of cells RER-defective. Therefore, the aim of this project was to explore and characterize this unexpected toxic activity shown by Pol  $\eta$  in the condition of low dNTPs and when cells are unable to repair embedded ribonucleotides.

# Results and Conclusions

## I - The incorporation of ribonucleotides induces structural and conformational changes in DNA

---

Alice Meroni<sup>1</sup>, Elisa Mentegari<sup>2</sup>, Emmanuele Crespan<sup>2</sup>, Marco Muzi-Falconi<sup>1,#</sup>, Federico Lazzaro<sup>1,\*</sup>, Alessandro Podestà<sup>3,#</sup>

<sup>1</sup>Dipartimento di Bioscienze, Università degli Studi di Milano, via Celoria 26, 20133 Milano, Italy.

<sup>2</sup>DNA Enzymology & Molecular Virology, Institute of Molecular Genetics IGM-CNR, via Abbiategrasso 207, 27100 Pavia, Italy.

<sup>3</sup>Dipartimento di Fisica and C.I.Ma.I.Na, Università degli Studi di Milano, via Celoria 16, 20133 Milano, Italy.

#Corresponding authors;

e-mail: [alessandro.podesta@mi.infn.it](mailto:alessandro.podesta@mi.infn.it), [marco.muzifalconi@unimi.it](mailto:marco.muzifalconi@unimi.it)

\*Co- last authors

**Biophysical Journal**, 113(7), 1373–1382. (2017)

<https://doi.org/10.1016/j.bpj.2017.07.013>

## Synopsis of the work and specific contributions

Ribonucleotides incorporation into the genome is the most frequent error committed by DNA polymerases during genome replication. Accordingly, the inability to remove and replace ribonucleotides causes genome instability and replication stress. In this work, we studied at nano-metric scale the impact of ribonucleotides persistence on DNA structure.

We develop a new strategy to produce long Ribonucleotides-Containing DNA (RC-DNA) molecules in large quantity that have been imaged by means of Atomic Force Microscopy (AFM). In detail, we set up a particular PCR reaction in presence of the four dNTPs and one ribonucleotide species (rCTP) where the DNA synthesis is carried out by a mutant *Taq* polymerases. This mutant polymerase was obtained by introducing a single amino acidic substitution in the nucleotide-binding pocket (I614K) that makes it wider and prone to ribonucleotides incorporation. After the purification of the I614K *Taq* Pol, we set up the PCR conditions in which we can obtain a discrete amount of DNA molecules with ribonucleotides embedded. We hence verified the effective ribonucleotides incorporation by the I614K *Taq* Pol and we also tried to roughly estimate at which extent RC-DNA molecules contain ribonucleotides, which seem the most of them. Therefore, we produced different molecules population of different lengths, from 464 to 1049 bp, with and without embedded ribonucleotides that have been subject to AFM imaging. We deposited molecules on mica using  $Mg^{2+}$  ions to mediate the interaction with DNA and the substrate; then we used AFM in the tapping operation mode to avoid any deformation of the sample and to scan the surface by a gentle touching. DNA control molecules were well equilibrated on the surface and retained the canonical B-conformation, while RC-DNA molecules showed different changes dependent upon ribonucleotides presence. Specifically, ribonucleotides incorporation induces significant shortening of the length of the molecules, measured by a semi-automatic tracking operation. Moreover, the presence of ribonucleotides affects the end-to-end distance and consequently the persistence length, by increasing molecules flexibility respect to their

counterpart without ribonucleotides. In summary, we provided new evidence of structural changes imposed by ribonucleotides persistence into DNA, trying to reproduce a physiological-like system, with long and equilibrated molecules respect to the past studies, done mainly with short crystallized oligos.

This project was entirely developed by me with the supervision of Prof. Alessandro Podestà, for the physics part, and Dott. Federico Lazzaro and Prof. Marco Muzi Falconi, for what concerned the RC-DNAs production. I produced all the figures presented in the manuscript, with the exception of Figure S2, that I did in collaboration with the CNR of Pavia. I also wrote the manuscript with Prof. Alessandro Podestà and I actively managed the process of revision. For this contribution I am the first author of the work.

# I - Characterization of structural and configurational properties of DNA by Atomic Force Microscopy

---

Alice Meroni<sup>1</sup>, Alessandro Podestà<sup>2,#</sup>

<sup>1</sup> Dipartimento di Bioscienze, Università degli Studi di Milano, via Celoria 26, 20133 Milano, Italy.

<sup>2</sup> Dipartimento di Fisica and C.I.Ma.I.Na, Università degli Studi di Milano, via Celoria 16, 20133 Milano, Italy.

# Corresponding author; e-mail: [alessandro.podesta@mi.infn.it](mailto:alessandro.podesta@mi.infn.it)

**Book Chapter in Methods in Molecular Biology Genome instability (pp. 557–573). Humana Press, New York, NY. (In Press, 2018)**

[https://doi.org/10.1007/978-1-4939-7306-4\\_37](https://doi.org/10.1007/978-1-4939-7306-4_37)

## Synopsis of the work and specific contributions

In this *Method in Molecular Biology*, we describe in detail how to study and characterize structural and configurational properties of DNA by Atomic Force Microscopy. This protocol was set and used to accomplish the work presented in the previous section *The incorporation of ribonucleotides induces structural and conformational changes in DNA (Meroni et al., 2017)*. Here we specifically describe how to perform AFM imaging on DNA and how to extrapolate and analyze the data.

This Method is part of a collection of Methods in Molecular Biology, published in the book entitled Genome Instability.

This work was done under the supervision of Prof. Alessandro Podestà, with whom I wrote this protocol and produced the presented figures.

## II - Measuring the levels of ribonucleotides embedded in genomic DNA

---

Meroni A., Nava G.M., Sertic S., Plevani P., Muzi-Falconi M.<sup>#\*</sup> and Lazzaro F.<sup>#\*</sup>  
Dipartimento di Bioscienze, Università degli Studi di Milano. Milano, Italy

<sup>#</sup>Co-last authors

<sup>\*</sup>Corresponding authors: [marco.muzifalconi@unimi.it](mailto:marco.muzifalconi@unimi.it);  
[federico.lazzaro@unimi.it](mailto:federico.lazzaro@unimi.it)

Book Chapter in **Methods in Molecular Biology Genome instability**  
(pp. 319–327). Humana Press, New York, NY. (In Press, 2018)

[https://doi.org/10.1007/978-1-4939-7306-4\\_22](https://doi.org/10.1007/978-1-4939-7306-4_22)

### **Synopsis of the work and specific contributions**

In this *Method in Molecular Biology*, we described in detail how to measure levels of ribonucleotides embedded in genomic DNA. This protocol was optimized for human and yeast, to compare ribonucleotides levels in different mutants. However, it is not yet present in any of our publication on yeast.

This Method is part of a collection of Methods in Molecular Biology, published in the book entitled Genome Instability.

For what concerns this work, I participated in the optimization of the protocol for yeast and I wrote the protocol, under the supervision of Dott. Federico Lazzaro.

## **II - Yeast DNA Polymerase $\eta$ is involved in genome replication under low deoxyribonucleotides pools situations**

---

The second aim was to unravel the function of the Translesion Synthesis (TLS) polymerase  $\eta$  when the genome is ribonucleotides-enriched and the deoxyribonucleotides pool is depleted. Yeast cells lacking the RNase H activities accumulate ribonucleotides into the genome and are sensitive to treatment with low doses of hydroxyurea (HU), a drug that affects DNA synthesis by decreasing the intracellular dNTPs pool (Lazzaro et al., 2012). Surprisingly, we found that the TLS DNA polymerase  $\eta$  is the one responsible for such HU-induced cell lethality, suggesting that it is performing a function with a negative impact on RNase H lacking cells exposed to HU.

In brief, I characterized the cellular response to acute and chronic HU treatment, trying to deepen the comprehension about the on-going process. In absence of RNase H activities, cells failed to switch off the DNA damage checkpoint when exposed to HU and, consequently, did not succeed in cell division, accumulating in the G<sub>2</sub>/M phase. These phenotypes were dependent upon the presence of Pol  $\eta$ , confirming its involvement in the response to hydroxyurea. Moreover, by conditionally over-expressing Pol  $\eta$  during the cell cycle, I found that this particular activity is restricted to HU-stressed DNA replication, and it is proportional to the protein abundance in cells. Finally, I produced several Pol  $\eta$  mutants, which revealed that the catalytic reaction performed by Pol  $\eta$  is responsible of its negative impact and, importantly, that this is strictly related to its ability to introduce ribonucleotides. We hence ended up with a model in which Pol  $\eta$  is involved in shaping ribonucleotides abundance into the genome under low dNTPs conditions, resulting in negative outcomes when the RNase H activities are absent.

I developed this project during my Ph.D. fellowship under the supervision and in collaboration with Dott. Federico Lazzaro. All the data obtained are part of a manuscript, which is actually in preparation (Part III of this Thesis).

# Discussion

Considering the various aspects and factors discussed in this thesis, I chose not to present a general discussion. Instead, a detailed discussion with future implications of the presented findings is presented in the dedicated session of each published and in preparation manuscript.

# References

- Abraham, R. T. (2001). Cell cycle checkpoint signaling through the ATM and ATR kinases. *Genes and Development*. <https://doi.org/10.1101/gad.914401>
- Acharya, N., Haracska, L., Johnson, R. E., Unk, I., Prakash, S., & Prakash, L. (2005). Complex Formation of Yeast Rev1 and Rev7 Proteins: a Novel Role for the Polymerase-Associated Domain. *Molecular and Cellular Biology*, 25(21), 9734–9740. <https://doi.org/10.1128/MCB.25.21.9734-9740.2005>
- Acharya, N., Haracska, L., Prakash, S., & Prakash, L. (2007). Complex Formation of Yeast Rev1 with DNA Polymerase  $\eta$ . *Molecular and Cellular Biology*, 27(23), 8401–8408. <https://doi.org/10.1128/MCB.01478-07>
- Acharya, N., Johnson, R. E., Prakash, S., & Prakash, L. (2006). Complex Formation with Rev1 Enhances the Proficiency of *Saccharomyces cerevisiae* DNA Polymerase  $\epsilon$  for Mismatch Extension and for Extension Opposite from DNA Lesions. *Molecular and Cellular Biology*, 26(24), 9555–9563. <https://doi.org/10.1128/MCB.01671-06>
- Acharya, N., Yoon, J.-H., Gali, H., Unk, I., Haracska, L., Johnson, R. E., ... Prakash, S. (2008). Roles of PCNA-binding and ubiquitin-binding domains in human DNA polymerase  $\epsilon$  in translesion DNA synthesis. *Proceedings of the National Academy of Sciences of the United States of America*, 105(46), 17724–9. <https://doi.org/10.1073/pnas.0809844105>
- Acharya, N., Yoon, J.-H., Hurwitz, J., Prakash, L., & Prakash, S. (2010). DNA polymerase  $\epsilon$  lacking the ubiquitin-binding domain promotes replicative lesion bypass in humans cells. *Proceedings of the National Academy of Sciences of the United States of America*, 107(23), 10401–5. <https://doi.org/10.1073/pnas.1005492107>
- Aguilera, A., & García-Muse, T. (2012). R Loops: From Transcription Byproducts to Threats to Genome Stability. *Molecular Cell*, 46(2), 115–124. <https://doi.org/10.1016/j.molcel.2012.04.009>
- Aguilera, A., & Gómez-González, B. (2008). Genome instability: a mechanistic view of its causes and consequences. *Nature Reviews Genetics*, 9(3), 204–217. <https://doi.org/10.1038/nrg2268>
- Ahel, I., Rass, U., El-Khamisy, S. F., Katyal, S., Clements, P. M., McKinnon, P. J., ... West, S. C. (2006). The neurodegenerative disease protein aprataxin resolves abortive DNA ligation intermediates. *Nature*, 443(7112), 713–716. <https://doi.org/10.1038/nature05164>
- Aicardi, J., & Goutières, F. (2000). Systemic Lupus Erythematosus or Aicardi-Goutières Syndrome? *Neuropediatrics*, 31(3), 113–113. <https://doi.org/10.1055/s-2000-7533>
- Alberts B, Johnson A, Lewis J, Raff M, R. K. & W. P. (2002). *Molecular Biology of the Cell*. Garland Science.
- Allen-Soltero, S., Martinez, S. L., Putnam, C. D., & Kolodner, R. D. (2014). A *Saccharomyces cerevisiae* RNase H2 Interaction Network Functions To Suppress Genome Instability. *Molecular and Cellular Biology*, 34(8), 1521–

34. <https://doi.org/10.1128/MCB.00960-13>
- Almeida, K. H., & Sobol, R. W. (2007). A unified view of base excision repair: Lesion-dependent protein complexes regulated by post-translational modification. *DNA Repair*, 6(6), 695–711.  
<https://doi.org/10.1016/j.dnarep.2007.01.009>
- Amon, J. D., & Koshland, D. (2016). RNase H enables efficient repair of R-loop induced DNA damage. *eLife*, 5. <https://doi.org/10.7554/eLife.20533>
- Arana, M. E., Kerns, R. T., Wharey, L., Gerrish, K. E., Bushel, P. R., & Kunkel, T. A. (2012). Transcriptional responses to loss of RNase H2 in *Saccharomyces cerevisiae*. *DNA Repair*, 11(12), 933–41.  
<https://doi.org/10.1016/j.dnarep.2012.09.006>
- Arora, R., Lee, Y., Wischnewski, H., Brun, C. M., Schwarz, T., & Azzalin, C. M. (2014). RNaseH1 regulates TERRA-telomeric DNA hybrids and telomere maintenance in ALT tumour cells. *Nature Communications*, 5, 5220.  
<https://doi.org/10.1038/ncomms6220>
- Arudchandran, A., Cerritelli, S., Narimatsu, S., Itaya, M., Shin, D. Y., Shimada, Y., & Crouch, R. J. (2000). The absence of ribonuclease H1 or H2 alters the sensitivity of *Saccharomyces cerevisiae* to hydroxyurea, caffeine and ethyl methanesulphonate: implications for roles of RNases H in DNA replication and repair. *Genes to Cells: Devoted to Molecular & Cellular Mechanisms*, 5(10), 789–802. Retrieved from  
<http://www.ncbi.nlm.nih.gov/pubmed/11029655>
- Balk, B., Maicher, A., Dees, M., Klermund, J., Luke-Glaser, S., Bender, K., & Luke, B. (2013). Telomeric RNA-DNA hybrids affect telomere-length dynamics and senescence. *Nat Struct Mol Biol*, 20(10), 1199–1205.  
<https://doi.org/10.1038/nsmb.2662\rnsmb.2662> [pii]
- Ban, C., Ramakrishnan, B., & Sundaralingam, M. (1994). A single 2'-hydroxyl group converts B-DNA to A-DNA. Crystal structure of the DNA-RNA chimeric decamer duplex d(CCGGC)r(G)d(CCGG) with a novel intermolecular G-C base-paired quadruplet. *Journal of Molecular Biology*, 236(1), 275–85. <https://doi.org/10.1006/jmbi.1994.1134>
- Barnes, R. P., Hile, S. E., Lee, M. Y., & Eckert, K. A. (2017). DNA polymerases eta and kappa exchange with the polymerase delta holoenzyme to complete common fragile site synthesis. *DNA Repair*, 57(April), 1–11.  
<https://doi.org/10.1016/j.dnarep.2017.05.006>
- Barnum, K. J., & O'Connell, M. J. (2014). Cell cycle regulation by checkpoints. *Methods in Molecular Biology (Clifton, N.J.)*, 1170, 29–40.  
[https://doi.org/10.1007/978-1-4939-0888-2\\_2](https://doi.org/10.1007/978-1-4939-0888-2_2)
- Beard, W. A., & Wilson, S. H. Structural insights into the origins of DNA polymerase fidelity, 11 *Structure* § (2003). [https://doi.org/10.1016/S0969-2126\(03\)00051-0](https://doi.org/10.1016/S0969-2126(03)00051-0)
- Bebenek, K., & Kunkel, T. A. (2004). Functions of DNA Polymerases. In *Advances in protein chemistry* (Vol. 69, pp. 137–165).  
[https://doi.org/10.1016/S0065-3233\(04\)69005-X](https://doi.org/10.1016/S0065-3233(04)69005-X)
- Bemark, M., Khamlichi, A. A., Davies, S. L., & Neuberger, M. S. (2000). Disruption of mouse polymerase ζ (Rev3) leads to embryonic lethality and impairs blastocyst development in vitro, 10(19).

- [https://doi.org/10.1016/S0960-9822\(00\)00724-7](https://doi.org/10.1016/S0960-9822(00)00724-7)
- Bergoglio, V., Boyer, A.-S., Walsh, E., Naim, V., Legube, G., Lee, M. Y. W. T. W. T., ... Hoffmann, J.-S. (2013). DNA synthesis by Pol  $\eta$  promotes fragile site stability by preventing under-replicated DNA in mitosis. *The Journal of Cell Biology*, 201(3), 395–408. <https://doi.org/10.1083/jcb.201207066>
- Bermejo, R., Lai, M. S., & Foiani, M. (2012). Preventing Replication Stress to Maintain Genome Stability: Resolving Conflicts between Replication and Transcription. *Molecular Cell*, 45(6), 710–718. <https://doi.org/10.1016/j.molcel.2012.03.001>
- Bienko, M., Green, C. M., Crosetto, N., Rudolf, F., Zapart, G., Coull, B., ... Dikic, I. (2005). Ubiquitin-Binding Domains in Y-Family Polymerases Regulate Translesion Synthesis. *Science*, 310(5755), 1821–1824. <https://doi.org/10.1126/science.1120615>
- Biertümpfel, C., Zhao, Y., Kondo, Y., Ramón-Maiques, S., Gregory, M., Lee, J. Y., ... Yang, W. (2010). Structure and mechanism of human DNA polymerase  $\epsilon$ . *Nature*, 465(7301), 1044–1048. <https://doi.org/10.1038/nature09196>
- Bonilla, C. Y., Melo, J. A., & Toczyski, D. P. (2008). Colocalization of Sensors Is Sufficient to Activate the DNA Damage Checkpoint in the Absence of Damage. *Molecular Cell*, 30(3), 267–276. <https://doi.org/10.1016/j.molcel.2008.03.023>
- Boulé, J. B., Rougeon, F., & Papanicolaou, C. (2001). Terminal Deoxynucleotidyl Transferase Indiscriminately Incorporates Ribonucleotides and Deoxyribonucleotides. *Journal of Biological Chemistry*, 276(33), 31388–31393. <https://doi.org/10.1074/jbc.M105272200>
- Branzei, D., & Foiani, M. (2005). The DNA damage response during DNA replication. *Current Opinion in Cell Biology*. <https://doi.org/10.1016/j.ceb.2005.09.003>
- Branzei, D., Vanoli, F., & Foiani, M. (2008). SUMOylation regulates Rad18-mediated template switch. *Nature*, 456(7224), 915–920. <https://doi.org/10.1038/nature07587>
- Broomfield, S., Chow, B. L., & Xiao, W. (1998). MMS2, encoding a ubiquitin-conjugating-enzyme-like protein, is a member of the yeast error-free postreplication repair pathway. *Proceedings of the National Academy of Sciences of the United States of America*, 95(10), 5678–83. Retrieved from <http://www.ncbi.nlm.nih.gov/pubmed/9576943>
- Brown, J. A., Fiala, K. A., Fowler, J. D., Sherrer, S. M., Newmister, S. A., Duym, W. W., & Suo, Z. (2010). A Novel Mechanism of Sugar Selection Utilized by a Human X-Family DNA Polymerase. *Journal of Molecular Biology*, 395(2), 282–290. <https://doi.org/10.1016/j.jmb.2009.11.003>
- Brown, J. A., & Suo, Z. (2011). Unlocking the sugar “steric gate” of DNA polymerases. *Biochemistry*, 50(7), 1135–42. <https://doi.org/10.1021/bi101915z>
- Bubeck, D., Reijns, M. A. M., Graham, S. C., Astell, K. R., Jones, E. Y., & Jackson, A. P. (2011). PCNA directs type 2 RNase H activity on DNA replication and repair substrates. *Nucleic Acids Research*, 39(9), 3652–3666. <https://doi.org/10.1093/nar/gkq980>
- Burgers, P. M. (1991). *Saccharomyces cerevisiae* replication factor C. II.

- Formation and activity of complexes with the proliferating cell nuclear antigen and with DNA polymerases delta and epsilon. *The Journal of Biological Chemistry*, 266(33), 22698–706. Retrieved from <http://www.ncbi.nlm.nih.gov/pubmed/1682322>
- Burgers, P. M. J., & Kunkel, T. A. (2017). Eukaryotic DNA Replication Fork. *Annual Review of Biochemistry*, 86(1), 417–438. <https://doi.org/10.1146/annurev-biochem-061516-044709>
- Byun, T. S., Pacek, M., Yee, M., Walter, J. C., & Cimprich, K. A. (2005). Functional uncoupling of MCM helicase and DNA polymerase activities activates the ATR-dependent checkpoint. *Genes & Development*, 19(9), 1040–52. <https://doi.org/10.1101/gad.1301205>
- Caldecott, K. W. (2007). Mammalian single-strand break repair: mechanisms and links with chromatin. *DNA Repair*, 6(4), 443–53. <https://doi.org/10.1016/j.dnarep.2006.10.006>
- Callebaut, I., & Mornon, J. P. (1997). From BRCA1 to RAP1: A widespread BRCT module closely associated with DNA repair. *FEBS Letters*, 400(1), 25–30. [https://doi.org/10.1016/S0014-5793\(96\)01312-9](https://doi.org/10.1016/S0014-5793(96)01312-9)
- Carthew, R. W., & Sontheimer, E. J. (2009). Origins and Mechanisms of miRNAs and siRNAs. *Cell*, 136(4), 642–55. <https://doi.org/10.1016/j.cell.2009.01.035>
- Castro, C., Smidansky, E., Maksimchuk, K. R., Arnold, J. J., Korneeva, V. S., Gotte, M., ... Cameron, C. E. (2007). Two proton transfers in the transition state for nucleotidyl transfer catalyzed by RNA- and DNA-dependent RNA and DNA polymerases. *Proceedings of the National Academy of Sciences*, 104(11), 4267–4272. <https://doi.org/10.1073/pnas.0608952104>
- Cech, T. R. (2012). The RNA Worlds in Context. *Cold Spring Harbor Perspectives in Biology*, 4(7), a006742–a006742. <https://doi.org/10.1101/cshperspect.a006742>
- Cerritelli, S. M., & Crouch, R. J. (2009). Ribonuclease H: the enzymes in eukaryotes. *The FEBS Journal*, 276(6), 1494–505. <https://doi.org/10.1111/j.1742-4658.2009.06908.x>
- Cerritelli, S. M., Frolova, E. G., Feng, C., Grinberg, A., Love, P. E., & Crouch, R. J. (2003). Failure to produce mitochondrial DNA results in embryonic lethality in Rnaseh1 null mice. *Molecular Cell*, 11(3), 807–815. [https://doi.org/10.1016/S1097-2765\(03\)00088-1](https://doi.org/10.1016/S1097-2765(03)00088-1)
- Chabes, A., Georgieva, B., Domkin, V., Zhao, X., Rothstein, R., & Thelander, L. (2003). Survival of DNA damage in yeast directly depends on increased dNTP levels allowed by relaxed feedback inhibition of ribonucleotide reductase. *Cell*, 112(3), 391–401. [https://doi.org/10.1016/S0092-8674\(03\)00075-8](https://doi.org/10.1016/S0092-8674(03)00075-8)
- Champoux, J. J. (2001). DNA topoisomerases: structure, function, and mechanism. *Annual Review of Biochemistry*, 70, 369–413. <https://doi.org/10.1146/annurev.biochem.70.1.369>
- Chan, Y. A., Aristizabal, M. J., Lu, P. Y. T., Luo, Z., Hamza, A., Kobor, M. S., ... Hieter, P. (2014). Genome-Wide Profiling of Yeast DNA:RNA Hybrid Prone Sites with DRIP-Chip. *PLoS Genetics*, 10(4), e1004288. <https://doi.org/10.1371/journal.pgen.1004288>

- Chang, D. J., & Cimprich, K. A. (2009). DNA damage tolerance: when it's OK to make mistakes. *Nature Chemical Biology*, 5(2), 82–90. <https://doi.org/10.1038/nchembio.139>
- Chargaff, E. (1950). Chemical specificity of nucleic acids and mechanism of their enzymatic degradation. *Experientia*, 6(6), 201–209. <https://doi.org/10.1007/BF02173653>
- Chen, J. Z., Qiu, J., Shen, B., & Holmquist, G. P. (2000). Mutational spectrum analysis of RNase H(35) deficient *Saccharomyces cerevisiae* using fluorescence-based directed termination PCR. *Nucleic Acids Research*, 28(18), 3649–56. <https://doi.org/10.1093/NAR/28.18.3649>
- Chen, T., & Romesberg, F. E. (2014). Directed polymerase evolution. *FEBS Letters*, 588(2), 219–29. <https://doi.org/10.1016/j.febslet.2013.10.040>
- Cheung, H. W., Chun, A. C. S., Wang, Q., Deng, W., Hu, L., Guan, X. Y., ... Wang, X. (2006). Inactivation of human MAD2b in nasopharyngeal carcinoma cells leads to chemosensitization to DNA-damaging agents. *Cancer Research*, 66(8), 4357–4367. <https://doi.org/10.1158/0008-5472.CAN-05-3602>
- Chiapperino, D., Kroth, H., Kramarczuk, I. H., Sayer, J. M., Masutani, C., Hanaoka, F., ... Cheh, A. M. (2002). Preferential misincorporation of purine nucleotides by human DNA polymerase  $\eta$  opposite benzo[a]pyrene 7,8-diol 9,10-epoxide deoxyguanosine adducts. *Journal of Biological Chemistry*, 277(14), 11765–11771. <https://doi.org/10.1074/jbc.M112139200>
- Chilkova, O., Stenlund, P., Isoz, I., Stith, C. M., Grabowski, P., Lundstrom, E.-B., ... Johansson, E. (2007). The eukaryotic leading and lagging strand DNA polymerases are loaded onto primer-ends via separate mechanisms but have comparable processivity in the presence of PCNA. *Nucleic Acids Research*, 35(19), 6588–6597. <https://doi.org/10.1093/nar/gkm741>
- Chiu, H.-C., Koh, K. D., Evich, M., Lesiak, A. L., Germann, M. W., Bongiorno, A., ... Storici, F. (2014). RNA intrusions change DNA elastic properties and structure. *Nanoscale*, 6(17), 10009. <https://doi.org/10.1039/C4NR01794C>
- Cho, J.-E., Kim, N., Li, Y. C., & Jinks-Robertson, S. (2013). Two distinct mechanisms of Topoisomerase 1-dependent mutagenesis in yeast. *DNA Repair*, 12(3), 205–211. <https://doi.org/10.1016/j.dnarep.2012.12.004>
- Cho, J. E., Kim, N., & Jinks-Robertson, S. (2015). Topoisomerase 1-dependent deletions initiated by incision at ribonucleotides are biased to the non-transcribed strand of a highly activated reporter. *Nucleic Acids Research*, 43(19), 9306–9313. <https://doi.org/10.1093/nar/gkv824>
- Chon, H., Vassilev, A., Depamphilis, M. L., Zhao, Y., Zhang, J., Burgers, P. M., ... Cerritelli, S. M. (2009). Contributions of the two accessory subunits, RNASEH2B and RNASEH2C, to the activity and properties of the human RNase H2 complex. *Nucleic Acids Research*, 37(1), 96–110. <https://doi.org/10.1093/nar/gkn913>
- Chou, S. H., Flynn, P., Wang, A., & Reid, B. (1991). High-resolution NMR studies of chimeric DNA-RNA-DNA duplexes, heteronomous base pairing, and continuous base stacking at junctions. *Biochemistry*, 30(21), 5248–5257. <https://doi.org/10.1021/bio0235a019>
- Chu, H., Cifuentes-Rojas, C., Kesner, B., Aeby, E., Lee, H., Wei, C., ... Lee, J. T.

- (2017). TERRA RNA Antagonizes ATRX and Protects Telomeres. *Cell*, 170(1), 86–101.e16. <https://doi.org/10.1016/j.cell.2017.06.017>
- Cilli, P., Minoprio, A., Bossa, C., Bignami, M., & Mazzei, F. (2015). Formation and Repair of Mismatches Containing Ribonucleotides and Oxidized Bases at Repeated DNA Sequences. *The Journal of Biological Chemistry*, 290(43), 26259–69. <https://doi.org/10.1074/jbc.M115.679209>
- Clark, A. B., Lujan, S. A., Kissling, G. E., & Kunkel, T. A. (2011). Mismatch repair-independent tandem repeat sequence instability resulting from ribonucleotide incorporation by DNA polymerase  $\epsilon$ . *DNA Repair*, 10(5), 476–482. <https://doi.org/10.1016/j.dnarep.2011.02.001>
- Clausen, A. R., Lujan, S. A., Burkholder, A. B., Orebaugh, C. D., Williams, J. S., Clausen, M. F., ... Kunkel, T. A. (2015). Tracking replication enzymology in vivo by genome-wide mapping of ribonucleotide incorporation. *Nature Structural & Molecular Biology*, 22(3), 185–91. <https://doi.org/10.1038/nsmb.2957>
- Clausen, A. R., Murray, M. S., Passer, A. R., Pedersen, L. C., & Kunkel, T. A. (2013). Structure-function analysis of ribonucleotide bypass by B family DNA replicases. *Proceedings of the National Academy of Sciences of the United States of America*, 110(42), 16802–7. <https://doi.org/10.1073/pnas.1309119110>
- Clausen, A. R., Zhang, S., Burgers, P. M., Lee, M. Y., & Kunkel, T. A. (2013). Ribonucleotide incorporation, proofreading and bypass by human DNA polymerase  $\delta$ . *DNA Repair*, 12(2), 121–7. <https://doi.org/10.1016/j.dnarep.2012.11.006>
- Cohen-Fix, O., & Koshland, D. (1997). The anaphase inhibitor of *Saccharomyces cerevisiae* Pds1p is a target of the DNA damage checkpoint pathway. *Proc Natl Acad Sci U S A*, 94(26), 14361–14366. <https://doi.org/10.1073/pnas.94.26.14361>
- Collins, K., & Greider, C. W. (1995). Utilization of ribonucleotides and RNA primers by *Tetrahymena* telomerase. *The EMBO Journal*, 14(21), 5422–32. Retrieved from <http://www.ncbi.nlm.nih.gov/pubmed/7489731>
- Compe, E., & Egly, J.-M. (2016). Nucleotide Excision Repair and Transcriptional Regulation: TFIIH and Beyond. *Annual Review of Biochemistry*, 85(1), 265–290. <https://doi.org/10.1146/annurev-biochem-060815-014857>
- Conover, H. N., Lujan, S. A., Chapman, M. J., Cornelio, D. A., Sharif, R., Williams, J. S., ... Argueso, J. L. (2015). Stimulation of Chromosomal Rearrangements by Ribonucleotides. *Genetics*, 201(3), 951–961. <https://doi.org/10.1534/genetics.115.181149>
- Cooper, D. L., Lahue, R. S., & Modrich, P. (1993). Methyl-directed mismatch repair is bidirectional. *Journal of Biological Chemistry*, 268(16), 11823–11829.
- Coutinho, P., & Barbot, C. (1993). *Ataxia with Oculomotor Apraxia Type 1*. *GeneReviews*(®). University of Washington, Seattle. Retrieved from <http://www.ncbi.nlm.nih.gov/pubmed/20301629>
- Crick, F. (1970). Central dogma of molecular biology. *Nature*, 227(5258), 561–3. <https://doi.org/10.1038/227561a0>
- Crick, F. H. C., & Watson, J. D. (1954). The Complementary Structure of Deoxyribonucleic Acid. *Proceedings of the Royal Society A: Mathematical*,

- Physical and Engineering Sciences*, 223(1152), 80–96.  
<https://doi.org/10.1098/rspa.1954.0101>
- Crow, Y. J., Hayward, B. E., Parmar, R., Robins, P., Leitch, A., Ali, M., ... Lindahl, T. (2006). Mutations in the gene encoding the 3′-5′ DNA exonuclease TREX1 cause Aicardi-Goutières syndrome at the AGS1 locus. *Nature Genetics*, 38(8), 917–920. <https://doi.org/10.1038/ng1845>
- Crow, Y. J., Leitch, A., Hayward, B. E., Garner, A., Parmar, R., Griffith, E., ... Jackson, A. P. (2006). Mutations in genes encoding ribonuclease H2 subunits cause Aicardi-Goutières syndrome and mimic congenital viral brain infection. *Nature Genetics*, 38(8), 910–916.  
<https://doi.org/10.1038/ng1842>
- D’Souza, S., & Walker, G. C. (2006). Novel role for the C terminus of *Saccharomyces cerevisiae* Rev1 in mediating protein-protein interactions. *Molecular and Cellular Biology*, 26(21), 8173–82.  
<https://doi.org/10.1128/MCB.00202-06>
- D’Souza, S., Waters, L. S., & Walker, G. C. (2008). Novel conserved motifs in Rev1 C-terminus are required for mutagenic DNA damage tolerance. *DNA Repair*, 7(9), 1455–1470. <https://doi.org/10.1016/j.dnarep.2008.05.009>
- Dahm, R. (2008). Discovering DNA: Friedrich Miescher and the early years of nucleic acid research. *Human Genetics*. <https://doi.org/10.1007/s00439-007-0433-0>
- Daigaku, Y., Keszthelyi, A., Müller, C. A., Miyabe, I., Brooks, T., Retkute, R., ... Carr, A. M. (2015). A global profile of replicative polymerase usage. *Nature Structural & Molecular Biology*, 22(3), 192–8.  
<https://doi.org/10.1038/nsmb.2962>
- Davies, A. A., Huttner, D., Daigaku, Y., Chen, S., & Ulrich, H. D. (2008). Activation of ubiquitin-dependent DNA damage bypass is mediated by replication protein a. *Molecular Cell*, 29(5), 625–36.  
<https://doi.org/10.1016/j.molcel.2007.12.016>
- de Feraudy, S., Limoli, C. L., Giedzinski, E., Karentz, D., Marti, T. M., Feeney, L., & Cleaver, J. E. (2007). Pol eta is required for DNA replication during nucleotide deprivation by hydroxyurea. *Oncogene*, 26(39), 5713–21.  
<https://doi.org/10.1038/sj.onc.1210385>
- DeRose, E. F., Perera, L., Murray, M. S., Kunkel, T. A., & London, R. E. (2012). Solution structure of the Dickerson DNA dodecamer containing a single ribonucleotide. *Biochemistry*, 51(12), 2407–16.  
<https://doi.org/10.1021/bi201710q>
- Dhar, M. K., Sehgal, S., & Kaul, S. (2012). Structure, replication efficiency and fragility of yeast ARS elements. *Research in Microbiology*, 163(4), 243–253.  
<https://doi.org/10.1016/j.resmic.2012.03.003>
- Dickerson, R. E., Drew, H. R., Conner, B. N., Wing, R. M., Fratini, A. V., & Kopka, M. L. (1982). The anatomy of A-, B-, and Z-DNA. *Science*, 216(4545), 475–485. <https://doi.org/10.1126/science.7071593>
- Diffley, J. F. X. (1995). The initiation of DNA replication in the budding yeast cell division cycle. *Yeast*, 11(16), 1651–1670.  
<https://doi.org/10.1002/yea.320111608>
- Dijk, M., Typas, D., Mullenders, L., & Pines, A. (2014). Insight in the multilevel

- regulation of NER. *Experimental Cell Research*, 329(1), 116–123.  
<https://doi.org/10.1016/j.yexcr.2014.08.010>
- Donigan, K. A., Cerritelli, S. M., McDonald, J. P., Vaisman, A., Crouch, R. J., & Woodgate, R. (2015). Unlocking the steric gate of DNA polymerase  $\eta$  leads to increased genomic instability in *Saccharomyces cerevisiae*. *DNA Repair*, 35, 1–12. <https://doi.org/10.1016/j.dnarep.2015.07.002>
- Donigan, K. A., McLenigan, M. P., Yang, W., Goodman, M. F., & Woodgate, R. (2014). The steric gate of DNA polymerase  $\iota$  regulates ribonucleotide incorporation and deoxyribonucleotide fidelity. *The Journal of Biological Chemistry*, 289(13), 9136–45. <https://doi.org/10.1074/jbc.M113.545442>
- Drury, L. S., Perkins, G., & Diffley, J. F. X. (2000). The cyclin-dependent kinase Cdc28p regulates distinct modes of Cdc6p proteolysis during the budding yeast cell cycle. *Current Biology*, 10(5), 231–240.  
[https://doi.org/10.1016/S0960-9822\(00\)00355-9](https://doi.org/10.1016/S0960-9822(00)00355-9)
- Durando, M., Tateishi, S., & Vaziri, C. (2013). A non-catalytic role of DNA polymerase  $\eta$  in recruiting Rad18 and promoting PCNA monoubiquitination at stalled replication forks. *Nucleic Acids Research*, 41(5), 3079–93. <https://doi.org/10.1093/nar/gkto16>
- Eder, P. S., Walder, R. Y., & Walder, J. A. (1993). Substrate specificity of human RNase H1 and its role in excision repair of ribose residues misincorporated in DNA. *Biochimie*, 75(1–2), 123–126. [https://doi.org/10.1016/0300-9084\(93\)90033-O](https://doi.org/10.1016/0300-9084(93)90033-O)
- Egli, M., Usman, N., & Rich, A. (1993). Conformational influence of the ribose 2'-hydroxyl group: Crystal structures of DNA-RNA chimeric duplexes. *Biochemistry*, 32(13), 3221–3237. <https://doi.org/10.1021/bi00064a004>
- El Hage, A., French, S. L., Beyer, A. L., & Tollervey, D. (2010). Loss of Topoisomerase I leads to R-loop-mediated transcriptional blocks during ribosomal RNA synthesis. *Genes & Development*, 24(14), 1546–58.  
<https://doi.org/10.1101/gad.573310>
- El Hage, A., Webb, S., Kerr, A., Tollervey, D., & Andujar, E. (2014). Genome-Wide Distribution of RNA-DNA Hybrids Identifies RNase H Targets in tRNA Genes, Retrotransposons and Mitochondria. *PLoS Genetics*, 10(10), e1004716. <https://doi.org/10.1371/journal.pgen.1004716>
- Esposito, G., Godin†, I., Klein, U., Yaspo, M.-L., Cumano, A., & Rajewsky, K. (2000). Disruption of the Rev3l-encoded catalytic subunit of polymerase  $\zeta$  in mice results in early embryonic lethality. *Current Biology*, 10(19), 1221–1224. [https://doi.org/10.1016/S0960-9822\(00\)00726-0](https://doi.org/10.1016/S0960-9822(00)00726-0)
- Essers, J., Theil, A. F., Baldeyron, C., van Cappellen, W. A., Houtsmuller, A. B., Kanaar, R., & Vermeulen, W. (2005). Nuclear dynamics of PCNA in DNA replication and repair. *Mol Cell Biol*, 25(21), 9350–9359.  
<https://doi.org/10.1128/MCB.25.21.9350-9359.2005>
- Faili, A., Aoufouchi, S., Weller, S., Vuillier, F., Stary, A., Sarasin, A., ... Weill, J.-C. (2004). DNA Polymerase  $\eta$  Is Involved in Hypermutation Occurring during Immunoglobulin Class Switch Recombination. *The Journal of Experimental Medicine*, 199(2), 265–270.  
<https://doi.org/10.1084/jem.20031831>
- Feng, W. (2016). Mec1/ATR, the Program Manager of Nucleic Acids Inc. *Genes*,

- 8(1), 10. <https://doi.org/10.3390/genes8010010>
- Figiel, M., Chon, H., Cerritelli, S. M., Cybulska, M., Crouch, R. J., & Nowotny, M. (2011). The structural and biochemical characterization of human RNase H2 complex reveals the molecular basis for substrate recognition and Aicardi-Goutières syndrome defects. *The Journal of Biological Chemistry*, 286(12), 10540–10550. <https://doi.org/10.1074/jbc.M110.181974>
- Fortune, J. M., Pavlov, Y. I., Welch, C. M., Johansson, E., Burgers, P. M. J., & Kunkel, T. A. (2005). *Saccharomyces cerevisiae* DNA Polymerase  $\delta$ : High fidelity for base substitutions but lower fidelity for single- and multi-base deletions. *Journal of Biological Chemistry*, 280(33), 29980–29987. <https://doi.org/10.1074/jbc.M505236200>
- Freudenthal, B. D., Gakhar, L., Ramaswamy, S., & Washington, M. T. (2010). Structure of monoubiquitinated PCNA and implications for translesion synthesis and DNA polymerase exchange. *Nature Structural & Molecular Biology*, 17(4), 479–84. <https://doi.org/10.1038/nsmb.1776>
- Gali, H., Juhasz, S., Morocz, M., Hajdu, I., Fatyol, K., Szukacsov, V., ... Haracska, L. (2012). Role of SUMO modification of human PCNA at stalled replication fork. *Nucleic Acids Research*, 40(13), 6049–59. <https://doi.org/10.1093/nar/gks256>
- Gangavarapu, V., Prakash, S., & Prakash, L. (2007). Requirement of RAD52 group genes for postreplication repair of UV-damaged DNA in *Saccharomyces cerevisiae*. *Molecular and Cellular Biology*, 27(21), 7758–64. <https://doi.org/10.1128/MCB.01331-07>
- Gao, G., Orlova, M., Georgiadis, M. M., Hendrickson, W. A., & Goff, S. P. (1997). Conferring RNA polymerase activity to a DNA polymerase: a single residue in reverse transcriptase controls substrate selection. *Proceedings of the National Academy of Sciences of the United States of America*, 94(2), 407–11. Retrieved from <http://www.ncbi.nlm.nih.gov/pubmed/9012795>
- Gao, R., Schellenberg, M. J., Huang, S.-Y. N., Abdelmalak, M., Marchand, C., Nitiss, K. C., ... Pommier, Y. (2014). Proteolytic degradation of topoisomerase II (Top2) enables the processing of Top2-DNA and Top2-RNA covalent complexes by tyrosyl-DNA-phosphodiesterase 2 (TDP2). *The Journal of Biological Chemistry*, 289(26), 17960–9. <https://doi.org/10.1074/jbc.M114.565374>
- Gao, Y., Mutter-Rottmayer, E., Zlatanou, A., Vaziri, C., & Yang, Y. (2017). Mechanisms of Post-Replication DNA Repair. *Genes*, 8(2). <https://doi.org/10.3390/genes8020064>
- Garcia-Diaz, M., & Kunkel, T. A. (2006). Mechanism of a genetic glissando\*: structural biology of indel mutations. *Trends in Biochemical Sciences*, 31(4), 206–214. <https://doi.org/10.1016/j.tibs.2006.02.004>
- García-Gómez, S., Reyes, A., Martínez-Jiménez, M. I., Chocrón, E. S., Mourón, S., Terrados, G., ... Blanco, L. (2013). PrimPol, an archaic primase/polymerase operating in human cells. *Molecular Cell*, 52(4), 541–53. <https://doi.org/10.1016/j.molcel.2013.09.025>
- Garg, P., Stith, C. M., Sabouri, N., Johansson, E., & Burgers, P. M. (2004). Idling by DNA polymerase  $\delta$  maintains a ligatable nick during lagging-strand DNA replication. *Genes and Development*, 18(22), 2764–2773.

- <https://doi.org/10.1101/gad.1252304>
- Gerlach, V. L., Aravind, L., Gotway, G., Schultz, R. A., Koonin, E. V., & Friedberg, E. C. (1999). Human and mouse homologs of *Escherichia coli* DinB (DNA polymerase IV), members of the UmuC/DinB superfamily. *Proceedings of the National Academy of Sciences of the United States of America*, 96(21), 11922–7. Retrieved from <http://www.ncbi.nlm.nih.gov/pubmed/10518552>
- Ghodgaonkar, M. M. M., Lazzaro, F., Olivera-Pimentel, M., Artola-Borán, M., Cejka, P., Reijns, M. A. A., ... Jiricny, J. (2013). Ribonucleotides Misincorporated into DNA Act as Strand-Discrimination Signals in Eukaryotic Mismatch Repair. *Molecular Cell*, 50(3), 323–32. <https://doi.org/10.1016/j.molcel.2013.03.019>
- Ghosal, G., & Chen, J. (2013). DNA damage tolerance: a double-edged sword guarding the genome. *Translational Cancer Research*, 2(3), 107–129. <https://doi.org/10.3978/j.issn.2218-676X.2013.04.01>
- Giannattasio, M., Lazzaro, F., Longhese, M. P., Plevani, P., & Muzi-Falconi, M. (2004). Physical and functional interactions between nucleotide excision repair and DNA damage checkpoint. *Embo J*, 23(2), 429–438. <https://doi.org/10.1038/sj.emboj.7600051>
- Giannattasio, M., Zwicky, K., Follonier, C., Foiani, M., Lopes, M., & Branzei, D. (2014). Visualization of recombination-mediated damage bypass by template switching. *Nature Structural & Molecular Biology*, 21(10), 884–92. <https://doi.org/10.1038/nsmb.2888>
- Gibbs, P. E. M., Borden, A., & Lawrence, C. W. (1995). The T-T pyrimidine (6–4) pyrimidinone UV photoproduct is much less mutagenic in yeast than in *Escherichia coli*. *Nucleic Acids Research*, 23(11), 1919–1922. <https://doi.org/10.1093/nar/23.11.1919>
- Gibbs, P. E., McGregor, W. G., Maher, V. M., Nisson, P., & Lawrence, C. W. (1998). A human homolog of the *Saccharomyces cerevisiae* REV3 gene, which encodes the catalytic subunit of DNA polymerase zeta. *Proceedings of the National Academy of Sciences of the United States of America*, 95(June), 6876–6880. <https://doi.org/10.1073/pnas.95.12.6876>
- Gibbs, P. E., Wang, X. D., Li, Z., McManus, T. P., McGregor, W. G., Lawrence, C. W., & Maher, V. M. (2000). The function of the human homolog of *Saccharomyces cerevisiae* REV1 is required for mutagenesis induced by UV light. *Proceedings of the National Academy of Sciences of the United States of America*, 97(8), 4186–91. <https://doi.org/10.1073/PNAS.97.8.4186>
- Gilbert, W. (1986). Origin of life: The RNA world. *Nature*, 319(6055), 618–618. <https://doi.org/10.1038/319618a0>
- Ginno, P. A., Lott, P. L., Christensen, H. C., Korf, I., & Chédin, F. (2012). R-loop formation is a distinctive characteristic of unmethylated human CpG island promoters. *Molecular Cell*, 45(6), 814–25. <https://doi.org/10.1016/j.molcel.2012.01.017>
- Göhler, T., Sabbioneda, S., Green, C. M., & Lehmann, A. R. (2011). ATR-mediated phosphorylation of DNA polymerase  $\eta$  is needed for efficient recovery from UV damage. *Journal of Cell Biology*, 192(2), 219–227. <https://doi.org/10.1083/jcb.201008076>
- Göksenin, A. Y., Zahurancik, W., LeCompte, K. G., Taggart, D. J., Suo, Z., &

- Pursell, Z. F. (2012). Human DNA polymerase  $\epsilon$  is able to efficiently extend from multiple consecutive ribonucleotides. *Journal of Biological Chemistry*, 287(51), 42675–42684. <https://doi.org/10.1074/jbc.M112.422733>
- Gómez-Herreros, F., Romero-Granados, R., Zeng, Z., Álvarez-Quilón, A., Quintero, C., Ju, L., ... Cortés-Ledesma, F. (2013). TDP2-Dependent Non-Homologous End-Joining Protects against Topoisomerase II-Induced DNA Breaks and Genome Instability in Cells and In Vivo. *PLoS Genetics*, 9(3). <https://doi.org/10.1371/journal.pgen.1003226>
- Goodman, M. F. (1997). Hydrogen bonding revisited: geometric selection as a principal determinant of DNA replication fidelity. *Proceedings of the National Academy of Sciences of the United States of America*, 94(20), 10493–5. Retrieved from <http://www.ncbi.nlm.nih.gov/pubmed/9380666>
- Goodman, M. F., Creighton, S., Bloom, L. B., Petruska, J., & Kunkel, T. A. (1993). Biochemical Basis of DNA Replication Fidelity. *Critical Reviews in Biochemistry and Molecular Biology*, 28(2), 83–126. <https://doi.org/10.3109/10409239309086792>
- Graf, M., Bonetti, D., Lockhart, A., Serhal, K., Kellner, V., Maicher, A., ... Luke, B. (2017). Telomere Length Determines TERRA and R-Loop Regulation through the Cell Cycle. *Cell*, 170(1), 72–85.e14. <https://doi.org/10.1016/j.cell.2017.06.006>
- Gratchev, A., Strein, P., Utikal, J., & Sergij, G. (2003). Molecular genetics of Xeroderma pigmentosum variant. *Experimental Dermatology*, 12(5), 529–36. Retrieved from <http://www.ncbi.nlm.nih.gov/pubmed/14705792>
- Gueranger, Q., Stary, A., Aoufouchi, S., Faili, A., Sarasin, A., Reynaud, C.-A., & Weill, J.-C. (2008). Role of DNA polymerases  $\eta$ ,  $\iota$  and  $\zeta$  in UV resistance and UV-induced mutagenesis in a human cell line. *DNA Repair*, 7(9), 1551–1562. <https://doi.org/10.1016/j.dnarep.2008.05.012>
- Gueven, N., Becherel, O. J., Kijas, A. W., Chen, P., Howe, O., Rudolph, J. H., ... Lavin, M. F. (2004). Aprataxin, a novel protein that protects against genotoxic stress. *Human Molecular Genetics*, 13(10), 1081–1093. <https://doi.org/10.1093/hmg/ddh122>
- Gulbis, J. M., Kelman, Z., Hurwitz, J., O'Donnell, M., & Kuriyan, J. (1996). Structure of the C-terminal region of p21(WAF1/CIP1) complexed with human PCNA. *Cell*, 87(2), 297–306. Retrieved from <http://www.ncbi.nlm.nih.gov/pubmed/8861913>
- Günther, C., Kind, B., Reijns, M. A. M., Berndt, N., Martinez-Bueno, M., Wolf, C., ... Lee-Kirsch, M. A. (2015). Defective removal of ribonucleotides from DNA promotes systemic autoimmunity. *Journal of Clinical Investigation*, 125(1), 413–424. <https://doi.org/10.1172/JCI78001>
- Guo, C. (2003). Mouse Rev1 protein interacts with multiple DNA polymerases involved in translesion DNA synthesis. *The EMBO Journal*, 22(24), 6621–6630. <https://doi.org/10.1093/emboj/cdg626>
- Guo, C., Sonoda, E., Tang, T. S., Parker, J. L., Bielen, A. B., Takeda, S., ... Friedberg, E. C. (2006). REV1 Protein Interacts with PCNA: Significance of the REV1 BRCT Domain In Vitro and In Vivo. *Molecular Cell*, 23(2), 265–271. <https://doi.org/10.1016/j.molcel.2006.05.038>
- Guo, C., Tang, T.-S., Bienko, M., Parker, J. L., Bielen, A. B., Sonoda, E., ...

- Friedberg, E. C. (2006). Ubiquitin-Binding Motifs in Rev1 Protein Are Required for Its Role in the Tolerance of DNA Damage. *Molecular and Cellular Biology*, 26(23), 8892–8900. <https://doi.org/10.1128/MCB.01118-06>
- Guo, C., Tang, T. S., Bienko, M., Dikic, I., & Friedberg, E. C. (2008). Requirements for the interaction of mouse Polk with ubiquitin and its biological significance. *Journal of Biological Chemistry*, 283(8), 4658–4664. <https://doi.org/10.1074/jbc.M709275200>
- Guo, D., Xie, Z., Shen, H., Zhao, B., & Wang, Z. (2004). Translesion synthesis of acetylaminofluorene-dG adducts by DNA polymerase  $\zeta$  is stimulated by yeast Rev1 protein. *Nucleic Acids Research*, 32(3), 1122–1130. <https://doi.org/10.1093/nar/gkh279>
- Haracska, L., Johnson, R. E., Unk, I., Phillips, B. B., Hurwitz, J., Prakash, L., & Prakash, S. (2001). Targeting of human DNA polymerase iota to the replication machinery via interaction with PCNA. *Proceedings of the National Academy of Sciences of the United States of America*, 98(25), 14256–61. <https://doi.org/10.1073/pnas.261560798>
- Haracska, L., Johnson, R. E., Unk, I., Phillips, B., Hurwitz, J., Prakash, L., & Prakash, S. (2001). Physical and functional interactions of human DNA polymerase eta with PCNA. *Mol Cell Biol*, 21(21), 7199–7206. <https://doi.org/10.1128/MCB.21.21.7199-7206.2001>
- Haracska, L., Kondratick, C. M., Unk, I., Prakash, S., & Prakash, L. (2001). Interaction with PCNA Is Essential for Yeast DNA Polymerase  $\eta$  Function. *Molecular Cell*, 8(2), 407–415. [https://doi.org/10.1016/S1097-2765\(01\)00319-7](https://doi.org/10.1016/S1097-2765(01)00319-7)
- Haracska, L., Prakash, L., & Prakash, S. (2002a). Role of human DNA polymerase kappa as an extender in translesion synthesis. *Proceedings of the National Academy of Sciences of the United States of America*, 99(25), 16000–5. <https://doi.org/10.1073/pnas.252524999>
- Haracska, L., Prakash, S., & Prakash, L. (2000). Replication past O(6)-methylguanine by yeast and human DNA polymerase eta. *Molecular and Cellular Biology*, 20(21), 8001–7. <https://doi.org/10.1128/MCB.20.21.8001-8007.2000>
- Haracska, L., Prakash, S., & Prakash, L. (2002b). Yeast Rev1 Protein Is a G Template-specific DNA Polymerase. *Journal of Biological Chemistry*, 277(18), 15546–15551. <https://doi.org/10.1074/jbc.M112146200>
- Haracska, L., Prakash, S., & Prakash, L. (2003). Yeast DNA polymerase zeta is an efficient extender of primer ends opposite from 7,8-dihydro-8-Oxoguanine and O6-methylguanine. *Molecular and Cellular Biology*, 23(4), 1453–9. <https://doi.org/10.1128/MCB.23.4.1453-1459.2003>
- Haracska, L., Torres-Ramos, C. A., Johnson, R. E., Prakash, S., & Prakash, L. (2004). Opposing effects of ubiquitin conjugation and SUMO modification of PCNA on replicational bypass of DNA lesions in *Saccharomyces cerevisiae*. *Molecular and Cellular Biology*, 24(10), 4267–74. <https://doi.org/10.1128/mcb.24.10.4267-4274.2004>
- Haracska, L., Unk, I., Johnson, R. E., Johansson, E., Burgers, P. M., Prakash, S., & Prakash, L. (2001). Roles of yeast DNA polymerases delta and zeta and of Rev1 in the bypass of abasic sites. *Genes & Development*, 15(8), 945–54. <https://doi.org/10.1101/gad.882301>

- Haracska, L., Unk, I., Johnson, R. E., Phillips, B. B., Hurwitz, J., Prakash, L., & Prakash, S. (2002). Stimulation of DNA synthesis activity of human DNA polymerase kappa by PCNA. *Molecular and Cellular Biology*, 22(3), 784–91. Retrieved from <http://www.ncbi.nlm.nih.gov/pubmed/11784855>
- Haracska, L., Washington, M. T., Prakash, S., & Prakash, L. (2001). Inefficient Bypass of an Abasic Site by DNA Polymerase  $\eta$ . *Journal of Biological Chemistry*, 276(9), 6861–6866. <https://doi.org/10.1074/jbc.M008021200>
- Harris, J. L., Jakob, B., Taucher-Scholz, G., Dianov, G. L., Becherel, O. J., & Lavin, M. F. (2009). Aprataxin, poly-ADP ribose polymerase 1 (PARP-1) and apurinic endonuclease 1 (APE1) function together to protect the genome against oxidative damage. *Human Molecular Genetics*, 18(21), 4102–4117. <https://doi.org/10.1093/hmg/ddp359>
- Harrison, J. C., & Haber, J. E. (2006). Surviving the Breakup: The DNA Damage Checkpoint. *Annual Review of Genetics*, 40(1), 209–235. <https://doi.org/10.1146/annurev.genet.40.051206.105231>
- Hartwell, L. H. (1974). *Saccharomyces cerevisiae* Cell Cycle. *BACTERIOLOGICAL REVIEWS*, 38(2), 164–198. Retrieved from <https://www.ncbi.nlm.nih.gov/pmc/articles/PMC413849/pdf/bactrev00045-0058.pdf>
- Hartwell, L. H., & Weinert, T. A. (1989). Checkpoints: controls that ensure the order of cell cycle events. *Science*, 246(4930), 629–634. <https://doi.org/10.1126/science.2683079>
- Hedglin, M., Pandey, B., & Benkovic, S. J. (2016). Characterization of human translesion DNA synthesis across a UV-induced DNA lesion. *eLife*, 5. <https://doi.org/10.7554/eLife.19788>
- Hegde, M. L., Hazra, T. K., & Mitra, S. (2008). Early steps in the DNA base excision/single-strand interruption repair pathway in mammalian cells. *Cell Research*, 18(1), 27–47. <https://doi.org/10.1038/cr.2008.8>
- Heider, M. R., Burkhart, B. W., Santangelo, T. J., & Gardner, A. F. (2017). Defining the RNaseH2 enzyme-initiated ribonucleotide excision repair pathway in Archaea. *Journal of Biological Chemistry*, 292(21), 8835–8845. <https://doi.org/10.1074/jbc.M117.783472>
- Herrick, J., & Sclavi, B. (2007). Ribonucleotide reductase and the regulation of DNA replication: an old story and an ancient heritage. *Molecular Microbiology*, 63(1), 22–34. <https://doi.org/10.1111/j.1365-2958.2006.05493.x>
- Hiller, B., Achleitner, M., Glage, S., Naumann, R., Behrendt, R., & Roers, A. (2012). Mammalian RNase H2 removes ribonucleotides from DNA to maintain genome integrity. *The Journal of Experimental Medicine*, 209(8), 1419–26. <https://doi.org/10.1084/jem.20120876>
- Hoege, C., Pfander, B., Moldovan, G.-L., Pyrowolakis, G., & Jentsch, S. (2002). RAD6-dependent DNA repair is linked to modification of PCNA by ubiquitin and SUMO. *Nature*, 419(6903), 135–141. <https://doi.org/10.1038/nature00991>
- Hoeijmakers, J. H. (1993). Nucleotide excision repair I: from E. coli to yeast. *Trends in Genetics : TIG*, 9(5), 173–7. Retrieved from <http://www.ncbi.nlm.nih.gov/pubmed/8337754>
- Hoeijmakers, J. H. J. (2001). Genome maintenance mechanisms for preventing

- cancer. *Nature*, 411(6835), 366–374. <https://doi.org/10.1038/35077232>
- Hofmann, R. M., & Pickart, C. M. (1999). Noncanonical MMS2-encoded ubiquitin-conjugating enzyme functions in assembly of novel polyubiquitin chains for DNA repair. *Cell*, 96(5), 645–53. Retrieved from <http://www.ncbi.nlm.nih.gov/pubmed/10089880>
- Huang, S.-Y. N., Ghosh, S., & Pommier, Y. (2015). Topoisomerase I alone is sufficient to produce short DNA deletions and can also reverse nicks at ribonucleotide sites. *The Journal of Biological Chemistry*, 290(22), 14068–76. <https://doi.org/10.1074/jbc.M115.653345>
- Huang, S.-Y. N., Williams, J. S., Arana, M. E., Kunkel, T. A., & Pommier, Y. (2016). Topoisomerase I-mediated cleavage at unrepaired ribonucleotides generates DNA double-strand breaks. *The EMBO Journal*, e201592426. <https://doi.org/10.15252/emj.201592426>
- Huertas, P. (2010). DNA resection in eukaryotes: deciding how to fix the break. *Nature Structural & Molecular Biology*, 17(1), 11–16. <https://doi.org/10.1038/nsmb.1710>
- Huttner, D., & Ulrich, H. D. (2008). Cooperation of replication Protein A with the ubiquitin ligase Rad18 in DNA damage bypass. *Cell Cycle*, 7(23), 3629–3633. <https://doi.org/10.4161/cc.7.23.7166>
- Jäger, J., & Pata, J. D. (1999). Getting a grip: polymerases and their substrate complexes. *Current Opinion in Structural Biology*, 9(1), 21–8. Retrieved from <http://www.ncbi.nlm.nih.gov/pubmed/10047577>
- Jaishree, T. N., van der Marel, G. A., van Boom, J. H., & Wang, A. H. (1993). Structural influence of RNA incorporation in DNA: quantitative nuclear magnetic resonance refinement of d(CG)r(CG)d(CG) and d(CG)r(C)d(TAGCG). *Biochemistry*, 32(18), 4903–11. Retrieved from <http://www.ncbi.nlm.nih.gov/pubmed/7683912>
- Jansen, J. G., Tsaalbi-Shtylik, A., Langerak, P., Calléja, F., Meijers, C. M., Jacobs, H., & de Wind, N. (2005). The BRCT domain of mammalian Rev1 is involved in regulating DNA translesion synthesis. *Nucleic Acids Research*, 33(1), 356–365. <https://doi.org/10.1093/nar/gki189>
- Jeong, H. S., Backlund, P. S., Chen, H. C., Karavanov, A. A., & Crouch, R. J. (2004). RNase H2 of *Saccharomyces cerevisiae* is a complex of three proteins. *Nucleic Acids Research*, 32(2), 407–414. <https://doi.org/10.1093/nar/gkh209>
- Jinks-Robertson, S., & Klein, H. L. (2015). Ribonucleotides in DNA: hidden in plain sight. *Nature Structural & Molecular Biology*, 22(3), 176–8. <https://doi.org/10.1038/nsmb.2981>
- Johnson, A., & O'Donnell, M. (2005). CELLULAR DNA REPLICASES: Components and Dynamics at the Replication Fork. *Annual Review of Biochemistry*, 74(1), 283–315. <https://doi.org/10.1146/annurev.biochem.73.011303.073859>
- Johnson, R. E., Kondratick, C. M., Prakash, S., & Prakash, L. (1999). hRAD30 mutations in the variant form of xeroderma pigmentosum. *Science (New York, N.Y.)*, 285(5425), 263–5. <https://doi.org/10.1126/science.285.5425.263>
- Johnson, R. E., Prakash, S., & Prakash, L. (1999). Efficient bypass of a thymine-thymine dimer by yeast DNA polymerase, Poleta. *Science*, 283(5404), 1001–

1004. <https://doi.org/10.1126/science.283.5404.1001>
- Johnson, R. E., Torres-Ramos, C. A., Izumi, T., Mitra, S., Prakash, S., & Prakash, L. (1998). Identification of APN<sub>2</sub>, the *Saccharomyces cerevisiae* homolog of the major human AP endonuclease HAP<sub>1</sub>, and its role in the repair of abasic sites. *Genes & Development*, *12*(19), 3137–3143. <https://doi.org/10.1101/gad.12.19.3137>
- Johnson, R. E., Washington, M. T., Haracska, L., Prakash, S., & Prakash, L. (2000). Eukaryotic polymerases iota and zeta act sequentially to bypass DNA lesions. *Nature*, *406*(6799), 1015–1019. <https://doi.org/10.1038/35023030>
- Johnson, S. J., & Beese, L. S. (2004). Structures of mismatch replication errors observed in a DNA polymerase. *Cell*, *116*(6), 803–16. Retrieved from <http://www.ncbi.nlm.nih.gov/pubmed/15035983>
- Joyce, C. M. (1997). Choosing the right sugar: how polymerases select a nucleotide substrate. *Proceedings of the National Academy of Sciences of the United States of America*, *94*(5), 1619–22. <https://doi.org/10.1073/pnas.94.5.1619>
- Jung, Y., Hakem, A., Hakem, R., & Chen, X. (2011). Pirh2 e3 ubiquitin ligase monoubiquitinates DNA polymerase eta to suppress translesion DNA synthesis. *Molecular and Cellular Biology*, *31*(19), 3997–4006. <https://doi.org/10.1128/MCB.05808-11>
- Kannouche, P., Broughton, B. C., Volker, M., Hanaoka, F., Mullenders, L. H., & Lehmann, A. R. (2001). Domain structure, localization, and function of DNA polymerase eta, defective in xeroderma pigmentosum variant cells. *Genes & Development*, *15*(2), 158–72. <https://doi.org/10.1101/GAD.187501>
- Kannouche, P. L., & Lehmann, A. R. (2004). Ubiquitination of PCNA and the polymerase switch in human cells. *Cell Cycle (Georgetown, Tex.)*, *3*(8), 1011–3. Retrieved from <http://www.ncbi.nlm.nih.gov/pubmed/15280666>
- Kannouche, P. L., Wing, J., & Lehmann, A. R. (2004). Interaction of human DNA polymerase eta with monoubiquitinated PCNA: a possible mechanism for the polymerase switch in response to DNA damage. *Molecular Cell*, *14*(4), 491–500. Retrieved from <http://www.ncbi.nlm.nih.gov/pubmed/15149598>
- Kasiviswanathan, R., & Copeland, W. C. (2011). Ribonucleotide Discrimination and Reverse Transcription by the Human Mitochondrial DNA Polymerase. *Journal of Biological Chemistry*, *286*(36), 31490–31500. <https://doi.org/10.1074/jbc.M111.252460>
- Kawamoto, T., Araki, K., Sonoda, E., Yamashita, Y. M., Harada, K., Kikuchi, K., ... Takeda, S. (2005). Dual Roles for DNA Polymerase η in Homologous DNA Recombination and Translesion DNA Synthesis. *Molecular Cell*, *20*(5), 793–799. <https://doi.org/10.1016/j.molcel.2005.10.016>
- Kim, N., Cho, J. E., Li, Y. C., & Jinks-Robertson, S. (2013). RNA:DNA Hybrids Initiate Quasi-Palindrome-Associated Mutations in Highly Transcribed Yeast DNA. *PLoS Genetics*, *9*(11). <https://doi.org/10.1371/journal.pgen.1003924>
- Kim, N., Huang, S. N. S., -y. N., Williams, J. S., Li, Y. C., Clark, A. B., Cho, J.-E. J., ... Jinks-Robertson, S. (2011). Mutagenic processing of ribonucleotides in

- DNA by yeast topoisomerase I. *Science (New York, N.Y.)*, 332(6037), 1561–4.  
<https://doi.org/10.1126/science.1205016>
- Kind, B., Muster, B., Staroske, W., Herce, H. D., Sachse, R., Rapp, A., ... Lee-Kirsch, M. A. (2014). Altered spatio-temporal dynamics of RNase H2 complex assembly at replication and repair sites in Aicardi-Goutières syndrome. *Human Molecular Genetics*, 23(22), 5950–5960.  
<https://doi.org/10.1093/hmg/ddu319>
- Koh, K. D., Balachander, S., Hesselberth, J. R., & Storici, F. (2015). Ribose-seq: global mapping of ribonucleotides embedded in genomic DNA. *Nature Methods*, 12(3), 251–7, 3 p following 257. <https://doi.org/10.1038/nmeth.3259>
- Kolodner, R. D., & Marsischky, G. T. (1999). Eukaryotic DNA mismatch repair. *Current Opinion in Genetics & Development*, 9(1), 89–96. Retrieved from <http://www.ncbi.nlm.nih.gov/pubmed/10072354>
- Kool, E. T. (2002). Active site tightness and substrate fit in DNA replication. *Annual Review of Biochemistry*, 71, 191–219.  
<https://doi.org/10.1146/annurev.biochem.71.110601.135453>
- Kornberg, R. D. (1974). Chromatin Structure: A Repeating Unit of Histones and DNA. *Science*, 184(4139), 868–871.  
<https://doi.org/10.1126/science.184.4139.868>
- Kosarek, J. N., Woodruff, R. V., Rivera-Begeman, A., Guo, C., D'Souza, S., Koonin, E. V., ... Friedberg, E. C. (2008). Comparative analysis of in vivo interactions between Rev1 protein and other Y-family DNA polymerases in animals and yeasts. *DNA Repair*, 7(3), 439–451.  
<https://doi.org/10.1016/j.dnarep.2007.11.016>
- Krejci, L., Van Komen, S., Li, Y., Villemain, J., Reddy, M. S., Klein, H., ... Sung, P. (2003). DNA helicase Srs2 disrupts the Rad51 presynaptic filament. *Nature*, 423(6937), 305–309. <https://doi.org/10.1038/nature01577>
- Krijger, P. H. L., Lee, K.-Y., Wit, N., van den Berk, P. C. M., Wu, X., Roest, H. P., ... Jacobs, H. (2011). HLTF and SHPRH are not essential for PCNA polyubiquitination, survival and somatic hypermutation: existence of an alternative E3 ligase. *DNA Repair*, 10(4), 438–44.  
<https://doi.org/10.1016/j.dnarep.2010.12.008>
- Kuchta, R. D., & Stengel, G. (2010). Mechanism and evolution of DNA primases. *Biochimica et Biophysica Acta (BBA) - Proteins and Proteomics*, 1804(5), 1180–1189. <https://doi.org/10.1016/j.bbapap.2009.06.011>
- Kunkel, T. A. (2004). DNA replication fidelity. *The Journal of Biological Chemistry*, 279(17), 16895–8. <https://doi.org/10.1074/jbc.R400006200>
- Kunkel, T. A., & Bebenek, K. (2000). DNA Replication Fidelity. *Annual Review of Biochemistry*, 1–5. <https://doi.org/10.1146/annurev.biochem.69.1.497>
- Kunkel, T. A., & Burgers, P. M. (2008). Dividing the workload at a eukaryotic replication fork. *Trends in Cell Biology*, 18(11), 521–7.  
<https://doi.org/10.1016/j.tcb.2008.08.005>
- Kunkel, T. A., & Erie, D. A. (2005). DNA mismatch repair. *Annual Review of Biochemistry*, 74(1), 681–710.  
<https://doi.org/10.1146/annurev.biochem.74.082803.133243>
- Kunkel, T. A., Hamatake, R. K., Motto-Fox, J., Fitzgerald, M. P., & Sugino, A. (1989). Fidelity of DNA polymerase I and the DNA polymerase I-DNA

- primase complex from *Saccharomyces cerevisiae*. *Molecular and Cellular Biology*, 9(10), 4447–58. Retrieved from <http://www.ncbi.nlm.nih.gov/pubmed/2555694>
- Kusumoto, R., Masutani, C., Iwai, S., & Hanaoka, F. (2002). Translesion synthesis by human DNA polymerase  $\eta$  across thymine glycol lesions. *Biochemistry*, 41(19), 6090–6099. <https://doi.org/10.1021/Bio25549k>
- Kusumoto, R., Masutani, C., Shimmyo, S., Iwai, S., & Hanaoka, F. (2004). DNA binding properties of human DNA polymerase  $\eta$ : implications for fidelity and polymerase switching of translesion synthesis. *Genes to Cells*, 9(12), 1139–1150. <https://doi.org/10.1111/j.1365-2443.2004.00797.x>
- Larimer, F. W., Perry, J. R., & Hardigree, A. A. (1989). The REV1 gene of *Saccharomyces cerevisiae*: isolation, sequence, and functional analysis. *Journal of Bacteriology*, 171(1), 230–237.
- Larralde, R., Robertson, M. P., & Miller, S. L. (1995). Rates of decomposition of ribose and other sugars: implications for chemical evolution. *Proceedings of the National Academy of Sciences of the United States of America*, 92(18), 8158–8160. <https://doi.org/10.1073/pnas.92.18.8158>
- Lawrence, C. W. (2004). Cellular Functions of DNA Polymerase  $\zeta$  and Rev1 Protein (pp. 167–203). [https://doi.org/10.1016/S0065-3233\(04\)69006-1](https://doi.org/10.1016/S0065-3233(04)69006-1)
- Lawrence, C. W., & Christensen, R. B. (1978). Ultraviolet-induced reversion of *cyc1* alleles in radiation-sensitive strains of yeast. *Journal of Molecular Biology*, 122(1), 1–21. [https://doi.org/10.1016/0022-2836\(78\)90104-3](https://doi.org/10.1016/0022-2836(78)90104-3)
- Lawrence, C. W., Das, G., & Christensen, R. B. (1985). REV7, a new gene concerned with UV mutagenesis in yeast. *MGG Molecular & General Genetics*, 200(1), 80–85. <https://doi.org/10.1007/BF00383316>
- Lawrence, C. W., Nisson, P. E., & Christensen, R. B. (1985). UV and chemical mutagenesis in *rev7* mutants of yeast. *Molecular & General Genetics: MGG*, 200(1), 86–91. Retrieved from <http://www.ncbi.nlm.nih.gov/pubmed/3897795>
- Lawrence, C. W., O'Brien, T., & Bond, J. (1984). UV-induced reversion of *his4* frameshift mutations in *rad6*, *rev1*, and *rev3* mutants of yeast. *Molecular & General Genetics: MGG*, 195(3), 487–90. Retrieved from <http://www.ncbi.nlm.nih.gov/pubmed/6381967>
- Lazzaro, F., Giannattasio, M., Puddu, F., Granata, M., Pelliccioli, A., Plevani, P., & Muzi-Falconi, M. (2009). Checkpoint mechanisms at the intersection between DNA damage and repair. *DNA Repair*, 8(9), 1055–1067. <https://doi.org/10.1016/j.dnarep.2009.04.022>
- Lazzaro, F., Novarina, D., Amara, F., Watt, D. L., Stone, J. E., Costanzo, V., ... Muzi-Falconi, M. (2012). RNase H and Postreplication Repair Protect Cells from Ribonucleotides Incorporated in DNA. *Molecular Cell*, 45(1), 99–110. <https://doi.org/10.1016/j.molcel.2011.12.019>
- Lee, S. H., Pan, Z. Q., Kwong, A. D., Burgers, P. M., & Hurwitz, J. (1991). Synthesis of DNA by DNA polymerase epsilon in vitro. *The Journal of Biological Chemistry*, 266(33), 22707–17. Retrieved from <http://www.ncbi.nlm.nih.gov/pubmed/1682323>
- Lehman, I. R. (1974). DNA Ligase: Structure, Mechanism, and Function. *Science*, 186(4166), 790–797. <https://doi.org/10.1126/science.186.4166.790>

- Lehman, I. R., Bessman, M. J., Simms, E. S., & Kornberg, A. (1958). Enzymatic synthesis of deoxyribonucleic acid. I. Preparation of substrates and partial purification of an enzyme from *Escherichia coli*. *The Journal of Biological Chemistry*, 233(1), 163–70. Retrieved from <http://www.ncbi.nlm.nih.gov/pubmed/13563462>
- Lehman, I. R., & Kaguni, L. S. (1989). DNA polymerase alpha. *The Journal of Biological Chemistry*, 264(8), 4265–8. Retrieved from <http://www.ncbi.nlm.nih.gov/pubmed/2647732>
- Lehmann, A. R. (2005). Replication of damaged DNA by translesion synthesis in human cells. In *FEBS Letters* (Vol. 579, pp. 873–876). <https://doi.org/10.1016/j.febslet.2004.11.029>
- Lehmann, A. R. (2006). New functions for Y family polymerases. *Molecular Cell*. <https://doi.org/10.1016/j.molcel.2006.10.021>
- Lehmann, A. R., & Fuchs, R. P. (2006). Gaps and forks in DNA replication: Rediscovering old models. *DNA Repair*, 5(12), 1495–1498. <https://doi.org/10.1016/j.dnarep.2006.07.002>
- Lehmann, A. R., Niimi, A., Ogi, T., Brown, S., Sabbioneda, S., Wing, J. F., ... Green, C. M. (2007). Translesion synthesis: Y-family polymerases and the polymerase switch. *DNA Repair*, 6(7), 891–899. <https://doi.org/10.1016/j.dnarep.2007.02.003>
- Leman, A. R., & Noguchi, E. (2013). The replication fork: understanding the eukaryotic replication machinery and the challenges to genome duplication. *Genes*, 4(1), 1–32. <https://doi.org/10.3390/genes4010001>
- Lemontt, J. F., Waters, L. S., Minesinger, B. K., Wiltrout, M. E., D'Souza, S., Woodruff, R. V., & Walker, G. C. (1971). Mutants of yeast defective in mutation induced by ultraviolet light. *Genetics*, 68(1), 21–33. <https://doi.org/10.1128/MMBR.00034-08>
- Lengauer, C., Kinzler, K. W., & Vogelstein, B. (1998). Genetic instabilities in human cancers. *Nature*, 396(6712), 643–649. <https://doi.org/10.1038/25292>
- Levikova, M., & Cejka, P. (2015). The *Saccharomyces cerevisiae* Dna2 can function as a sole nuclease in the processing of Okazaki fragments in DNA replication. *Nucleic Acids Research*, 43(16), 7888–7897. <https://doi.org/10.1093/nar/gkv710>
- Levine, R. L., Miller, H., Grollman, A., Ohashi, E., Ohmori, H., Masutani, C., ... Moriya, M. (2001). Translesion DNA Synthesis Catalyzed by Human Pol  $\eta$  and Pol  $\kappa$  across 1, N 6 -Ethenodeoxyadenosine. *Journal of Biological Chemistry*, 276(22), 18717–18721. <https://doi.org/10.1074/jbc.M102158200>
- Li, G., & Reinberg, D. (2011). Chromatin higher-order structures and gene regulation. *Current Opinion in Genetics and Development*. <https://doi.org/10.1016/j.gde.2011.01.022>
- Li, Y., & Breaker, R. R. (1999). Kinetics of RNA degradation by specific base catalysis of transesterification involving the 2'-hydroxyl group. *Journal of the American Chemical Society*, 121(23), 5364–5372. <https://doi.org/10.1021/ja990592p>
- Li, Z., Pearlman, A. H., & Hsieh, P. (2016). DNA mismatch repair and the DNA damage response. *DNA Repair*, 38, 94–101. <https://doi.org/10.1016/j.dnarep.2015.11.019>

- Lieber, M. R. (2010). The mechanism of double-strand DNA break repair by the nonhomologous DNA end-joining pathway. *Annual Review of Biochemistry*, 79, 181–211.  
<https://doi.org/10.1146/annurev.biochem.052308.093131>
- Lin, W., Xin, H., Zhang, Y., Wu, X., Yuan, F., & Wang, Z. (1999). The human REV1 gene codes for a DNA template-dependent dCMP transferase. *Nucleic Acids Research*, 27(22), 4468–4475.  
<https://doi.org/10.1093/nar/27.22.4468>
- Lindahl, T., & Barnes, D. E. (2000). Repair of endogenous DNA damage. *Cold Spring Harbor Symposia on Quantitative Biology*, 65, 127–33. Retrieved from <http://www.ncbi.nlm.nih.gov/pubmed/12760027>
- Lindsey-Boltz, L. A., Kemp, M. G., Hu, J., & Sancar, A. (2015). Analysis of Ribonucleotide Removal from DNA by Human Nucleotide Excision Repair. *The Journal of Biological Chemistry*, 290(50), 29801–7.  
<https://doi.org/10.1074/jbc.M115.695254>
- Ling, H., Boudsocq, F., Woodgate, R., & Yang, W. (2001). Crystal structure of a Y-family DNA polymerase in action: A mechanism for error-prone and lesion-bypass replication. *Cell*, 107(1), 91–102. [https://doi.org/10.1016/S0092-8674\(01\)00515-3](https://doi.org/10.1016/S0092-8674(01)00515-3)
- Longhese, M. P., Bonetti, D., Manfrini, N., & Clerici, M. (2010). Mechanisms and regulation of DNA end resection. *The EMBO Journal*, 29(17), 2864–74.  
<https://doi.org/10.1038/emboj.2010.165>
- Longhese, M. P., Foiani, M., Muzi-Falconi, M., Lucchini, G., & Plevani, P. (1998). DNA damage checkpoint in budding yeast. *The EMBO Journal*, 17(19), 5525–5528. Retrieved from <https://www.ncbi.nlm.nih.gov/pmc/articles/PMC1170880/pdf/005525.pdf>
- Lowdon, M., & Vitols, E. (1973). Ribonucleotide reductase activity during the cell cycle of *Saccharomyces cerevisiae*. *Archives of Biochemistry and Biophysics*, 158(1), 177–184. [https://doi.org/10.1016/0003-9861\(73\)90611-5](https://doi.org/10.1016/0003-9861(73)90611-5)
- Lujan, S. A., Williams, J. S., Clausen, A. R., Clark, A. B., & Kunkel, T. A. (2013). Ribonucleotides Are Signals for Mismatch Repair of Leading-Strand Replication Errors. *Molecular Cell*, 50(3), 437–443.  
<https://doi.org/10.1016/j.molcel.2013.03.017>
- Majka, J., Binz, S. K., Wold, M. S., & Burgers, P. M. J. (2006). Replication protein a directs loading of the DNA damage checkpoint clamp to 5'??-DNA junctions. *Journal of Biological Chemistry*, 281(38), 27855–27861.  
<https://doi.org/10.1074/jbc.M605176200>
- Masai, H., Matsumoto, S., You, Z., Yoshizawa-Sugata, N., & Oda, M. (2010). Eukaryotic Chromosome DNA Replication: Where, When, and How? *Annual Review of Biochemistry*, 79(1), 89–130.  
<https://doi.org/10.1146/annurev.biochem.052308.103205>
- Masuda, Y., Ohmae, M., Masuda, K., & Kamiya, K. (2003). Structure and Enzymatic Properties of a Stable Complex of the Human REV1 and REV7 Proteins. *Journal of Biological Chemistry*, 278(14), 12356–12360.  
<https://doi.org/10.1074/jbc.M211765200>
- Masutani, C., Kusumoto, R., Iwai, S., & Hanaoka, F. (2000). Mechanisms of accurate translesion synthesis by human DNA polymerase  $\epsilon$ . *The EMBO*

- Journal*, 19(12), 3100–3109. <https://doi.org/10.1093/emboj/19.12.3100>
- Masutani, C., Kusumoto, R., Yamada, A., Dohmae, N., Yokoi, M., Yuasa, M., ... Hanaoka, F. (1999). The XPV (xeroderma pigmentosum variant) gene encodes human DNA polymerase  $\eta$ . *Nature*, 399(6737), 700–4. <https://doi.org/10.1038/21447>
- Matsuda, T., Bebenek, K., Masutani, C., Rogozin, I. B., Hanaoka, F., & Kunkel, T. A. (2001). Error rate and specificity of human and murine DNA polymerase  $\eta$ . *Journal of Molecular Biology*, 312(2), 335–346. <https://doi.org/10.1006/jmbi.2001.4937>
- Matzke, M. A., & Matzke, A. J. M. (2004). Planting the seeds of a new paradigm. *PLoS Biology*, 2(5), E133. <https://doi.org/10.1371/journal.pbio.0020133>
- McCulloch, S. D., Kokoska, R. J., Masutani, C., Iwai, S., Hanaoka, F., & Kunkel, T. A. (2004). Preferential cis-syn thymine dimer bypass by DNA polymerase  $\eta$  occurs with biased fidelity. *Nature*, 428(6978), 97–100. <https://doi.org/10.1038/nature02352>
- McCulloch, S. D., & Kunkel, T. A. (2008). The fidelity of DNA synthesis by eukaryotic replicative and translesion synthesis polymerases. *Cell Research Cell Research*, 184(18). <https://doi.org/10.1038/cr.2008.4>
- McDonald, J. P., Levine, A. S., & Woodgate, R. (1997). The *Saccharomyces cerevisiae* RAD30 gene, a homologue of *Escherichia coli* dinB and umuC, is DNA damage inducible and functions in a novel error-free postreplication repair mechanism. *Genetics*, 147(4), 1557–1568. <https://doi.org/10.1128/MCB.23.7.2463>
- McDonald, J. P., Rapić-Otrin, V., Epstein, J. A., Broughton, B. C., Wang, X., Lehmann, A. R., ... Woodgate, R. (1999). Novel human and mouse homologs of *Saccharomyces cerevisiae* DNA polymerase  $\eta$ . *Genomics*, 60(1), 20–30. <https://doi.org/10.1006/geno.1999.5906>
- McDonald, J. P., Vaisman, A., Kuban, W., Goodman, M. F., & Woodgate, R. (2012). Mechanisms Employed by *Escherichia coli* to Prevent Ribonucleotide Incorporation into Genomic DNA by Pol V. *PLoS Genetics*, 8(11). <https://doi.org/10.1371/journal.pgen.1003030>
- McIlwraith, M. J., Vaisman, A., Liu, Y., Fanning, E., Woodgate, R., & West, S. C. (2005). Human DNA polymerase  $\eta$  promotes DNA synthesis from strand invasion intermediates of homologous recombination. *Molecular Cell*, 20(5), 783–792. <https://doi.org/10.1016/j.molcel.2005.10.001>
- McNally, K., Neal, J. A., McManus, T. P., McCormick, J. J., & Maher, V. M. (2008). hRev7, putative subunit of hPol $\zeta$ , plays a critical role in survival, induction of mutations, and progression through S-phase, of UV(254nm)-irradiated human fibroblasts. *DNA Repair*, 7(4), 597–604. <https://doi.org/10.1016/j.dnarep.2007.12.013>
- Meroni, A., Lazzaro, F., Muzi-Falconi, M., & Podestà, A. (2018). Characterization of Structural and Configurational Properties of DNA by Atomic Force Microscopy (pp. 557–573). Humana Press, New York, NY. [https://doi.org/10.1007/978-1-4939-7306-4\\_37](https://doi.org/10.1007/978-1-4939-7306-4_37)
- Meroni, A., Mentegari, E., Crespan, E., Muzi-Falconi, M., Lazzaro, F., & Podestà, A. (2017). The Incorporation of Ribonucleotides Induces Structural and Conformational Changes in DNA. *Biophysical Journal*, 113(7), 1373–1382.

- <https://doi.org/10.1016/j.bnpj.2017.07.013>
- Meroni, A., Nava, G. M., Sertic, S., Plevani, P., Muzi-Falconi, M., & Lazzaro, F. (2018). Measuring the Levels of Ribonucleotides Embedded in Genomic DNA (pp. 319–327). Humana Press, New York, NY.  
[https://doi.org/10.1007/978-1-4939-7306-4\\_22](https://doi.org/10.1007/978-1-4939-7306-4_22)
- Meselson, M., & Stahl, F. W. (1958). The replication of DNA in *Escherichia coli*. *Proceedings of the National Academy of Sciences*, 44(7), 671–682.  
<https://doi.org/10.1073/pnas.44.7.671>
- Mimitou, E. P., & Symington, L. S. (2011). DNA end resection—Unraveling the tail. *DNA Repair*, 10(3), 344–348.  
<https://doi.org/10.1016/j.dnarep.2010.12.004>
- Minca, E. C., & Kowalski, D. (2010). Multiple Rad5 activities mediate sister chromatid recombination to bypass DNA damage at stalled replication forks. *Molecular Cell*, 38(5), 649–661.  
<https://doi.org/10.1016/j.molcel.2010.03.020>
- Minko, I. G., Washington, M. T., Kanuri, M., Prakash, L., Prakash, S., & Lloyd, R. S. (2003). Translesion Synthesis past Acrolein-derived DNA Adduct,  $\gamma$ -Hydroxypropanodeoxyguanosine, by Yeast and Human DNA Polymerase  $\eta$ . *Journal of Biological Chemistry*, 278(2), 784–790.  
<https://doi.org/10.1074/jbc.M207774200>
- Minko, I. G., Washington, M. T., Prakash, L., Prakash, S., & Lloyd, R. S. (2001). Translesion DNA Synthesis by Yeast DNA Polymerase  $\eta$  on Templates Containing N<sup>2</sup>-Guanine Adducts of 1,3-Butadiene Metabolites. *Journal of Biological Chemistry*, 276(4), 2517–2522.  
<https://doi.org/10.1074/jbc.M007867200>
- Moldovan, G.-L., Pfander, B., & Jentsch, S. (2007). PCNA, the Maestro of the Replication Fork. *Cell*, 129(4), 665–679.  
<https://doi.org/10.1016/j.cell.2007.05.003>
- Morrison, A., & Sugino, A. (1994). The 3'  $\rightarrow$  5' exonucleases of both DNA polymerases  $\alpha$  and  $\delta$  participate in correcting errors of DNA replication in *Saccharomyces cerevisiae*. *MGG Molecular & General Genetics*, 242(3), 289–296. <https://doi.org/10.1007/BF00280418>
- Morrison, a, Johnson, a L., Johnston, L. H., & Sugino, a. (1993). Pathway correcting DNA replication errors in *Saccharomyces cerevisiae*. *The EMBO Journal*, 12(4), 1467–1473.
- Murakumo, Y., Ogura, Y., Ishii, H., Numata, S., Ichihara, M., Croce, C. M., ... Takahashi, M. (2001). Interactions in the Error-prone Postreplication Repair Proteins hREV1, hREV3, and hREV7. *Journal of Biological Chemistry*, 276(38), 35644–35651. <https://doi.org/10.1074/jbc.M102051200>
- Murante, R. S., Henricksen, L. A., & Bambara, R. A. (1998). Junction ribonuclease: An activity in Okazaki fragment processing. *Proceedings of the National Academy of Sciences of the United States of America*, 95(5), 2244–2249. <https://doi.org/10.1073/pnas.95.5.2244>
- Murray, a W. (1992). Creative blocks: cell-cycle checkpoints and feedback controls. *Nature*, 359(6396), 599–604. <https://doi.org/10.1038/359599a0>
- Nair, D. T., Johnson, R. E., Prakash, L., Prakash, S., & Aggarwal, A. K. (2005). Rev1 employs a novel mechanism of DNA synthesis using a protein

- template. *Science (New York, N.Y.)*, 309(5744), 2219–2222.  
<https://doi.org/10.1126/science.1116336>
- Nair, D. T., Johnson, R. E., Prakash, S., Prakash, L., & Aggarwal, A. K. (2004). Replication by human DNA polymerase- $\alpha$  occurs by Hoogsteen base-pairing. *Nature*, 430(6997), 377–380. <https://doi.org/10.1038/nature02692>
- Negrini, S., Gorgoulis, V. G., & Halazonetis, T. D. (2010). Genomic instability — an evolving hallmark of cancer. *Nature Reviews Molecular Cell Biology*, 11(3), 220–228. <https://doi.org/10.1038/nrm2858>
- Nelson, J. R., Lawrence, C. W., & Hinkle, D. C. (1996). Deoxycytidyl transferase activity of yeast REV1 protein. *Nature*, 382(6593), 729–731.  
<https://doi.org/10.1038/382729a0>
- Nelson, J. R., Lawrence, C. W., & Hinkle, D. C. (1996). Thymine-thymine dimer bypass by yeast DNA polymerase zeta. *Science (New York, N.Y.)*, 272(5268), 1646–1649. <https://doi.org/10.1126/science.272.5268.1646>
- Newlon, C. S., & Theis, J. F. (2002). DNA replication joins the revolution: whole-genome views of DNA replication in budding yeast. *BioEssays: News and Reviews in Molecular, Cellular and Developmental Biology*, 24(4), 300–4.  
<https://doi.org/10.1002/bies.10075>
- Nguyen, T. A., Tak, Y. S., Lee, C. H., Kang, Y. H., Cho, I. T., & Seo, Y. S. (2011). Analysis of subunit assembly and function of the *Saccharomyces cerevisiae* RNase H2 complex. *FEBS Journal*, 278(24), 4927–4942.  
<https://doi.org/10.1111/j.1742-4658.2011.08394.x>
- Nick McElhinny, S. A., Kumar, D., Clark, A. B., Watt, D. L., Watts, B. E., Lundström, E.-B., ... Kunkel, T. A. (2010). Genome instability due to ribonucleotide incorporation into DNA. *Nature Chemical Biology*, 6(10), 774–81. <https://doi.org/10.1038/nchembio.424>
- Nick McElhinny, S. A., & Ramsden, D. A. (2003). Polymerase mu is a DNA-directed DNA/RNA polymerase. *Molecular and Cellular Biology*, 23(7), 2309–15. <https://doi.org/10.1128/mcb.23.7.2309-2315.2003>
- Nick McElhinny, S. A., Watts, B. E., Kumar, D., Watt, D. L., Lundström, E.-B., Burgers, P. M. J., ... Kunkel, T. A. (2010). Abundant ribonucleotide incorporation into DNA by yeast replicative polymerases. *Proceedings of the National Academy of Sciences of the United States of America*, 107(11), 4949–54. <https://doi.org/10.1073/pnas.0914857107>
- Nick McElhinny, S. a, Kissling, G. E., & Kunkel, T. a. (2010). Differential correction of lagging-strand replication errors made by DNA polymerases {alpha} and {delta}. *Proceedings of the National Academy of Sciences of the United States of America*, 107(49), 21070–21075.  
<https://doi.org/10.1073/pnas.1013048107>
- Nigg, E. A. (1995). Cyclin-dependent protein kinases: Key regulators of the eukaryotic cell cycle. *BioEssays*, 17(6), 471–480.  
<https://doi.org/10.1002/bies.950170603>
- Nishizaki, T., Iwai, S., Ohkubo, T., Kojima, C., Nakamura, H., Kyogoku, Y., & Ohtsuka, E. (1996). Solution Structures of DNA duplexes containing a DNA x RNA hybrid region, d(GG)r(AGAU)d(GAC) x d(GTCATCTCC) and d(GGAGA)r(UGAC) x d(GTCATCTCC). *Biochemistry*, 35(13), 4016–25.  
<https://doi.org/10.1021/bi951982i>

- Nitiss, J. L. (2009a). DNA topoisomerase II and its growing repertoire of biological functions. *Nature Reviews. Cancer*, 9(5), 327–337. <https://doi.org/10.1038/nrc2608>
- Nitiss, J. L. (2009b). Targeting DNA topoisomerase II in cancer chemotherapy. *Nature Reviews. Cancer*, 9(5), 338–350. <https://doi.org/10.1038/nrc2607>
- Nyberg, K. A., Michelson, R. J., Putnam, C. W., & Weinert, T. A. (2002). Toward Maintaining the Genome: DNA Damage and Replication Checkpoints. *Annual Review of Genetics*, 36(1), 617–656. <https://doi.org/10.1146/annurev.genet.36.060402.113540>
- O’Connell, K., Jinks-Robertson, S., & Petes, T. D. (2015). Elevated Genome-Wide Instability in Yeast Mutants Lacking RNase H Activity. *Genetics*, 201(3), 963–975. <https://doi.org/10.1534/genetics.115.182725>
- Ochoa, S. (1961). Enzymatic synthesis of ribonucleic acid. *Radioactive Isotopes in Physiology Diagnostics and ...*. Retrieved from [http://link.springer.com/chapter/10.1007/978-3-642-49761-2\\_31](http://link.springer.com/chapter/10.1007/978-3-642-49761-2_31)
- Ogi, T., Kannouche, P., & Lehmann, A. R. (2005). Localisation of human Y-family DNA polymerase kappa: relationship to PCNA foci. *Journal of Cell Science*, 118, 129–136. <https://doi.org/10.1242/jcs.01603>
- Ogi, T., Kato, T., Kato, T., & Ohmori, H. (1999). Mutation enhancement by DINB1, a mammalian homologue of the Escherichia coli mutagenesis protein dinB. *Genes to Cells: Devoted to Molecular & Cellular Mechanisms*, 4(11), 607–18. Retrieved from <http://www.ncbi.nlm.nih.gov/pubmed/10620008>
- Ogi, T., Limsirichaikul, S., Overmeer, R. M., Volker, M., Takenaka, K., Cloney, R., ... Lehmann, A. R. (2010). Three DNA Polymerases, Recruited by Different Mechanisms, Carry Out NER Repair Synthesis in Human Cells. *Molecular Cell*, 37(5), 714–727. <https://doi.org/10.1016/j.molcel.2010.02.009>
- Ogi, T., Shinkai, Y., Tanaka, K., & Ohmori, H. (2002). Polkappa protects mammalian cells against the lethal and mutagenic effects of benzo[a]pyrene. *Proceedings of the National Academy of Sciences of the United States of America*, 99(24), 15548–53. <https://doi.org/10.1073/pnas.222377899>
- Ohashi, E., Murakumo, Y., Kanjo, N., Akagi, J. I., Masutani, C., Hanaoka, F., & Ohmori, H. (2004). Interaction of hREV1 with three human Y-family DNA polymerases. *Genes to Cells*, 9(6), 523–531. <https://doi.org/10.1111/j.1356-9597.2004.00747.x>
- Okazaki, R., Okazaki, T., Sakabe, K., Sugimoto, K., & Sugino, A. (1968). Mechanism of DNA chain growth. I. Possible discontinuity and unusual secondary structure of newly synthesized chains. *Proceedings of the National Academy of Sciences of the United States of America*, 59(2), 598–605. Retrieved from <http://www.ncbi.nlm.nih.gov/pubmed/4967086>
- Papouli, E., Chen, S., Davies, A. A., Huttner, D., Krejci, L., Sung, P., & Ulrich, H. D. (2005). Crosstalk between SUMO and Ubiquitin on PCNA Is Mediated by Recruitment of the Helicase Srs2p. *Molecular Cell*, 19(1), 123–133. <https://doi.org/10.1016/j.molcel.2005.06.001>
- Parker, J. L., Bielen, A. B., Dikic, I., & Ulrich, H. D. (2007). Contributions of ubiquitin- and PCNA-binding domains to the activity of Polymerase eta in

- Saccharomyces cerevisiae. *Nucleic Acids Research*, 35(3), 881–9.  
<https://doi.org/10.1093/nar/gkl1102>
- Pata, J. D. (2010). Structural diversity of the Y-family DNA polymerases. *Biochimica et Biophysica Acta*, 1804(5), 1124–35.  
<https://doi.org/10.1016/j.bbapap.2010.01.020>
- Patel, P. H., Kawate, H., Adman, E., Ashbach, M., & Loeb, L. A. (2001). A single highly mutable catalytic site amino acid is critical for DNA polymerase fidelity. *The Journal of Biological Chemistry*, 276(7), 5044–51.  
<https://doi.org/10.1074/jbc.M008701200>
- Patel, P. H., & Loeb, L. A. (2000). Multiple amino acid substitutions allow DNA polymerases to synthesize RNA. *Journal of Biological Chemistry*, 275(51), 40266–40272. <https://doi.org/10.1074/jbc.M005757200>
- Patel, S. S., Wong, I., & Johnson, K. A. (1991). Pre-Steady-State Kinetic Analysis of Processive DNA Replication Including Complete Characterization of an Exonuclease-Deficient Mutant. *Biochemistry*, 30(2), 511–525.  
<https://doi.org/10.1021/bi00216a029>
- Paulovich, A. G., & Hartwell, L. H. (1995). A checkpoint regulates the rate of progression through S phase in *S. cerevisiae* in Response to DNA damage. *Cell*, 82(5), 841–847. [https://doi.org/10.1016/0092-8674\(95\)90481-6](https://doi.org/10.1016/0092-8674(95)90481-6)
- Pavlov, Y. I., Maki, S., Maki, H., & Kunkel, T. A. (2004). Evidence for interplay among yeast replicative DNA polymerases alpha, delta and epsilon from studies of exonuclease and polymerase active site mutations. *BMC Biology*, 2(1), 11. <https://doi.org/10.1186/1741-7007-2-11>
- Pavlov, Y. I., Shcherbakova, P. V., & Kunkel, T. A. (2001). In vivo consequences of putative active site mutations in yeast DNA polymerases  $\alpha$ ,  $\epsilon$ ,  $\delta$  and  $\zeta$ . *Genetics*, 159(1), 47–64.
- Pelliccioli, A., & Foiani, M. (2005). Signal transduction: How Rad53 kinase is activated. *Current Biology*. <https://doi.org/10.1016/j.cub.2005.08.057>
- Pelliccioli, A., Lucca, C., Liberi, G., Marini, F., Lopes, M., Plevani, P., ... Wold, M. (1999). Activation of Rad53 kinase in response to DNA damage and its effect in modulating phosphorylation of the lagging strand DNA polymerase. *EMBO Journal*, 18(22), 6561–6572.  
<https://doi.org/10.1093/emboj/18.22.6561>
- Petruska, J., Goodman, M. F., Boosalis, M. S., Sowers, L. C., Cheong, C., & Tinoco, I. (1988). Comparison between DNA melting thermodynamics and DNA polymerase fidelity. *Proceedings of the National Academy of Sciences of the United States of America*, 85(17), 6252–6.  
<https://doi.org/10.1073/pnas.85.17.6252>
- Pfander, B., Moldovan, G.-L., Sacher, M., Hoege, C., & Jentsch, S. (2005). SUMO-modified PCNA recruits Srs2 to prevent recombination during S phase. *Nature*, 436(7049), 428–33. <https://doi.org/10.1038/nature03665>
- Pikor, L., Thu, K., Vucic, E., & Lam, W. (2013). The detection and implication of genome instability in cancer. *Cancer Metastasis Reviews*, 32(3–4), 341–52.  
<https://doi.org/10.1007/s10555-013-9429-5>
- Pileur, F., Toulme, J. J., & Cazenave, C. (2000). Eukaryotic ribonucleases HI and HII generate characteristic hydrolytic patterns on DNA-RNA hybrids: further evidence that mitochondrial RNase H is an RNase HII. *Nucleic*

- Acids Research*, 28(18), 3674–83. <https://doi.org/10.1093/nar/28.18.3674>
- Pizzi, S., Sertic, S., Orcesi, S., Cereda, C., Bianchi, M., Jackson, A. P., ... Muzi-Falconi, M. (2015). Reduction of hRNase H2 activity in Aicardi-Goutières syndrome cells leads to replication stress and genome instability. *Human Molecular Genetics*, 24(3), 649–58. <https://doi.org/10.1093/hmg/ddu485>
- Plevani, P., & Chang, L. M. (1977). Enzymatic initiation of DNA synthesis by yeast DNA polymerases. *Proceedings of the National Academy of Sciences of the United States of America*, 74(5), 1937–41. Retrieved from <http://www.ncbi.nlm.nih.gov/pubmed/325562>
- Plosky, B. S., Vidal, A. E., Fernández de Henestrosa, A. R., McLenigan, M. P., McDonald, J. P., Mead, S., & Woodgate, R. (2006). Controlling the subcellular localization of DNA polymerases iota and eta via interactions with ubiquitin. *The EMBO Journal*, 25(12), 2847–55. <https://doi.org/10.1038/sj.emboj.7601178>
- Pomerantz, R. T., & O'Donnell, M. (2008). The replisome uses mRNA as a primer after colliding with RNA polymerase. *Nature*, 456(7223), 762–766. <https://doi.org/10.1038/nature07527>
- Pommier, Y. (2013). Drugging topoisomerases: Lessons and Challenges. *ACS Chemical Biology*. <https://doi.org/10.1021/cb300648v>
- Potenski, C. J., Niu, H., Sung, P., & Klein, H. L. (2014). Avoidance of ribonucleotide-induced mutations by RNase H2 and Srs2-Exo1 mechanisms. *Nature*, 511(7508), 251–4. <https://doi.org/10.1038/nature13292>
- Prakash, S., Johnson, R., & Prakash, L. (2005). EUKARYOTIC TRANSLESION SYNTHESIS DNA POLYMERASES: Specificity of Structure and Function. *Annual Review of Biochemistry*, 74(1), 317–353. <https://doi.org/10.1146/annurev.biochem.74.082803.133250>
- Qiu, J., Qian, Y., Frank, P., Wintersberger, U., & Shen, B. (1999). Saccharomyces cerevisiae RNase H(35) Functions in RNA Primer Removal during Lagging-Strand DNA Synthesis, Most Efficiently in Cooperation with Rad27 Nuclease. *Molecular and Cellular Biology*, 19(12), 8361–8371. Retrieved from <http://www.ncbi.nlm.nih.gov/pmc/articles/PMC84926/> <http://www.ncbi.nlm.nih.gov/pmc/articles/PMC84926/pdf/mbo08361.pdf>
- Raghuraman, M. K., Winzeler, E. A., Collingwood, D., Hunt, S., Wodicka, L., Conway, A., ... Fangman, W. L. (2001). Replication Dynamics of the Yeast Genome. *Science*, 294(5540), 115–121. <https://doi.org/10.1126/science.294.5540.115>
- Rao, P. N., & Johnson, R. T. (1970). Mammalian Cell Fusion: Studies on the Regulation of DNA Synthesis and Mitosis. *Nature*, 225(5228), 159–164. <https://doi.org/10.1038/225159a0>
- Rasmussen, A. K., Chatterjee, A., Rasmussen, L. J., & Singh, K. K. (2003). Mitochondria-mediated nuclear mutator phenotype in Saccharomyces cerevisiae. *Nucleic Acids Research*, 31(14), 3909–3917. <https://doi.org/10.1093/nar/gkg446>
- Ratray, A. J., & Strathern, J. N. (2005). Homologous Recombination Is Promoted by Translesion Polymerase Pol $\eta$ . *Molecular Cell*, 20(5), 658–659. <https://doi.org/10.1016/j.molcel.2005.11.018>
- Reha-Krantz, L. J. (2010). DNA polymerase proofreading: Multiple roles

- maintain genome stability. *Biochimica et Biophysica Acta (BBA) - Proteins and Proteomics*, 1804(5), 1049–1063.  
<https://doi.org/10.1016/j.bbapap.2009.06.012>
- Reichard, P. (1985). Ribonucleotide reductase and deoxyribonucleotide pools. *Basic Life Sci.*, 31, 33–45. Retrieved from  
<http://eutils.ncbi.nlm.nih.gov/entrez/eutils/elink.fcgi?dbfrom=pubmed&mp;id=3888178&retmode=ref&cmd=prlinks>
- Reijns, M. A. M., & Jackson, A. P. (2014). Ribonuclease H2 in health and disease. *Biochemical Society Transactions*, 42(4), 717–725.  
<https://doi.org/10.1042/BST20140079>
- Reijns, M. A. M., Kemp, H., Ding, J., de Procé, S. M., Jackson, A. P., & Taylor, M. S. (2015). Lagging-strand replication shapes the mutational landscape of the genome. *Nature*, 518(7540), 502–506.  
<https://doi.org/10.1038/nature14183>
- Reijns, M. A. M. M., Bubeck, D., Gibson, L. C. D. D., Graham, S. C., Baillie, G. S., Jones, E. Y., & Jackson, A. P. (2011). The structure of the human RNase H2 complex defines key interaction interfaces relevant to enzyme function and human disease. *Journal of Biological Chemistry*, 286(12), 10530–10539.  
<https://doi.org/10.1074/jbc.M110.177394>
- Reijns, M. A. M., Rabe, B., Rigby, R. E., Mill, P., Astell, K. R., Lettice, L. A., ... Jackson, A. P. (2012). Enzymatic removal of ribonucleotides from DNA is essential for mammalian genome integrity and development. *Cell*, 149(5), 1008–1022. <https://doi.org/10.1016/j.cell.2012.04.011>
- Rey, L., Sidorova, J. M., Puget, N., Boudsocq, F., Biard, D. S. F., Monnat, R. J., ... Hoffmann, J.-S. J.-S. (2009). Human DNA polymerase eta is required for common fragile site stability during unperturbed DNA replication. *Molecular and Cellular Biology*, 29(12), 3344–3354.  
<https://doi.org/10.1128/MCB.00115-09>
- Rice, G. I., Bond, J., Asipu, A., Brunette, R. L., Manfield, I. W., Carr, I. M., ... Crow, Y. J. (2009). Mutations involved in Aicardi-Goutières syndrome implicate SAMHD1 as regulator of the innate immune response. *Nature Genetics*, 41(7), 829–32. <https://doi.org/10.1038/ng.373>
- Rice, G. I., del Toro Duany, Y., Jenkinson, E. M., Forte, G. M. A., Anderson, B. H., Ariaudo, G., ... Crow, Y. J. (2014). Gain-of-function mutations in IFIH1 cause a spectrum of human disease phenotypes associated with upregulated type I interferon signaling. *Nature Genetics*, 46(5), 503–9.  
<https://doi.org/10.1038/ng.2933>
- Rice, G. I., Kasher, P. R., Forte, G. M. A., Mannion, N. M., Greenwood, S. M., Szykiewicz, M., ... Crow, Y. J. (2012). Mutations in ADAR1 cause Aicardi-Goutières syndrome associated with a type I interferon signature. *Nature Genetics*, 44(11), 1243–1248. <https://doi.org/10.1038/ng.2414>
- Rice, G., Patrick, T., Parmar, R., Taylor, C. F., Aeby, A., Aicardi, J., ... Crow, Y. J. (2007). Clinical and molecular phenotype of Aicardi-Goutières syndrome. *American Journal of Human Genetics*, 81(4), 713–25.  
<https://doi.org/10.1086/521373>
- Rippe, K., & Luke, B. (2015). TERRA and the state of the telomere. *Nature Structural & Molecular Biology*, 22(11), 853–858.

- <https://doi.org/10.1038/nsmb.3078>
- Rosebrock, A. P. (2017). Synchronization and Arrest of the Budding Yeast Cell Cycle Using Chemical and Genetic Methods. *Cold Spring Harbor Protocols*, 2017(1), pdb.proto88724. <https://doi.org/10.1101/pdb.proto88724>
- Ross, A. L., Simpson, L. J., & Sale, J. E. (2005). Vertebrate DNA damage tolerance requires the C-terminus but not BRCT or transferase domains of REV1. *Nucleic Acids Research*, 33(4), 1280–1289. <https://doi.org/10.1093/nar/gki279>
- Roush, A. A., Suarez, M., Friedberg, E. C., Radman, M., & Siede, W. (1998). Deletion of the *Saccharomyces cerevisiae* gene RAD30 encoding an *Escherichia coli* DinB homolog confers UV radiation sensitivity and altered mutability. *Molecular and General Genetics*, 257(6), 686–692. <https://doi.org/10.1007/s004380050698>
- Rychlik, M. P., Chon, H., Cerritelli, S. M., Klimek, P., Crouch, R. J., & Nowotny, M. (2010). Crystal structures of RNase H2 in complex with nucleic acid reveal the mechanism of RNA-DNA junction recognition and cleavage. *Molecular Cell*, 40(4), 658–70. <https://doi.org/10.1016/j.molcel.2010.11.001>
- Rydberg, B., & Game, J. (2002). Excision of misincorporated ribonucleotides in DNA by RNase H (type 2) and FEN-1 in cell-free extracts. *Proceedings of the National Academy of Sciences of the United States of America*, 99(26), 16654–9. <https://doi.org/10.1073/pnas.262591699>
- Sabbioneda, S., Bortolomai, I., Giannattasio, M., Plevani, P., & Muzi-Falconi, M. (2007). Yeast Rev1 is cell cycle regulated, phosphorylated in response to DNA damage and its binding to chromosomes is dependent upon MEC1. *DNA Repair*, 6(1), 121–7. <https://doi.org/10.1016/j.dnarep.2006.09.002>
- Sabbioneda, S., Gourdin, A. M., Green, C. M., Zotter, A., Giglia-Mari, G., Houtsmuller, A., ... Lehmann, A. R. (2008). Effect of proliferating cell nuclear antigen ubiquitination and chromatin structure on the dynamic properties of the Y-family DNA polymerases. *Molecular Biology of the Cell*, 19(12), 5193–202. <https://doi.org/10.1091/mbc.E08-07-0724>
- Sale, J. E., Lehmann, A. R., & Woodgate, R. (2012). Y-family DNA polymerases and their role in tolerance of cellular DNA damage. *Nature Reviews. Molecular Cell Biology*, 13(3), 141–52. <https://doi.org/10.1038/nrm3289>
- San Filippo, J., Sung, P., & Klein, H. (2008). Mechanism of Eukaryotic Homologous Recombination. *Annual Review of Biochemistry*, 77(1), 229–257. <https://doi.org/10.1146/annurev.biochem.77.061306.125255>
- Sanchez, Y., Bachant, J., Wang, H., Hu, F., Liu, D., Tetzlaff, M., & Elledge, S. J. (1999). Control of the DNA damage checkpoint by chk1 and rad53 protein kinases through distinct mechanisms. *Science (New York, N.Y.)*, 286(5442), 1166–1171. <https://doi.org/10.1126/science.286.5442.1166>
- Sayrac, S., Vengrova, S., Godfrey, E. L., & Dalgaard, J. Z. (2011). Identification of a novel type of spacer element required for imprinting in fission yeast. *PLoS Genetics*, 7(3). <https://doi.org/10.1371/journal.pgen.1001328>
- Schellenberg, M. J., Tumbale, P. P., & Williams, R. S. (2015). Molecular underpinnings of Aprataxin RNA/DNA deadenylase function and dysfunction in neurological disease. *Progress in Biophysics and Molecular Biology*. <https://doi.org/10.1016/j.pbiomolbio.2015.01.007>

- Schiestl, R. H., Prakash, S., & Prakash, L. (1990). The SRS2 suppressor of rad6 mutations of *Saccharomyces cerevisiae* acts by channeling DNA lesions into the RAD52 DNA repair pathway. *Genetics*, *124*(4), 817–31. Retrieved from <http://www.ncbi.nlm.nih.gov/pubmed/2182387>
- Sekiguchi, J., & Shuman, S. (1997). Site-specific ribonuclease activity of eukaryotic DNA topoisomerase I. *Molecular Cell*, *1*(1), 89–97. Retrieved from <http://www.ncbi.nlm.nih.gov/pubmed/9659906>
- Sertic, S., Pizzi, S., Lazzaro, F., Plevani, P., & Muzi-Falconi, M. (2012). NER and DDR: Classical music with new instruments. *Cell Cycle*, *11*(4), 668–674. <https://doi.org/10.4161/cc.11.4.19117>
- Shachar, S., Ziv, O., Avkin, S., Adar, S., Wittschieben, J., Reißner, T., ... Livneh, Z. (2009). Two-polymerase mechanisms dictate error-free and error-prone translesion DNA synthesis in mammals. *The EMBO Journal*, *28*(4), 383–393. <https://doi.org/10.1038/emboj.2008.281>
- Sharp, S. J., Schaack, J., Cooley, L., Burke, D. J., & Soil, D. (1985). Structure and Transcription of Eukaryotic tRNA Gene. *Critical Reviews in Biochemistry*, *19*(2), 107–144. <https://doi.org/10.3109/10409238509082541>
- Shcherbakova, P. V., Pavlov, Y. I., Chilkova, O., Rogozin, I. B., Johansson, E., & Kunkel, T. A. (2003). Unique Error Signature of the Four-subunit Yeast DNA Polymerase  $\epsilon$ . *Journal of Biological Chemistry*, *278*(44), 43770–43780. <https://doi.org/10.1074/jbc.M306893200>
- Shen, W., Sun, H., De Hoyos, C. L., Bailey, J. K., Liang, X., & Crooke, S. T. (2017). Dynamic nucleoplasmic and nucleolar localization of mammalian RNase H1 in response to RNAP I transcriptional R-loops. *Nucleic Acids Research*, *34*, 875–880. <https://doi.org/10.1093/nar/gkx710>
- Shen, Y., Koh, K. D., Weiss, B., & Storici, F. (2012). Mismatched rNMPs in DNA are mutagenic and are targets of mismatch repair and RNases H. *Nature Structural & Molecular Biology*, *19*(1), 98–104. <https://doi.org/10.1038/nsmb.2176>
- Shen, Z. (2011). Genomic instability and cancer: an introduction. *Journal of Molecular Cell Biology*, *3*(1), 1–3. <https://doi.org/10.1093/jmcb/mjq057>
- Sheu, Y.-J., & Stillman, B. (2006). Cdc7-Dbf4 phosphorylates MCM proteins via a docking site-mediated mechanism to promote S phase progression. *Molecular Cell*, *24*(1), 101–113. <https://doi.org/10.1016/j.molcel.2006.07.033>
- Shimizu, T., Tateishi, S., Tanoue, Y., Azuma, T., & Ohmori, H. (2017). Somatic hypermutation of immunoglobulin genes in Rad18 knockout mice. *DNA Repair*, *50*, 54–60. <https://doi.org/10.1016/j.dnarep.2016.12.008>
- Sible, J. C., Tyson, J. J., & Novák, B. (2002). Checkpoints in the Cell Cycle. *Encyclopedia of Life Sciences*, (August), 1–8. <https://doi.org/10.1038/npg.els.0001355>
- Siede, W., Friedberg, A. S., Dianova, I., & Friedberg, E. C. (1994). Characterization of G1 checkpoint control in the yeast *Saccharomyces cerevisiae* following exposure to DNA-damaging agents. *Genetics*, *138*(2), 271–281.
- Simpson, L. J., Ross, A.-L., Szüts, D., Alviani, C. A., Oestergaard, V. H., Patel, K. J., & Sale, J. E. (2006). RAD18-independent ubiquitination of proliferating-cell nuclear antigen in the avian cell line DT40. *EMBO Reports*, *7*(9), 927–

32. <https://doi.org/10.1038/sj.embor.7400777>
- Skoneczna, A., McIntyre, J., Skoneczny, M., Policinska, Z., & Sledziwska-Gojska, E. (2007). Polymerase eta is a short-lived, proteasomally degraded protein that is temporarily stabilized following UV irradiation in *Saccharomyces cerevisiae*. *Journal of Molecular Biology*, 366(4), 1074–1086. <https://doi.org/10.1016/j.jmb.2006.11.093>
- Skourti-Stathaki, K., & Proudfoot, N. J. (2014). A double-edged sword: R loops as threats to genome integrity and powerful regulators of gene expression. *Genes and Development*. <https://doi.org/10.1101/gad.242990.114>
- Sogo, J. M., Lopes, M., & Foiani, M. (2002). Fork Reversal and ssDNA Accumulation at Stalled Replication Forks Owing to Checkpoint Defects. *Science*, 297(5581), 599–602. <https://doi.org/10.1126/science.1074023>
- Sparks, J. L., & Burgers, P. M. (2015). Error-free and mutagenic processing of topoisomerase 1-provoked damage at genomic ribonucleotides. *The EMBO Journal*, 34(9), 1259–69. <https://doi.org/10.15252/embj.201490868>
- Sparks, J. L., Chon, H., Cerritelli, S. M., Kunkel, T. A., Johansson, E., Crouch, R. J., & Burgers, P. M. (2012). *RNase H2-Initiated Ribonucleotide Excision Repair*. *Molecular Cell* (Vol. 47). <https://doi.org/10.1016/j.molcel.2012.06.035>
- Stary, A., Kannouche, P., Lehmann, A. R., & Sarasin, A. (2003). Role of DNA polymerase eta in the UV mutation spectrum in human cells. *J Biol Chem*, 278(21), 18767–18775. <https://doi.org/10.1074/jbc.M211838200>
- Stein, H., & Hausen, P. (1969). Enzyme from calf thymus degrading the RNA moiety of DNA-RNA Hybrids: effect on DNA-dependent RNA polymerase. *Science (New York, N.Y.)*. <https://doi.org/10.1126/science.166.3903.393>
- Stelter, P., & Ulrich, H. D. (2003). Control of spontaneous and damage-induced mutagenesis by SUMO and ubiquitin conjugation. *Nature*, 425(6954), 188–191. <https://doi.org/10.1038/nature01965>
- Stetson, D. B., Ko, J. S., Heidmann, T., & Medzhitov, R. (2008). Trex1 prevents cell-intrinsic initiation of autoimmunity. *Cell*, 134(4), 587–98. <https://doi.org/10.1016/j.cell.2008.06.032>
- Stinchcomb, D. T., Struhl, K., & Davis, R. W. (1979). Isolation and characterisation of a yeast chromosomal replicator. *Nature*, 282(5734), 39–43. Retrieved from <http://www.ncbi.nlm.nih.gov/pubmed/388229>
- Sugawara, N., & Haber, J. E. (1992). Characterization of double-strand break-induced recombination: homology requirements and single-stranded DNA formation. *Molecular and Cellular Biology*, 12(2), 563–75. <https://doi.org/10.1128/MCB.12.2.563>. Updated
- Sun, Z., Hsiao, J., Fay, D. S., & Stern, D. F. (1998). Rad53 FHA Domain Associated with Phosphorylated Rad9 in the DNA Damage Checkpoint. *Science*, 281(5374), 272–274. <https://doi.org/10.1126/science.281.5374.272>
- Suzuki, Y., Holmes, J. B., Cerritelli, S. M., Sakhuja, K., Minczuk, M., Holt, I. J., & Crouch, R. J. (2010). An Upstream Open Reading Frame and the Context of the Two AUG Codons Affect the Abundance of Mitochondrial and Nuclear RNase H1. *Molecular and Cellular Biology*, 30(21), 5123–5134. <https://doi.org/10.1128/MCB.00619-10>
- T.-C. Lin, Chun Xia Wang, Catherine M. Joyce, A., & Konigsberg\*, W. H. (2001). 3′–5′ Exonucleolytic Activity of DNA Polymerases: Structural Features That

- Allow Kinetic Discrimination between Ribo- and Deoxyribonucleotide Residues†. <https://doi.org/10.1021/BI0105936>
- Takisawa, H., Mimura, S., & Kubota, Y. (2000). Eukaryotic DNA replication: From pre-replication complex to initiation complex. *Current Opinion in Cell Biology*. [https://doi.org/10.1016/S0955-0674\(00\)00153-8](https://doi.org/10.1016/S0955-0674(00)00153-8)
- Tercero, J. A., Labib, K., & Diffley, J. F. (2000). DNA synthesis at individual replication forks requires the essential initiation factor Cdc45p. *The EMBO Journal*, 19(9), 2082–2093. <https://doi.org/10.1093/emboj/19.9.2082>
- Theis, J. F., & Newlon, C. S. (1997). The ARS309 chromosomal replicator of *Saccharomyces cerevisiae* depends on an exceptional ARS consensus sequence. *Proceedings of the National Academy of Sciences*, 94(20), 10786–10791. <https://doi.org/10.1073/pnas.94.20.10786>
- Tian, F., Sharma, S., Zou, J., Lin, S.-Y., Wang, B., Rezvani, K., ... Zhang, D. (2013). BRCA1 promotes the ubiquitination of PCNA and recruitment of translesion polymerases in response to replication blockade. *Proceedings of the National Academy of Sciences of the United States of America*, 110(33), 13558–63. <https://doi.org/10.1073/pnas.1306534110>
- Tinoco, I., & Bustamante, C. (1999). How RNA folds. *Journal of Molecular Biology*, 293(2), 271–281. <https://doi.org/10.1006/jmbi.1999.3001>
- Tishkoff, D. X., Boerger, A. L., Bertrand, P., Filosi, N., Gaida, G. M., Kane, M. F., & Kolodner, R. D. (1997). Identification and characterization of *Saccharomyces cerevisiae* EXO1, a gene encoding an exonuclease that interacts with MSH2. *Proceedings of the National Academy of Sciences*, 94(14), 7487–7492. <https://doi.org/10.1073/pnas.94.14.7487>
- Tissier, A., Kannouche, P., Reck, M.-P., Lehmann, A. R., Fuchs, R. P. P., & Cordonnier, A. (2004). Co-localization in replication foci and interaction of human Y-family members, DNA polymerase pol $\eta$  and REV1 protein. *DNA Repair*, 3(11), 1503–1514. <https://doi.org/10.1016/j.dnarep.2004.06.015>
- Tissier, A., McDonald, J. P., Frank, E. G., & Woodgate, R. (2000). pol iota, a remarkably error-prone human DNA polymerase. *Genes & Development*, 14(13), 1642–1650. <https://doi.org/10.1101/gad.14.13.1642>
- Tissier, A., McDonald, J. P., Frank, E. G., & Woodgate, R. (2000). poliota, a remarkably error-prone human DNA polymerase. *Genes & Development*, 14(13), 1642–50. Retrieved from <http://www.ncbi.nlm.nih.gov/pubmed/10887158>
- Torres-Ramos, C. A., Prakash, S., & Prakash, L. (1997). Requirement of yeast DNA polymerase delta in post-replicative repair of UV-damaged DNA. *The Journal of Biological Chemistry*, 272(41), 25445–8. Retrieved from <http://www.ncbi.nlm.nih.gov/pubmed/9325255>
- Traut, T. W. (1994). Physiological concentrations of purines and pyrimidines. *Molecular and Cellular Biochemistry*. <https://doi.org/10.1007/BF00928361>
- Trincao, J., Johnson, R. E., Escalante, C. R., Prakash, S., Prakash, L., & Aggarwal, A. K. (2001). Structure of the catalytic core of *S. cerevisiae* DNA polymerase eta: implications for translesion DNA synthesis. *Molecular Cell*, 8(2), 417–26. Retrieved from <http://www.ncbi.nlm.nih.gov/pubmed/11545743>
- Trincao, J., Johnson, R. E., Escalante, C. R., Prakash, S., Prakash, L., & Aggarwal, A. K. (2001). Structure of the Catalytic Core of *S. cerevisiae* DNA

- Polymerase  $\eta$ . *Molecular Cell*, 8(2), 417–426. [https://doi.org/10.1016/S1097-2765\(01\)00306-9](https://doi.org/10.1016/S1097-2765(01)00306-9)
- Tsuji, Y., Watanabe, K., Araki, K., Shinohara, M., Yamagata, Y., Tsurimoto, T., ... Tateishi, S. (2008). Recognition of forked and single-stranded DNA structures by human RAD18 complexed with RAD6B protein triggers its recruitment to stalled replication forks. *Genes to Cells*, 13(4), 343–354. <https://doi.org/10.1111/j.1365-2443.2008.01176.x>
- Tumbale, P., Appel, C. D., Kraehenbuehl, R., Robertson, P. D., Williams, J. S., Krahn, J., ... Williams, R. S. (2011). Structure of an aprataxin–DNA complex with insights into AOA1 neurodegenerative disease. *Nature Structural & Molecular Biology*, 18(11), 1189–1195. <https://doi.org/10.1038/nsmb.2146>
- Tumbale, P., Williams, J. S., Schellenberg, M. J., Kunkel, T. A., & Williams, R. S. (2013). Aprataxin resolves adenylated RNA–DNA junctions to maintain genome integrity. *Nature*, 506(7486), 111–115. <https://doi.org/10.1038/nature12824>
- Turchi, J. J., Huang, L., Murante, R. S., Kim, Y., & Bambara, R. A. (1994). Enzymatic completion of mammalian lagging-strand DNA replication. *Proceedings of the National Academy of Sciences of the United States of America*, 91(21), 9803–7. Retrieved from <http://www.ncbi.nlm.nih.gov/pubmed/7524089>
- Uljon, S. N., Johnson, R. E., Edwards, T. A., Prakash, S., Prakash, L., & Aggarwal, A. K. (2004). Crystal Structure of the Catalytic Core of Human DNA Polymerase Kappa. *Structure*, 12(8), 1395–1404. <https://doi.org/10.1016/j.str.2004.05.011>
- Unk, I., Hajdú, I., Fátýol, K., Hurwitz, J., Yoon, J.-H., Prakash, L., ... Haracska, L. (2008). Human HLTF functions as a ubiquitin ligase for proliferating cell nuclear antigen polyubiquitination. *Proceedings of the National Academy of Sciences of the United States of America*, 105(10), 3768–73. <https://doi.org/10.1073/pnas.0800563105>
- Unk, I., Hajdú, I., Fátýol, K., Szakál, B., Blastyák, A., Bermudez, V., ... Haracska, L. (2006). Human SHPRH is a ubiquitin ligase for Mms2-Ubc13-dependent polyubiquitylation of proliferating cell nuclear antigen. *Proceedings of the National Academy of Sciences of the United States of America*, 103(48), 18107–12. <https://doi.org/10.1073/pnas.0608595103>
- Usui, T., Ogawa, H., & Petrini, J. H. J. (2001). A DNA damage response pathway controlled by Tel1 and the Mre11 complex. *Molecular Cell*, 7(6), 1255–1266. [https://doi.org/10.1016/S1097-2765\(01\)00270-2](https://doi.org/10.1016/S1097-2765(01)00270-2)
- Vaisman, A., Kuban, W., McDonald, J. P., Karata, K., Yang, W., Goodman, M. F., & Woodgate, R. (2012). Critical amino acids in Escherichia coli UmuC responsible for sugar discrimination and base-substitution fidelity. *Nucleic Acids Research*, 40(13), 6144–57. <https://doi.org/10.1093/nar/gks233>
- Vaisman, A., Masutani, C., Hanaoka, F., & Chaney, S. G. (2000). Efficient translesion replication past oxaliplatin and cisplatin GpG adducts by human DNA polymerase  $\eta$ . *Biochemistry*, 39(16), 4575–4580. <https://doi.org/10.1021/bio00130k>
- Vaisman, A., McDonald, J. P., Huston, D., Kuban, W., Liu, L., Van Houten, B., & Woodgate, R. (2013). Removal of Misincorporated Ribonucleotides from

- Prokaryotic Genomes: An Unexpected Role for Nucleotide Excision Repair. *PLoS Genetics*, 9(11), e1003878. <https://doi.org/10.1371/journal.pgen.1003878>
- Vaisman, A., McDonald, J. P., Noll, S., Huston, D., Loeb, G., Goodman, M. F., & Woodgate, R. (2014). Investigating the mechanisms of ribonucleotide excision repair in *Escherichia coli*. *Mutation Research - Fundamental and Molecular Mechanisms of Mutagenesis*, 761, 21–33. <https://doi.org/10.1016/j.mrfmmm.2014.01.005>
- Vaisman, A., & Woodgate, R. (2017). Translesion DNA polymerases in eukaryotes: what makes them tick? *Critical Reviews in Biochemistry and Molecular Biology*, 9238(June), 1–30. <https://doi.org/10.1080/10409238.2017.1291576>
- Vanderstraeten, S., Van den Brûle, S., Hu, J., & Foury, F. (1998). The role of 3'-5' exonucleolytic proofreading and mismatch repair in yeast mitochondrial DNA error avoidance. *The Journal of Biological Chemistry*, 273(37), 23690–7. Retrieved from <http://www.ncbi.nlm.nih.gov/pubmed/9726974>
- Vengrova, S., & Dalgaard, J. Z. (2006). The wild-type *Schizosaccharomyces pombe* mat1 imprint consists of two ribonucleotides. *EMBO Reports*, 7(1), 59–65. <https://doi.org/10.1038/sj.embor.7400576>
- Voet, D., & Voet, J. G. (2010). *Biochemistry 4e. Zhurnal Eksperimental'noi i Teoreticheskoi Fiziki*.
- Vujcic, M., Miller, C. A., & Kowalski, D. (1999). Activation of silent replication origins at autonomously replicating sequence elements near the HML locus in budding yeast. *Molecular and Cellular Biology*, 19(9), 6098–109. Retrieved from <http://www.ncbi.nlm.nih.gov/pubmed/10454557>
- Wahba, L., Amon, J. D., Koshland, D., & Vuica-Ross, M. (2011). RNase H and Multiple RNA Biogenesis Factors Cooperate to Prevent RNA:DNA Hybrids from Generating Genome Instability. *Molecular Cell*, 44(6), 978–988. <https://doi.org/10.1016/j.molcel.2011.10.017>
- Wahl, M. C., & Sundaralingam, M. (2000). B-form to A-form conversion by a 3'-terminal ribose: crystal structure of the chimera d(CCACTAGTG)r(G). *Nucleic Acids Research*, 28(21), 4356–63. Retrieved from <http://www.ncbi.nlm.nih.gov/pubmed/11058136>
- Wallace, B. D., & Williams, R. S. (2014, November 2). Ribonucleotide triggered DNA damage and RNA-DNA damage responses. *RNA Biology*. <https://doi.org/10.4161/15476286.2014.992283>
- Walter, J., & Newport, J. (2000). Initiation of eukaryotic DNA replication: origin unwinding and sequential chromatin association of Cdc45, RPA, and DNA polymerase alpha. *Molecular Cell*, 5(4), 617–27. Retrieved from <http://www.ncbi.nlm.nih.gov/pubmed/10882098>
- Wang, A. H., Quigley, G. J., Kolpak, F. J., Crawford, J. L., van Boom, J. H., van der Marel, G., & Rich, A. (1979). Molecular structure of a left-handed double helical DNA fragment at atomic resolution. *Nature*, 282(5740), 680–686. <https://doi.org/10.1038/282680a0>
- Wang, W., Wu, E. Y., Hellinga, H. W., & Beese, L. S. (2012). Structural factors that determine selectivity of a high fidelity DNA polymerase for deoxy-, dideoxy-, and ribonucleotides. *The Journal of Biological Chemistry*, 287(34), 28215–26. <https://doi.org/10.1074/jbc.M112.366609>

- Wang, Y., Knudsen, B. R., Bjergbaek, L., Westergaard, O., & Andersen, A. H. (1999). Stimulated activity of human topoisomerases IIalpha and IIbeta on RNA-containing substrates. *The Journal of Biological Chemistry*, 274(32), 22839–46. <https://doi.org/10.1074/JBC.274.32.22839>
- Wang, Y., Woodgate, R., McManus, T. P., Mead, S., McCormick, J. J., & Maher, V. M. (2007). Evidence that in Xeroderma Pigmentosum Variant Cells, which Lack DNA Polymerase eta, DNA Polymerase iota Causes the Very High Frequency and Unique Spectrum of UV-Induced Mutations. *Cancer Research*, 67(7), 3018–3026. <https://doi.org/10.1158/0008-5472.CAN-06-3073>
- Washington, M. T., Johnson, R. E., Prakash, L., & Prakash, S. (2002). Human DINB1-encoded DNA polymerase kappa is a promiscuous extender of mispaired primer termini. *Proceedings of the National Academy of Sciences of the United States of America*, 99(4), 1910–4. <https://doi.org/10.1073/pnas.032594399>
- Washington, M. T., Johnson, R. E., Prakash, L., & Prakash, S. (2004). Human DNA polymerase iota utilizes different nucleotide incorporation mechanisms dependent upon the template base. *Molecular and Cellular Biology*, 24(2), 936–43. <https://doi.org/10.1128/MCB.24.2.936>
- Washington, M. T., Minko, I. G., Johnson, R. E., Wolffe, W. T., Harris, T. M., Lloyd, R. S., ... Prakash, L. (2004). Efficient and error-free replication past a minor-groove DNA adduct by the sequential action of human DNA polymerases iota and kappa. *Molecular and Cellular Biology*, 24(13), 5687–93. <https://doi.org/10.1128/MCB.24.13.5687-5693.2004>
- Watanabe, K., Tateishi, S., Kawasuji, M., Tsurimoto, T., Inoue, H., & Yamaizumi, M. (2004). Rad18 guides poleta to replication stalling sites through physical interaction and PCNA monoubiquitination. *The EMBO Journal*, 23(19), 3886–96. <https://doi.org/10.1038/sj.emboj.7600383>
- Waters, L. S., Minesinger, B. K., Wiltrout, M. E., D'Souza, S., Woodruff, R. V., & Walker, G. C. (2009). Eukaryotic translesion polymerases and their roles and regulation in DNA damage tolerance. *Microbiology and Molecular Biology Reviews : MMBR*, 73(1), 134–154. <https://doi.org/10.1128/MMBR.00034-08>
- Waters, L. S., & Walker, G. C. (2006). The critical mutagenic translesion DNA polymerase Rev1 is highly expressed during G(2)/M phase rather than S phase. *Proceedings of the National Academy of Sciences of the United States of America*, 103(24), 8971–8976. <https://doi.org/10.1073/pnas.0510167103>
- Watson, J. D., & Crick, F. H. C. (1953). Molecular structure of nucleic acids. *Nature*. <https://doi.org/10.1097/BLO.obo13e3181468780>
- Watt, D. L., Johansson, E., Burgers, P. M., & Kunkel, T. A. (2011). Replication of ribonucleotide-containing DNA templates by yeast replicative polymerases. *DNA Repair*, 10(8), 897–902. <https://doi.org/10.1016/j.dnarep.2011.05.009>
- Weinert, T. A., & Hartwell, L. H. (1988). The RAD9 gene controls the cell cycle response to DNA damage in *Saccharomyces cerevisiae*. *Science (New York, N.Y.)*, 241(4863), 317–22. <https://doi.org/10.1126/science.3291120>
- Weinert, T. A., Kiser, G. L., & Hartwell, L. H. (1994). Mitotic checkpoint genes in budding yeast and the dependence of mitosis on DNA replication and

- repair. *Genes and Development*, 8(6), 652–665.  
<https://doi.org/10.1101/gad.8.6.652>
- Williams, J. S., Clausen, A. R., Lujan, S. a, Marjavaara, L., Clark, A. B., Burgers, P. M., ... Morris, D. (2015). Evidence that processing of ribonucleotides in DNA by topoisomerase 1 is leading-strand specific. *Nature Structural & Molecular Biology*, 22(4), 291–297. <https://doi.org/10.1038/nsmb.2989>
- Williams, J. S., Clausen, A. R., Nick McElhinny, S. A., Watts, B. E., Johansson, E., & Kunkel, T. A. (2012). Proofreading of ribonucleotides inserted into DNA by yeast DNA polymerase  $\epsilon$ . *DNA Repair*, 11(8), 649–656.  
<https://doi.org/10.1016/j.dnarep.2012.05.004>
- Williams, J. S., Gehle, D. B., & Kunkel, T. A. (2017). The role of RNase H2 in processing ribonucleotides incorporated during DNA replication. *DNA Repair*, 53, 52–58.  
<https://doi.org/http://dx.doi.org/10.1016/j.dnarep.2017.02.016>
- Williams, J. S., Lujan, S. A., & Kunkel, T. A. (2016). Processing ribonucleotides incorporated during eukaryotic DNA replication. *Nature Reviews Molecular Cell Biology*, 17(6), 350–363. <https://doi.org/10.1038/nrm.2016.37>
- Williams, J. S., Smith, D. J., Marjavaara, L., Lujan, S. A., Chabes, A., & Kunkel, T. A. (2013). Topoisomerase 1-Mediated Removal of Ribonucleotides from Nascent Leading-Strand DNA. *Molecular Cell*, 49(5), 1010–1015.  
<https://doi.org/10.1016/j.molcel.2012.12.021>
- Wilson, R. C., Jackson, M. A., & Pata, J. D. (2013). Y-Family Polymerase Conformation Is a Major Determinant of Fidelity and Translesion Specificity. *Structure*, 21(1), 20–31. <https://doi.org/10.1016/j.str.2012.11.005>
- Wing, R., Drew, H., Takano, T., Broka, C., Takana, S., Itakura, K., & Dickerson, R. E. (1980). Crystal structure analysis of a complete turn of B-DNA. *Nature*, 287(October), 755–758. <https://doi.org/10.1038/287755a0>
- Wittschieben, J. P., Reshmi, S. C., Gollin, S. M., & Wood, R. D. (2006). Loss of DNA Polymerase  $\zeta$  Causes Chromosomal Instability in Mammalian Cells. *Cancer Research*, 66(1), 134–142. <https://doi.org/10.1158/0008-5472.CAN-05-2982>
- Wong, I., Patel, S. S., & Johnson, K. A. (1991). An Induced-Fit Kinetic Mechanism for DNA Replication Fidelity: Direct Measurement by Single-Turnover Kinetics. *Biochemistry*, 30(2), 526–537.  
<https://doi.org/10.1021/bi00216a030>
- Woodgate, R. (2001). Evolution of the two-step model for UV-mutagenesis. *Mutation Research*, 485(1), 83–92. Retrieved from <http://www.ncbi.nlm.nih.gov/pubmed/11341996>
- Xiao, W., Chow, B. L., Broomfield, S., & Hanna, M. (2000). The *Saccharomyces cerevisiae* RAD6 group is composed of an error-prone and two error-free postreplication repair pathways. *Genetics*, 155(4), 1633–41. Retrieved from <http://www.ncbi.nlm.nih.gov/pubmed/10924462>
- Xie, W., Yang, X., Xu, M., & Jiang, T. (2012). Structural insights into the assembly of human translesion polymerase complexes. *Protein and Cell*, 3(11), 864–874. <https://doi.org/10.1007/s13238-012-2102-x>
- Yamada, a, Masutani, C., Iwai, S., & Hanaoka, F. (2000). Complementation of defective translesion synthesis and UV light sensitivity in xeroderma

- pigmentosum variant cells by human and mouse DNA polymerase  $\eta$ . *Nucleic Acids Research*, 28(13), 2473–2480.  
<https://doi.org/10.1093/nar/28.13.2473>
- Yanagihara, H., Kobayashi, J., Tateishi, S., Kato, A., Matsuura, S., Tauchi, H., ... Komatsu, K. (2011). NBS1 Recruits RAD18 via a RAD6-like Domain and Regulates Pol  $\eta$ -Dependent Translesion DNA Synthesis. *Molecular Cell*, 43(5), 788–797. <https://doi.org/10.1016/j.molcel.2011.07.026>
- Yang, W. (2014). An Overview of Y-Family DNA Polymerases and a Case Study of Human DNA Polymerase  $\eta$ . *Biochemistry*, 53(17), 2793–2803.  
<https://doi.org/10.1021/bi500019s>
- Yang, W., Lee, J. Y., & Nowotny, M. (2006). Making and Breaking Nucleic Acids: Two-Mg<sup>2+</sup>-Ion Catalysis and Substrate Specificity. *Molecular Cell*, 22(1), 5–13. <https://doi.org/10.1016/j.molcel.2006.03.013>
- Yang, W., & Woodgate, R. (2007). What a difference a decade makes: Insights into translesion DNA synthesis. *Proceedings of the National Academy of Sciences*, 104(40), 15591–15598. <https://doi.org/10.1073/pnas.0704219104>
- Yang, Y. G., Lindahl, T., & Barnes, D. E. (2007). Trex1 Exonuclease Degrades ssDNA to Prevent Chronic Checkpoint Activation and Autoimmune Disease. *Cell*, 131(5), 873–886. <https://doi.org/10.1016/j.cell.2007.10.017>
- Yao, N. Y., Schroeder, J. W., Yurieva, O., Simmons, L. A., & O'Donnell, M. E. (2013). Cost of rNTP/dNTP pool imbalance at the replication fork. *Proceedings of the National Academy of Sciences*, 110(32), 12942–12947.  
<https://doi.org/10.1073/pnas.1309506110>
- Yeeles, J. T. P., Poli, J., Mariani, K. J., & Pasero, P. (2013). Rescuing stalled or damaged replication forks. *Cold Spring Harbor Perspectives in Biology*.  
<https://doi.org/10.1101/cshperspect.a012815>
- Yu, C., Bonaduce, M. J., & Klar, A. J. S. (2012). Defining the Epigenetic Mechanism of Asymmetric Cell Division of *Schizosaccharomyces japonicus* Yeast. *Genetics*, 193(1). Retrieved from  
<http://www.genetics.org/content/193/1/85>
- Yu, H., & Dröge, P. (2014). Replication-induced supercoiling: a neglected DNA transaction regulator? *Trends in Biochemical Sciences*, 39(5), 219–220.  
<https://doi.org/10.1016/j.tibs.2014.02.009>
- Yu, T. Y., Kao, Y. W., Lin, J. J., West, J. A., Chapman, B. A., Alekseyenko, A. A., ... Lee, J. T. (2014). Approaching TERRA Firma: Genomic Functions of Telomeric Noncoding RNA. *Proc. Natl. Acad. Sci. USA*, 111(1), 3377–3382.  
<https://doi.org/10.1016/j.cell.2017.06.020>
- Yuan, F., Zhang, Y., Rajpal, D. K., Wu, X., Guo, D., Wang, M., ... Wang, Z. (2000). Specificity of DNA lesion bypass by the yeast DNA polymerase  $\eta$ . *Journal of Biological Chemistry*, 275(11), 8233–8239.  
<https://doi.org/10.1074/jbc.275.11.8233>
- Zeng, X., Winter, D. B., Kasmer, C., Kraemer, K. H., Lehmann, A. R., & Gearhart, P. J. (2001). DNA polymerase  $\eta$  is an A-T mutator in somatic hypermutation of immunoglobulin variable genes. *Nature Immunology*, 2(6), 537–541. <https://doi.org/10.1038/88740>
- Zeng, Z., Cortés-Ledesma, F., El Khamisy, S. F., & Caldecott, K. W. (2011). TDP2/TTRAP is the major 5'-tyrosyl DNA phosphodiesterase activity in

- vertebrate cells and is critical for cellular resistance to topoisomerase II-induced DNA damage. *Journal of Biological Chemistry*, 286(1), 403–409. <https://doi.org/10.1074/jbc.M110.181016>
- Zhang, H., Chatterjee, A., & Singh, K. K. (2006). Saccharomyces cerevisiae polymerase zeta functions in mitochondria. *Genetics*, 172(4), 2683–8. <https://doi.org/10.1534/genetics.105.051029>
- Zhang, H., & Lawrence, C. W. (2005). The error-free component of the RAD6/RAD18 DNA damage tolerance pathway of budding yeast employs sister-strand recombination. *Proceedings of the National Academy of Sciences of the United States of America*, 102(44), 15954–9. <https://doi.org/10.1073/pnas.0504586102>
- Zhang, Y., Yuan, F., Wu, X., Rechkoblit, O., Taylor, J. S., Geacintov, N. E., & Wang, Z. (2000). Error-prone lesion bypass by human DNA polymerase eta. *Nucleic Acids Research*, 28(23), 4717–24. Retrieved from <http://www.ncbi.nlm.nih.gov/pubmed/11095682>
- Zhang, Y., Yuan, F., Wu, X., Taylor, J. S., & Wang, Z. (2001). Response of human DNA polymerase iota to DNA lesions. *Nucleic Acids Research*, 29(4), 928–35. Retrieved from <http://www.ncbi.nlm.nih.gov/pubmed/11160925>
- Zhang, Y., Yuan, F., Wu, X., & Wang, Z. (2000). Preferential incorporation of G opposite template T by the low-fidelity human DNA polymerase iota. *Molecular and Cellular Biology*, 20(19), 7099–108. <https://doi.org/10.1128/MCB.20.19.7099-7108.2000>. Updated
- Zhao, X., Chabes, a, Domkin, V., Thelander, L., & Rothstein, R. (2001). The ribonucleotide reductase inhibitor Sml1 is a new target of the Mec1/Rad53 kinase cascade during growth and in response to DNA damage. *The EMBO Journal*, 20(13), 3544–3553. <https://doi.org/10.1093/emboj/20.13.3544>
- Zhao, X., & Rothstein, R. (2002). The Dun1 checkpoint kinase phosphorylates and regulates the ribonucleotide reductase inhibitor Sml1. *Proceedings of the National Academy of Sciences of the United States of America*, 99(6), 3746–51. <https://doi.org/10.1073/pnas.062502299>
- Zhao, Y., Gregory, M. T., Biertümpfel, C., Hua, Y.-J., Hanaoka, F., & Yang, W. (2013). Mechanism of somatic hypermutation at the WA motif by human DNA polymerase η. *Proceedings of the National Academy of Sciences of the United States of America*, 110(20), 8146–51. <https://doi.org/10.1073/pnas.1303126110>
- Zheng, L., & Shen, B. (2011). Okazaki fragment maturation: nucleases take centre stage. *Journal of Molecular Cell Biology*, 3(1), 23–30. <https://doi.org/10.1093/jmcb/mjq048>
- Zhou, B. L., Pata, J. D., & Steitz, T. A. (2001). Crystal structure of a DinB lesion bypass DNA polymerase catalytic fragment reveals a classic polymerase catalytic domain. *Molecular Cell*, 8(2), 427–37. Retrieved from <http://www.ncbi.nlm.nih.gov/pubmed/11545744>
- Zhu, H., & Shuman, S. (2008). Bacterial nonhomologous end joining ligases preferentially seal breaks with a 3'-OH monoribonucleotide. *Journal of Biological Chemistry*, 283(13), 8331–8339. <https://doi.org/10.1074/jbc.M705476200>
- Zhuang, Z., Johnson, R. E., Haracska, L., Prakash, L., Prakash, S., & Benkovic, S.

- J. (2008). Regulation of polymerase exchange between Pol $\epsilon$  and Pol $\delta$  by monoubiquitination of PCNA and the movement of DNA polymerase holoenzyme. *Proceedings of the National Academy of Sciences of the United States of America*, 105(14), 5361–6. <https://doi.org/10.1073/pnas.0801310105>
- Zimmer, A. D., & Koshland, D. (2016). Differential roles of the RNases H in preventing chromosome instability. *Proceedings of the National Academy of Sciences*, 201613448. <https://doi.org/10.1073/pnas.1613448113>
- Zou, L. (2003). Sensing DNA Damage Through ATRIP Recognition of RPA-ssDNA Complexes. *Science*, 300(5625), 1542–1548. <https://doi.org/10.1126/science.1083430>
- Zou, L., & Stillman, B. (2000). Assembly of a complex containing Cdc45p, replication protein A, and Mcm2p at replication origins controlled by S-phase cyclin-dependent kinases and Cdc7p-Dbf4p kinase. *Molecular and Cellular Biology*, 20(9), 3086–96. Retrieved from <http://www.ncbi.nlm.nih.gov/pubmed/10757793>

# Part II

## Published Paper I

---

### **The incorporation of ribonucleotides induces structural and conformational changes in DNA**

Alice Meroni<sup>1</sup>, Elisa Mentegari<sup>2</sup>, Emmanuele Crespan<sup>2</sup>, Marco Muzi-Falconi<sup>1,#</sup>,  
Federico Lazzaro<sup>1,\*</sup>, Alessandro Podestà<sup>3,#</sup>

<sup>1</sup>Dipartimento di Bioscienze, Università degli Studi di Milano, via Celoria 26,  
20133 Milano, Italy.

<sup>2</sup>DNA Enzymology & Molecular Virology, Institute of Molecular Genetics  
IGM-CNR, via Abbiategrasso 207, 27100 Pavia, Italy.

<sup>3</sup>Dipartimento di Fisica and C.I.Ma.I.Na, Università degli Studi di Milano, via  
Celoria 16, 20133 Milano, Italy.

#Corresponding authors;

e-mail: [alessandro.podesta@mi.infn.it](mailto:alessandro.podesta@mi.infn.it), [marco.muzifalconi@unimi.it](mailto:marco.muzifalconi@unimi.it)

\*Co- last authors

**Biophysical Journal**, 113(7), 1373–1382. (2017)

<https://doi.org/10.1016/j.bpj.2017.07.013>

# The Incorporation of Ribonucleotides Induces Structural and Conformational Changes in DNA

Alice Meroni,<sup>1</sup> Elisa Mentegari,<sup>2</sup> Emmanuele Crespan,<sup>2</sup> Marco Muzi-Falconi,<sup>1,\*</sup> Federico Lazzaro,<sup>1</sup> and Alessandro Podestà<sup>3,\*</sup>

<sup>1</sup>Dipartimento di Bioscienze, Università degli Studi di Milano, Milano, Italy; <sup>2</sup>DNA Enzymology and Molecular Virology, Institute of Molecular Genetics IGM-CNR, Pavia, Italy; and <sup>3</sup>Dipartimento di Fisica and C.I.Ma.I.Na, Università degli Studi di Milano, Milano, Italy

**ABSTRACT** Ribonucleotide incorporation is the most common error occurring during DNA replication. Cells have hence developed mechanisms to remove ribonucleotides from the genome and restore its integrity. Indeed, the persistence of ribonucleotides into DNA leads to severe consequences, such as genome instability and replication stress. Thus, it becomes important to understand the effects of ribonucleotides incorporation, starting from their impact on DNA structure and conformation. Here we present a systematic study of the effects of ribonucleotide incorporation into DNA molecules. We have developed, to our knowledge, a new method to efficiently synthesize long DNA molecules (hundreds of basepairs) containing ribonucleotides, which is based on a modified protocol for the polymerase chain reaction. By means of atomic force microscopy, we could therefore investigate the changes, upon ribonucleotide incorporation, of the structural and conformational properties of numerous DNA populations at the single-molecule level. Specifically, we characterized the scaling of the contour length with the number of basepairs and the scaling of the end-to-end distance with the curvilinear distance, the bending angle distribution, and the persistence length. Our results revealed that ribonucleotides affect DNA structure and conformation on scales that go well beyond the typical dimension of the single ribonucleotide. In particular, the presence of ribonucleotides induces a systematic shortening of the molecules, together with a decrease of the persistence length. Such structural changes are also likely to occur *in vivo*, where they could directly affect the downstream DNA transactions, as well as interfere with protein binding and recognition.

## INTRODUCTION

Current opinion on the evolution of genetic information suggests that DNA was selected as the storage molecule because it is more stable with respect to its ancient precursor, RNA (1). The only difference between DNA and RNA is the presence of a hydroxyl group on the ribose of RNA monomers (rNMPs). Such group makes RNA unstable and less suitable to safely store genetic information (2).

Recent works reported that large amounts of ribonucleotides are misincorporated into chromosomes during DNA replication, even though DNA polymerases are extremely accurate enzymes (3–5). The frequency of incorporation in budding yeast is estimated to be ~1 every 700 nucleotides, making ribonucleotides the most frequent noncanonical nucleotides incorporated into the genome (6).

The elevated levels of ribonucleotides incorporated may suggest that this is not a mere error of DNA polymerases, but that it may have some beneficial roles. Indeed, it was recently demonstrated that ribonucleotides help a specific DNA repair pathway in discriminating the newly synthesized strand from the template filament (7,8). However, ribonucleotides are not permanent in DNA, because cells possess specific mechanisms to remove them from the genome (6,9). The persistence of rNMPs is an endogenous source of genome instability and replication stress (5,10–12).

RNase H enzymes are able to recognize and cleave embedded rNMPs (13), and are responsible for the major pathway that processes genomic rNMPs. Interestingly, defects in RNase H2 function represent the major cause of a rare genetic disorder, Aicardi-Goutieres syndrome (14).

How rNMPs embedded in chromosomal DNA may interfere with DNA-protein interactions has not been investigated yet, although it has been reported that nucleosomes assembly on DNA is reduced when even a single ribonucleotide is present (15). Understanding the structural changes imposed upon DNA molecules by the presence of

Submitted March 6, 2017, and accepted for publication July 25, 2017.

\*Correspondence: marco.muzifalconi@unimi.it or alessandro.podesta@mi.infn.it

Federico Lazzaro and Alessandro Podestà contributed equally to this article.

Editor: Karin Musier-Forsyth.

<http://dx.doi.org/10.1016/j.bpj.2017.07.013>

© 2017 Biophysical Society.

This is an open access article under the CC BY-NC-ND license (<http://creativecommons.org/licenses/by-nc-nd/4.0/>).



ribonucleotides is essential to determine the biological impact of their persistence in the genome. It is thus crucial to explore and investigate those effects at the single-molecule level.

During the 1990s, the first ribonucleotides containing DNA (RC-DNA) molecules were crystallized. These were very short self-complementary oligonucleotides with embedded ribonucleotides. X-ray diffraction analyses suggested that the presence of ribonucleotides induce a complete change toward the A-conformation, both when they are in the middle or at the ends of the molecules (16–18). In solution studies, such as nuclear magnetic resonance, the transition observed was partial (19,20). Molecular dynamics simulations suggested that even with 50% of ribonucleotide substitutions, B-DNA is not fully converted to A-DNA, although the ribose caused local perturbations (21). In addition, atomic force microscopy (AFM) measurements showed that ribonucleotides also perturb the backbone elasticity (22–24) with respect to DNA in the B-form, although these studies report different trends of the persistence length in relation to the presence of ribonucleotides. In conclusion, only a few single-molecule studies on the structural properties of RC-DNAs are available in the literature, and furthermore, in some cases apparently contradictory results are reported. And in most cases, short RC-DNA molecules are studied, although in biologically relevant cases (such as *in vivo*), the molecules are much longer.

Here we present the results of a systematic study of the structural effects of ribonucleotide incorporation into DNA carried out taking advantage of, to our knowledge, a novel protocol to synthesize several-hundred-of-basepairs-long RC-DNA molecules. RC-DNA molecules were produced via enzymatic synthesis by a mutant *Taq* polymerase (I614K), able to introduce ribonucleotides (rNTPs) in addition to deoxynucleotides (dNTPs). We were therefore able to produce numerous populations of RC-DNA molecules, as well as their controls without ribonucleotides, that have been studied at the single-molecule level by means of AFM. The main advantage of AFM is the possibility of studying large ensembles of molecules, by quantitatively analyzing each molecule individually, therefore obtaining robust average values of relevant structural and conformational observables (25–28). In particular, we have characterized the scaling of the contour length with the number of basepairs, the scaling of the end-to-end distance with the curvilinear distance, the bending angle distribution, and the persistence length of DNA molecules, showing that the presence of ribonucleotides affects the DNA structure and conformation well beyond the scale of the single ribonucleotide, up to full molecular length. The observed changes are also likely to take place in physiological conditions such as the cell environment, and consequently influence DNA transactions occurring *in vivo*.

## MATERIALS AND METHODS

### *Taq* polymerase production

The pTaq plasmid was site-directed mutagenized using primers TAQI614K for 5'-TGG CCC TGG ACT ATA GCC AGA AGC TCA GGG TGC TGG CCC A-3' and TAQI614Krev 5'-TGG GCC AGC ACC CTG AGC TCT TTC TGG CTA TAG TCC AGG GCC A-3'. BL21(DE3) *Escherichia coli* cells harboring pTaq or pTaqI614K were grown in selective medium and protein expression was induced by IPTG addition. Protein extraction and purification was done by GeneSpin (Milan, Italy).

### RC-DNAs synthesis

Polymerase chain reaction (PCR) was performed with either wild-type (WT) or I614K *Taq* polymerase in the presence of dATP, dGTP, and dTTP 0.2 mM, dCTP 0.1 mM for normal DNAs, and plus rCTP 0.8 mM only for RC-DNAs. Nucleotides were purchased from GeneSpin. The 464- and 727-basepair (bp) fragments were amplified from pGEM3Zf plasmid using primer pairs 5'-TCG GGA AAC CTG TCG TGC C-3'/5'-CAG CGT GAG CTA TGA GAA AG-3' and 5'-TCG GGA AAC CTG TCG TGC C-3'/5'-TCA GCA GAG CGC AGATAC CA-3', respectively. The 646-bp fragment was amplified from pNB187 plasmid using primers 5'-TAG TTG AAG CAT TAG GTC CC-3'/5'-CTT CTC AAA TAT GCT TCC CA-3'; the 960- and the 1079-bp fragments were amplified from pFL39.3 with primers 5'-AAA GAG TTA CTC AAG AAT AA-3'/5'-CAA AAC GGC ATT TAA GAA GC-3' and 5'-GGA CGA GGC AAG CTA AAC AG-3'/5'-CAA AAC GGC ATT TAA GAA GC-3', respectively. The complete sequences are reported in Fig. S8. PCR reactions were carried out in multiple independent samples and then pooled to increase the product yield. The samples were loaded onto 1% agarose gel and the band corresponding to the amplification product was excised and purified using silica columns (The Wizard SV Gel and PCR Clean-Up System; Promega, Fitchburg, WI) according to the manufacturer's instructions. This last step was necessary to further clean the samples from template plasmid and primers. All the samples were finally resuspended in ultrapure Milli-Q water (Millipore, Billerica, MA).

### PCR with radiolabeled nucleotides

PCR reactions were performed adding  $\alpha^{32}\text{P}$ -dCTP or  $\alpha^{32}\text{P}$ -rCTP (PerkinElmer, Waltham, MA) in addition to the nonradioactive dCTP or rCTP, respecting the final concentrations described above for RC-DNAs. Samples were drop-dialyzed on 0.025- $\mu\text{m}$  membranes (Millipore) and further cleaned by ethanol precipitation. Samples were then run in a 2% agarose gel that was dried and exposed on a phosphor storage screen; images were acquired using a PhosphorImager (Typhoon FLA 7000; GE Healthcare, Buckinghamshire, UK).

### Alkaline gel and Southern blot

Alkaline gel electrophoresis was performed as described in (29). Briefly, samples were incubated for 2 h at 55°C in 0.3 M NaOH and then run in alkaline gel (1% agarose in Milli-Q water with 1 mM EDTA and 250 mM NaOH) previously equilibrated in its alkaline running buffer (1 mM EDTA, 250 mM NaOH). DNA was transferred to a charged nylon membrane (GeneScreen Plus Hybridization Transfer Membrane; PerkinElmer) by Southern blotting and hybridized with the radiolabeled 464-bp fragment as a probe (prepared by a DECAprime II DNA Labeling Kit; Ambion, Austin, TX). Images were acquired using a PhosphorImager (Typhoon FLA 7000; GE Healthcare).

### AFM imaging

The procedure is described in detail in (30). Samples were deposited on freshly cleaved mica of the highest quality (V1, ruby muscovite; Ted Pella,

Redding, CA) in a  $Mg^{2+}$ -containing buffer (5 mM  $MgCl_2$ , 10 mM NaCl, 10 mM HEPES-Na, pH 7.5 in Milli-Q  $H_2O$ ). Incubation time ranged from 2 to 10 min at room temperature, then the samples were gently washed dropwise with 1–2 mL of Milli-Q water, and dried under a clean nitrogen stream. Images were captured in air, using a Multimode Nanoscope IV AFM (Bruker, Billerica, MA) working in tapping mode, equipped with rigid cantilevers ( $\sim 300$  kHz resonance frequency) and single-crystal silicon tips with nominal radius of curvature below 10 nm. The scan rate was typically 1.5–2 Hz, the scan area  $2 \times 1 \mu m$ , with a sampling resolution of 1 and 2 nm/pixel in the fast and slow scan directions, respectively.

## Analysis of AFM data

Raw images were first flattened by subtracting polynomials up to the third order, using only the flat mica surface as reference for the fit. DNA and RC-DNA molecules were semiautomatically traced using FiberApp software (31), to obtain the spatial coordinates of the backbones. Calibration of the scanner was checked by scanning a calibration grating and the determined correction factors (always  $< 2\text{--}3\%$ ) were applied to the coordinates, when needed. The traces were analyzed using custom MATLAB (The MathWorks, Natick, MA) routines. We evaluated the following statistical quantities describing structural/mechanical and conformational properties of semirigid polymers, as described in our previous works (26,30): the mean contour length  $\langle l \rangle$ , the mean squared end-to-end distance  $\langle R^2(L) \rangle$  of segments of the molecules with a curvilinear length (curvilinear distance)  $L$ , the distribution of bending angles  $\theta(L)$  (as well as  $\langle \cos(\theta(L)) \rangle$  and  $\langle \theta^2(L) \rangle$ ), and the persistence length  $P$ . If DNA molecules are in a well-defined form (either B or A), the  $\langle l \rangle$  versus  $n$  of the bp curve is a straight line with a slope equal to  $r_A$  or  $r_B$ , the rise per residues of the A and B forms, respectively, with units nm/bp. A reduction of the contour length independent on bp simply shifts the curve vertically by a constant offset  $c$ , but does not alter the slope of the curve. According to the wormlike chain (WLC) model, in two dimensions the mean squared end-to-end distance  $\langle R^2 \rangle_{2D}$  increases as the curvilinear distance  $L$  increases, and depends on the persistence length  $P$  of DNA as (25,26):

$$\langle R^2(L) \rangle_{2D} = 4PL \left[ 1 - \frac{2P}{L} \left( 1 - e^{-\frac{L}{2P}} \right) \right]. \quad (1)$$

*Estimation of the fraction of incorporated rCTP.* To estimate the percentage %rCTP of rCTP incorporated into RC-DNA molecules, we use Eq. 2, i.e., we multiply the fraction of sites along the DNA backbone available for rCTP incorporation (the GC content %GC) by the estimated frequency of incorporation,  $f_{\text{incorporation}}$  (defined and calculated with Eq. 3 in the Results and Discussion):

$$\%rCTP_{\text{incorporated}} = \%GC \cdot f_{\text{incorporation}} \cdot 100. \quad (2)$$

*Apparent B to A transition fraction.* An apparent fraction of basepairs in the DNA molecules that have switched from B to A conformation can be calculated by assuming that whenever an rCTP is incorporated, the hosting basepair switches from the B to the A form. The B-to-A transition fraction represents the fraction of basepairs that undergo such transition. Following (32,33), the total number of available basepairs before rCTP incorporation is  $N = (l_0 - c)/r_B$ , where  $l_0$  is the measured contour length;  $c$  is a possible systematic shortening of the molecules, as discussed before (the negative intercept of the  $\langle l \rangle$  versus  $n$  of basepairs curve shown in Fig. 4); and  $r_B = 0.34$  nm/bp is the B-form helical rise. After rCTP incorporation,  $N_A$  basepairs switch to the A conformation whereas  $N_B$  basepairs remain in the B conformation, such that  $N = N_B + N_A$ . In terms of contour length,  $N_B r_B + N_A r_A = (l_0 - c) - |\Delta l|$ , where  $r_A = 0.26$  nm/bp is the A-form helical rise and  $\Delta l$  is the measured difference in contour length upon ribonucleotide introduction. It follows that the bases in A form are  $N_A = |\Delta l|/(r_B - r_A)$ , and the B to A transition fraction  $N_A/N$  can be calculated as  $N_A/N = [|\Delta l|/(l_0 - c)] \times [r_B/(r_B - r_A)]$ .

*Statistical analysis.* Length data are reported in the figures and tables as mean value  $\pm$  effective error. The mean values and the SDs have been obtained by a Gaussian fit of the distributions of experimental values (see Fig. S4 for some representative distributions of contour length values). The effective errors have been calculated by summing in quadrature the SDs of the mean and a systematic error of  $\pm 1\%$  due to the  $z$ -piezo calibration. The error associated to the persistence length, extracted by fitting Eq. 1 to the average end-to-end distance curves of the samples, has been estimated by applying the fit to a few set of data obtained by adding a Gaussian noise to the average curves, whose width was set equal to the SD of the mean associated to each experimental value (the resulting error bar is comparable to the marker size, and it is not shown in the graphs). The significance of the observed differences in the value of relevant parameters was evaluated applying a two-tailed  $t$ -test.

## RESULTS AND DISCUSSION

### Synthesis of RC-DNA molecules

DNA molecules with incorporated ribonucleotides are generally synthesized chemically by a stepwise addition of nucleotides, whose limit is the chain extension step; as a result, with this methodology, only relatively short molecules are produced. Such short RC-DNAs molecules (10–30 bp) have been studied by several techniques (16,21,22), reproducing environments quite far from the physiological one.

We propose, to our knowledge, a new approach to synthesize RC-DNA molecules that exploits many consecutive cycles of an enzymatic reaction known as PCR. PCR is performed with the *Thermus aquaticus* DNA Polymerase (*Taq* pol), a very versatile enzyme, able to sustain multiple reaction cycles to amplify a defined DNA sequence exponentially (34). *Taq* pol is endowed with a high capability of discrimination between dNTPs and rNTPs; we took advantage of a known mutant version that is able to incorporate ribonucleotides more efficiently (35). We mutated the *Taq* pol with a single amino acid substitution at Isoleucine 614 to Lysine, making the enzyme more prone to binding and introducing rNTPs (35). The incorporation rates range from 150- to 1500-fold with respect to the WT *Taq* pol, depending on the rNTP species (rCTP, rATP, rGTP, or rTTP) (35). We expressed and purified both the WT and I614K *Taq* pols from *E. coli* cells, as described in Materials and Methods.

PCR allows the synthesis of a significant number of linear molecules, thanks to repetitive cycles of reaction. We set PCR conditions for the I614K *Taq* pol, in the presence of all four dNTPs and of rCTP, the most common ribonucleotide found in the DNA of living cells (36,37). To verify the effective rCTP incorporation, PCRs were performed using radiolabeled  $\alpha^{32}P$ -rCTP, and the amplification products (464 bp) were then purified and visualized by autoradiography after agarose gel electrophoresis. The radioactive signal corresponding to a band of 464 bp indicates that the I614K *Taq* pol is indeed introducing  $\alpha^{32}P$ -rCTP, although with low efficiency compared to  $\alpha^{32}P$ -dCTP (Fig. 1).

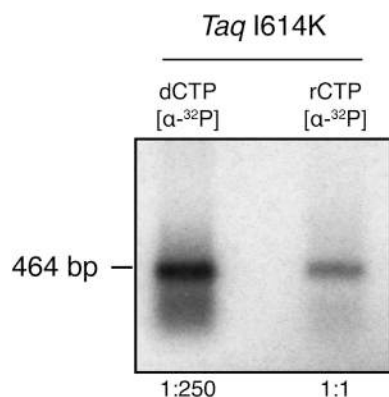


FIGURE 1 *Taq* polymerase I614K introduces rCTP in PCR products. DNA is amplified by I614K *Taq* pol mutant in the presence of radiolabeled  $\alpha^{32}\text{P}$ -dCTP or  $\alpha^{32}\text{P}$ -rCTP, and then it is separated onto an agarose gel, after purification through drop-dialysis and ethanol precipitation. The radioactive signal visible in the rCTP lane confirms that PCR products contain rNMPs.

From the published kinetic parameters of I614K *Taq* pol (35) it is possible to theoretically estimate such frequency of incorporation, using

$$f_{\text{incorporation}} = \frac{v_{d\text{CTP}}}{v_{r\text{CTP}}} = \frac{\frac{K_{\text{cat}}^{d\text{CTP}}}{K_m^{d\text{CTP}}} [d\text{CTP}]}{\frac{K_{\text{cat}}^{r\text{CTP}}}{K_m^{r\text{CTP}}} [r\text{CTP}]} \quad (3)$$

In our PCR conditions, the mutant *Taq* pol introduces one rCTP every 19 dCTP, in front of each guanosine residue (G), respecting the Watson-Crick basepairing. In fact, its misincorporation rates are small, regardless of the fact that I614K mutation confers less fidelity to the polymerase (38), as we verified by sequencing (data not shown).

To assess to what extent ribonucleotides are present in RC-DNA molecules, we exploited alkaline gel electrophoresis. PCR reactions were performed with I614K *Taq* pol in the presence or absence of rCTP and the products (see Fig. S1) were separated by gel electrophoresis in alkaline conditions; here the DNA is denatured and its backbone hydrolyzed at ribonucleotide positions, generating smaller fragments (4). Fig. 2 shows the degree of alkaline degradation of the 464-bp fragments, synthesized either in the absence or presence of rCTP. The molecules produced without rCTP migrate as a sharp band, whereas the ones containing rCTP generate a smear of smaller fragments, confirming the presence of ribonucleotides in most of them.

The presence of rNMPs in the template strand could interfere with the *Taq* pol activity in the following reaction cycles, as reported for other polymerases (39,40). To exclude this, we tested the ability of the mutant *Taq* pol to bypass ribonucleotides in the template by using a primer extension assay. The I614K *Taq* polymerase efficiently bypasses embedded rCMP in DNA (Fig. S2); a slight

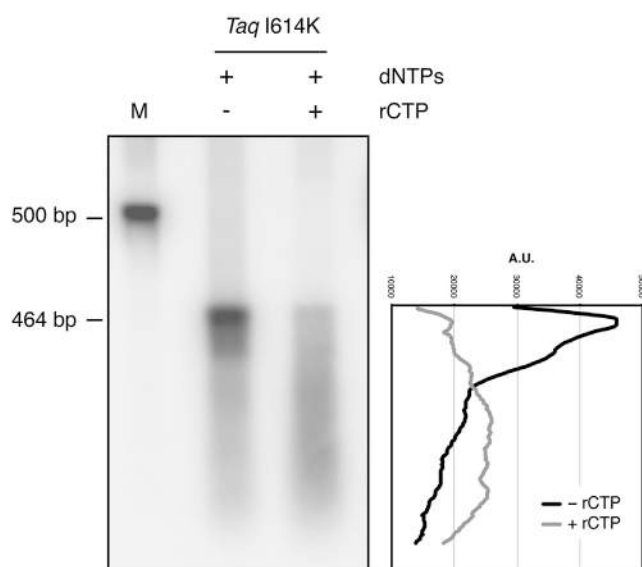


FIGURE 2 RC-DNA molecules are sensitive to alkaline hydrolysis. DNA is amplified in the presence or absence of rCTP and run in alkaline conditions. The DNA backbone is hydrolyzed in correspondence to ribonucleotides, resulting in a population of smaller molecules. Only molecules produced in the presence of rCTP are hydrolyzed and their corresponding band is converted to a smear signal. DNA is detected by Southern blotting hybridization, using the radiolabeled 464-bp fragment as a probe. The chart on the right displays the lane profiles in the presence or absence of rCTP.

pausing before the rNMP can be detected at enzyme concentrations much lower than those used in PCR reactions. Our synthesis strategy allows us, therefore, to obtain full-length amplified sequences.

### AFM imaging and characterization of RC-DNAs

Once the RC-DNA production has been validated, we generated several DNA molecules with different lengths and features. We produced and purified DNA and RC-DNA molecules with five different lengths in basepairs (464, 646, 727, 960, and 1079), and subjected them to AFM imaging. As described in detail in the Materials and Methods, DNA molecules were deposited onto a negatively charged mica surface, where they adsorb thanks to the mediation of magnesium divalent ions, which bridge the negative charges of the DNA backbone and the mica surface. Fig. 3 shows three representative AFM images of DNA and RC-DNA molecules produced with either WT or I614K *Taq* polymerases. Typically, the DNA molecules are well contrasted, thanks to the  $\text{Mg}^{2+}$  buffer, which provides a clean way to bind the molecules to the mica surface, preserving the atomic smoothness and cleanliness of the freshly cleaved substrates. Because the efficiency of PCR decreases when the mutated *Taq* is used, and when ribonucleotides are added to the reaction, AFM maps typically feature a decreasing number of molecules per unit area. Some molecules from both WT and I614K *Taq* pol (~20%) exhibited severe

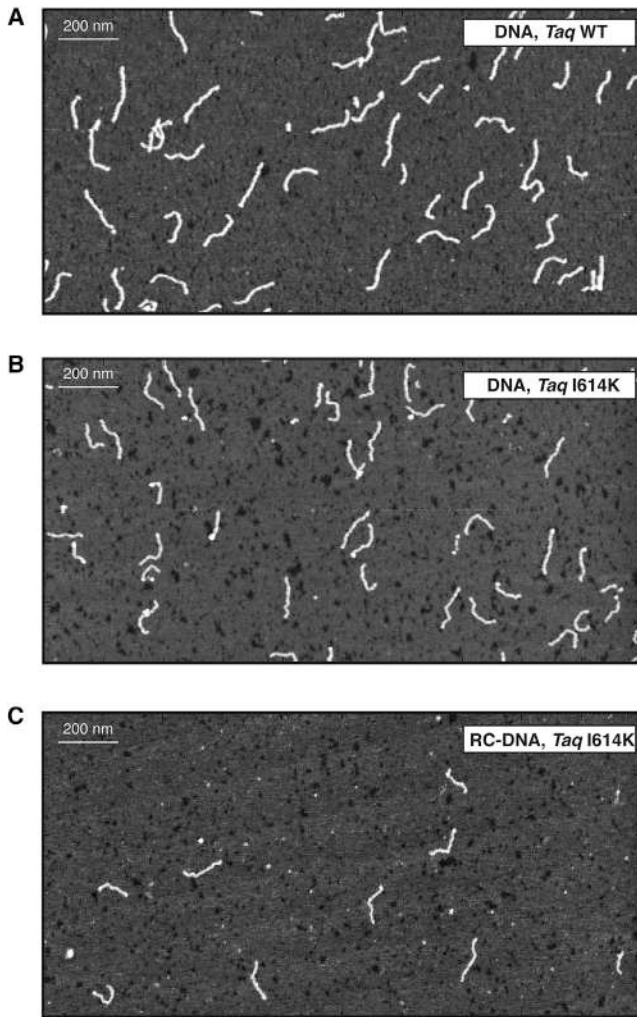


FIGURE 3 Representative AFM topographies of 464-bp molecules. Molecules are deposited on mica and imaged in air by AFM. (A) Shown here are DNA molecules synthesized with WT and (B) I614K *Taq* pol in the presence of dNTPs, and (C) RC-DNA molecules synthesized with the addition of rCTP by the I614K *Taq* polymerase. The size of the image is  $2 \times 1 \mu\text{m}^2$ .

irregularities in their shape and dimensions, such as overlapping and condensed regions, protruding asperities, etc., and were not considered for the analysis. These molecules were excluded on the basis of a visual analysis as well as of the analysis of representative profiles, as shown in Fig. S3. As detailed in Materials and Methods, molecules from several AFM topographic profiles were semiautomatically traced to calculate the relevant structural and conformational quantities (contour length, rise per residue, bending angle distribution, and end-to-end distance curve).

To validate our experimental imaging conditions, we have first characterized the conformational properties of DNA molecules produced by the WT *Taq* pol with dNTPs only. The scaling of the average contour length of linear DNA molecules with respect to the number of basepairs (464, 646, 727, 960, and 1079) is shown in Fig. 4.

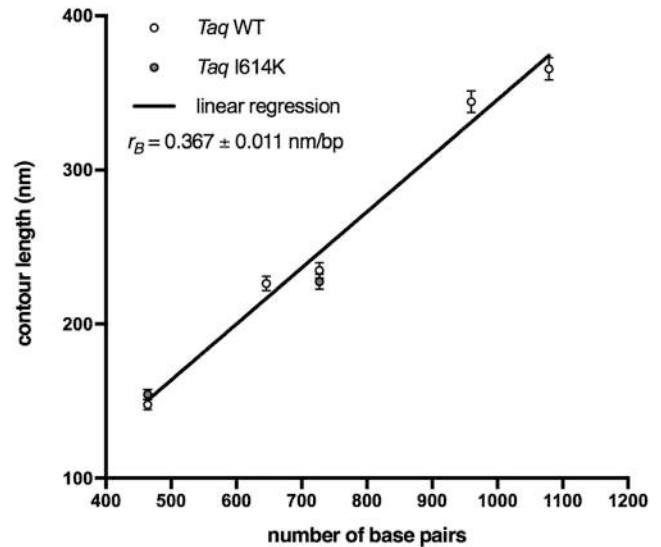


FIGURE 4 DNA molecules from WT and I614K *Taq* pol retain canonical B conformation. Measured contour length values are plotted versus the number of basepairs of each DNA population analyzed (464, 646, 727, 960, and 1079), produced either by WT or I614K *Taq* polymerases. The linear fit ( $R^2 = 0.9851$ ) exhibits a slope ( $r_B = 0.367 \pm 0.011$  nm/bp) close to the one typical of B DNA conformation. The length of the molecules produced by the mutated I614K *Taq* pol agrees with the length of the corresponding molecules produced by the WT *Taq* pol, within the error. The number of analyzed 464-, 646-, 727-, 960-, and 1079-bp WT *Taq* pol molecules is 146, 92, 74, 67, and 46, respectively; the number of analyzed 464- and 727-bp I614K *Taq* pol molecules is 176 and 47, respectively.

The slope of the contour length versus number-of-basepairs curve represents the rise per residue  $r$  of the molecules. We found  $r_B = 0.367 \pm 0.011$  nm/bp, which is close to the value for the B form of DNA ( $r_B = 0.34$  nm/bp), and significantly larger than the rise per residue of the A form ( $r_A = 0.26$  nm/bp). Notably, the intercept  $c$  of the fitting line in Fig. 4 is negative ( $c = -21.3 \pm 7.2$  nm), witness to a reduction of the contour length of the molecules, irrespective of the number of basepairs, of  $\sim 60$  bp in the B form. The reduction of the length of DNA molecules imaged in air is commonly observed (32,33,41), and the reason is still debated, although the prevalent hypothesis is that of a partial transition from B to A conformation. Such transition is often assessed based on the comparison of the measured contour length to the one expected for the B form, by considering only one molecular length (i.e., a given number of basepairs). This procedure, however, cannot capture accurately the scaling of the contour length with the number of basepairs, especially in those cases when a systematic alteration of the contour length is not attributable to a distributed, yet partial, transition. In the case of this study, we have evidence that the scaling of the DNA lengths, despite a systematic shortening, is the one typical of the B form (Fig. 4); we argue therefore that the constant shortening must be well localized within the molecule, which is at odds with the idea of a uniformly distributed shortening as expected by

a uniform (yet only partial) B to A transition. Recently, Japaridze et al. (32) reported a similar evidence of molecular shortening, and by means of tip-enhanced Raman spectroscopy they were able to localize the shortened DNA tracts at the molecules' free ends. We have carefully checked the calibration of our instrument, and we exclude this as the reason for the observed shortening (data not shown).

Reference DNA molecules synthesized by the I614K *Taq* pol have also been characterized (for a few selected lengths), and the measured lengths agree within error with those of the WT *Taq* pol, indicating that there is no alteration of DNA synthesized by the mutant *Taq* polymerase (Fig. 4). Our data suggest therefore that reference DNA molecules (WT and I614K *Taq* pol) are in the B-form, although there are shortened domains within the molecules. These samples represent the controls for the investigation of the effects of ribonucleotide incorporation. The latter have been assessed first by looking at changes of the contour length of the molecules upon ribonucleotide incorporation.

Interestingly, when comparing RC-DNA samples (464, 646, 727, and 960 bp) to their reference molecules without ribonucleotides, we observed a systematic shortening, except in the case of the 960-bp population (see Figs. 5 and S4 for the distribution of measured length values). We

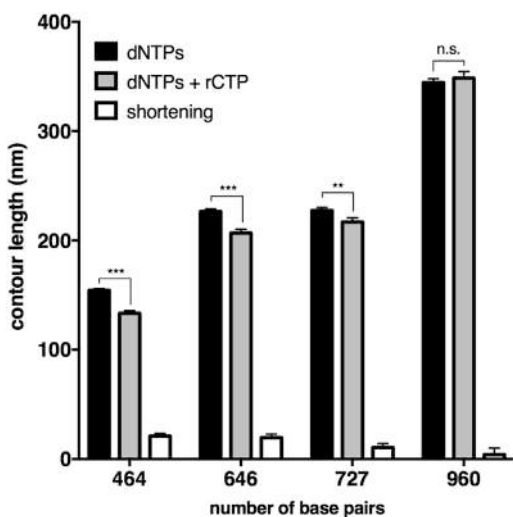


FIGURE 5 The incorporation of rCTPs induces shortening of DNA molecules. Solid bars represent the mean contour length of four different sets of molecules, produced with dNTPs or with the addition of rCTP. Open bars represent the difference in contour length (shortening) observed upon ribonucleotide incorporation. In the case of 464-, 646-, and 727-bp populations, the shortening of the contour length is significant according to the two-tailed *t*-test (with  $p \leq 0.001$ , 0.001, and 0.010, respectively), and this can be attributed to ribonucleotide incorporation. The 960-bp sample did not show a significant decrease in length ( $p = 0.50$ ). Error bars represent the combination of the standard deviation of the mean and the calibration error, as explained in Materials and Methods. The number of analyzed 464-, 646-, 727-, and 960-bp dNTPs/dNTPs+rCTP molecules is 176/157, 92/92, 47/57, and 61/26, respectively. All plotted values are reported in Table S1.

attribute the shortening of the contour length to the presence of rCTP. In fact, apart from the rCTP incorporation, nothing else is different from the control DNA molecules; moreover, the molecules generated by the I614K *Taq* pol have been shown to be equivalent in terms of length to the ones from the WT *Taq* (Fig. 4). We also exclude that the shortening effect is due to increased truncation of PCR products when ribonucleotides are present in the template DNA strand: the primer extension assay described above demonstrated that the I614K *Taq* polymerase efficiently bypasses embedded rCMP, without prematurely ending the synthesis reaction (see Fig. S2 and Supporting Materials and Methods). The measured length differences between DNA and RC-DNA molecules are all significant according to the two-tailed *t*-test, with the exception of the 960-bp DNA sample that is not significant. Indeed, this is the sample with the lowest expected percentage of basepairs containing an rCMP (1.8%, and reported in Table 1) that was determined by Eq. 2, which considers the GC content and the ribonucleotide incorporation frequency. As for the others, we expect a 3.1% of basepairs containing a ribonucleotide in the 464-bp, 2.3% in the 646-bp, and 3.0% in the 727-bp molecules (Table 1). These data suggest that the number of embedded ribonucleotides could be crucial to induce detectable alterations of the contour length; however, there seems to be no clear correlation of the contour length shortening with the original GC content (reported in Table 1), especially when comparing the 646- and 727-bp samples (the shortening is more pronounced in 646-bp RC-DNAs, despite the smaller GC content). In addition to the absolute amount of GC pairs, it is important to consider their spatial distribution along the molecules (see Fig. S5 for a graphical representation of the distribution of GCs). We notice that in the case of the 646-bp sequence, the majority of available positions for rCTP incorporation consist of single bases, and that G or C clusters contain a maximum of three adjacent bases (as detailed in Table 1). Although the I614K *Taq* polymerase could be able to insert consecutive ribonucleotides, this would be a very inefficient and unfavorable reaction (35). As a consequence, despite the higher expected quantity of rCTP in the 727 bp, this sample probably presents a lesser degree of incorporation. In its sequence, there are actually fewer single positions available, and more, and longer, GC clusters, made of two to six consecutive C or G (Table 1).

Because double-stranded RNA molecules are known to be in the A form (42,43), and RNA-containing oligonucleotides have been shown to undergo a partial B to A transition (19,21), one can tentatively estimate an apparent fraction of basepairs that underwent a B to A transition upon rCTP incorporation, assuming that whenever an rCTP is incorporated, the hosting basepair switches from the B to the A form. The extent of such transition is calculated using the equations given in Materials and Methods. Fractions of the B-to A apparent transitions are 0.67, 0.41, 0.22, and

**TABLE 1** Features of RC-DNA Molecules

bp	%GC (%)	Total Number of G+C	Number of Clusters with 6–4 G or C	Number of Clusters with 2–3 G or C	Number of Single G or C	Total Number of rCTP Incorporated	%rCTP (%)
464	58	269	4	50	143	14	3.1
646	43	279	0	51	159	15	2.3
727	57	413	5	77	224	22	3.0
960	34	325	3	45	215	17	1.8

GC content percentage, the GC clustering degree, and the estimated rCTP incorporation (absolute and percentage content) in the investigated DNA sequences. Clusters consist of consecutive nucleotides of the same species; here we have reported the sum of G and C clusters in one DNA strand, which is identical in the other complementary strand. Clusters are divided into two main groups: one made from 6 to 4 units, the other from 2 to 3. The number of isolated G or C present in the sequence is also reported. The total number of rCTP incorporated represents the estimated amount of rCTP incorporated into the molecule (with the percentage value) calculated using Eq. 2, as described in [Materials and Methods](#).

0.05 for 464-, 646-, 727-, and 960-bp fragments, respectively. These estimated fractions are surprisingly high, because the ribonucleotide incorporation ratio (one rCTP every 19 bp) would lead to a B to A transition fraction up to one order-of-magnitude smaller. A reasonable explanation could be that the incorporation of one rCTP triggers the transition from the B to A form not only in correspondence to that single basepair, but also along the surrounding nucleotides (a B/A junction), extending across several tens of basepairs (corresponding to a few cooperative lengths,  $\sim 10$  basepairs each (44,45)). At present, however, we do not have clear evidence that a (partial) B to A transition is the leading mechanism behind the observed shortening of DNA molecules upon ribonucleotide incorporation.

To further investigate the nature of the rCTP action on the DNA structure, we have investigated the mesoscopic conformation and elasticity of RC-DNAs. To this purpose, we have characterized the distribution of bending angles along the molecules' backbones as a function of the curvilinear separation  $L$ , as well as the scaling of the mean squared end-to-end distance  $\langle R^2 \rangle_{2D}$  (Eq. 1), as described in the [Materials and Methods](#). Equation 1 is valid for molecules equilibrated on two dimensions, where  $P$  refers to the persistence length of the molecules in the three dimensions, i.e., in the bulk solution. Noticeably, the ratio  $(R/L)^2$  depends only on the ratio  $P/L$ , which also represents the asymptotic scaling of the normalized curves at large distances. The measured ratio of higher moments of the angle distribution  $\langle \theta^4 \rangle / \langle \theta^2 \rangle^2$  is close to three (see [Supporting Materials and Methods](#) and [Fig. S6](#)), which is the theoretical WLC value for full equilibration of the molecules in two dimensions (25). The values of  $P$  for DNA and RC-DNA samples are obtained by fitting Eq. 1 to the  $R^2$  versus  $L$  curves (the representative curve for the 464-bp sample is shown in [Fig. S7](#)). Typically, the WLC model fitted with good accuracy the experimental data across the 0–120-nm distance range. [Fig. 6, A–C](#), shows the scaling of the normalized mean squared end-to-end distance  $(R/L)^2$ . The mean squared end-to-end distance  $R^2$  has been normalized by  $L^2$  to better appreciate the change in the slope (i.e., in the persistence lengths  $P$ ) upon incorporation of rCTP, and the extrapolated persistence length values are plotted in [Fig. 6 D](#) and reported in [Table S1](#). First, we

noticed that for the 464- and 727-bp samples (from I614K *Taq* pol) the measured values of the persistence length are higher than the value of  $\sim 50$  nm, typically for DNA molecules with a  $\sim 50\%$  GC content (25,26). However, this is consistent with the fact that high GC content is known to induce stiffening, with an increase of the persistence length (46). Remarkably, the incorporation of ribonucleotides into the molecules with higher GC content (464 and 727 bp) induced a significant shortening of the persistence length, according to the two-tailed  $t$ -test ([Fig. 6 D](#); [Table S1](#)).

The 960-bp sample is the only one not showing any appreciable reduction of the persistence length, in addition to the absence of the shortening of the contour length, as shown previously. However, as for the shortening of contour length, we could not define a clear trend of the persistence length shortening with the GC content, probably because the rCTP incorporation is not simply proportional to the available sites; the latter in turn are not uniformly distributed along the molecules, but present with different degrees of clustering and spatial distribution ([Fig. S5](#); [Table 1](#)).

The molecules containing rCTP seem to be equilibrated to a good extent on the mica surface, and their  $R^2$  versus  $L$  curves can be fitted by the WLC model across a wide range of distances; these evidences suggest that the incorporation of rCTP exerts an influence on the DNA structure that goes well beyond the scale of the single ribonucleotide. In this study, we observe that, upon rCTP incorporation, the structure and conformation of DNA molecules change significantly and on the mesoscopic scale. In particular, the observed reduction of the persistence length  $P$  suggests that ribonucleotides induce a softening of DNA molecules ([Fig. 6 D](#)) in addition to causing a significant shortening ([Fig. 5](#)). The extension of the effects of the rCTP incorporation in dsDNA is remarkable, because one would expect an effective rCTP content of a few percent ([Table 1](#)). The action of a single ribonucleotide, namely its effect on the DNA structure, extends far beyond its linear dimension. Attributing the observed changes of conformational and elastic properties to a B to A transition—based on the fact that RNA is in the A form—is not at all straightforward, and this conclusion would not at present be fully supported by the data. On one side, DNA in the A form in

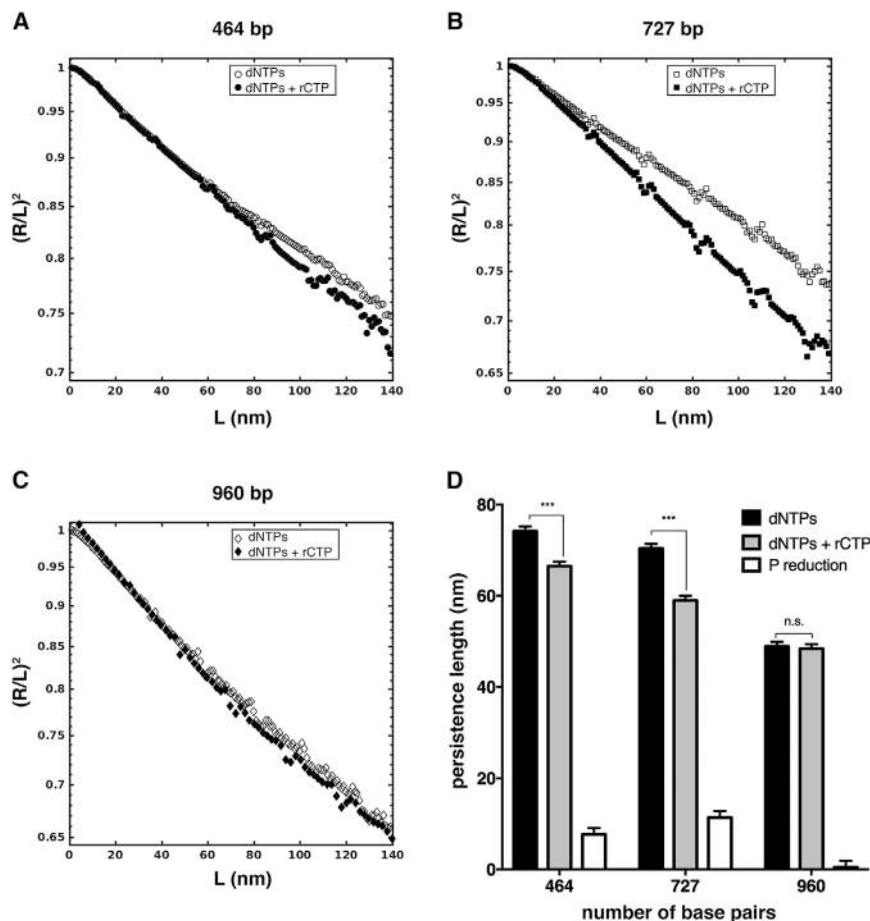


FIGURE 6 rCTP incorporation affects end-to-end distance and persistence length of DNA molecules. (A–C) Shown here is the scaling of the normalized mean squared end-to-end distance  $(R/L)^2$  as a function of the curvilinear distance  $L$  for 464-, 727-, and 960-bp samples. Differences in the slope of the curves are appreciable for 464- and 727 bp, but not for 960 bp. In (D) are represented persistence length values of the same samples (solid bars): 464- and 727 bp showed extremely significant decrease in  $P$  upon rCTP incorporation (with  $p \leq 0.001$ , according to the two-tailed  $t$ -test), whereas the 960-bp samples did not show any difference ( $p = 0.10$ ). Open bars represent the persistence length shortening between the two compared samples. See [Materials and Methods](#) for details on error bars. The number of analyzed 464-, 727-, and 960-bp dNTPs/dNTPs+rCTP molecules is 176/157, 47/57, and 61/26, respectively. All plotted values are reported in [Table S1](#).

solution is reported to be stiffer than in the B form (47), at odd with our observations; on the other side, DNA in the A form deposited on mica at different ethanol concentrations showed decreasing values of the persistence length at increasing B to A transition fractions, a trend similar to that observed by us, at least in the general terms. Concerning the published single-molecule studies on the bending rigidity (persistence length) of ribonucleotide-containing DNA molecules, including double-stranded RNA, either stiffer (23) or softer and slightly stiffer molecules (22) have been reported, depending on the sequence context and the positions of ribonucleotides. It emerged that besides the absolute content, which determines the extent of the incorporation, the distribution of ribonucleotide along the molecular backbone also is important in determining structural changes (22). Chiu et al. (22) concluded that the incorporation of ribonucleotides locally induces a significant (torsional) distortion of the sugar-phosphate backbone, affecting the elastic, and structural properties of the molecule as a whole. Relating such a torsional alteration to the observed mesoscopic changes of the DNA molecules conformation, namely the shortening of the molecules, and the reduction of the persistent length, is not trivial. Intuitively, a torsional alteration, especially if distributed along

the molecular backbone, even if not uniformly, can lead to a shortening of the molecule. It was recently proposed that the rotational stiffening caused by the ribonucleotide-induced torsion of the sugar-phosphate backbone can hamper the rotational fluctuations, resulting in bending stiffening, rather than the opposite, at least as long as the electrostatic component of the persistence length is concerned (48). Under the hypothesis that the incorporation of ribonucleotides induces the formation of B/A junctions, which are known to be significantly bent (49), one could also consider the role of these bent domains in decreasing the apparent persistence length of DNA molecules (50). Further investigations are therefore required, by means of both experimental techniques and structural simulations, to unravel the fine mechanisms underlying the observed structural and conformational changes in DNA molecules upon ribonucleotide incorporation. In particular, the influence of the base sequence should be directly investigated and assessed, at similar GC content.

## CONCLUSIONS

In this work, we present, to our knowledge, a novel approach to study the effects of ribonucleotides

incorporation into DNA. Our synthesis strategy exploited the use of a mutant version of the *Taq* polymerase (I614K) in PCR reactions allowing us to generate populations of long (several hundreds of basepairs) RC-DNAs, which are more biologically relevant than short oligonucleotides. In particular, we have studied the ribonucleotides-induced changes in the structural and conformational properties of DNA at the single-molecule level by means of atomic force microscopy. Our systematic and statistical study highlighted the impact of ribonucleotides intrusions on the DNA double helix. We found that their presence alters DNA structural properties. All the investigated DNA molecules, with the exception of the longest molecules with the lowest GC content (960 bp), showed a significant reduction in the contour length upon rCTP introduction compared to their cognate molecules without rCTP. As observed in RNA molecules, it is the presence of the extra hydroxyl group on ribonucleotides that leads to a compaction of the DNA backbone. From the biochemical parameters of the I614K *Taq* polymerase (38) we estimated an incorporation frequency of 1/19 (rCTP/dCTP), representing 2–3% of the total number of basepairs. By contrast, the calculated apparent B to A transition fraction ranges between 20 and 60%. Although we do not have concluding evidence that this structural transition is the mechanism triggered by the ribonucleotide insertion, these figures suggest that the ribonucleotide effect on DNA structure extends remarkably on a scale that goes well beyond the typical dimension of a single ribonucleotide, affecting the full length of the molecule. Together with the shortening, RC-DNA molecules become more flexible, as demonstrated by the reduction of the persistence length. This is another indication that the effect of even a tiny fraction of incorporated ribonucleotides affects the DNA molecules on a global scale. A deeper understanding of the observed phenomena would require a precise quantification of the extent of rCTP incorporation, as well as of their spatial distribution along the RC-DNA molecules. Nevertheless, rCTP incorporation is nearly controlled by the number of positions available, given by the GC content.

In our system, control DNA molecules retain their native B conformation, supporting the idea that changes upon ribonucleotide introduction are likely to occur also in vivo. Along the genome of living cells there are hotspots of ribonucleotide incorporation, and the most frequently incorporated ribonucleotide is rCTP (36,37). We speculate that the induced structural and conformational alterations can contribute to the negative outcome of ribonucleotide persistence in DNA. These alterations could be easily transferred to DNA transactions that rely on structure recognition, such as protein binding. For instance, it is reported that ribonucleotides prevent nucleosome assembly on DNA (15), probably reshaping their positioning. Therefore, our strategy to study the effect of ribonucleotide incorporation of long supported DNA fragments could contribute to a better un-

derstanding of their harmful consequences upon genome stability.

## SUPPORTING MATERIAL

Supporting Materials and Methods, eight figures, and one table are available at [http://www.biophysj.org/biophysj/supplemental/S0006-3495\(17\)30811-1](http://www.biophysj.org/biophysj/supplemental/S0006-3495(17)30811-1).

## AUTHOR CONTRIBUTIONS

M.M.-F., F.L., and A.P. conceived the study and designed the experiments. A.M. and A.P. performed the main experiments and analyzed the data. E.M. and E.C. performed the control experiment reported in Fig. S2. A.M. and A.P. wrote the manuscript. M.M.-F. and F.L. revised the manuscript. All authors participated in scientific discussions.

## ACKNOWLEDGMENTS

A.M. thanks Francesca Borghi for support in AFM imaging, and Barbara Sciandrone for support in radioactive DNA dialysis. We thank Prof. A. Aliverti and Prof. P. Plevani for critical discussions, and G. Maga for support in the control experiments.

A.P. thanks the Department of Physics of the University of Milano for financial support under the project “Piano di Sviluppo dell’Ateneo per la Ricerca 2014. Linea B: Supporto per i Giovani Ricercatori”. The M.M.-F. lab is funded by AIRC (no. 15631), MIUR, and Telethon (GGP15227). F.L. is funded by AIRC and Fondazione Cariplo (TRIDEO 2014 Id. 15724) and Fondazione CARIPO (RIF. 2013-0798). E.M. and E.C. are supported by AIRC individual grant MFAG2016 18811.

## REFERENCES

- Gilbert, W. 1986. Origin of life: the RNA world. *Nature*. 319:618.
- Li, Y., and R. R. Breaker. 1999. Kinetics of RNA degradation by specific base catalysis of transesterification involving the 2'-hydroxyl group. *J. Am. Chem. Soc.* 121:5364–5372.
- Hiller, B., M. Achleitner, ..., A. Roers. 2012. Mammalian RNase H2 removes ribonucleotides from DNA to maintain genome integrity. *J. Exp. Med.* 209:1419–1426.
- Nick McElhinny, S. A., B. E. Watts, ..., T. A. Kunkel. 2010. Abundant ribonucleotide incorporation into DNA by yeast replicative polymerases. *Proc. Natl. Acad. Sci. USA*. 107:4949–4954.
- Nick McElhinny, S. A., D. Kumar, ..., T. A. Kunkel. 2010. Genome instability due to ribonucleotide incorporation into DNA. *Nat. Chem. Biol.* 6:774–781.
- Sparks, J. L., H. Chon, ..., P. M. Burgers. 2012. RNase H2-initiated ribonucleotide excision repair. *Mol. Cell.* 47:980–986.
- Ghodegaonkar, M. M. M., F. Lazzaro, ..., J. Jiricny. 2013. Ribonucleotides misincorporated into DNA act as strand-discrimination signals in eukaryotic mismatch repair. *Mol. Cell.* 50:323–332.
- Lujan, S. A., J. S. Williams, ..., T. A. Kunkel. 2013. Ribonucleotides are signals for mismatch repair of leading-strand replication errors. *Mol. Cell.* 50:437–443.
- Kim, N., S. N. Huang, ..., S. Jinks-Robertson. 2011. Mutagenic processing of ribonucleotides in DNA by yeast topoisomerase I. *Science*. 332:1561–1564.
- Conover, H. N., S. A. Lujan, ..., J. L. Argueso. 2015. Stimulation of chromosomal rearrangements by ribonucleotides. *Genetics*. 201:951–961.

11. Lazzaro, F., D. Novarina, ..., M. Muzi-Falconi. 2012. RNase H and postreplication repair protect cells from ribonucleotides incorporated in DNA. *Mol. Cell.* 45:99–110.
12. Reijns, M. A. M., B. Rabe, ..., A. P. Jackson. 2012. Enzymatic removal of ribonucleotides from DNA is essential for mammalian genome integrity and development. *Cell.* 149:1008–1022.
13. Cerritelli, S. M., and R. J. Crouch. 2009. Ribonuclease H: the enzymes in eukaryotes. *FEBS J.* 276:1494–1505.
14. Crow, Y. J., A. Leitch, ..., A. P. Jackson. 2006. Mutations in genes encoding ribonuclease H2 subunits cause Aicardi-Goutières syndrome and mimic congenital viral brain infection. *Nat. Genet.* 38:910–916.
15. Hovatter, K. R., and H. G. Martinson. 1987. Ribonucleotide-induced helical alteration in DNA prevents nucleosome formation. *Proc. Natl. Acad. Sci. USA.* 84:1162–1166.
16. Egli, M., N. Usman, and A. Rich. 1993. Conformational influence of the ribose 2'-hydroxyl group: crystal structures of DNA-RNA chimeric duplexes. *Biochemistry.* 32:3221–3237.
17. Ban, C., B. Ramakrishnan, and M. Sundaralingam. 1994. A single 2'-hydroxyl group converts B-DNA to A-DNA. Crystal structure of the DNA-RNA chimeric decamer duplex d(CCGGC)r(G)d(CCGG) with a novel intermolecular G-C base-paired quadruplet. *J. Mol. Biol.* 236:275–285.
18. Wahl, M. C., and M. Sundaralingam. 2000. B-form to A-form conversion by a 3'-terminal ribose: crystal structure of the chimera d(CCAC TAGTG)r(G). *Nucleic Acids Res.* 28:4356–4363.
19. Jaishree, T. N., G. A. van der Marel, ..., A. H. Wang. 1993. Structural influence of RNA incorporation in DNA: quantitative nuclear magnetic resonance refinement of d(CG)r(CG)d(CG) and d(CG)r(C)d(TAGCG). *Biochemistry.* 32:4903–4911.
20. Chou, S. H., P. Flynn, ..., B. Reid. 1991. High-resolution NMR studies of chimeric DNA-RNA-DNA duplexes, heteronomous basepairing, and continuous base stacking at junctions. *Biochemistry.* 30:5248–5257.
21. DeRose, E. F., L. Perera, ..., R. E. London. 2012. Solution structure of the Dickerson DNA dodecamer containing a single ribonucleotide. *Biochemistry.* 51:2407–2416.
22. Chiu, H.-C., K. D. Koh, ..., F. Storici. 2014. RNA intrusions change DNA elastic properties and structure. *Nanoscale.* 6:10009–10017.
23. Abels, J. A., F. Moreno-Herrero, ..., N. H. Dekker. 2005. Single-molecule measurements of the persistence length of double-stranded RNA. *Biophys. J.* 88:2737–2744.
24. Herrero-Galán, E., M. E. Fuentes-Perez, ..., J. R. Arias-Gonzalez. 2013. Mechanical identities of RNA and DNA double helices unveiled at the single-molecule level. *J. Am. Chem. Soc.* 135:122–131.
25. Rivetti, C., M. Guthold, and C. Bustamante. 1996. Scanning force microscopy of DNA deposited onto mica: equilibration versus kinetic trapping studied by statistical polymer chain analysis. *J. Mol. Biol.* 264:919–932.
26. Podestà, A., M. Indrieri, ..., D. Dunlap. 2005. Positively charged surfaces increase the flexibility of DNA. *Biophys. J.* 89:2558–2563.
27. Lia, G., M. Indrieri, ..., D. Dunlap. 2008. ATP-dependent looping of DNA by ISWI. *J. Biophotonics.* 1:280–286.
28. Podestà, A., L. Imperadori, ..., D. Dunlap. 2004. Atomic force microscopy study of DNA deposited on poly L-ornithine-coated mica. *J. Microsc.* 215:236–240.
29. Sambrook, J., and D. W. Russell. 2006. Alkaline agarose gel electrophoresis. *CSH Protoc.*:2006 Jun 1;2006(1). pii: pdb.prot4027. <http://dx.doi.org/10.1101/pdb.prot4027>.
30. Meroni, A., F. Lazzaro, ..., A. Podestà. 2017. Characterization of structural and configurational properties of DNA by atomic force microscopy. *In* Methods in Molecular Biology. J. M. Walker, editor. Humana Press, New York, NY.
31. Usov, I., and R. Mezzenga. 2015. FiberApp: an open-source software for tracking and analyzing polymers, filaments, biomacromolecules, and fibrous objects. *Macromolecules.* 48:1269–1280.
32. Japaridze, A., D. Vobornik, ..., G. Dietler. 2016. Toward an effective control of DNA's submolecular conformation on a surface. *Macromolecules.* 49:643–652.
33. Rivetti, C., and S. Codeluppi. 2001. Accurate length determination of DNA molecules visualized by atomic force microscopy: evidence for a partial B- to A-form transition on mica. *Ultramicroscopy.* 87:55–66.
34. Chien, A., D. B. Edgar, and J. M. Trela. 1976. Deoxyribonucleic acid polymerase from the extreme thermophile *Thermus aquaticus*. *J. Bacteriol.* 127:1550–1557.
35. Patel, P. H., and L. A. Loeb. 2000. Multiple amino acid substitutions allow DNA polymerases to synthesize RNA. *J. Biol. Chem.* 275:40266–40272.
36. Koh, K. D., S. Balachander, ..., F. Storici. 2015. Ribose-seq: global mapping of ribonucleotides embedded in genomic DNA. *Nat. Methods.* 12:251–257, 3, 257.
37. Clausen, A. R., S. A. Lujan, ..., T. A. Kunkel. 2015. Tracking replication enzymology in vivo by genome-wide mapping of ribonucleotide incorporation. *Nat. Struct. Mol. Biol.* 22:185–191.
38. Patel, P. H., H. Kawate, ..., L. A. Loeb. 2001. A single highly mutable catalytic site amino acid is critical for DNA polymerase fidelity. *J. Biol. Chem.* 276:5044–5051.
39. Clausen, A. R., S. Zhang, ..., T. A. Kunkel. 2013. Ribonucleotide incorporation, proofreading and bypass by human DNA polymerase  $\delta$ . *DNA Repair (Amst.)*. 12:121–127.
40. Clausen, A. R., M. S. Murray, ..., T. A. Kunkel. 2013. Structure-function analysis of ribonucleotide bypass by B family DNA replicases. *Proc. Natl. Acad. Sci. USA.* 110:16802–16807.
41. Sanchez-Sevilla, A., J. Thimonier, ..., J. Barbet. 2002. Accuracy of AFM measurements of the contour length of DNA fragments adsorbed on mica in air and in aqueous buffer. *Ultramicroscopy.* 92:151–158.
42. Langridge, R., and P. J. Gomas. 1963. The structure of RNA. *Science.* 141:1024.
43. Arnott, S., D. W. L. Hukins, and S. D. Dover. 1972. Optimised parameters for RNA double-helices. *Biochem. Biophys. Res. Commun.* 48:1392–1399.
44. Ivanov, V. I., L. E. Minchenkova, ..., C. Zimmer. 1996. The detection of B-form/A-form junction in a deoxyribonucleotide duplex. *Biophys. J.* 71:3344–3349.
45. Ivanov, V. I., D. Y. Krylov, ..., L. E. Minchenkova. 1983. B-A transition in DNA. *J. Biomol. Struct. Dyn.* 1:453–460.
46. Hormeño, S., B. Ibarra, ..., J. R. Arias-Gonzalez. 2011. Mechanical properties of high-G-C content DNA with A-type base-stacking. *Biophys. J.* 100:1996–2005.
47. Charney, E., H.-H. Chen, and D. C. Rau. 1991. The flexibility of A-form DNA. *J. Biomol. Struct. Dyn.* 9:353–362.
48. Dobrynin, A. V. 2005. Electrostatic persistence length of semiflexible and flexible polyelectrolytes. *Macromolecules.* 38:9304–9314.
49. Selsing, E., R. D. Wells, ..., S. Arnott. 1979. Bent DNA: visualization of a base-paired and stacked A-B conformational junction. *J. Biol. Chem.* 254:5417–5422.
50. Rouzina, I., and V. A. Bloomfield. 1998. DNA bending by small, mobile multivalent cations. *Biophys. J.* 74:3152–3164.

**Biophysical Journal, Volume 113**

**Supplemental Information**

**The Incorporation of Ribonucleotides Induces Structural and Conformational Changes in DNA**

**Alice Meroni, Elisa Mentegari, Emmanuele Crespan, Marco Muzi-Falconi, Federico Lazzaro, and Alessandro Podestà**

# The incorporation of ribonucleotides induces structural and conformational changes in DNA

Alice Meroni<sup>1</sup>, Elisa Mentegari<sup>2</sup>, Emmanuele Crespan<sup>2</sup>, Marco Muzi-Falconi<sup>1,#</sup>, Federico Lazzaro<sup>1,\*</sup>, Alessandro Podestà<sup>3,\*,#</sup>

<sup>1</sup>Dipartimento di Bioscienze, Università degli Studi di Milano, via Celoria 26, 20133 Milano, Italy.

<sup>2</sup>DNA Enzymology & Molecular Virology, Institute of Molecular Genetics IGM-CNR, via Abbiategrosso 207, 27100 Pavia, Italy.

<sup>3</sup>Dipartimento di Fisica and C.I.Ma.I.Na, Università degli Studi di Milano, via Celoria 16, 20133 Milano, Italy.

#Corresponding authors; e-mail: [alessandro.podesta@mi.infn.it](mailto:alessandro.podesta@mi.infn.it), [marco.muzifalconi@unimi.it](mailto:marco.muzifalconi@unimi.it)

\*Co- last authors

## Supplemental Information

### Table of contents

Visualization of PCR products with and without ribonucleotides .....	2
Ribonucleotide bypass by I614K <i>Taq</i> polymerase.....	3
Molecules with irregular shape .....	4
Structural and conformational data for DNA molecules.....	5
Distributions of contour length in DNA and RC-DNA populations.....	6
Spatial distribution of GC positions in the investigated DNA sequences.....	7
Surface equilibration of DNA molecules.....	8
Scaling of the squared end to end distance $R^2(L)$ .....	9
Sequence of DNA molecules .....	10

## Visualization of PCR products with and without ribonucleotides

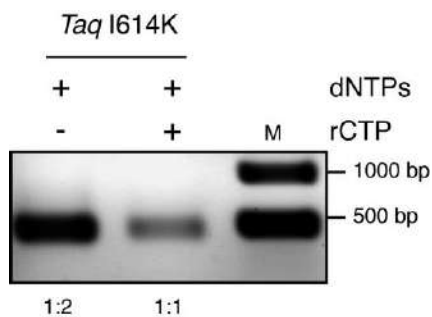


**Figure S1. PCR products with and without rCTP synthesized by I614K *Taq* pol.** PCR are performed in presence of all the four dNTPs either with or without the addition of rCTP. Products are loaded on 1% agarose gel after purification. Bands are then quantified and normalized prior to alkaline gel electrophoresis.

## Ribonucleotide bypass by I614K *Taq* polymerase

**Primer Extension Assay.** The DNA substrate (50 nM) was incubated with different units of I614K *Taq* polymerase (indicated in the figure) in the reaction buffer (10 mM Tris HCl pH 8.0 @ 25°C, 50 mM KCl, 1.5 mM MgCl<sub>2</sub>, 0.08% NP40). Reactions were incubated at 55°C for 10 minutes and stopped by adding standard denaturing gel loading buffer (95% formamide, 10 mM ethylenediaminetetraacetic acid and bromophenol blue), heated at 95°C for 5 min and loaded on a 7M urea 12% polyacrylamide gel. Images were acquired using Molecular Dynamycs Phosphoimager (Typhoon Trio, GE Healthcare, Buckinghamshire, UK).

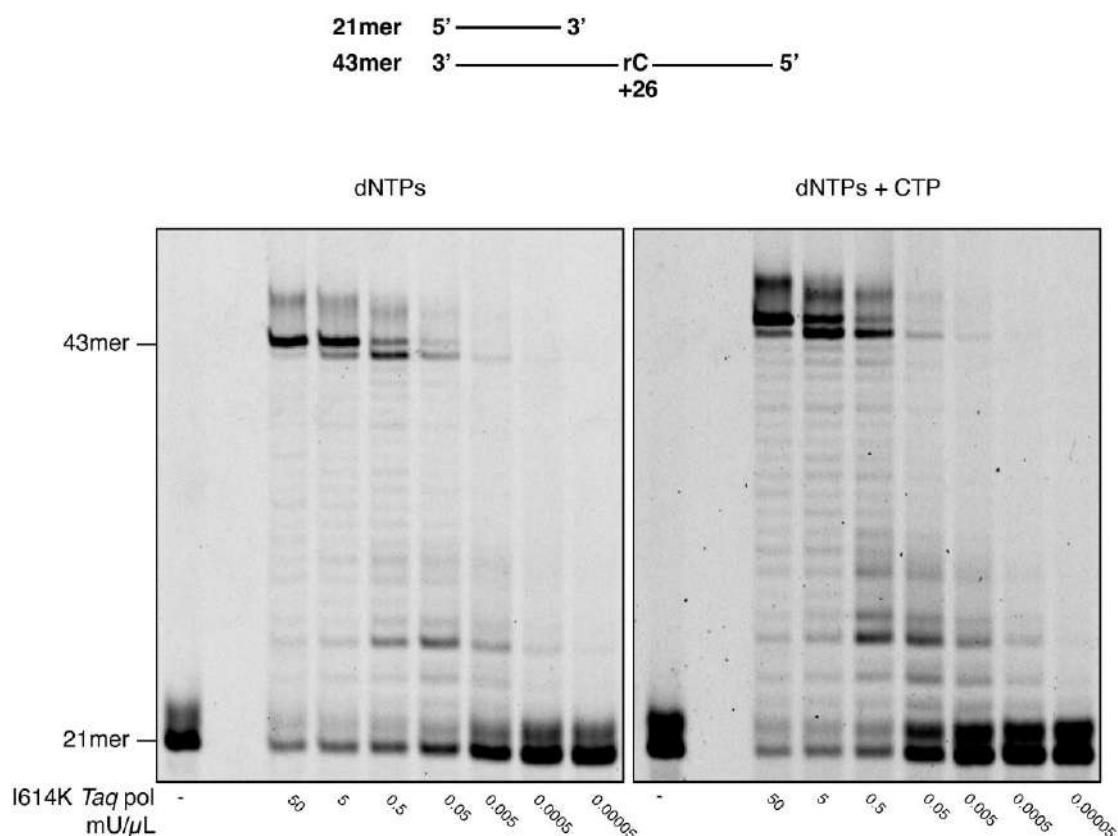


**Fig. S2. I614K *Taq* polymerase is able to bypass rCMP embedded in the DNA template.** The primer extension reactions are performed with decreasing units of I614K *Taq* pol, in presence of dNTPs or dNTPs and CTP. The 21mer primer is labelled at 5' with the ATTO-647N fluorescent dye and annealed to a 43mer template with a rCMP embedded at position +26, as indicated in the top of the panel. The concentration of dNTPs is 10 μM while, in the reaction with the addition of ribonucleotides, dATP, dGTP and dTTP are 10 μM, dCTP is 5 μM and rCTP 40 μM. The I614K *Taq* pol is able to bypass rCMP, replicating the full-length template. It slightly pauses at +25 position, before rCMP, then proceed with the synthesis reaction.

## Molecules with irregular shape

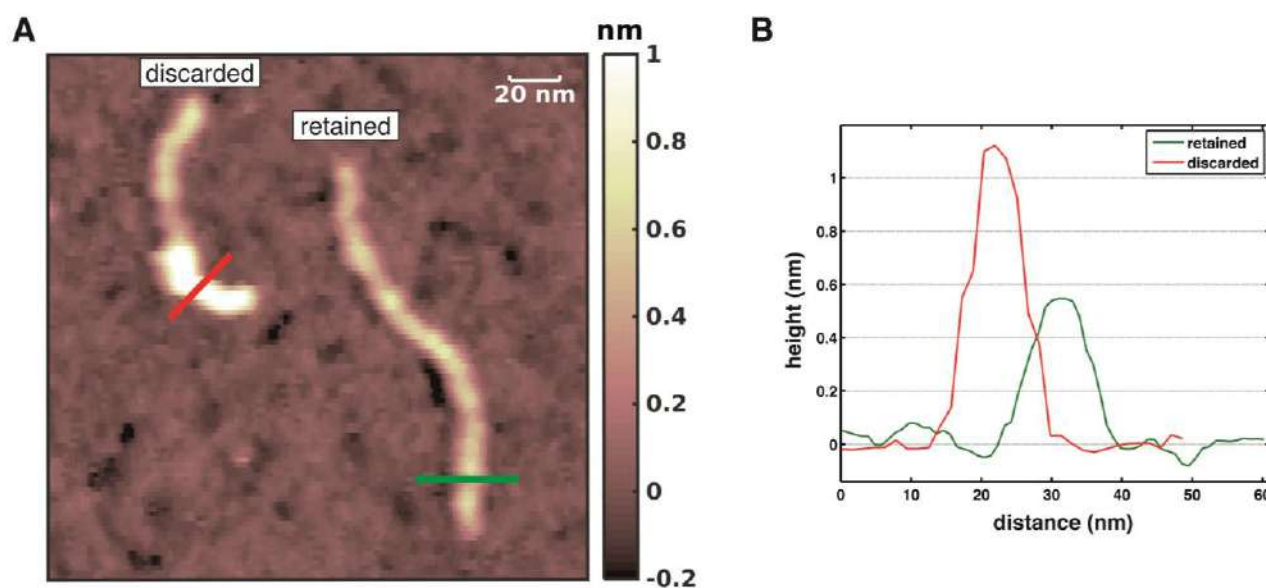


**Figure S3. Molecules with irregular shape are excluded from the analysis based on their height and upon visual inspection.** (A) AFM image of two representative 464 bp molecules, one considered good for the analysis (retained) and the other discarded. The discarded molecule is clearly higher than the retained one, especially at one extremity. In (B) are plotted the height profiles of the indicated lines in panel (A): the red line transects the discarded molecule, while the green line transects the regular molecule, included in the analysis.

## Structural and conformational data for DNA molecules

bp	% GC	$l_0$ (nm)	$\Delta l$ (nm)	P <sub>two-tailed</sub>		P <sub>two-tailed</sub>		dof	N <sub>ref</sub> /N <sub>ribo</sub>
				t-test	P (nm)	$\Delta P$ (nm)	t-test		
464	58	154.3 ± 1.7	-21.0 ± 2.4	≤0.001	74.2 ± 1.0	-7.7 ± 1.4	≤0.001	331	176/157
646	43	226.4 ± 2.5	-19.6 ± 3.4	≤0.001				182	92/92
727	57	227.5 ± 2.7	-10.5 ± 3.8	≤0.01	70.4 ± 1.0	-11.4 ± 1.4	≤0.001	102	47/57
960	34	344.4 ± 3.4	+4.1 ± 6.0	0.50	48.9 ± 1.0	-0.5 ± 1.4	1	85	61/26
1079	35	365.6 ± 3.9							46

**Table S1. Structural data for DNA molecules.** The data plotted in the figures of the main text are here reported. For details on data analysis see the Methods section.  $l_0$  is the average contour length of the reference molecules (typically from the I614K or WT *Taq* pol, when the former was not available).  $\Delta l$  refers to the average length variation upon rCTP introduction (always by I614K *Taq* pol) with respect to the reference molecules. Similarly, the persistence length data ( $P$  and  $\Delta P$ ) are reported. Dof (degrees of freedom) is the sum of the numbers of reference and RC-DNA molecules analyzed (for the contour length estimation) and considered for the two-tailed t-test, minus 2.

## Distributions of contour length in DNA and RC-DNA populations

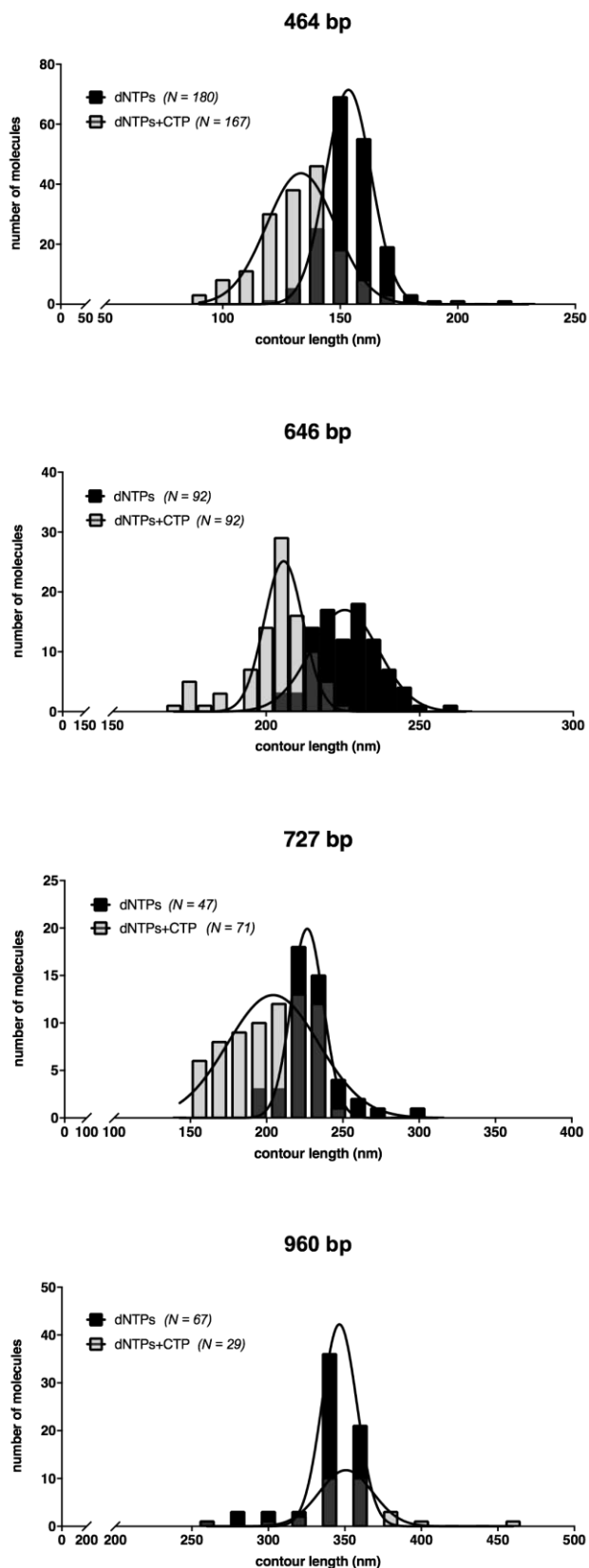


**Figure S4. Distributions of contour length values of DNA and RC-DNA molecules.** Histograms represent the distribution of measured contour length values for each sample. Gaussian fits are also shown. The mean values extracted by the Gaussian fit and the associated errors (calculated as described in the Methods) are reported in Table S1.

## Spatial distribution of GC positions in the investigated DNA sequences

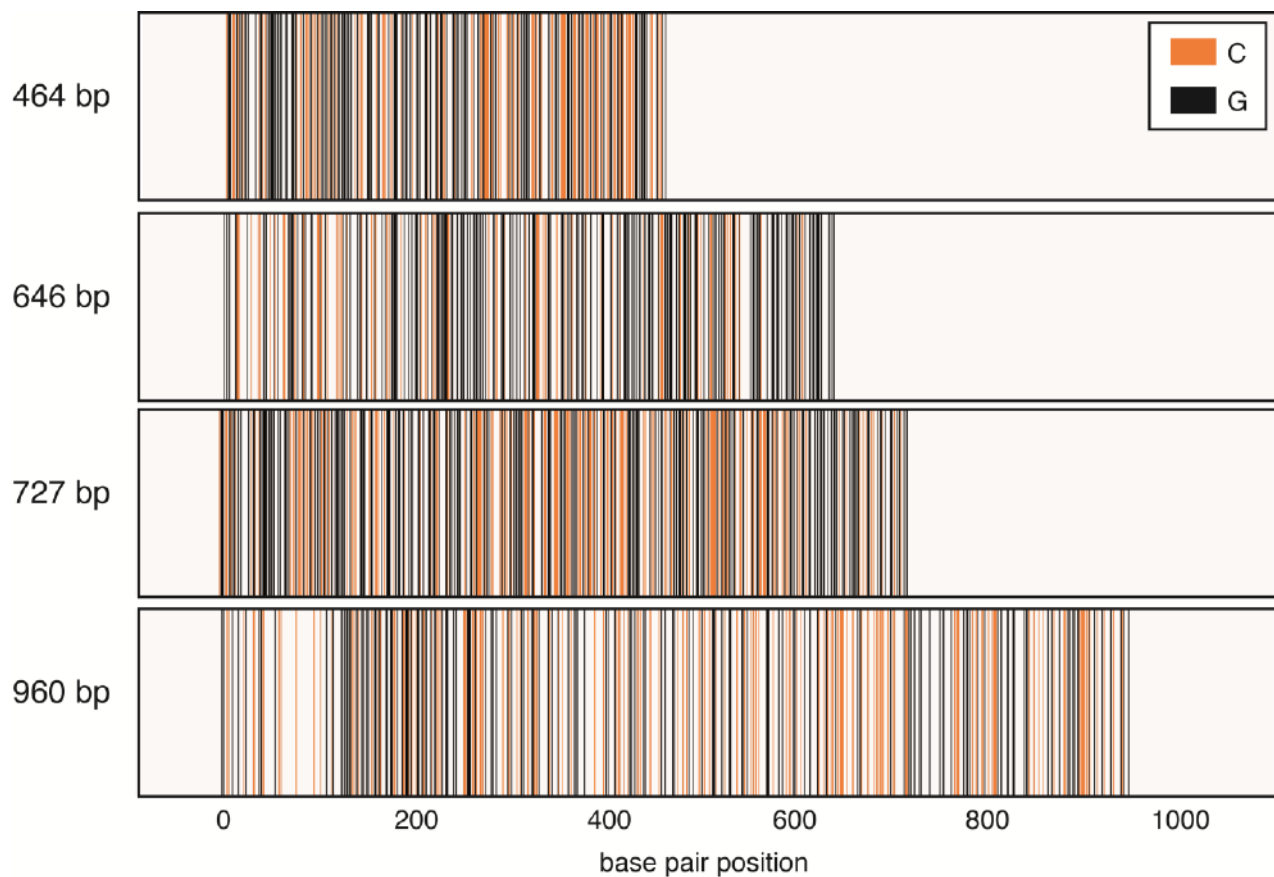


**Figure S5. Spatial distribution of GC positions in the investigated DNA molecules.** Graphical representation of the distribution of GC positions along the molecules sequence. Cs and Gs positions for only one DNA strand are represented as orange and black bars respectively, the GC distribution of the complementary strand is the same but with C in place of G and vice versa. G positions (black bars) are the ones available for rCTP incorporation in one DNA strand, while C positions (orange bars) are available for the complementary DNA strand.

## Surface equilibration of DNA molecules

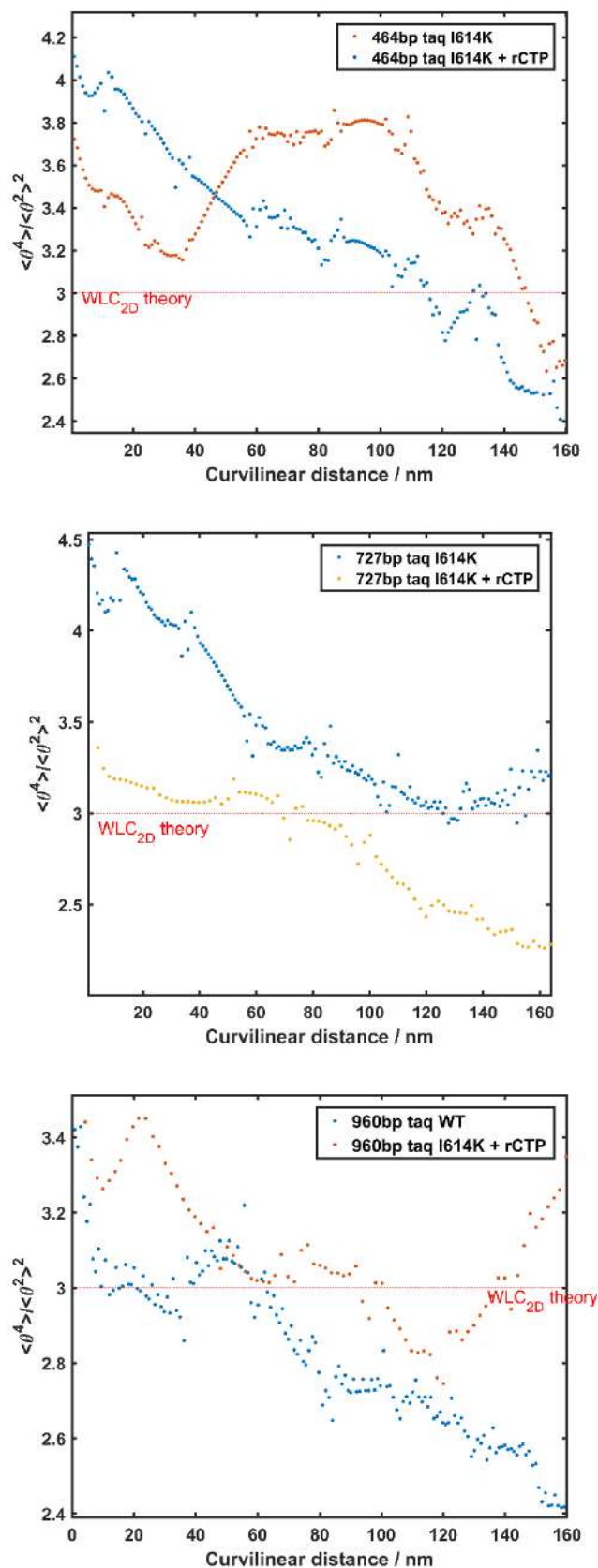


**Figure S6. The ratio of higher moments of the bending angle distribution of studied DNA molecules.** Across a broad distance range, the measured value is close to the ideal value of 3 expected from the WLC theory for fully equilibrated molecules in two dimensions.

## Scaling of the squared end to end distance $R^2(L)$

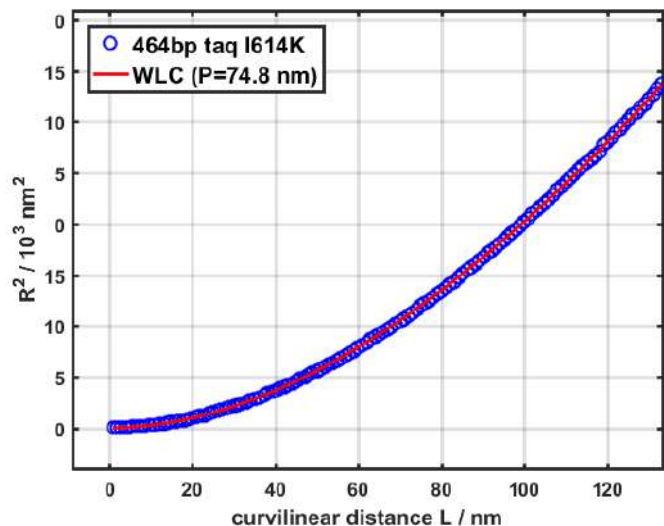


**Figure S7. Representative  $R^2$  vs  $L$  curve, showing the typical scaling of the average squared end-to-end distance with the curvilinear distance along the DNA molecule.** The curve for the 464 bp sample (from I614K *Taq* pol) is shown, with the best WLC fit. The curves of other molecules (727bp and 960bp) are similar. All curves can be fitted accurately on the 0-150 nm distance range. For the sake of better comparison, the normalized curves  $R^2/L^2$  are shown in the main text.

## Sequence of DNA molecules

### 464 bp

TCGGGAAACCTGTCGTGCCAGCTGCATTAATGAATCGGCCAACGCGCGGGGAGAGGCGGTTTGC GTATT  
GGGCGCTCTTCCGCTTCCCTCGCTCACTGACTCGCTGCGCTCGGTCGTTTCGGCTGCGGCGAGCGGTATCAG  
CTCACTCAAAGGCGGTAATACGGTTATCCACAGAATCAGGGGATAACGCAGGAAAGAACATGTGAGCA  
AAAGGCCAGCAAAGGCCAGGAACCGTAAAAAGGCCGCGTTGCTGGCGTTTTTCGATAGGCTCCGCCCC  
CCTGACGAGCATCACAAAAATCGACGCTCAAGTCAGAGGTGGCGAAACCCGACAGGACTATAAAGATA  
CCAGGCGTTTTCCCCCTGGAAGCTCCCTCGTGCGCTCTCCTGTTCCGACCCTGCCGCTTACCGGATACCTG  
TCCGCCTTTCTCCCTTCGGGAAGCGTGGCGCTTTCTCATAGCTCACGCTG

### 646 bp

TAGTTGAAGCATTAGGTCCCAAATTTGTTTACTAAAAACACATGTGGATATCTTGACTGATTTTTCCAT  
GGAGGGCACAGTTAAGCCGCTAAAGGCATTATCCGCCAAGTACAATTTTTTACTCTTCGAAGACAGAAA  
ATTTGCTGACATTGGTAATACAGTCAAATTGCAGTACTCTGCGGGTGTATACAGAATAGCAGAATGGGC  
AGACATTACGAATGCACACGGTGTGGTGGGCCAGGTATTGTTAGCGGTTTGAAGCAGGCGGCAGAAG  
AAGTAACAAAGGAACCTAGAGGCCTTTTGATGTTAGCAGAATTGTCATGCAAGGGCTCCCTATCTACTG  
GAGAATATACTAAGGGTACTGTTGACATTGCGAAGAGCGACAAAGATTTTGTTATCGGCTTTATTGCTCA  
AAGAGACATGGGTGGAAGAGATGAAGGTTACGATTGGTTGATTATGACACCCGGTGTGGGTTTAGATGA  
CAAGGGAGACGCATTGGGTCAACAGTATAGAACCGTGGATGATGTGGTCTCTACAGGATCTGACATTAT  
TATTGTTGGAAGAGGACTATTTGCAAAGGGAAGGGATGCTAAGGTAGAGGGTGAACGTTACAGAAAAG  
CAGGCTGGGAAGCATATTTGAGAAG

### 727 bp

TCGGGAAACCTGTCGTGCCAGCTGCATTAATGAATCGGCCAACGCGCGGGGAGAGGCGGTTTGC GTATT  
GGGCGCTCTTCCGCTTCCCTCGCTCACTGACTCGCTGCGCTCGGTCGTTTCGGCTGCGGCGAGCGGTATCAG  
CTCACTCAAAGGCGGTAATACGGTTATCCACAGAATCAGGGGATAACGCAGGAAAGAACATGTGAGCA  
AAAGGCCAGCAAAGGCCAGGAACCGTAAAAAGGCCGCGTTGCTGGCGTTTTTCGATAGGCTCCGCCCC  
CCTGACGAGCATCACAAAAATCGACGCTCAAGTCAGAGGTGGCGAAACCCGACAGGACTATAAAGATA  
CCAGGCGTTTTCCCCCTGGAAGCTCCCTCGTGCGCTCTCCTGTTCCGACCCTGCCGCTTACCGGATACCTG  
TCCGCCTTTCTCCCTTCGGGAAGCGTGGCGCTTTCTCATAGCTCACGCTGTAGGTATCTCAGTTCGGTGTA  
GGTCGTTTCGCTCCAAGCTGGGCTGTGTGCACGAACCCCCGTTTCAGCCCGACCGCTGCGCCTTATCCGGT  
AACTATCGTCTTGAGTCCAACCCGTAAGACACGACTTATCGCCACTGGCAGCAGCCACTGGTAACAGG  
ATTAGCAGAGCGAGGTATGTAGGCGGTGCTACAGAGTTCTTGAAGTGGTGGCCTAACTACGGCTACACT  
AGAAGGACAGTATTTGGTATCTGCGCTCTGCTGA

**960 bp**

AAAGAGTTACTCAAGAATAAGAATTTTCGTTTTAAAACCTAAGAGTCACTTTAAAATTTGTATACACTTA  
TTTTTTTTATAACTTATTTAATAATAAAAATCATAAATCATAAGAAATTCGCTTATTTAGAAAGTGGCGCG  
CCTCAGCACTGAGCAGCGTAATCTGGAACGTCATATGGATAGGATCCTGCATAGTCCGGGACGTCATAC  
GGATAGCCCGCATAGTCAGGAACATCGTATGGGTAAAAGATGTTAATTAACCCGGGGATCCGTCTAACC  
TCAGAAATAGTGTTGTATATATCATTGTCCGTAATATCATCGTGAAAACCAGTGTCCCTCGTTAATTATTG  
TCTGAATTAGCCATTCTTTAGATTTCAGTGTGAAATATGTAATTAATTTCTTAAATTTTCAGTGATATTTGA  
CTTCTCAATCTTTCGAGAAGCTTCATCTGAGATTTACCATTATTTTCGTTAGCATATATGAGAACTTTAA  
CTTTCGATTAGATAAATTCTGATCCTATTCTGGGTACTAAAGAATCTAAGGCATTTAACAATGGCTCTGTA  
TCATCTACATCAATATTGGGTAAATCAATTGTAAGCATTCTACCTGCGCTCAAACATGCAAAAAGCAAATT  
TGACAAAACCTGTCCAACCTCAGATCTACCCCAAACAATAACAATGTAGTCATTTAACATTTTCTTCACTCC  
ACATATCTGATCTCTTAAATTAGATCCGCGTAAGAATTGTGTATAAAAATGAAAAAATATTGTTGGATTTA  
ATGATTCCTCCCTTTGATGGAGAATCTAACGATAACCGAAAACCTTTCACCCGAAGGTAATAGGTATTGGT  
ATATTAATGTGGTACTATTCTTTTCTTTTCAATGCATGCACTTATGAATTTCCAGTGTAGTGTAGGCCAC  
CCCAACGCCAAAGTTTCTAAGTACTTTAAGCTTCTTAAATGCCGTTTTG

**1079 bp**

GGACGAGGCAAGCTAAACAGATCTATATTACCCTGTTATCCCTAGCGGATCTGCCGGTAGAGGTGTGGT  
CAATAAGAGCGACCTCATACTATACTGAGAAAGCAACCTGACCTACAGGAAAGAGTTACTCAAGAAT  
AAGAATTTTCGTTTTAAAACCTAAGAGTCACTTTAAAATTTGTATACACTTATTTTTTTTATAACTTATTT  
AATAATAAAAATCATAAATCATAAGAAATTCGCTTATTTAGAAAGTGGCGCGCCTCAGCACTGAGCAGCG  
TAATCTGGAACGTCATATGGATAGGATCCTGCATAGTCCGGGACGTCATACGGATAGCCCGCATAGTCA  
GGAACATCGTATGGGTAAAAGATGTTAATTAACCCGGGGATCCGTCTAACCTCAGAAATAGTGTTGTAT  
ATATCATTGTCCGTAATATCATCGTGAAAACCAGTGTCCCTCGTTAATTATTGTCTGAATTAGCCATTCTTT  
AGATTCAGTGTGAAATATGTAATTAATTTCTTAAATTTTCAGTGATATTTGACTTCTCAATCTTTCGAGA  
AGCTTCATCTGAGATTTACCATTATTTTCGTTAGCATATATGAGAACTTTAACTTTCGATTAGATAATTC  
TGATCCTATTCTGGGTACTAAAGAATCTAAGGCATTTAACAATGGCTCTGTATCATCTACATCAATATTG  
GGTAAATCAATTGTAAGCATTCTACCTGCGCTCAAACATGCAAAAAGCAAATTTGACAAAACCTGTCCAAC  
TCAGATCTACCCCAAACAATAACAATGTAGTCATTTAACATTTTCTTCACTCCACATATCTGATCTCTTAA  
ATTAGATCCGCGTAAGAATTGTGTATAAAAATGAAAAAATATTGTTGGATTTAATGATTCCTCCCTTTGAT  
GGAGAATCTAACGATAACCGAAAACCTTTCACCCGAAGGTAATAGGTATTGGTATATTAATGTGGTACT  
ATTCTTTTCTTTTCAATGCATGCACTTATGAATTTCCAGTGTAGTGTAGGCCACCCCAACGCCAAAGTTTC  
TAAGTACTTTAAGCTTCTTAAATGCCGTTTTG

**Figure S8. DNA Sequences.** Sequences of 464, 646, 727, 960 and 1079 bp fragments used in this study.

## Published Paper II

---

### **Characterization of structural and configurational properties of DNA by Atomic Force Microscopy**

Alice Meroni<sup>1</sup>, Alessandro Podestà<sup>2,#</sup>

<sup>1</sup> Dipartimento di Bioscienze, Università degli Studi di Milano, via Celoria 26, 20133 Milano, Italy.

<sup>2</sup> Dipartimento di Fisica and C.I.Ma.I.Na, Università degli Studi di Milano, via Celoria 16, 20133 Milano, Italy.

# Corresponding author; e-mail: [alessandro.podesta@mi.infn.it](mailto:alessandro.podesta@mi.infn.it)

**Book Chapter in Methods in Molecular Biology Genome instability (pp. 557–573). Humana Press, New York, NY. (In Press, 2018)**

[https://doi.org/10.1007/978-1-4939-7306-4\\_37](https://doi.org/10.1007/978-1-4939-7306-4_37)

## Characterization of Structural and Configurational Properties of DNA by Atomic Force Microscopy

Alice Meroni, Federico Lazzaro, Marco Muzi-Falconi,  
and Alessandro Podestà

### Abstract

We describe a method to extract quantitative information on DNA structural and configurational properties from high-resolution topographic maps recorded by atomic force microscopy (AFM). DNA molecules are deposited on mica surfaces from an aqueous solution, carefully dehydrated, and imaged in air in Tapping Mode. Upon extraction of the spatial coordinates of the DNA backbones from AFM images, several parameters characterizing DNA structure and configuration can be calculated. Here, we explain how to obtain the distribution of contour lengths, end-to-end distances, and gyration radii. This modular protocol can be also used to characterize other statistical parameters from AFM topographies.

**Key words** Atomic force microscope/microscopy (AFM), DNA, Mica, DNA conformation

---

### 1 Introduction

Across more than three decades, atomic force microscopy (AFM) has become a technique of choice for the quantitative investigation of biomolecules such as DNA, proteins, and their complexes (for an overview, *see* [1] and references therein). The success of AFM relies on its ability to provide nanometer spatial resolution in  $XY$ , sub-nanometer resolution in  $Z$ , as well as on the capability of imaging biological samples in their physiological conditions. Since the advent of AFM, DNA has been the privileged target of innumerable studies, due to its paramount biological relevance (for a review, *see* [2]). Being a semirigid, charged, strong polyelectrolyte, DNA concentrates in itself a wealth of interesting physics, and has a great potential for nanobiotechnological applications [3, 4]; for this reasons, DNA has been an ideal benchmark for biophysical studies [5–17]. Such studies mostly rely on the statistical characterization of structural and configurational properties of a population of double stranded DNA molecules with fixed length. Several

parameters describe the equilibrium configuration of DNA molecules: contour length, end-to-end distance, rise per residue, radius of gyration, bending angle distribution along the DNA backbone, persistence length, to cite the most important. The statistical mechanics of semirigid polymers describes the distribution of these parameters in equilibrium conditions [5]. Structural and configurational changes of DNA molecule can occur as a consequence of modification of the DNA environment (ionic strength, pH, surface charge density) [6, 7, 18], as well as a consequence of internal changes at the base pairs level (such as mispaired and damaged bases [19, 20]); it follows that high-resolution imaging of DNA molecules, as provided by AFM, can be a very valuable complement of biomolecular studies.

Here, we describe a general protocol for acquiring high-resolution images of DNA molecules, either linear fragments or plasmids, using an atomic force microscope operated in Tapping (or intermittent contact) Mode in air. In Tapping (or intermittent contact) Mode, a sharp oscillating probe periodically touches the surface under investigation [21]. During each gentle tap, lateral forces are minimized, and this provides high spatial resolution and overall noninvasiveness of the measurement. DNA must be well attached to a smooth, flat substrate, so to obtain well-contrasted, well-resolved topographic maps. At the same time, the sample preparation procedure must preserve as much as possible the native DNA characteristics, so to avoid trapping the molecules in out-of-equilibrium configurations. We present all the steps required for extracting quantitative information on the structural and configurational properties of a population of DNA molecules: the preparation of DNA samples on mica surface; the imaging in air by AFM in Tapping Mode; the preparation of images for the analysis and the digitization of the DNA traces; the calculation of selected statistical parameters describing the state of the system (contour length, radius of gyration, and end-to-end distance). The approach here described is rather general and modular, and can be easily implemented to add the calculation of other statistical descriptors of the DNA structural properties, such as the persistence length or the bending angle distribution. The protocol here presented can be easily adapted to other imaging modes and conditions.

---

## 2 Materials

1. Cyanoacrylate glue (such as Loctite 406 or similar).
2. Steel magnetic disks, diameter 11–15 mm, thickness 0.2–0.5 mm.

3. Mica disks of the highest quality grade (V1, ruby muscovite), with thickness 0.2–0.6 mm and diameter 6–12 mm. (*see Notes 1 and 2*).
4. Ethanol (laboratory grade,  $\geq 95\%$  v/v).
5. Eppendorf tubes, 1.5 mL.
6. Plastic tubes, 50 mL.
7. Pipettes with plastic tips (p20, p200, and p1000).
8. Scotch-like adhesive tape (such as the Magic Transparent Tape).
9. Ultrapure MilliQ (typical resistivity  $\rho = 18.2 \text{ M}\Omega \text{ cm}$  at  $25 \text{ }^\circ\text{C}$ ) to prepare samples and solution for AFM imaging.
10. Nitrogen from a reservoir (purity  $\geq 99.999\%$ ).
11. Blotting paper to remove drops of water after rinsing.
12. Tweezers.
13. AFM tips for dynamic (or Tapping) Mode (*see Note 3*).
14. Deposition buffer: 2–5 mM  $\text{MgCl}_2$ , 10 mM NaCl, 10 mM HEPES-Na pH 7.5 in MilliQ  $\text{H}_2\text{O}$  (*see Note 4*).
15. Stock DNA in MilliQ water (at least  $0.05 \text{ ng}/\mu\text{L}$ ).

---

## 3 Methods

### 3.1 Sample Preparation

#### 3.1.1 Substrate Preparation

A mica disk must be glued to a rigid support, whose dimensions and geometry can vary according to the instrument specifications. In most cases this support can be a metal disk with diameter 11–15 mm (at least 2 mm larger than the mica disk) and thickness 0.5–1 mm (*see Note 5*).

1. Clean the mica and the metallic surfaces with ethanol and dry all surfaces using blotting paper.
2. Glue the mica disk to the steel disk using cyanoacrylate-based adhesive (*see Note 6*).
3. Prepare at least 3–4 similar substrates, to be able to prepare many samples in parallel for quickly testing different deposition conditions.

#### 3.1.2 DNA Deposition on Mica

1. Freshly cleave the mica surface to be used for DNA deposition (*see Note 7*).
2. Dilute DNA to a final concentration of  $0.05 \text{ ng}/\mu\text{L}$  in the deposition buffer (so to have typically a 1–2 nM DNA solution) (*see Note 8*).
3. Put a 15–20  $\mu\text{L}$  drop of diluted DNA solution on the freshly cleaved mica (*see Note 9*). Avoid touching the mica surface with the pipette tip.

4. Incubate at room temperature for 2–10 min (longer incubation times will provide higher surface densities of DNA molecules).
5. Gently rinse the sample dropwise several times, using each time up to 1 mL of MilliQ water to remove the exceeding and loosely bound molecules. During the rinsing procedure, keep the sample tilted to help water slipping away.
6. Blot the remaining water placing the corner of a piece of blot paper next to the lower mica disk edge. Make sure the paper is not in contact with the surface.
7. Dry the sample under a gentle stream of clean nitrogen from a reservoir. Set a mild stream flux and keep the nozzle a few centimeter away from the surface (*see Note 10*).
8. The DNA sample is ready to be imaged (*see Note 11* for troubleshooting).

### 3.2 AFM Imaging in Air in Tapping Mode

AFM imaging is aimed at collecting a statistically meaningful number of high-quality, well-contrasted, high-resolution images of DNA molecules, which must then be digitized so to produce a large collection of molecular traces to be further analyzed. The general requirements are:

1. to collect in a single scan a reasonable number of molecules, so to obtain a good statistical sample (several hundred molecules) within 5–10 images;
2. to have a good sampling resolution overall in each image, in order to calculate accurate values of conformational parameters from the molecular traces.

Additional information can be found in **Note 12**.

Typical surface density of molecules on good samples is 15–40 molecules/ $\mu\text{m}^2$ , depending on the DNA length. Imaging of DNA samples in air can be performed in dynamic mode (usually called Tapping Mode, intermittent-contact or oscillating mode). Recently, new imaging modes based on a vertical tip-sample approach have been developed, which provide accurate control of applied force, low-invasiveness in air as well as in liquid and high spatial resolution (described briefly in **Note 13**); these modes could represent an alternative to the Tapping Mode, that we will considered hereafter.

We suggest the following scanning parameters and conditions for imaging DNA in air in Tapping Mode with a well-calibrated instrument (*see Note 14* on AFM calibration):

1. Mount a rigid cantilever for dynamic or Tapping Mode.
2. Set a free oscillation amplitude (target amplitude) of 10 nm or less. Smaller amplitudes provide high-quality and less-invasive imaging conditions, but require very clean, nonadhesive surfaces.

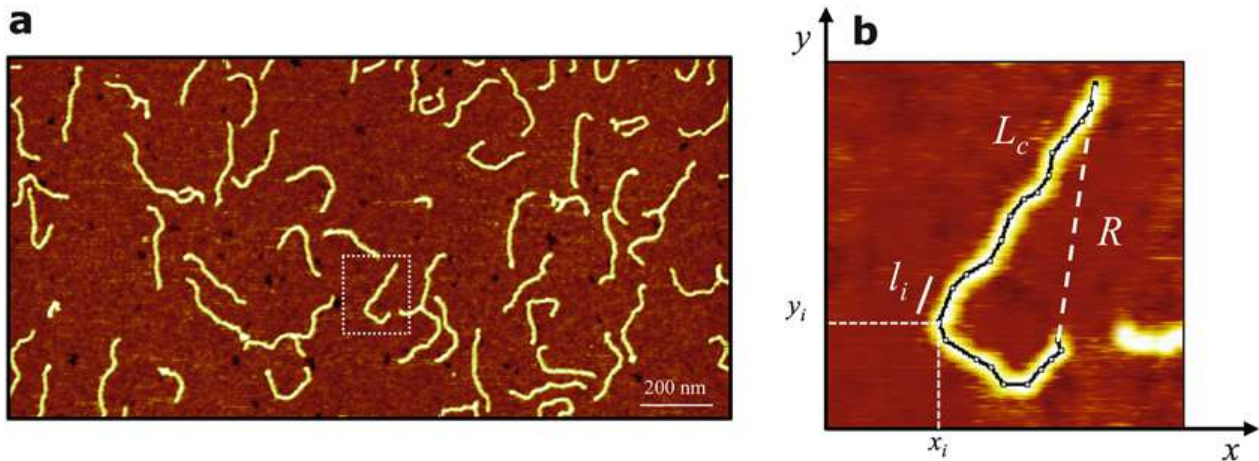
3. Initially, after engaging the tip on the sample surface, adjust the minimal amplitude (force) setpoint to track the surface while keeping the scan size to  $<1$  nm.
4. Initially, set a small scan size (100–500 nm) and optimize the gains and the amplitude setpoint to achieve optimal tracking conditions at the lowest applied force (*see Note 17*). Good tracking is witnessed by a good overlap of topographic profiles in both scan directions. Check the tracking in correspondence of points where a sudden change in surface slope occurs (typically, at the mica–DNA border). Poor tracking results in a loss of contact when the tip is crossing the DNA molecule downhill. Increase gradually the scan size up to  $2\ \mu\text{m} \times 1\ \mu\text{m}$  (aspect-ratio 2:1, *see Note 15*).
5. Set the sampling resolution to  $2048 \times 512$  points (number of points per line  $\times$  number of lines). This choice provides a sampling resolution of 1 nm/pixel and 2 nm/pixel in the fast and in the slow scan directions, respectively.
6. Set the scan rate to 1–4 Hz (*see Note 16*).
7. We suggest acquiring up to five images in each location, according to the simple scheme described below, then to withdraw the tip and engage some 100–500  $\mu\text{m}$  away. Three–four different macroscopic locations will provide several hundred molecules for the statistical analysis. The image acquisition scheme is the following: in each location, acquire the first image with no offsets in  $X$  and  $Y$  directions, at (0,0). Acquire the other images at points  $(X_0,0)$ ,  $(-X_0,0)$ ,  $(Y_0,0)$ ,  $(-Y_0,0)$ , set  $X_0 = 3\ \mu\text{m}$ ,  $Y_0 = 2\ \mu\text{m}$ , so to avoid overlap among the scan areas (*see Note 18*).
8. In order to maintain stable imaging conditions, in particular to minimize capillary adhesion at the tip–sample interface, the AFM head and the sample with the scanning stage can be hosted in a small chamber, inside which a dry  $\text{N}_2$  atmosphere is maintained, with relative humidity below 5%.

Figure 1a shows a typical topographic map of DNA molecules (727 bp) on mica, imaged in air in Tapping Mode, according to the described methodology.

### 3.3 Data Analysis (See Note 19)

#### 3.3.1 Image Preprocessing

Images must be prepared for the analysis, by removing standard artifacts related to the image formation process and by removing high-frequency noise, typically related to the feedback loop operation. Artifacts typically manifest themselves as baselines superimposed to the true topographic profiles. Identification and subtraction of the baseline from each topographic profile is essential for the accurate analysis of the AFM images. Details on the origin of artifacts and on the baseline subtraction procedures are provided in Note 20.



**Fig. 1** 727 bp DNA molecules on mica and details of the single-molecule analysis of AFM images. **(a)** Top-view AFM image showing molecules equilibrated on a mica surface, after gentle dehydration of the sample (the vertical range is 1 nm; heights increase from dark to bright colors). **(b)** A representative DNA molecule with highlighted the relevant parameters used for the characterization of configurational properties, as described in Subheading 3.3

1. Apply a global plane-fitting of the first order to the image, so to get rid of the global tilt of the sample. This operation will level the height values in the image, offering a complete overview of the molecules and of the overall image quality.
2. Apply a line-by-line flattening to the image by subtracting higher-order polynomials (usually up to the third order is enough) through suitable masks excluding features that do not belong to the reference substrate.
3. Check the quality of the flattening by looking at the height histogram of the image: a sharp Gaussian peak centered around the average height  $z_0$  of the substrate (typically  $z_0 = 0$  nm) with FWHM of a few Å should be present; DNA molecules will typically contribute a broader short tail in the height distribution.
4. Apply a median filter (with  $3 \times 3$ , maximum  $5 \times 5$  kernel) to the flattened image, to smooth high-frequency noise.

### 3.3.2 Tracing DNA Molecules

Once the images have been flattened and smoothed, the set of spatial coordinates  $\{x_i, y_i\}_{i=1:N}$  defining the backbone of each molecule for each particular experimental condition (i.e., for each particular length of the DNA molecules) must be determined. Here  $N$  is the total number of molecules in all the AFM images that can be used for the analysis. The tracking can be done manually or by means of (semi)automatic algorithms; some of them are freely available upon request to the developers (*see Note 21*). Here we describe how to manually trace the molecules using ImageJ/Fiji, an open-source software written in Java and supported by a broad community of scientists.

1. Export topographical maps in a format compatible with the ImageJ software (i.e., .tif). Resize the image to include the scanned area only.
2. Import the AFM image into ImageJ/Fiji and define image size and sampling resolution.
  - (a) Define the image size using the command: Image → Scale, and set width and height (in pixels).
  - (b) Define the scale using the command: Analyze → Set Scale, and set the scale (in nanometer).
3. Use the “Segmented Line” command to draw by hand the backbone of the molecule. Keep possibly a constant distance between each point that should not be too far or too close from each other. Consider to maintain a point-to-point distance from 1/2 to 2/3 of the molecule width.
4. Save the molecule trace using the command: “Save As  $XY$  Coordinates”. With this operation ImageJ/Fiji saves an ASCII (.txt) file containing the  $XY$  coordinates of the selected track, columnwise.

An example of the manual tracking of a DNA molecule is shown in Fig. 1b.

### 3.3.3 Basic Structural Analysis

Once the spatial coordinates of each molecule have been obtained, several statistical parameters, describing the structural and configurational properties of DNA in the studied conditions, can be determined (see among the others [5, 6, 8, 9, 11, 15, 22]). First, the contour length of DNA depends on the conformation adopted. Generally, DNA assumes the B-form in physiological conditions, but it can adopt other different conformations, like A- and Z-form. Moreover, DNA can display more open or compact configurations depending on its persistence length, which in turn is sensitively dependent on the ionic strength of the buffer and on the nature of the surrounding ions. Here we focus our attention on a selection of parameters that can be readily obtained by the  $XY$  coordinates: the contour length  $L_c$ , the end-to-end distance  $R$ , the gyration radius  $R_g$  [5, 8, 22, 23]. All these parameters depend on DNA form, base-pair composition, and persistence length; therefore, their accurate statistical determination can provide important information on the structural properties of a DNA population under study. Typically, the configurational parameters are evaluated from digitized traces, and then the average values with standard deviations are calculated from the distributions of these parameters.

1. Calculate  $L_c$ ,  $R$ , and  $R_g$  according to the following equations (refer to Fig. 1b; see also Note 22):

$$L_c = \sum_{i=1}^{N-1} l_i = \sum_{i=1}^{N-1} \sqrt{(x_{i+1} - x_i)^2 + (y_{i+1} - y_i)^2} \quad (1)$$

$$R = \sqrt{(x_N - x_1)^2 + (y_N - y_1)^2} \quad (2)$$

$$R_g = \sqrt{1/N \sum_{i=1}^N r_i^2} \quad (3)$$

where:

$$r_i^2 = (x_i - x_{CM})^2 + (y_i - y_{CM})^2 \quad (4)$$

$$(x_{CM}, y_{CM}) = 1/N \left( \sum_{i=1}^N x_i, \sum_{i=1}^N y_i \right) \quad (5)$$

In Eq. 5 ( $x_{CM}, y_{CM}$ ) are the coordinates of the center of mass of the molecule.

2. Calculate the histograms of the values of the above observables, in order to represent their statistical distributions. Always look first at distributions, and then calculate suitable estimators of the true values and their dispersions.
3. Calculate mean (median) values, standard deviations and standard deviations of the mean, or other suitable statistical estimators, depending on the particular statistical properties of the given observable [5].

An example of the analysis performed on DNA according to the presented protocol is shown in Fig. 2.

---

## 4 Notes

1. The typical substrate used for DNA immobilization is mica, a mineral belonging to the sheet silicate groups. There are many varieties of mica and Muscovite is the most used form. It is constituted by tetrahedral sheets of  $(Si,Al)_2O_5$  ionically linked by a central layer of  $Al_2(OH)_2$  [24]. The net negative charge of the basal oxygen between these double layers is balanced by a layer of hexagonally coordinates cations ( $K^+$  in Muscovite). This negatively charged layer becomes exposed after the standard cleavage procedure and the dissociation of  $K^+$  ions. The most prominent characteristic of mica is the nearly perfect cleavage, due to its intrinsic atomic structure [25]. Due to its chemical composition, the outmost layer of mica after cleavage

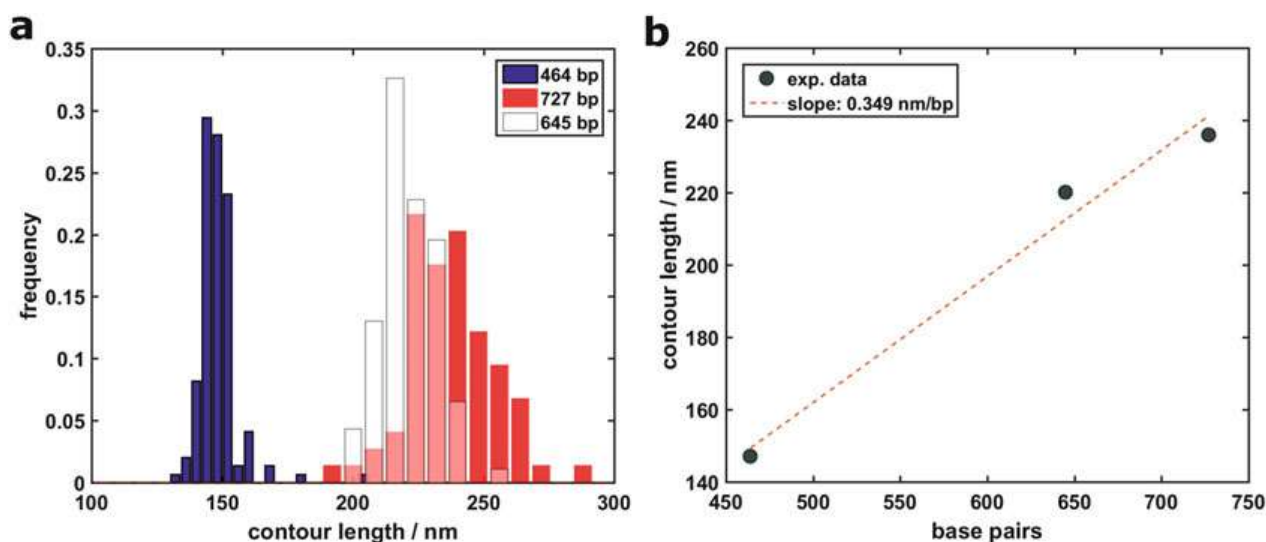


**Fig. 2** Distribution of contour length ( $L_c$ ) values and assessment of the form of DNA molecules upon dehydration on mica, according to the proposed protocol. Three populations of DNA molecules have been investigated, with lengths 464 bp, 645 bp, and 727 bp, respectively. **(a)** The distribution of contour length values is calculated according to Eq. 1. About 150, 80, and 80 molecules have been traced, respectively, for the 464 bp, 645 bp, and 727 bp populations. The measured average lengths agree with those expected for the B-form of DNA within 5–10%. **(b)** A linear fit of the curve  $L_c$  vs. bp provides a value of the rise per residue parameter of 0.349 nm/bp, confirming unambiguously that DNA molecules, despite the dehydration, are in the B form. The discrepancy between absolute observed values and the expected ones could be due to the partial transition towards the A-form that DNA faces when deposited on mica [22], with the A-form domains likely located at the DNA free ends [8]

is negatively charged in humid air and in particular in water. Freshly cleaved mica could hence provide negative, ultra-flat and clean surfaces, functional for high-quality AFM measurements [26]. By using divalent positive ions ( $Mg^{2+}$ ,  $Ca^{2+}$ ,  $Mn^{2+}$ ,  $Ni^{2+}$ , and  $Zn^{2+}$ ) [7], or molecules carrying a positive charge, as in the case of natural or artificial polyamines (poly-L-lysine and poly-L-ornithine [27, 28]) it is possible to bind the negatively charged DNA backbone to the mica surface, to the purpose of imaging DNA by AFM.

2. A cheaper alternative to pre-cut mica (and Teflon) disks is represented by mica (and Teflon) sheets of the same quality and thickness, from which disks of the desired diameter can be obtained using a hole punch.
3. Rigid cantilevers for dynamic modes must be used. Typical parameters characterizing these cantilevers are: resonance frequency  $f \approx 300$  kHz; single-crystal silicon tips with radius of curvature  $R < 10$  nm; force constant  $k \approx 40$  N/m; optionally, a gold or aluminium reflective coating on the back of the cantilever.
4. All the stock saline solutions are prepared starting from the powder that is dissolved in MilliQ water. Filtering should

possibly be avoided, as in general the entities that are removed are very large compared to DNA and would not represent a serious issue. The sample has to be as clean as possible in order to achieve the best condition of imaging, and clean buffers are a fundamental prerequisite. For this reason all dilutions and samples must be prepared using ultrapure MilliQ water based buffers. Never use simple (bi)distilled water, and never sterilize buffers.

5. If imaging in liquid is envisaged, it can be useful to put in between the mica disk and the metal support a Teflon spacer, about 2 mm larger than the mica disk and up to 2 mm thick, aimed at blocking the spread of the liquid used as imaging buffer, so that a stable droplet is obtained for in-liquid imaging. In this case, it is better to use different adhesive depending on the surfaces to be bound together. Mica on Teflon: two-component epoxy glue; Teflon on metal disk: cyanoacrylate glue. This metal–Teflon–mica substrate can be used of course also for imaging DNA in air.
6. A tiny amount of glue must be used, initially placed in the middle of the disk. Apply a gentle pressure so that the glue is distributed uniformly in between the mica disk and the support. Carefully dose the amount of glue so to avoid it spreading outside the mica disk area; this will likely cement the mica layers together from the side and will disturb the stripping procedure.
7. Mica disks should be always freshly cleaved immediately before the deposition of DNA, using soft adhesive tape to peel the topmost layers away. In this way it is possible to create a flat atomically smooth clean surface free of contaminants. To this purpose, firmly attach the scotch tape over the supported mica surface and remove it so to peel the topmost layers away. Repeat the operation using a clean portion of tape until a uniform thin circular layer remains on it (repeat in any case 2–3 times). To achieve a homogeneous stripping no air bubbles must be present below the adhesive tape. Apply a constant tension to the adhesive tape while peeling the mica. Remove the tape in one continuous movement.
8. DNA must be used freshly prepared, resuspended in MilliQ water. For best results, it can be stored at 4 °C for possibly no more than 1–2 weeks. Repeated thawing and freezing damages the DNA backbone [29].
9. The layer used for the imaging has to be cleaved just before sample deposition. It is a good practice to protect the surface from the contact with air, if it is not used immediately.
10. When significant amount of water remains on the surface upon drying, in the form of water islands, it may be the case that something went wrong either during the deposition of DNA

or the cleavage of the mica disk. Sticky/dirty/overcoated surfaces retain water, indeed. Such surfaces may result from the deposition of contaminated/degraded solutions or from remnants of the scotch tape adhesive.

11. In principle, the incubation time of the DNA solution on mica determines the number and density of molecules on the mica surface [5, 10, 12], and typically a few minutes are enough to obtain optimal imaging and analysis conditions. It may happen however that poor reproducibility and deviations from the expected behavior during sample preparation are observed. This problem typically occurs when the DNA concentration in solution and the incubation time are changed in the effort of obtaining the desired density of molecules. Usually, this anomalous behavior is also accompanied by the poor quality of the deposited molecules (condensed in blobs, totally or partially, or with small blobs at the free ends; aggregated or associated in complex two-dimensional structures or networks; etc.). All these can be symptoms that either the molecules in solution, or the buffer, or both, have some problems. For instance, a bad PCR reaction can produce weak DNA molecules with open, and therefore, sticky ends; because of the intrinsic DNA complementarity, several molecule ends will anneal between each other assembling networks, which will be mostly washed away, but also remain on the mica surface to some extent. A dirty buffer containing nanoscopic contaminants (*see* **Notes 4** and **8**) can promote DNA denaturation or aggregation, with similar effects. Large complexes will be typically washed away, as mentioned; therefore, only the minoritarian fraction of small objects will remain on the surface, with a density largely independent on both initial DNA concentration and incubation time. If similar issues are faced, it is usually wise to first prepare fresh clean buffers, then if needed fresh DNA stocks. Although only rarely observed in our experience, similar problems can also be due to poor quality of the mica surface (only use mica of the highest grade) or to issues in mica cleavage (including those due to the poor quality of the scotch tape, which can leave residues of glue on the mica surface).
12. AFM measurements can be carried out in air, as described in the present manuscript, as well as in a suitable saline buffer. Imaging DNA in liquid does not necessarily provides more accurate information, as long as one focuses on structural data, because the latter mostly rely on the accurate characterization of lengths along the DNA backbone, rather than on the measurement of heights. Tip convolution affects only at minor extent such measurements, at least for relatively long molecules (>100 bp). Moreover, there is evidence that dehydration required for sample preparation has little impact on the DNA

properties, probably due to the fact that the truly DNA–mica interface remains always partially hydrated (by a few monolayers of water) [5, 9, 28]. Nevertheless, the fine conformational changes induced by dehydration, as well as by the different sample preparation methods and choices of the bridging cations are still matter of discussion [8, 22]. The general methodology presented here applies irrespective to the imaging method adopted (air, liquid, Tapping Mode, Peak Force Tapping, etc.). For some specific indications in the case of imaging in liquid, *see* **Note 5**.

13. Imaging methods based on the vertical approach of the tip towards the sample have recently been introduced [30], and represent valid alternatives to dynamic (tapping) modes and contact modes, especially in liquid. The general idea, besides specificities related to the different implementations, is to record a set of force curves on a grid spanning the scan area, with a carefully controlled maximum force setpoint; during imaging in fluid, the maximum force can be kept on the 10–100 pN level, while lateral forces are minimized thanks to the vertical approach mode, similarly to Tapping or other dynamic modes. In Tapping Mode, however, peak forces are significantly higher.
14. Calibration of the piezo-scanners should be checked periodically (every 6–12 months) by imaging the surface of a calibration grating, with repeated morphological features of appropriate dimensions (in the present case, the  $XY$  period should be 1  $\mu\text{m}$ , the depths 10–200 nm). Unless a certified grating is used, the  $XYZ$  accuracy after the calibration procedure can be reasonably assumed to be  $\leq 2\%$ .
15. The number of scanned lines impacts on the acquisition time of a single image. Setting an aspect-ratio 2:1 allows reducing the number of scanned lines, i.e., the acquisition time, without affecting dramatically the image resolution in the slow scan direction. Given a target sampling resolution in the image, the scanned area can be kept large, for the sake of a better statistics, by increasing the scan size and the aspect-ratio value, and setting suitable values of the points per line and number of lines parameters. The main limit to be considered is that the scanning speed cannot grow arbitrarily, otherwise the feedback loop will not be able to track accurately the surface.
16. Scanning speed (which changes when either scan rate or scan size are changed) should not be too small, otherwise drifts could produce significant distortions in the image. At the same time, too high scan speeds will challenge the feedback loop of the AFM and determine inaccurate tracking.
17. Typically the integral gain has the highest impact on image quality. Each instrument has its own gain optimal settings.

Increase the integral gain until oscillations appear in the height and error signals. Then decrease the integral gain just below the critical value. Increase the proportional gain until the quality of the image starts worsening. Setting high gains gives advantages in terms of tracking stability and scanning velocity that overcompensates the introduction of high-frequency noise in the image; the latter can be effectively removed a posteriori by applying a median filter with a  $3 \times 3$  kernel on the image.

18. Drifts must be minimized in order to obtain accurate topographic maps. Drifts can be due to thermal equilibration of the system components (sample, laser, cantilever, electronics as well as the scanner) or to mechanical hysteresis of the piezo elements. When a different scan area is selected by applying offsets to the piezo, the latter will typically keep some memory of the previous static deformation, resulting in a constant drift across the new image. In order to minimize this effect and completely refresh the scanner motion, after setting the new offsets it is effective to reduce significantly the number of lines and complete a few low-resolution images moving quickly up and down, until the hysteresis is lost. Also reverting a few times the slow scan direction (up-bottom/bottom-up) helps removing the hysteresis of the piezo scanner.
19. The data analysis procedures described in general terms in this manuscript can be implemented by means of custom routines, as well as by means of commercial and open-source software. Basic image processing tools are typically included in the control software of the AFM. The authors have developed their own libraries of data analysis routines in the MATLAB environment (many research groups use their own libraries). Some open-source software packages are listed below (this list is neither meant to be complete, nor is it expected to remain up to date for a long time):
  - (a) ImageJ/Fiji, <http://rsb.info.nih.gov/ij/>
  - (b) Gwyddion, <http://gwyddion.net/>
  - (c) WSxM, <http://www.wsxmsolutions.com/>
  - (d) FiberApp, <http://www.fsm.ethz.ch/publications-list/software.html>
  - (e) Image SXM, <https://www.liverpool.ac.uk/%7Esdb/ImageSXM/>
20. Mica is atomically smooth and overall flat. Deviations from a flat baseline can therefore be attributed to scanning artifacts, with the obvious exception of those due to the presence of a DNA molecule. A global tilt of the sample adds a linear baseline to each profile, and globally a plane to the topographic map as a whole. Tubular scanners will add an approximately parabolic

baseline to each profile (a bow), because the displacement of the sample placed on top of the tube follows a curved trajectory rather than a linear one (ideally an arc of circumference). Generally, each scanner will add its own polynomial distortion to the AFM topographic map. Drifts of different nature can add additional shifts between adjacent profiles (approximately constant along each profile, i.e., along the fast-scan direction, but appreciable along the slow-scan direction); the presence of these line-by-line deviations usually requires the application of line-by-line polynomial subtraction (also known as flattening) rather than simply the subtraction of a two-dimensional plane, or paraboloid, or higher-order surface (also known as plane-fitting). It is essential, in order to accurately determine the image baseline, to mask (i.e., not to consider in the polynomial fit) all the surface features that do not belong to the flat reference substrate (the DNA molecules, surface defects, ...). Masks are typically built by thresholding (flooding) algorithms, determining image segmentation; only the substrate is considered for the flattening. The absence of masking in the fitting procedure will introduce artifacts in the topographic maps (the ubiquitous black stripes), because in the presence of bumps and/or depressions the fitted polynomial typically deviates from the baseline. Masking is typically a feature of the analysis software. The flattening process is described in Fig. 3.

21. A semiautomatic tracing algorithm is in principle preferable to the manual tracing of DNA molecules, as the latter is more prone to introduce bias from the operator. An automatic algorithm can of course introduce systematic errors, although these would be the same for all molecules, irrespective to the operator. Ivan Usov's FiberApp is a free comprehensive suite of (MATLAB) routines with a GUI for "Tracking and Analyzing Polymers, Filaments, Biomacromolecules, and Fibrous Objects" (available at <http://www.fsm.ethz.ch/publications-list/software.html> [31]).
22. The formulas reported in the text for the calculation of basic structural parameters provide in general accurate results as long as the digitization of the molecules in the image is not poor, which in the case of DNA means that the point-to-point distance should be of the order of 0.5–1 nm. Separations significantly smaller than 0.5–1 nm are unreasonable, considered that the nominal width of DNA is 2 nm; oversampling can introduce spurious high-frequency components to the trace, that will affect the angle distribution as well as the calculated contour length. The contour length  $L_c$  is the most sensitive parameter, indeed. Optimized estimators for  $L_c$  have been developed, and can be used instead of Eq. 1 [32–34].

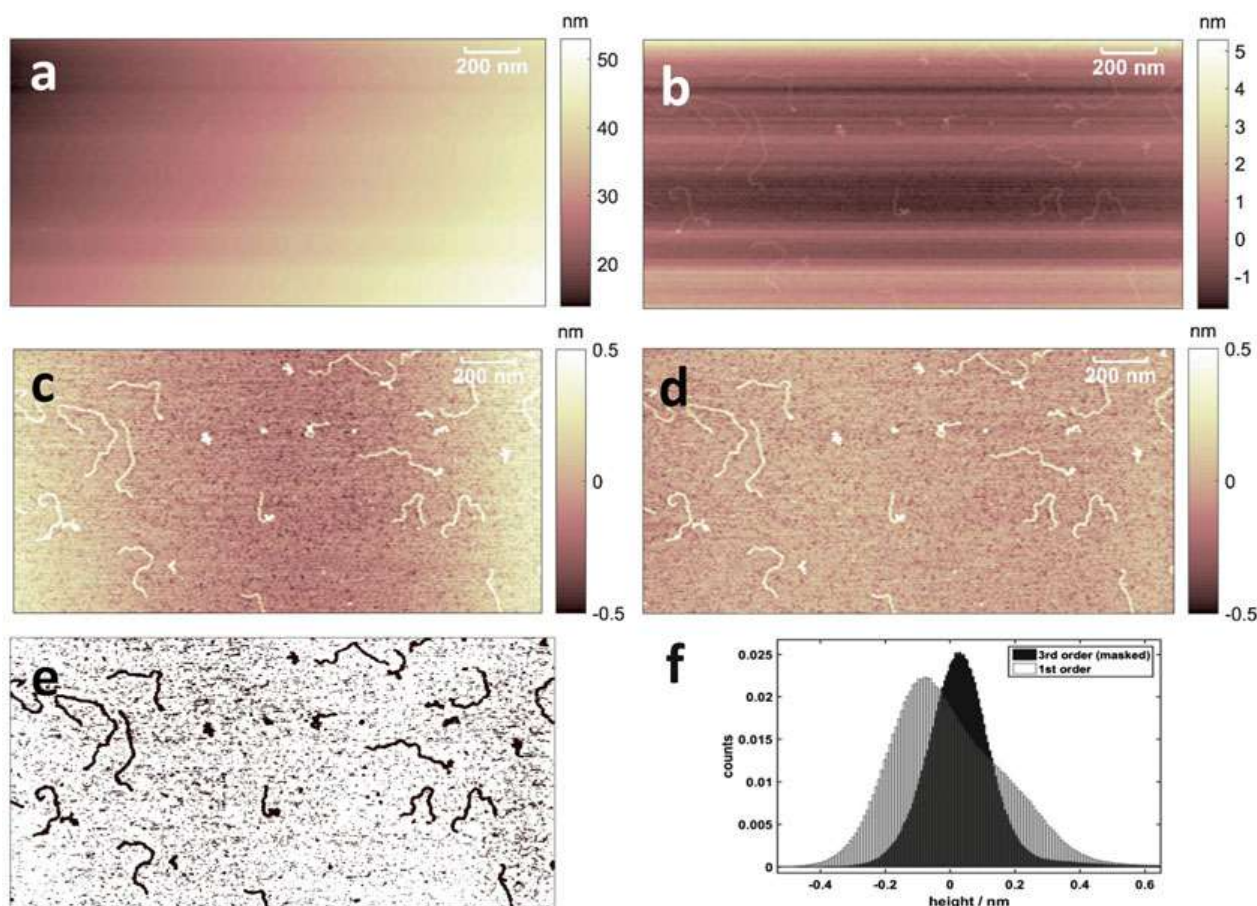


**Fig. 3** Overview of the image pre-processing procedure. The process starts with (a) a raw AFM image, where the sample tilt and line-by-line distortions hinder the target topographical features (the DNA molecules in this case); after (b) a global plane-fitting of the first order, and a series of line-by-line flattening of the (c) first, and (d) third order, the baseline is effectively removed and the molecules emerge, well-contrasted with respect to the smooth, flat substrate. In (e) the mask built to apply the third-order flattening is shown. This logical mask assigns a value of 1 to the points that must be considered for the fitting, i.e., those belonging to the substrate, and 0 elsewhere. In (f) the distributions of surface heights after the first and third order flattening are compared. A well-shaped, nearly symmetric dominant mode, representing the height values of the substrate, is typical of a properly flattened image

---

## Acknowledgments

We thank Francesca Borghi for support in AFM analysis. A.P. thanks the Dept. of Physics of the University of Milano for financial support under the project “Piano di Sviluppo dell’Ateneo per la Ricerca 2014. Linea B: Supporto per i giovani ricercatori”. Work in M.M-F lab is supported by AIRC (n.15631) and Telethon (GGP15227).

## References

- Alessandrini A, Facci P (2005) AFM: a versatile tool in biophysics. *Meas Sci Technol* 16: R65–R92. doi:[10.1088/0957-0233/16/6/R01](https://doi.org/10.1088/0957-0233/16/6/R01)
- Kalle W, Strappe P (2012) Atomic force microscopy on chromosomes, chromatin and DNA: a review. *Micron* 43:1224–1231. doi:[10.1016/j.micron.2012.04.004](https://doi.org/10.1016/j.micron.2012.04.004)
- Podgornik Rudolf (2011) Physics of DNA. <http://www.fmf.uni-lj.si/~podgornik/download/physics-of-DNA-1.1.pdf>
- Pinheiro AV, Han D, Shih WM, Yan H (2011) Challenges and opportunities for structural DNA nanotechnology. *Nat Nanotechnol* 6:763–772. doi:[10.1038/nnano.2011.187](https://doi.org/10.1038/nnano.2011.187)
- Rivetti C, Guthold M, Bustamante C (1996) Scanning force microscopy of DNA deposited onto mica: equilibration versus kinetic trapping studied by statistical polymer chain analysis. *J Mol Biol* 264:919–932. doi:[10.1006/jmbi.1996.0687](https://doi.org/10.1006/jmbi.1996.0687)
- Podestà A, Indrieri M, Brogioli D, Manning GS, Milani P, Guerra R, Finzi L, Dunlap D (2005) Positively charged surfaces increase the flexibility of DNA. *Biophys J* 89:2558–2563
- Pastré D, Piétrement O, Fusil S, Landousy F, Jeusset J, David M-O, Hamon L, Le Cam E, Zozime A (2003) Adsorption of DNA to mica mediated by divalent counterions: a theoretical and experimental study. *Biophys J* 85:2507–2518. doi:[10.1016/S0006-3495\(03\)74673-6](https://doi.org/10.1016/S0006-3495(03)74673-6)
- Japaridze A, Vobornik D, Lipiec E, Cerreta A, Szczerbinski J, Zenobi R, Dietler G (2016) Toward an effective control of DNA's submolecular conformation on a surface. *Macromolecules* 49:643–652. doi:[10.1021/acs.macromol.5b01827](https://doi.org/10.1021/acs.macromol.5b01827)
- Buzio R, Repetto L, Giacomelli F, Ravazzolo R, Valbusa U (2014) Symmetric curvature descriptors for label-free analysis of DNA. *Sci Rep* 4:6459. doi:[10.1038/srep06459](https://doi.org/10.1038/srep06459)
- Bustamante C, Rivetti C (1996) Visualizing protein-nucleic acid interactions on a large scale with the scanning force microscope. *Annu Rev Biophys Biomol Struct* 25:395–429. doi:[10.1146/annurev.bb.25.060196.002143](https://doi.org/10.1146/annurev.bb.25.060196.002143)
- Valle F, Favre M, De Los RP, Rosa A, Dietler G (2005) Scaling exponents and probability distributions of DNA end-to-end distance. *Phys Rev Lett* 95:158105. doi:[10.1103/PhysRevLett.95.158105](https://doi.org/10.1103/PhysRevLett.95.158105)
- Fang Y, Spisz TS, Wiltshire T, D'Costa NP, Bankman IN, Reeves RH, Hoh JH (1998) Solid-state DNA sizing by atomic force microscopy. *Anal Chem* 70:2123–2129. doi:[10.1021/ac971187o](https://doi.org/10.1021/ac971187o)
- Santos S, Stefancich M, Hernandez H, Chiesa M, Thomson NH (2012) Hydrophilicity of a single DNA molecule. *J Phys Chem C* 116:2807–2818. doi:[10.1021/jp211326c](https://doi.org/10.1021/jp211326c)
- Thomson NH, Santos S, Mitchenall LA, Stuchinskaya T, Taylor JA, Maxwell A (2014) DNA G-segment bending is not the sole determinant of topology simplification by type II DNA topoisomerases. *Sci Rep* 4:6158. doi:[10.1038/srep06158](https://doi.org/10.1038/srep06158)
- Wiggins PA, van der Heijden T, Moreno-Herrero F, Spakowitz A, Phillips R, Widom J, Dekker C, Nelson PC (2006) High flexibility of DNA on short length scales probed by atomic force microscopy. *Nat Nanotechnol* 1:137–141. doi:[10.1038/nnano.2006.63](https://doi.org/10.1038/nnano.2006.63)
- Savelyev A, Materese CK, Papoian GA (2011) Is DNA's rigidity dominated by electrostatic or nonelectrostatic interactions? *J Am Chem Soc* 133:19290–19293. doi:[10.1021/ja207984z](https://doi.org/10.1021/ja207984z)
- Lia G, Indrieri M, Owen-Hughes T, Finzi L, Podesta A, Milani P, Dunlap D (2008) ATP-dependent looping of DNA by ISWI. *J Biophotonics* 1:280–286
- Fang Y, Hoh JH, Spisz TS (1999) Ethanol-induced structural transitions of DNA on mica. *Nucleic Acids Res* 27:1943–1949. doi:[10.1093/nar/27.8.1943](https://doi.org/10.1093/nar/27.8.1943)
- Parker SCJ, Margulies EH, Tullius TD (2008) The relationship between fine scale DNA structure, GC content, and functional elements in 1% of the human genome. *Genome Inform* 20:199–211
- Knips A, Zacharias M (2015) Influence of a cis, syn-cyclobutane pyrimidine dimer damage on DNA conformation studied by molecular dynamics simulations. *Biopolymers* 103:215–222. doi:[10.1002/bip.22586](https://doi.org/10.1002/bip.22586)
- García R, Perez R (2002) Dynamic atomic force microscopy methods. *Surf Sci Rep* 47:197. doi:[10.1016/S0167-5729\(02\)00077-8](https://doi.org/10.1016/S0167-5729(02)00077-8)
- Rivetti C, Codeluppi S (2001) Accurate length determination of DNA molecules visualized by atomic force microscopy: evidence for a partial B- to A-form transition on mica. *Ultramicroscopy* 87:55–66. doi:[10.1016/S0304-3991\(00\)00064-4](https://doi.org/10.1016/S0304-3991(00)00064-4)
- Shi Y (1996) Statistical mechanics of the extensible and shearable elastic rod and of DNA. *J*

- Chem Phys 105:714–731. doi:[10.1063/1.471927](https://doi.org/10.1063/1.471927)
24. Kuwahara Y (1999) Muscovite surface structure imaged by fluid contact mode AFM. *Phys Chem Miner* 26:198–205. doi:[10.1007/s002690050177](https://doi.org/10.1007/s002690050177)
  25. Ostendorf F, Schmitz C, Hirth S, Kühnle A, Kolodziej JJ, Reichling M (2008) How flat is an air-cleaved mica surface? *Nanotechnology* 19:305705. doi:[10.1088/0957-4484/19/30/305705](https://doi.org/10.1088/0957-4484/19/30/305705)
  26. Thundat T, Allison DP, Warmack RJ, Brown GM, Jacobson KB, Schrick JJ, Ferrell TL (1992) Atomic force microscopy of DNA on mica and chemically modified mica. *Scanning Microsc* 6:911–918
  27. Bussiek M, Mücke N, Langowski J (2003) Polylysine-coated mica can be used to observe systematic changes in the supercoiled DNA conformation by scanning force microscopy in solution. *Nucleic Acids Res* 31:e137. doi:[10.1093/nar/gng137](https://doi.org/10.1093/nar/gng137)
  28. Podesta A, Imperadori L, Colnaghi W, Finzi L, Milani P, Dunlap D (2004) Atomic force microscopy study of DNA deposited on poly L-ornithine-coated mica. *J Microsc* 215:236–240. doi:[10.1111/j.0022-2720.2004.01372.x](https://doi.org/10.1111/j.0022-2720.2004.01372.x)
  29. Bustamante C, Vesenka J, Tang CL, Rees W, Guthold M, Keller R (1992) Circular DNA molecules imaged in air by scanning force microscopy. *Biochemistry* 31:22–26
  30. Adamcik J, Berquand A, Mezzenga R (2011) Single-step direct measurement of amyloid fibrils stiffness by peak force quantitative nano-mechanical atomic force microscopy. *Appl Phys Lett* 98:193701. doi:[10.1063/1.3589369](https://doi.org/10.1063/1.3589369)
  31. Usov I, Mezzenga R (2015) FiberApp: an open-source software for tracking and analyzing polymers, filaments, biomacromolecules, and fibrous objects. *Macromolecules* 48:1269–1280. doi:[10.1021/ma502264c](https://doi.org/10.1021/ma502264c)
  32. Sanchez-Sevilla A, Thimonier J, Marilley M, Rocca-Serra J, Barbet J (2002) Accuracy of AFM measurements of the contour length of DNA fragments adsorbed on mica in air and in aqueous buffer. *Ultramicroscopy* 92:151–158. doi:[10.1016/S0304-3991\(02\)00128-6](https://doi.org/10.1016/S0304-3991(02)00128-6)
  33. Rivetti C (2009) A simple and optimized length estimator for digitized DNA contours. *Cytom Part A* 75:854–861. doi:[10.1002/cyto.a.20781](https://doi.org/10.1002/cyto.a.20781)
  34. Gomez AI, Cruz M, Cruz-Orive LM (2016) On the precision of curve length estimation in the plane. *Image Anal Stereol* 35:1. doi:[10.5566/ias.1412](https://doi.org/10.5566/ias.1412)

## Published Paper III

---

### Measuring the levels of ribonucleotides embedded in genomic DNA

Meroni A., Nava G.M., Sertic S., Plevani P., Muzi-Falconi M. <sup>#\*</sup> and Lazzaro F. <sup>#\*</sup>  
Dipartimento di Bioscienze, Università degli Studi di Milano. Milano, Italy

<sup>#</sup>Co-last authors

<sup>\*</sup>Corresponding authors: [marco.muzifalconi@unimi.it](mailto:marco.muzifalconi@unimi.it);  
[federico.lazzaro@unimi.it](mailto:federico.lazzaro@unimi.it)

Book Chapter in **Methods in Molecular Biology Genome instability**  
(pp. 319–327). Humana Press, New York, NY. (In Press, 2018)

[https://doi.org/10.1007/978-1-4939-7306-4\\_22](https://doi.org/10.1007/978-1-4939-7306-4_22)

## Measuring the Levels of Ribonucleotides Embedded in Genomic DNA

Alice Meroni, Giulia M. Nava, Sarah Sertic, Paolo Plevani, Marco Muzi-Falconi, and Federico Lazzaro

### Abstract

Ribonucleotides (rNTPs) are incorporated into genomic DNA at a relatively high frequency during replication. They have beneficial effects but, if not removed from the chromosomes, increase genomic instability. Here, we describe a fast method to easily estimate the amounts of embedded ribonucleotides into the genome. The protocol described is performed in *Saccharomyces cerevisiae* and allows us to quantify altered levels of rNMPs due to different mutations in the replicative polymerase  $\epsilon$ . However, this protocol can be easily applied to cells derived from any organism.

**Key words** DNA replication, DNA repair, DNA polymerase, Ribonucleotides incorporation, RNase H, Genome stability, Genomic rNMPs

---

### 1 Introduction

During evolution, DNA was selected as the principal molecule to preserve genetic information likely due to its greater stability compared to RNA, whose 3' hydroxyl group increases its susceptibility to hydrolysis.

At every cell cycle, genomic DNA is duplicated by DNA polymerases, enzymes that are specialized to copy a single-stranded DNA template and polymerize deoxyribonucleotides (dNTPs) accordingly, forming a complementary DNA strand. Given the much greater abundance of rNTPs compared to dNTPs in the nucleus, DNA polymerases evolved a steric gate to help preventing rNTPs from entering the active site [1].

However, recent data revealed that large amounts of rNTPs are incorporated in genomic DNA during replication [2]. The presence of rNMPs in the chromosomes has physiological roles [3–5] and is

---

M. Muzi-Falconi and F. Lazzaro are co-last authors.

normally transient: specific RNase H-based pathways excise them before mitosis [6]. Failure to remove genomic rNMPs causes replication stress and genome instability in yeast and human cells [7–12]. Mutations in the genes coding for RNase H2 in humans are responsible for the rare Aicardi-Goutieres Syndrome (AGS) [13]. Intriguingly, cells derived from AGS patients accumulate rNMPs in their chromosomes and exhibit constitutively activated DNA damage response and post-replication repair mechanisms [8, 10].

To investigate the mechanisms underlying incorporation and removal of ribonucleotides in chromosomes and to determine their effect on genome integrity, it is important to determine rapidly and semiquantitatively the amounts of ribonucleotides present genomic DNA. Here, we describe an experimental strategy based on the approach originally described by Hiller and colleagues [12] and then in [8]. Briefly, genomic DNA is extracted and treated in vitro with bacterial RNase HII, which introduces nicks at every ribonucleotides site. These nicks are radioactively labeled taking advantage of the DNA Polymerase I nick translation capability (Fig. 1). In this chapter, we describe the procedure starting from the preparation of genomic DNA from yeast cells and compare the effect of two mutations affecting the steric gate of pol  $\epsilon$ , M644G and M644L, that respectively increase and decrease rNTPs incorporation [9].

---

## 2 Materials

1. Eppendorf tubes 1.5 and 2 mL.
2. Pipettes and tips.
3. Glass Pasteur pipette.
4. MilliQ water.
5. 250 mL glass flasks.
6. Stirrer.
7. Gel electrophoresis apparatus.
8. Power supply.
9. UV transilluminator and digital camera.
10. Plastic wrap.
11. Tape.
12. Scalpel.
13. Thermomixer.
14. Geiger counter.
15. Gel dryer.

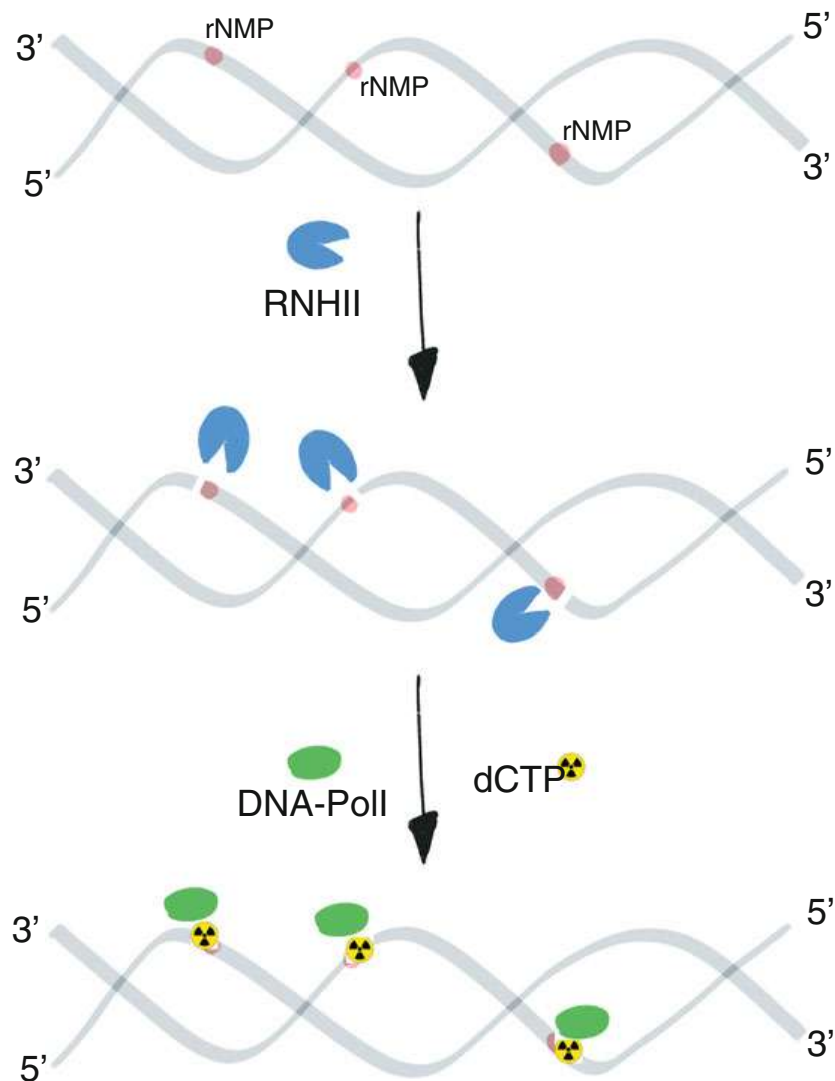


**Fig. 1** Representative scheme for ribonucleotides incorporation assay. RNHII recognizes and cleaves ribonucleotides embedded into genomic DNA (*red dot*) leaving 5' P-ribose ends. The DNA-Poll enzyme, through nick translation, marks RNHII-induced nicks with radiolabeled dCTP

16. 3 MM Whatman blotting papers.
17. Towel papers.
18. Weight ( $\geq 400$  g).
19. Phosphorimager and screen.
20. YDER Yeast DNA Extraction kit, materials and reagents listed in the kit instructions (Thermo Scientific).
21. RNase A 10 mg/mL.
22. Phenol:Chloroform:Isoamyl Alcohol 25:24:1 v/v/v (Saturated with 10 mM Tris-HCl, pH 8.0, 1 mM EDTA). Stored at 4 °C.
23. 100% ethanol. Stored at -20 °C.
24. 3 M sodium acetate, pH 7.0. Stored at 4 °C.
25. 70% ethanol. Stored at -20 °C.

26. Agarose powder.
27. 10 mg/mL ethidium bromide (EtBr).
28. TAE 1×: 40 mM Tris-HCl, pH 8.0, 20 mM acetic acid, and 1 mM EDTA. Stored at room temperature.
29. Lambda DNA marker.
30. RNase HII 5000 U/mL.
31. 10× ThermoPol<sup>®</sup> Reaction Buffer: 200 mM Tris-HCl, 100 mM (NH<sub>4</sub>)<sub>2</sub>SO<sub>4</sub>, 100 mM KCl, 20 mM MgSO<sub>4</sub>, 1% Triton<sup>®</sup> X-100 (New England Biolabs).
32. 10× dNTPs mix (without dCTP); 200 μM dATP, 200 μM dGTP and 200 μM dTTP.
33. NEBuffer 2; 500 mM NaCl, 100 mM Tris-HCl, 100 mM MgCl<sub>2</sub>, 10 mM DTT (New England Biolabs).
34. DNA Polymerase I 10,000 U/mL.
35. α<sup>32</sup>P-dCTP, 3000 Ci/mmol.
36. STOP solution: 30% glycerol, 200 mM EDTA, bromophenol blue, in MilliQ water.
37. TCA 30%.
38. Software for quantification and analysis: ImageQuant and Microsoft Excel.

---

### 3 Methods

#### 3.1 Genomic DNA Preparation

1. Isolate yeast genomic DNA using the Y-DER extraction Kit according to the manufacturer's instructions. All the steps are performed as described in the kit's instructions, with the following modifications:
  - (a) Use 50 mL cultures with an OD<sub>600</sub> between 0.3 and 0.8.
  - (b) RNase A 10 mg/mL is diluted 1:1000 in the Y-PER reagent.
2. Resuspend DNA in 200 μL of MilliQ water and add an equal volume of Phenol:Chloroform:Isoamyl Alcohol 25:24:1 v/v/v saturated with 10 mM Tris-HCl, pH 8.0, 1 mM EDTA (*see Note 1*).
3. Vortex vigorously for 15 s.
4. Centrifuge at maximum speed for 10 min at RT.
5. Carefully transfer only the aqueous phase (upper phase) to a new 1.5 mL eppendorf tube. That phase contains DNA. Do not transfer material from the interface or the lower phase. If so, repeat the procedure from **step 2**, adding an equal volume of Phenol:Chloroform:Isoamyl Alcohol 25:24:1 v/v/v saturated with 10 mM Tris-HCl, pH 8.0, 1 mM EDTA.

6. Precipitate DNA by adding three volumes of ice-cold 100% ethanol and 1/10 of the volume of sodium acetate 3 M, pH 7.0. Mix well and keep overnight at  $-20^{\circ}\text{C}$ .
7. Spin down the precipitate at maximum speed for 45' at  $4^{\circ}\text{C}$ . Draw off the supernatant.
8. Wash adding 1 mL of ice-cold 70% ethanol. Spin at maximum speed for 30 min at  $4^{\circ}\text{C}$ . Draw off the supernatant and dry the pellet at  $42\text{--}44^{\circ}\text{C}$  (*see Note 2*).
9. Resuspend gently the pellet with 50  $\mu\text{L}$  of MilliQ water.

### 3.2 Nicking DNA at Ribonucleotide Sites

1. Quantify genomic DNA by loading 2  $\mu\text{L}$  on a 1% agarose gel in TAE (with 0.67  $\mu\text{g}/\text{mL}$  EtBr) next to 1  $\mu\text{L}$  of Lambda DNA marker. Run for 10 min at 8–10 V/cm. The genomic DNA band should be compact and easily quantifiable (*see Note 3*).
2. Normalize DNA in each sample to 25 ng/ $\mu\text{L}$  by adding MilliQ water.
3. Prepare two new 1.5 mL eppendorf tubes per sample. Label the tubes with the sample name plus “–” and “+” (e.g., Sample 1– and Sample 1+) (*see Note 4*), and transfer 20  $\mu\text{L}$  (500 ng) of normalized genomic DNA to each tube.
4. Dilute 1:10 the RNase HII in ThermoPol Buffer 1 $\times$ . Prepare the two reaction mixtures (mix “–” and mix “+”) in new 1.5 mL tubes in excess with respect to the number of samples. Keep the mixtures on ice.  
1 $\times$  reaction mix recipe (Note that the final reaction volume is 50  $\mu\text{L}$ ):

	Mix “–”	Mix “+”
ThermoPol Buffer 10 $\times$	5 $\mu\text{L}$	5 $\mu\text{L}$
RNase HII	/	1 $\mu\text{L}$
ThermoPol Buffer 1 $\times$	1 $\mu\text{L}$	/
H <sub>2</sub> O MilliQ	24 $\mu\text{L}$	24 $\mu\text{L}$
Total volume	30 $\mu\text{L}$	30 $\mu\text{L}$

5. Vortex briefly and add 30  $\mu\text{L}$  of each mixture to the appropriate labeled tube containing genomic DNA.
6. Incubate at  $37^{\circ}\text{C}$  with 550 rpm agitation in a thermomixer for 2.30 h.
7. Add 50  $\mu\text{L}$  of MilliQ water and precipitate DNA following **steps 6–8** of section 3.1, consider 100  $\mu\text{L}$  of total volume.
8. Resuspend gently the pellet in 20  $\mu\text{L}$  of MilliQ water.

### 3.3 Radioactive Labeling of Nicks

1. Quantify and normalize DNA by loading 2  $\mu\text{L}$  on a 1% agarose gel in TAE (with 0.67  $\mu\text{g}/\text{mL}$  EtBr) next to 1  $\mu\text{L}$  of Lambda DNA marker. Run for 10 min at 9–10 V/cm (*see* Note for gel preparation).
2. Transfer 300 ng of DNA to a new 1.5 mL tube and add MilliQ water to 15  $\mu\text{L}$  of total volume.
3. Prepare the common DNA Polymerase I reaction mixture, keep it on ice.

1  $\times$  DNA Polymerase I reaction mix recipe:

10 $\times$ dNTPs mix (without dCTP):	2 $\mu\text{L}$
DNA Pol I 10 $\times$ buffer NEBuffer 2	2 $\mu\text{L}$
DNA Pol I 10,000 U/mL	0.5 $\mu\text{L}$
$\alpha^{32}\text{P}$ -dCTP 3000 Ci/mmol	0.3 $\mu\text{L}$
H <sub>2</sub> O MilliQ	0.2 $\mu\text{L}$

4. Add 5  $\mu\text{L}$  of the DNA Polymerase I reaction mix to the each sample and incubate at 16  $^{\circ}\text{C}$  for 30 min (*see* Note 5).
5. Add 4  $\mu\text{L}$  of the STOP solution (*see* Notes 5 and 6).
6. Load 20  $\mu\text{L}$  on a 1% agarose gel in TAE (with 0.67  $\mu\text{g}/\text{mL}$  EtBr). Here the DNA size marker is dispensable.
7. Run at 7 V/cm for 1.20 h.
8. Cut the gel immediately under the bromophenol blue line (*see* Note 7).
9. Examine the gel by UV light and photograph it digitally. This will allow normalization of the radioactive signal with respect to the DNA loaded in the gel.
10. Soak the gel in TCA 30% for half an hour to precipitate the DNA. The bromophenol blue turns yellow.
11. Assemble the sandwich on a glass tray: cover completely the inner part with plastic wrap. Layer three pieces of 3MM Whatman blotting paper larger than the gel. Take out the gel from TCA 30% and place it on the top of the blotting paper. Place in order: three more sheets of blotting paper on the gel, a stack of paper towels, and a weight (0.3–0.5 kg) (Fig. 2).
12. Let the gel dry overnight at room temperature.
13. Remove the paper towels and the blotting papers above the gel. Transfer the desiccated gel on a new 3MM blotting paper.
14. Dry the gel on the blotting paper using a gel dryer for 20 min at 80  $^{\circ}\text{C}$ . Use more than one blotting paper and cover the gel with plastic wrap to avoid radioactive contamination of the instrument.

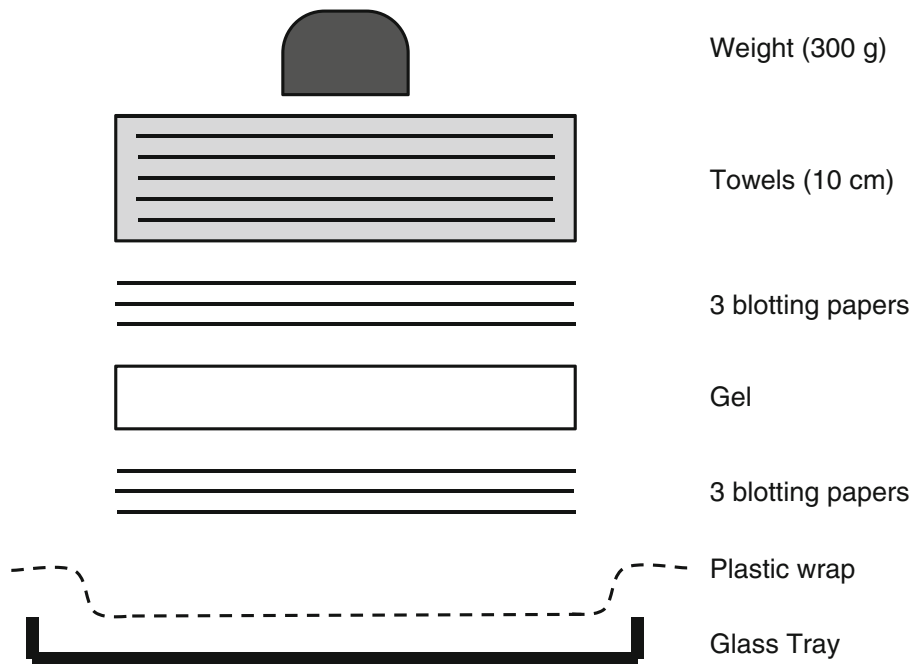


**Fig. 2** Scheme to assemble paper sandwich to dry the agarose gel

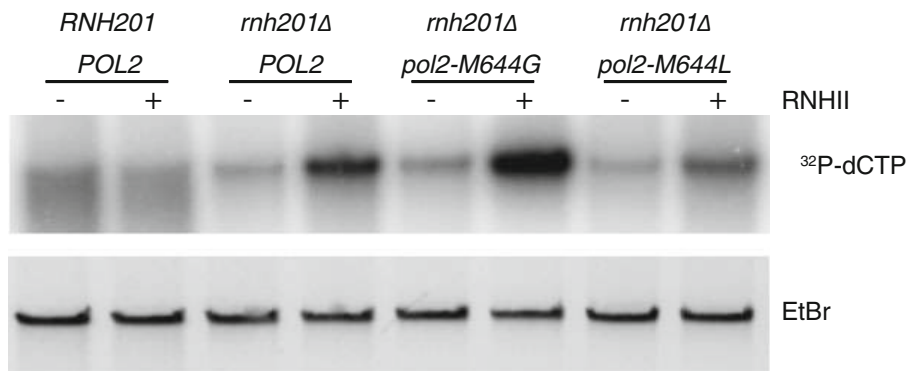


**Fig. 3** Visualization of ribonucleotides incorporation assay results. The strains tested are derivatives of a W303 background (*MATa ade2-1 trp1-1 leu2-3112 his3-11,15 ura3-1 can1-100 RAD5*) with a deletion of gene coding for the catalytic subunit of RNase H2 (*rnh201Δ*) combined with wt or mutated *POL2* gene. The *RNH201 POL2* wt strain is used as control. The radiolabeled signal represents the nicks labeled by PolI. The signal dependent upon RNHII treatment is proportional to the genomic ribonucleotides levels. The EtBr panel represents the loading control, acquired before gel drying and necessary for radioactive quantification

15. Expose the dried gel on a phosphorimager screen for 5–15 min (*see Note 8*).
16. Scan the screen in a phosphorimager. To quantify the result *see Note 9*. An Example is shown in Fig. 3.

---

## 4 Notes

1. DNA has to be clean and as little nicked as possible to achieve the best resolution. For these reasons it is strongly recommended to clean DNA through phenol:chloroform extraction and ethanol precipitation. We also found that the YDER preparation yields a genomic DNA with fewer nicks compared with other methods.
2. Draw off as much supernatant as possible with a glass Pasteur pipette, this would ensure removing the majority of the ethanol, and then place the eppendorf tubes in a heater at 42–44 °C. Drying time depends on how much ethanol is left in the samples. Check the samples after 20 min, if the ethanol is still there, leave them in the heater and check later. Note that excessive drying would damage the sample, for this reason keep checking samples every 20 min until the pellet is completely dry.
3. To normalize DNA in the samples take a digital image and use quantifying tools such as ImageQuant or ImageLab (BioRad).
4. Here, each sample is split into two: one half is digested with purified bacterial RNase HII, the other half is left untreated. This allows discrimination between the ribonucleotide-dependent nicks and the nicks generated during DNA preparation.
5. Labeling the nicks is the key step of this protocol. For this reason the procedure needs strict standardization. We suggest proceeding sample by sample adding the reaction mix to each tube every 15–30 s. After 30 min of incubation, repeat this procedure with the STOP solution. In this way, all the samples would be incubated for exactly 30 min at 16 °C.
6. As most DNA polymerases, DNA polymerase I needs magnesium ions. In this case the high concentration of EDTA in the STOP solution will stop the reaction, while the glycerol and the bromophenol blue make the samples ready to be loaded on a gel.
7. Labeled genomic DNA is loaded on the agarose gel together with the DNA Polymerase I reaction mix, including the unincorporated radioactive nucleotides. The nucleotides migrate faster than genomic DNA and the long run ensures complete separation. Free nucleotides migrate immediately below the bromophenol blue; therefore, the gel is cut immediately after the run to avoid their diffusion through the gel. The bromophenol blue is also a pH-indicator, used to monitor the change in the gel pH while soaking in 30% TCA. When it turns yellow

the agarose gel pH has become acid so DNA would be precipitated into it.

8. The exposure time could vary depending on the  $\alpha^{32}\text{P}$ -dCTP activity. With fresh and fully active  $\alpha^{32}\text{P}$ -dCTP the signal is saturated in 15 min.
9. Signal quantification. To quantify the resulting signal proceed with the following step. Quantify the bands corresponding to the genomic DNA, including the ones from the EtBr capture. Use the Volume Tool of ImageQuant software drawing a rectangle around the right band. Normalize each radioactive value to the corresponding EtBr value. This would ensure the correct interpretation of the radioactive signal. Then for each sample subtract the “–” signal from the “+” signal as a background normalization.

---

## Acknowledgments

This work was supported by grants from AIRC (n.15631) and Telethon (GGP15227) to M.M.-F., from AIRC and Fondazione Cariplo (TRIDEO 2014 Id. 15724) to F.L., and from Fondazione Cariplo (grant number 2013-0798) to P.P.

## References

1. Joyce CM (1997) Choosing the right sugar: how polymerases select a nucleotide substrate. *Proc Natl Acad Sci U S A* 94:1619–1622
2. McElhinny SAN, Watts BE, Kumar D et al (2010) Abundant ribonucleotide incorporation into DNA by yeast replicative polymerases. *Proc Natl Acad Sci U S A* 107:4949–4954
3. Ghodgaonkar MM, Lazzaro F, Olivera-Pimentel M et al (2013) Ribonucleotides misincorporated into DNA act as strand-discrimination signals in eukaryotic mismatch repair. *Mol Cell* 50:323–332
4. Lujan SA, Williams JS, Clausen AR et al (2013) Ribonucleotides are signals for mismatch repair of leading-strand replication errors. *Mol Cell* 50:437–443
5. Dalgaard JZ (2012) Causes and consequences of ribonucleotide incorporation into nuclear DNA. *Trends Genet* 28:592–597
6. Sparks JL, Chon H, Cerritelli SM et al (2012) RNase H2-initiated ribonucleotide excision repair. *Mol Cell* 47:980–986
7. Lazzaro F, Novarina D, Amara F et al (2012) RNase H and postreplication repair protect cells from ribonucleotides incorporated in DNA. *Mol Cell* 45:99–110
8. Pizzi S, Sertic S, Orcesi S et al (2015) Reduction of hRNase H2 activity in Aicardi-Goutières syndrome cells leads to replication stress and genome instability. *Hum Mol Genet* 24:649–658
9. Nick McElhinny SA, Kumar D, Clark AB et al (2010) Genome instability due to ribonucleotide incorporation into DNA. *Nat Chem Biol* 6:774–781
10. Günther C, Kind B, Reijns MAM et al (2014) Defective removal of ribonucleotides from DNA promotes systemic autoimmunity. *J Clin Invest* 125(1):413–424
11. Reijns MAM, Rabe B, Rigby RE et al (2012) Enzymatic removal of ribonucleotides from DNA is essential for mammalian genome integrity and development. *Cell* 149:1008–1022
12. Hiller B, Achleitner M, Glage S et al (2012) Mammalian RNase H2 removes ribonucleotides from DNA to maintain genome integrity. *J Exp Med* 209:1419–1426
13. Crow YJ, Manel N (2015) Aicardi-Goutières syndrome and the type I interferonopathies. *Nat Rev Immunol* 15(7):429–440

# Part III

### **Yeast DNA Polymerase $\eta$ is involved in genome replication under low deoxyribonucleotides pools conditions**

**Alice Meroni**<sup>1</sup>, Giulia M. Nava<sup>1</sup>, Eliana Bianco<sup>2</sup>, Marco Muzi-Falconi<sup>1#</sup>, Federico Lazzaro<sup>1#</sup>

<sup>1</sup>Dipartimento di Bioscienze, Università degli Studi di Milano, via Celoria 26, 20133 Milano, Italy.

<sup>2</sup>Department of Molecular Mechanisms of Disease, University of Zurich-Irchel, Winterthurerstrasse 190 CH-8057 Zurich, Switzerland.

<sup>#</sup>Corresponding author

## ABSTRACT

RNA:DNA hybrids could arise during several cellular processes and, among them, the DNA replication. Cells possess RNase H activities to deal with these particular substrates and restore the correct DNA:DNA sequence, avoiding potential negative outcomes as genome instability. Yeast cells lacking RNases H are negatively affected by hydroxyurea, which lowers the deoxyribonucleotides pool, necessary for DNA replication. Here we show that the Translesion Synthesis polymerase  $\eta$  (Pol  $\eta$ ) plays a key role in DNA replication under low deoxyribonucleotides condition. In particular, the catalysis reaction performed by Pol  $\eta$  results detrimental for cells lacking RNases H, leading to DNA damage checkpoint activation and G<sub>2</sub>/M arrest. Moreover, a Pol  $\eta$  mutant allele with enhanced ribonucleotides incorporation further exacerbates the sensitivity to hydroxyurea of cells lacking RNase H activities. We thus propose a model in which Pol  $\eta$  is helping hydroxyurea-stalled replication forks by introducing ribonucleotides, and that becomes ultimately injurious if cells are not able to remove ribonucleotides, as in absence of RNases H.

## INTRODUCTION

The accuracy of genome duplication is mainly guaranteed by the high fidelity of replicative DNA polymerases, which insert the correct deoxyribonucleotide respecting the base pairing with the template. Besides discriminating between the different bases, replicative polymerases have to choose also the right sugar [1]. In doing so, they are challenged by the high ribonucleotides (rNTPs) physiological concentrations, that exceed the ones of deoxyribonucleotides (dNTPs) up to hundreds of times [2]. Specific residues acting as a steric gate in the nucleotide binding site help DNA polymerases to select dNTPs, lacking an oxygen at the 2' carbon of the sugar, over rNTPs [1]. Nonetheless, during DNA replication, a huge number of ribonucleotides is introduced into the nascent strand [2]. In yeast, at least 1 rNTP is incorporated every 1000 dNTPs, making

rNTPs the most frequent non-canonical nucleotides introduced into the genome [3].

Embedded ribonucleotides are usually processed by RNase H enzymes, which contribute to the re-establishment of the correct DNA sequence [3]. Eukaryotic cells possess two types of RNase H enzymes: RNase H<sub>1</sub>, which cleaves RNA:DNA hybrids where at least four consecutive ribonucleotides are present; RNase H<sub>2</sub>, which processes both multiple and single embedded ribonucleotides [4]. In absence of RNase H activities, ribonucleotides are not repaired and cells display phenotypes linked to replication stress and genome instability (reviewed in [5,6]). Noteworthy, dysfunctions of the RNase H<sub>2</sub> complex are the major cause of the Aicardi-Goutières syndrome, a rare disorder that mainly affects brain, skin and the immune system [7]. Additionally, ribonucleotides can be subjected to alternative and mutagenic processing by Topoisomerase 1, which can lead to the formation of short deletions and ultimately double-strand breaks [8–10]. In general, the inability to remove ribonucleotides leads to severe consequences, as their persistence in DNA distorts the helix structure [11–14] and therefore affects DNA transactions.

Ribonucleotide incorporation is further increased in situations where the cellular dNTPs pools are reduced, such as when cells are treated with the ribonucleotide reductase inhibitor hydroxyurea (HU) [15]. As a consequence, cells lacking RNase H activities are hypersensitive to HU [15–17]. During replication, rNTPs are not efficiently bypassed by replicative DNA polymerases [18,19] and cells rely on post-replication repair mechanisms to overcome these blocks [17]. Indeed, following HU treatment, template switching or Pol ζ-mediated Trans-Lesion Synthesis (TLS) become essential to bypass rNTPs in the template DNA, and to complete genome duplication [17]. Intriguingly, we found that the increased sensitivity to HU observed in yeast cells lacking RNase H activities (*rnh1Δ rnh201Δ*) is almost totally dependent upon the presence of the TLS polymerase η (*RAD30*). Pol η belongs to the Y-family polymerases and has a major role in the bypass of several adducts that halt replication forks progression. It is a very versatile polymerase, known for its excellent ability in bypassing thymidine adducts and 8-oxo-guanines in an error-free manner [20–22]. In humans, defects in the gene

encoding Pol  $\eta$  (*POLH*) lead to the onset of the *xeroderma pigmentosum* variant (XP-V) genetic syndrome [23], characterized by high incidence of skin cancer and sunlight sensitivity, due to the inability to deal with UV lesions sun-induced [24]. Besides the TLS function, the human ortholog of Pol  $\eta$  has been implicated in other processes as class switch recombination [25,26] and common fragile sites (CFSs) stability [27–29]. Recently, yeast and human Pol  $\eta$  have been reported able to efficiently insert rNTPs and also to extend RNA primers with ribonucleotides, *in vitro* [30–32].

In this work, we identify and characterize this unexpected role of Pol  $\eta$ . In particular, we show that Pol  $\eta$  catalytic activity becomes harmful in the absence of RNase H activities and under low dNTPs conditions. The steric gate mutant of Pol  $\eta$ , with enhanced ribonucleotides incorporation [33], further exacerbates this phenomenon. During an S phase with low levels of dNTPs, Pol  $\eta$  activity leads to the activation of the DNA damage checkpoint and cell cycle arrest. We also demonstrate that the detrimental activity of Pol  $\eta$  is not dependent upon the presence of ribonucleotides in template DNA, and that RNase H activities are essential to resolve the toxic products of Pol  $\eta$ . We propose that Pol  $\eta$  actively participates to DNA replication in low dNTPs conditions. This function is important to achieve full genome duplication, thanks to Pol  $\eta$  ability to incorporate rNTPs or extend RNA stretches, generating multiple insertions or longer stretches of consecutive ribonucleotides. While in wild type cells, this is a perfectly acceptable compromise; this activity is indeed highly toxic for cells lacking RNases H, which are unable to restore the correct DNA composition and structure.

## RESULTS

### **DNA polymerase $\eta$ is responsible for HU-induced cell lethality in absence of RNase H activities.**

Yeast cells lacking both RNase H activities (*rnh1 $\Delta$ rnh201 $\Delta$* ) exhibit sensitivity to several genotoxic and replication stress-inducing agents, such as MMS, CPT, and HU [17,34,35]. In particular, following HU stress, Post Replication Repair (PRR) pathways become crucial for cell survival, and TLS polymerase  $\zeta$  likely helps replicative polymerases to deal with ribonucleotides persisting in genomic DNA [17]. Unexpectedly, we found that simultaneous deletion of all the yeast TLS polymerases, Pol  $\zeta$ , Pol  $\eta$  and Rev1 (*rev3 $\Delta$  rev7 $\Delta$  rad30 $\Delta$  rev1 $\Delta$* ) suppresses almost completely the HU sensitivity phenotype of *rnh1 $\Delta$  rnh201 $\Delta$*  cells, suggesting that one or all the TLS polymerases exert a toxic effect in RNase H lacking cells treated with HU. By studying different deletion combinations, we analyzed the individual contribution of each TLS polymerase (**Figure 1A**), and we found that the suppression of HU sensitivity is almost completely dependent upon the loss of DNA polymerase  $\eta$  (Rad30). Moreover, Pol  $\eta$  affects *rnh1 $\Delta$  rnh201 $\Delta$*  cell viability specifically following treatment with HU, but not with other genotoxic agents impacting on S phase, like MMS (**Figure 1B**). These observations suggest that Pol  $\eta$  is toxic when dNTP pools are lowered and genomic rNMPs cannot be removed.

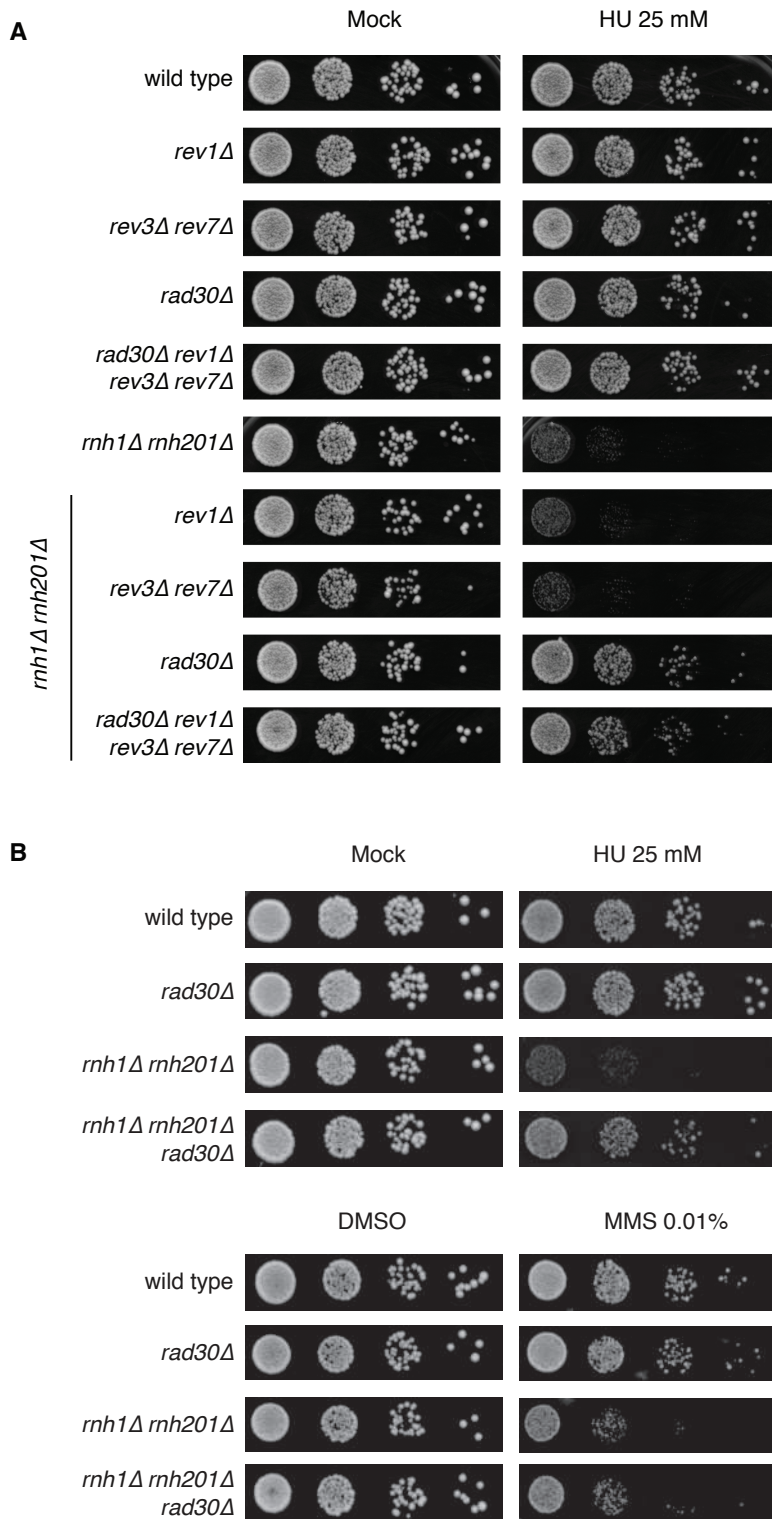


**Figure 1. Pol  $\eta$  is the only TLS responsible for HU sensitivity of cell lacking RNase H activities.**

10-fold serial dilutions of the indicated strains were plated on (A) YEPD and YEPD + 25 mM and (B) on YEPD, YEPD + 25 mM HU and YEPD + 0.01% MMS. Plates are incubated at 28°C and pictures were taken after 3 days of incubation.

## **Under low HU concentrations, DNA damage checkpoint activation and mitotic arrest in RNase H deficient cells is dependent upon Pol $\eta$ .**

We have previously shown that RNase H lacking cells exhibit DNA damage checkpoint activation and cell cycle arrest in G<sub>2</sub>/M phase during treatment with low doses of HU [17]. Given the involvement of Pol  $\eta$  in HU sensitivity, we tested its role in checkpoint activation under the same conditions.

The phosphorylation state of the checkpoint effector kinase Rad53 was used as a readout for DNA damage checkpoint (DDC) activation [36]. Cells were synchronized in G<sub>1</sub> with  $\alpha$ -factor, released in 25 mM HU, and collected at the indicated time points (**Figure 2A and B**). In such low doses of HU, wild type cells slightly activate the DDC in S phase; the checkpoint response is then turned off and cells proceed with cell division. *rnh1 $\Delta$  rnh201 $\Delta$*  cells, however, do not dephosphorylate Rad53 after S phase and this, in turn, prevents them from completing the cell cycle and entering the next G<sub>1</sub> phase; these cells accumulate in G<sub>2</sub>/M with 2C DNA content, consistently with their reduced viability.

Intriguingly, deletion of *RAD30* rescues almost completely all the phenotypes of RNase H mutants. Indeed, *rnh1 $\Delta$  rnh201 $\Delta$  rad30 $\Delta$*  cells exhibit an almost wild type kinetics of cell cycle progression and most cells dephosphorylate Rad53 (**Figure 2A and 2B**). Noteworthy, all these results are specific to HU treatment, as in untreated conditions the strains did not show any defects and behave similarly (**Figure S1**). In conclusion, when cells lacking RNase H activities are subjected to dNTPs pool depletion, Pol  $\eta$  is responsible for a DNA damage checkpoint activation that ultimately leads to the block of cell division and proliferation.

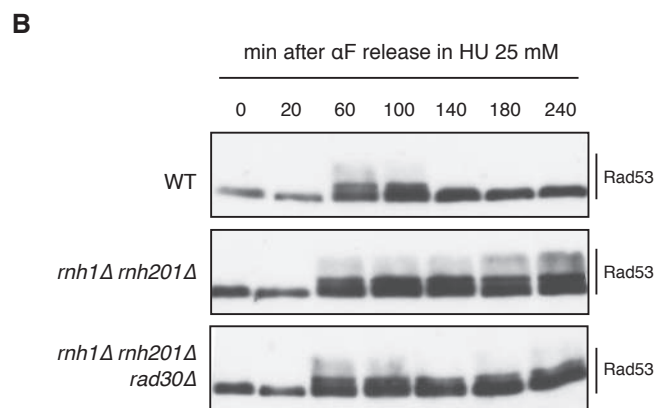
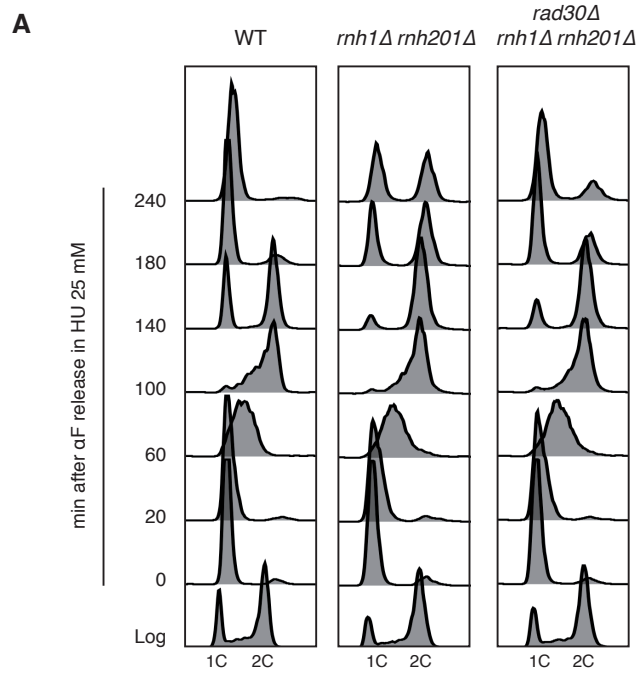


**Figure 2. In HU, RNase H deficient cells exhibit DNA damage checkpoint activation and G<sub>2</sub>/M arrest that are dependent upon Pol  $\eta$ .**

(A-B) Exponentially growing cells were synchronized in G<sub>1</sub> phase by  $\alpha$ -factor addition (4  $\mu$ g/mL) and released in 25 mM HU;  $\alpha$ -factor (10  $\mu$ g/mL) was re-added to the medium 90 after the release to block cells in the next G<sub>1</sub> phase. (A) Cell cycle progression was followed by cytofluorimetry (FACS) and (B) Rad53 phosphorylation state was monitored anti-Rad53 antibodies in western blots of cell extracts obtained at the indicated time points.

## **Pol $\eta$ exerts its toxicity through its ribonucleotide incorporation activity.**

To deepen our comprehension on the negative impact of Pol  $\eta$ , we evaluated the effect of overexpressing a catalytic-dead allele (*rad30-D155A-E156A*) or a mutant with enhanced ribonucleotide incorporation activity (*rad30-F35A*) [33,37]. Due to the catalytic inefficiency of the latter [33], we opted for the overexpression rather than using endogenous expression, in order to have comparable results between the mutants. Pol  $\eta$  alleles were then cloned under GAL<sub>1</sub>/10 promoter and overexpression was induced by addition of galactose; cell viability in 25 mM HU was calculated and is reported in **Figure 3A**. Overexpression of either wild type or mutant forms of Pol  $\eta$  was achieved at similar levels (**Figure 3B**) and did not affect wild type cell viability both in untreated or HU-treated conditions (**Figure 3A, grey bars and Figure S2**). In a RNase H deleted background (**Figure 3A, black bars**), overexpression of wild type Pol  $\eta$  exacerbated the HU sensitivity, linking the extent of its negative impact to the protein abundance in cells. On the other hand, cells carrying the catalytic-dead mutant (*rad30-D155A-E156A*) were almost completely viable, implying that Pol  $\eta$  catalytic activity is responsible for the observed phenotypes. This was confirmed by using the steric gate mutant *rad30-F35A*, which exhibits enhanced ribonucleotide incorporation activity [30,33]. In absence of RNase H, overexpression of the *rad30-F35A* allele caused a drastic reduction of cell viability, suggesting that the extra incorporation of ribonucleotides is the cause of cell lethality (**Figure 3A, black bars**). In summary, these results confirm that the observed Pol  $\eta$  toxic activity depends on its nucleotide polymerization activity and it is increased when more ribonucleotides are selected.

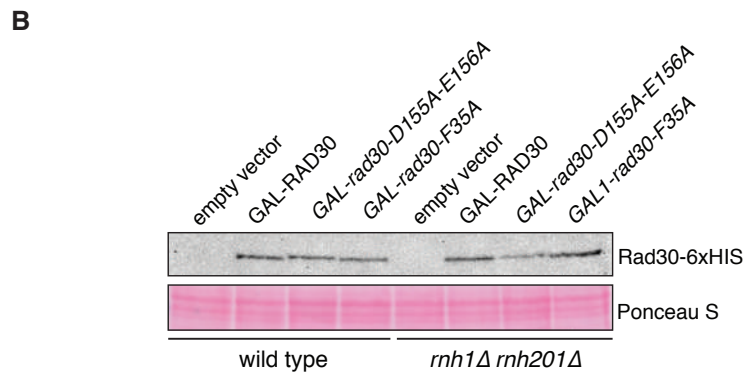
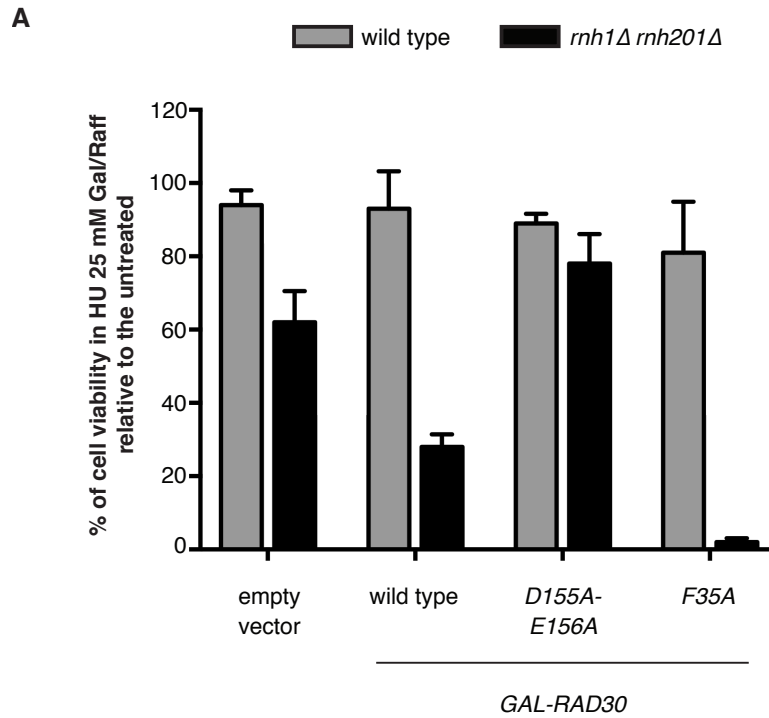


**Figure 3. Pol  $\eta$  toxicity depends on its catalytic and ribonucleotide-incorporation activity.**

(A) Cells were grown in SC-URA Raffinose 2% and arrested with  $\alpha$ -factor. Cultures were then appropriately diluted and plated on SC-URA supplemented with Galactose 2% and Raffinose 2%, either with or without 25 mM HU. Colonies were counted after 4 days at 28°C. Histogram bars represent the ratio between colonies counted on plates with and without hydroxyurea. Error bars represent the standard error of the mean (SEM), calculated on three independent experiments. (B) Overexpression levels of wild type and mutants Rad30 were checked by western blotting with anti-HIS antibodies 4 hours after Galactose induction.

## Pol $\eta$ toxicity is restricted to HU-stressed DNA replication

Hydroxyurea is known to induce replication forks stalling and consequently ssDNA gaps that are filled in late S phase, mainly by TLS polymerases [38–40]. On the other hand, Pol  $\eta$  was found in the proximity of replication origins during HU stress [41,42] and, in human cells, Pol  $\eta$  actively participates to CFSs replication, possibly by substituting Pol  $\delta$ [28,29] and forms foci upon hydroxyurea exposure [43]. Thus we asked whether the HU-dependent Pol  $\eta$  toxicity occurs during either DNA replication under low dNTPs conditions or post-replication, in late S phase/G<sub>2</sub>.

We choose to pulse cells with a high dose of HU after the  $\alpha$ -factor release, and then to remove the stress, in order to let cells complete replication without HU. With this experimental set up, cells still showed similar outcomes as with 25 mM HU, even with less extent (**Figure S3**). Regardless of the absence of HU in the medium, Pol  $\eta$  is still responsible for the activation of the DDC and for the G<sub>2</sub>/M cell cycle arrest in *rnh1 $\Delta$  rnh201 $\Delta$*  cells (**Figure S3**).

To discriminate between the two hypotheses, we used *rnh1 $\Delta$  rnh201 $\Delta$  rad30 $\Delta$*  synchronized cell populations where we conditionally overexpressed *RAD30* either before or after a short 200 mM HU treatment. In the first case (early induction), cells would be subjected to nucleotide depletion in the presence of Pol  $\eta$ , while in the latter (late induction), cells would experience the HU stress in the absence of Pol  $\eta$ , which would be expressed after HU removal. *RAD30* overexpression was achieved by using the galactose inducible promoter and was verified by western blotting, while cell cycle progression and DDC activation were monitored as previously described (**Figure 4A and 4B**). Intriguingly, with this experimental setup, we observed strong accumulation of G<sub>2</sub>/M arrested cells and Rad53 phosphorylation only if Pol  $\eta$  was present concomitantly with hydroxyurea during DNA replication (**Figure 4A and 4B, early induction lanes**). Whereas, when Pol  $\eta$  was overexpressed after HU removal, allowing it to fill HU-induced gaps in late S/ G<sub>2</sub>, most cells did not exhibit cell cycle problems or DDC activation (**Figure 4A and 4B, late induction lanes**). These data

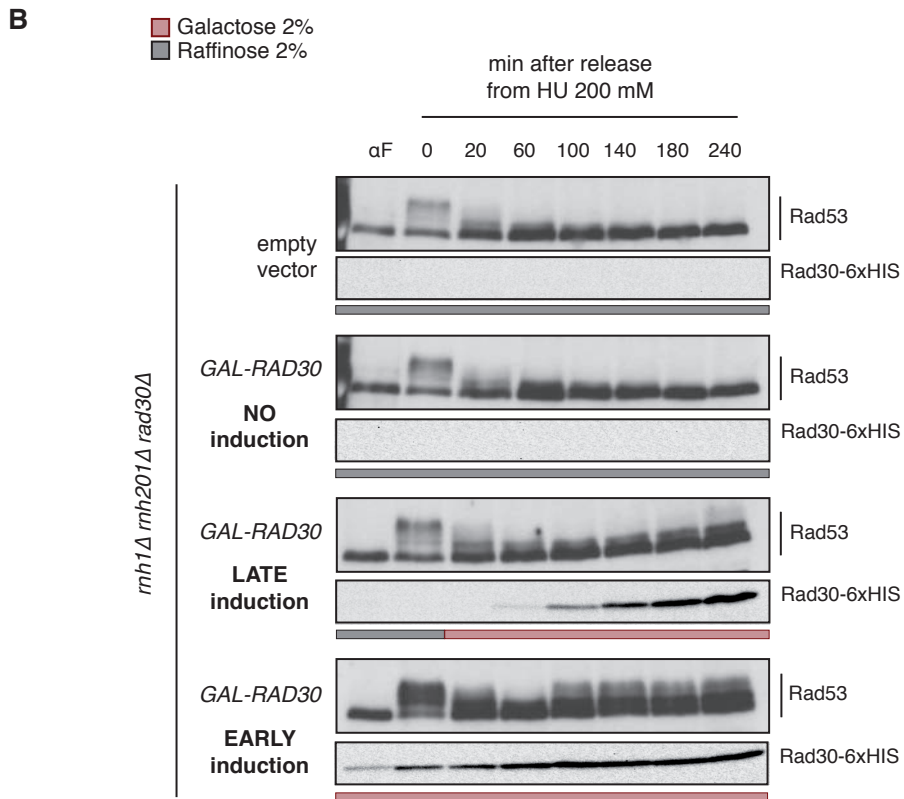
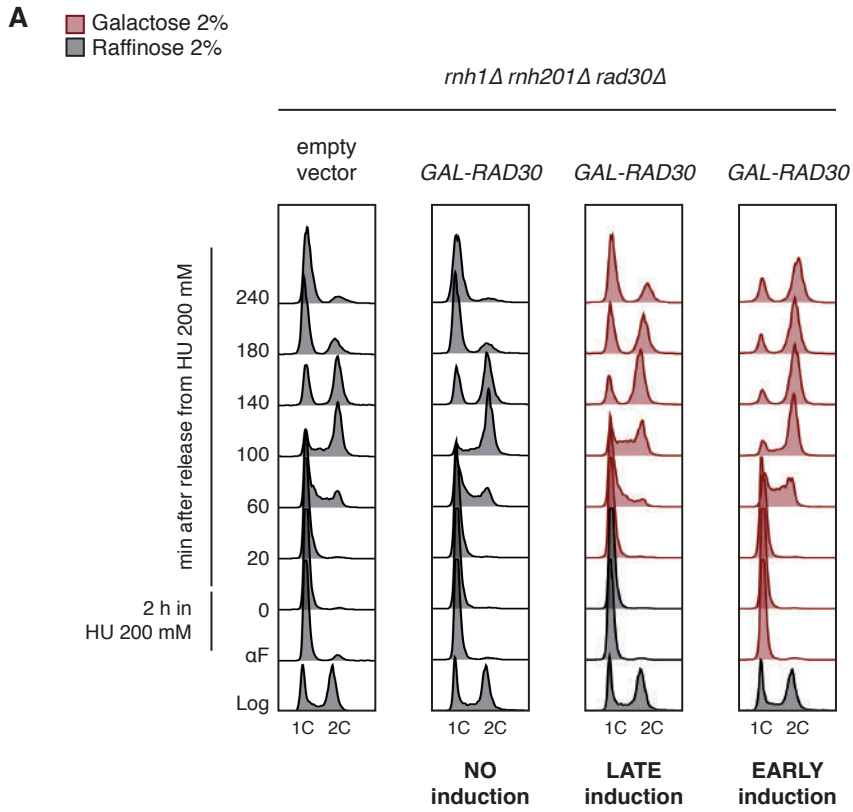
indicate that Pol  $\eta$  exerts its toxic effect when replication forks are slowed down and challenged by low dNTPs conditions.

Since Pol  $\eta$  toxic activity becomes relevant in the absence of RNase H, it is important to assess how the two are related to each other. Lack of RNase H leads to accumulation of unprocessed ribonucleotides in the genome, which presence could be required to trigger Pol  $\eta$  activity and consequently additional rNTP insertions. On the other hand, Pol  $\eta$  may be recruited by the stalling of replication forks induced by the low dNTP levels and then it incorporates rNTPs. In this scenario, the inability to process ribonucleotides becomes critical due to their Pol  $\eta$ -dependent improper placing, starting from the first replication cycle, when the template DNA is free from ribonucleotides. To discriminate between these two hypotheses, we generated a heterologous RNase H2 inducible system. The RNase H2 activity was provided by *E. coli* RnhB that is able to complement the absence of RNase H1 and H2 in yeast cells, suppressing the HU sensitivity (**Figure S4**). *rnhB* gene was cloned under the TetOFF promoter, so its transcription can be switched off by addition of doxycycline (DOXY). *rnhB* coding sequence was also fused to the AID-degron, so that the chimeric protein is degraded following addition of auxin (IAA) [44,45]. *rnh1 $\Delta$  rnh201 $\Delta$*  cells carrying the conditional *rnhB* construct were grown in the presence of the RnhB (ON); this allows the correct removal of ribonucleotides from the genome. RnhB was then turned off (OFF) during  $\alpha$ -factor synchronization, prior to the release in 25 mM HU, and cells were collected at the indicated time points. Cell cycle progression was monitored by FACS analysis and DDC activation was evaluated by western blotting (**Figure 5A and 5B**). In the presence of RnhB activity, *rnh1 $\Delta$  rnh201 $\Delta$*  cells progressed throughout the cell cycle in presence of hydroxyurea as the wild type strain, reaching the next G<sub>1</sub> phase without any arrest. This result confirms that the RnhB is properly working. On the contrary, when RnhB was turned off prior to the HU release, *rnh1 $\Delta$  rnh201 $\Delta$*  cells experienced the first DNA replication in the presence of hydroxyurea and in the absence of RNase H activity. In these conditions, they activated Rad53 and arrested in G<sub>2</sub>/M, similarly to *rnh1 $\Delta$  rnh201 $\Delta$*  cells carrying the empty plasmid. This observation indicates that these phenotypes are directly due replicating DNA in the presence of HU

and are the consequence of the inability to process newly incorporated genomic rNMPs (**Figure 5A and 5B**). Moreover, deletion of *RAD30* suppressed the phenotypes showed by *rnh1Δ rnh201Δ* cells released in HU in the absence of RnhB (OFF), confirming that loss of cell viability is independent of the presence of ribonucleotide in the DNA template, but dependent on Pol  $\eta$ .

**Figure 4 (next page). Pol  $\eta$  exerts its toxic activity only during HU-stressed DNA replication.**

Cells were grown in SC-URA Raffinose 2%, arrested with  $\alpha$ -factor (4  $\mu$ g/mL) and released from the G<sub>1</sub> block by transferring them in SC-URA Raffinose 2% with 200 mM HU for 2 hours. HU was then washed out and cells were transferred to fresh medium to allow completion of the cell cycle.  $\alpha$ -factor (10  $\mu$ g/mL) was re-added 90 min after HU wash out to block cells in the next G<sub>1</sub> phase. Media were supplemented with Galactose 2% when indicated (red). (A) FACS profiles, (B) Rad53 and Rad30-6xHIS western blots using appropriate antibodies are shown at the indicated time points.



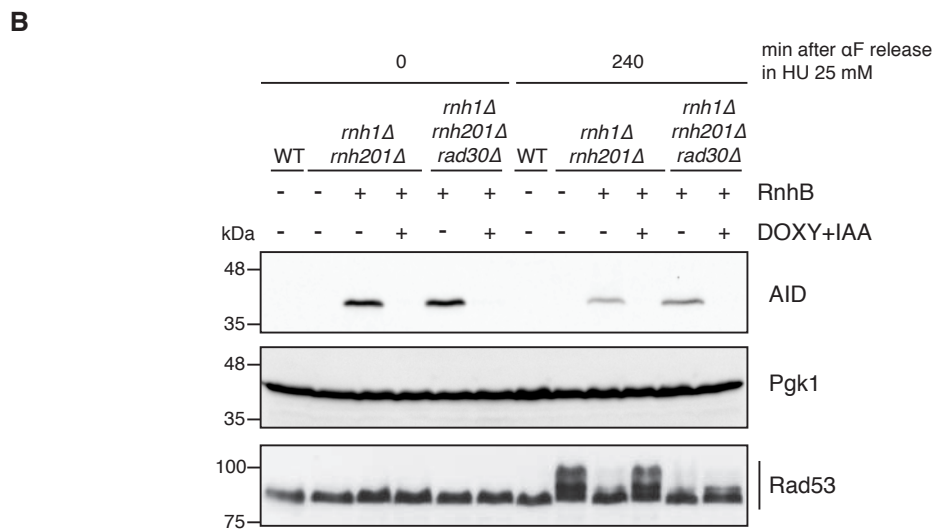
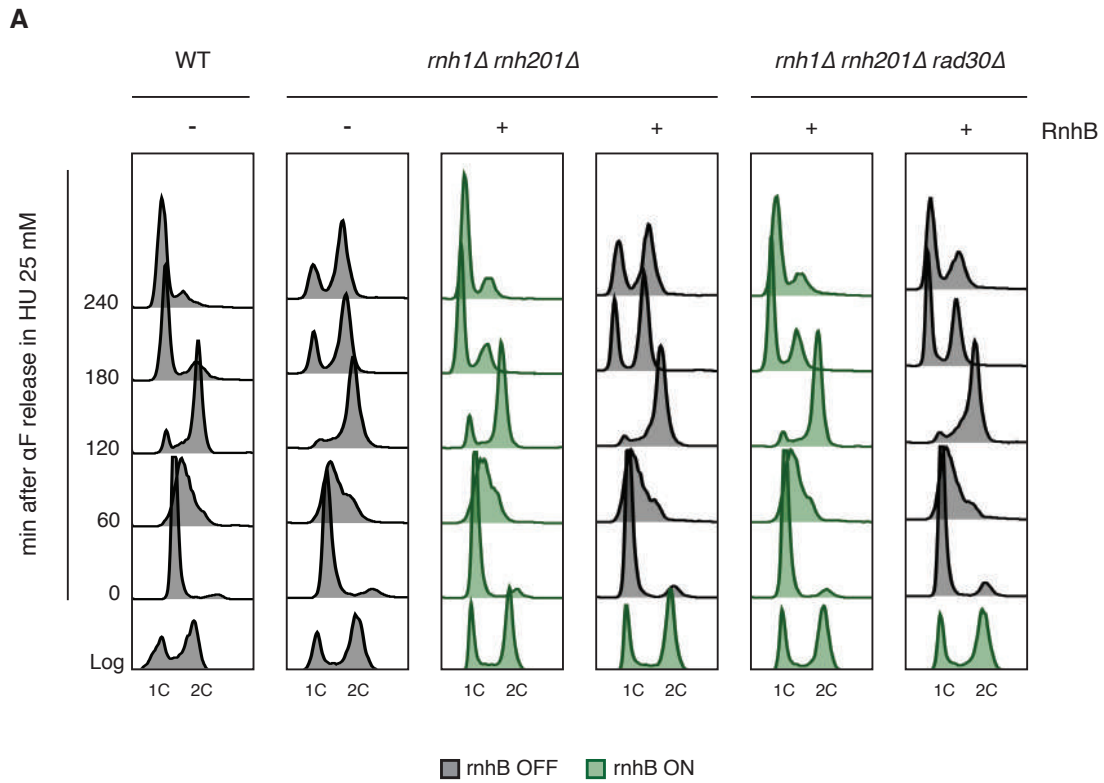


**Figure 5. Pol  $\eta$  generates toxic intermediates during the first round of replication in HU.**

Exponentially growing cells were synchronized in SC-TRP Glucose 2% by  $\alpha$ -factor addition (4  $\mu$ g/mL) and released in YEPD + 25 mM HU.  $\alpha$ -factor (10  $\mu$ g/mL) was re-added 90 min after the release. RnhB was expressed (rnhB ON, in green) and was depleted as needed by addition of 10  $\mu$ g/mL Doxycycline (DOXY) and 0.5 mM Auxin (IAA) (rnhB OFF, in gray). (A) FACS profiles, (B) Rad53 activation, RnhB-AID and Pgk1 western blots are shown at the indicated time points.

## DISCUSSION

TLS DNA polymerase  $\eta$  is well known for its roles in accurate damage bypass, thus contributing to fully genome duplication [20,21]. Here we describe a novel function for Pol  $\eta$ , during DNA replication under low dNTPs condition. Our results indicate that Pol  $\eta$  may be involved in chromosomal replication when normal replicative polymerases are challenged by deoxyribonucleotide depletion. We propose that in these conditions Pol  $\eta$  allows completion of genome duplication by promoting replication fork progression through the incorporation of ribonucleotides, whose concentrations are much higher respect to dNTPs, especially in hydroxyurea [46]. Though this function would be important to complete DNA replication and tolerate temporary decreases in dNTP pools, it would also become problematic for cell viability if RNases H activities are absent and chromosomally embedded ribonucleotides are excessively accumulated (**Figure 6**).

In the present work we show that TLS DNA polymerase  $\eta$  is responsible for most of the cell lethality induced by hydroxyurea treatment in cells lacking RNases H (*rnh1 $\Delta$ rnh201 $\Delta$* ). Indeed, loss of Pol  $\eta$  (Rad30) almost completely abrogates this sensitivity. Hydroxyurea inhibits replicative DNA synthesis depleting dNTP pools and augments the relative abundance of rNTPs, an effect that generates genome instability in cells defective for ribonucleotides removal. Indeed, exposure of *rnh1 $\Delta$ rnh201 $\Delta$*  cells to even low levels of HU leads to DNA damage checkpoint activation and G<sub>2</sub>/M arrest. These phenotypes are dependent upon the catalytic activity of Pol  $\eta$ , and are exacerbated in cells expressing a form of Pol  $\eta$  where the steric gate is mutated, allowing greater rNTP incorporation. Such toxic effect of Pol  $\eta$  is generated when cells lacking RNase H replicate in the presence of HU and it does not depend upon the presence of residual rNMPs in template DNA from the previous cell cycle. These data suggest that Pol  $\eta$  actively participates in DNA replication under low dNTPs conditions, but its activity turns out to be harmful if cells cannot process RNA:DNA hybrids. According to the literature, during HU-treated S phase, Pol  $\eta$  is bound to several DNA loci that correspond to actively replicating regions [41,42] and moreover, it is able to incorporate

ribonucleotides *in vitro* [30,33]. We thus propose that in low dNTPs situations, Pol  $\eta$  is contributing to genome duplication by introducing ribonucleotides, which are extremely abundant and available [46]. Pol  $\eta$  results hence suitable for this function thanks to its ability to extend DNA or RNA primers with ribonucleotides [30], unlike replicative DNA polymerases, which exhibit lower incorporation capability and are blocked by dNTPs shortage [2,3]. As a consequence, RNA:DNA hybrids are formed. While normally these would be corrected by RNase H activities, they become lethal structures in absence of RNase H [2,47,48]. Even if we did not directly assess the presence of Pol  $\eta$ -dependent ribonucleotides, genetic data suggest that the observed phenotypes are strictly related to unresolved RNA stretches. In fact, this Pol  $\eta$  function is only detectable in the simultaneous absence of the two RNases H (H1 and H2), which are both involved in cleaving embedded RNA stretches, while the RNase H2 fixes also single rNMPs [4]. Biochemical data support this model, and revealed that Pol  $\eta$  is indeed able to incorporate consecutive ribonucleotides [30]. Recently Pol  $\eta$  has been also shown to be able to extend RNA primers with dNTPs *in vitro* [30], therefore we cannot exclude this as another possible mechanism by which Pol  $\eta$  contributes in fixing RNA:DNA hybrids in the genome. In both cases, its synthesis reaction would result in the introduction of multiple ribonucleotides in DNA. Importantly, unprocessed ribonucleotides present in template DNA in *rnh1 $\Delta$ rnh201 $\Delta$*  cells do not seem to be involved. In fact, exploiting a conditional RNase H activity, we proved that Pol  $\eta$  exerts its toxic effect during HU-stressed DNA replication independently from embedded rNMPs in the template strand. These ribonucleotides actually halt forks progression, but are efficiently bypassed by the TLS polymerase  $\zeta$  or the template switch (TS) mechanism [17]. Remarkably, cells die because they cannot divide and the DDC seems to be switched off after S phase and re-activated when cells have 2C DNA content. Taken together, these observations may correlate RNA:DNA hybrids with chromosome segregation. Their presence could compromise chromosomes structure [11–14] and for this reason they are detected in G2/M and DDC is turned on. They could be placed in particular regions, as centromeres, important for proper cell division. Another possibility is that they trigger aberrant repair

systems impairing chromosomes structure, as the one dependent on Top1, which leads to deletions and breaks [9,10]. Supporting these hypotheses, the deletion of the Spindle Assembly Checkpoint factor Mad2 partially rescues the HU sensitivity of cells lacking RNase H (**Figure S5A**). As expected, *rnh1Δrnh201Δmad2Δ* cells success in cell division, being unable to activate Spindle Assembly Checkpoint and stop aberrant division. On the contrary, even achieving the G<sub>1</sub> phase, they show persistent DNA damage checkpoint activation (**Figure S5B**).

This scenario could be conserved in higher eukaryotes as well; this mechanism could resemble the one observed at CFSs replication. CFSs are peculiar sequences that assume non-B DNA structures that block replication forks [49,50]. Pol η is hence able to exchange with Pol δ and carry on DNA synthesis, avoiding the formation of breaks or under-replicated DNA entering in mitosis [27–29]. As in hydroxyurea, Pol η seems able to act when replication forks are stalled. Moreover, human Pol η showed *in vitro* ability of ribonucleotides incorporation and seems to be required for S phase progression in hydroxyurea [31,43]. In conclusion, this work presents new evidence on how TLS polymerase η contributes preserving genome stability, helping cells in completing genome duplication, albeit with rNTPs, when forks are stalled by the reduction of dNTPs.

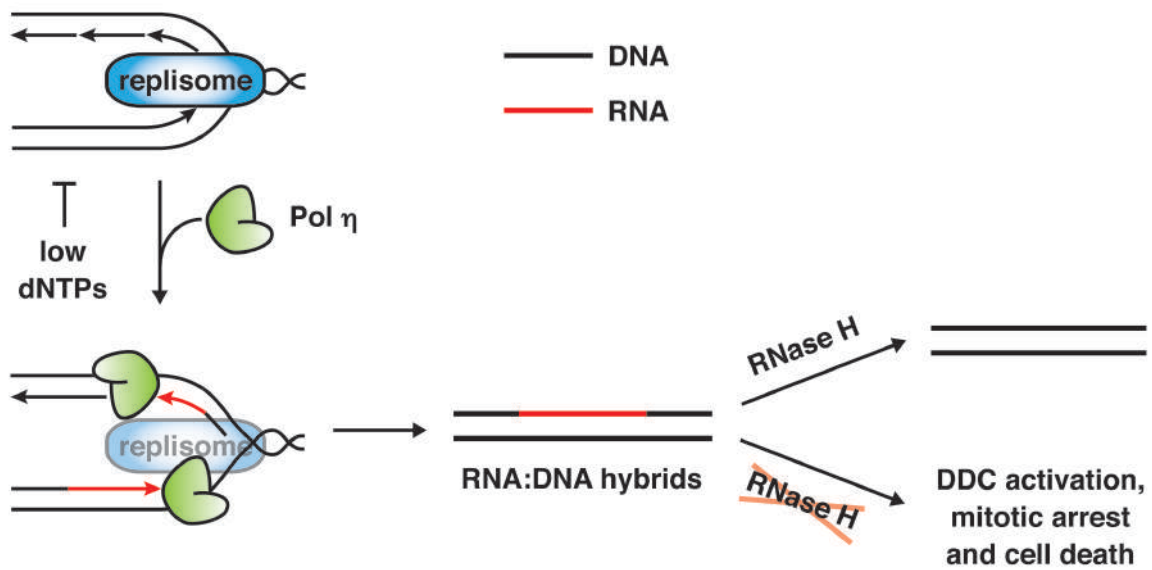


**Figure 6. Proposed model of Pol  $\eta$  function during hydroxyurea-mediated fork stalling.**

Replication forks are stalled by hydroxyurea that causes dNTPs pool depletion. Pol  $\eta$  is then recruited to help forks movement by introducing ribonucleotides in the newly synthesized strand. As a consequence, RNA:DNA hybrids are formed, which are later processed by RNase H activities. In absence of RNase H, RNA:DNA hybrids are not removed from the genome and lead to DNA damage checkpoint activation, cell cycle arrest and ultimately cell death.

## **AUTHOR CONTRIBUTIONS**

M.M.-F., F.L. conceived the study, secured funding and revised the manuscript. A.M., G-M.N., E.B. and F.L. designed and performed experiments. A.M. wrote the manuscript with input from all authors.

## **ACKNOWLEDGEMENTS**

We thank Prof. P. Plevani for critical discussions and T.A. Kunkel for providing us plasmids. M.M.-F. lab is funded by AIRC (n.15631), MIUR and Telethon (GGP15227). F.L is funded by AIRC and Fondazione Cariplo (TRIDEO 2014 Id. 15724) and Fondazione CARIPLLO (RIF. 2013-0798).

## MATERIALS AND METHODS

### Yeast strains, plasmids, media and growth conditions

All the strains used in this work are listed in Table S1 and are derivative of W303 *RAD5+* background. Strains are generated by standard genetic procedures for cell transformation and tetrad analysis. Deletions were made by the one-step PCR system [51].

For the indicated experiments, cell cultures were grown at 28°C in YEP medium (1% Yeast extract, 2% peptone) containing 2% glucose (YEPR), 2% raffinose (YEPR), or 2% galactose and 2% raffinose (YEPRG). For strains carrying plasmids, cells were grown in Synthetic-Complete medium added with appropriate sugar(s) and nutrients to maintain the selection. The addition and dose of drugs/chemicals are indicated on the figures and in their captions.

Hydroxyurea is purchased from US Biological (Salem, Massachusetts USA), Auxin (IAA), Doxycycline (DOXY), and MMS are purchased from Sigma (Saint Louis, Missouri USA).

The pJH2488 (*GAL1-RAD30-6xHIS*) and pJH2489 (*GAL1-rad30-D155A-E156A-6xHIS*) plasmids have been kindly provided by T.A. Kunkel and are described in [58]. pFL166.4 (*GAL1-rad30-F35A-6xHIS*) was obtained by site-directed mutagenesis (QuikChange Site-Directed Mutagenesis Kit) on pJH2488 using oligos 3'-ACA TAG ATA TGA ATG CCT TTG CTG CAC AGG TTG AGC AGA TGC G-5' and 3'-CGC ATC TGC TCA ACC TGT GCA GCA AAG GCA TTC ATA TCT ATG T-5', and then verified by DNA sequencing.

The pFL160.1 plasmid carrying the *rnhB*-3xminiAID-HA under TetOFF promoter was prepared as follows. The *rnhB* gene was cloned from MG1655 *E. coli* strain using primers 3'-TTA ACA TCG ATA GCG GCC GCA TGA TCG AAT TTG TTT ATC CGC ACA CG-5' and 3'-GAC TTT TGA CAA GAA ACC ATG GAC GCA AGT CCC AGT GCG C-5'. The 3X-miniAID sequence was amplified from the plasmid BYP7432 [45] using primers 3'-GCG CAC TGG GAC TTG CGT CCA TGG TTT CTT GTC AAA AGT C-5' and 3'-TGC AGG GCC CTA GCG GCC GCT CAC GCA TAG TCA GGA ACA TCG TAT GGG TAT TTA TAC ATT CTC AAG TCT A-5'. The two

amplicons were purified and then digested simultaneously with NotI and PshAI restriction enzymes. Ligation reaction was performed with NotI-digested pCM185 [44]. The sequence of the insert and junction regions was then verified by DNA sequencing.

### **Drop Test assays**

Log-phase yeast cultures were diluted at  $2 \times 10^6$  cells/mL. A series of 10-fold dilutions were prepared and 10 L drops were spotted on YEP plates or selective plates, supplemented with appropriate sugar and the indicated drugs. Pictures were taken after incubation at 28°C for 2 to 3 days.

### **Sensitivity Assay**

Exponentially growing cells were synchronized in the G<sub>1</sub> phase by adding  $\alpha$ -factor (4  $\mu$ g /mL) (Primm, Milano, Italy). After appropriate dilutions, 100 CFU of each strain were plated on YEPRG  $\pm$  25 mM HU. After 4 days of incubation the number of grown colonies was counted and normalized. The standard error of the mean (SEM) was calculated on three independent experiments.

### **SDS-PAGE and western blot**

TCA protein extracts were prepared and an equal amount for each sample was separated by SDS-PAGE [52]. Western blotting were performed with anti-Rad53 (C. Santocanale), anti-HIS-tag (70796-3 Novagen) or anti-miniAID-tag (MBL, [45]) anti-Pgk1 (22c5d8 Abcam, Cambridge UK) using standard techniques.

### **FACS analysis**

Cells were fixed in 70% ethanol and treated with RNase A and proteinase K. DNA was stained with Sytox Green and cell cycle distribution was estimated by cytofluorimetric analysis with a FACScan machine. Data were plotted using FlowJo® Software.

**Table S1**

Strain	Genotype	Ref.
SY2080	<i>W303 MATa ade2-1 trp1-1 leu2-3,112 his3-11,15 ura3-1 can1-100 RAD5</i>	M. Foiani
YFL1213	<i>(SY2080) MATa rnh1::HIS3 rnh201::KANMX6</i>	[17]
YFL1773	<i>(SY2080) MATa rnh1::HIS3 rnh201::KANMX6 rad30::TRP1</i>	This Study
YSS21	<i>(SY2080) MATa rad30::KANMX6</i>	[53]
YMG1082	<i>(SY2080) rad30::KanMX6 rev1::KanMX6 rev3::TRP1 rev7::HIS3</i>	[53]
YFL1271	<i>(SY2080) rad30::KanMX6 rev1::KanMX6 rev3::TRP1 rev7::HIS3 rnh1::HIS3 rnh201::KanMX6</i>	[17]
YSS17	<i>(SY2080) rev1::KanMX6</i>	This Study
YFL2485	<i>(SY2080) rev1::HPH rnh1::HIS3 rnh201::KanMX6</i>	This Study
YMG1096	<i>(SY2080) rev3::TRP1 rev7::HIS3</i>	This Study
YFL1389	<i>(SY2080) rev3::TRP1 rev7::HIS3 rnh1::HIS3 rnh201::KanMX6</i>	This Study
YFL1419	<i>(SY2080) + pRS426</i>	This Study
YFL1420	<i>(SY2080) + pJH2488 [GAL1-RAD30-6XHIS-URA]</i>	This Study
YFL1421	<i>(SY2080) + pJH2489 [GAL1-rad30-D155A-E156A-6XHIS-URA]</i>	This Study
YFL2567	<i>(SY2080) + pFL166.4 [GAL1-rad30-F355A-6XHIS-URA]</i>	This Study
YFL1422	<i>(SY2080) MATa rnh1::HIS3 rnh201::KANMX6 + pRS426</i>	This Study
YFL1423	<i>(SY2080) MATa rnh1::HIS3 rnh201::KANMX6 + pJH2488 [GAL1-rad30-6XHIS-URA]</i>	This Study
YFL1424	<i>(SY2080) MATa rnh1::HIS3 rnh201::KANMX6 + pJH2489 [GAL1-rad30-D155A-E156A-6XHIS-URA]</i>	This Study
YFL2569	<i>(SY2080) MATa rnh1::HIS3 rnh201::KANMX6 + pFL166.4 [GAL1-rad30-F355A-6XHIS-URA]</i>	This Study
YFL2591	<i>(SY2080) ura3::ADH1-AtTIR1-9MYC:URA3 + pCM185</i>	This Study
YFL2596	<i>(SY2080) ura3::ADH1-AtTIR1-9MYC:URA3 MATa rnh1::HIS3 rnh201::KANMX6 + pCM185</i>	This Study
YFL2598	<i>(SY2080) ura3::ADH1-AtTIR1-9MYC:URA3 MATa rnh1::HIS3 rnh201::KANMX6 + pFL160.1</i>	This Study
YFL2604	<i>(SY2080) ura3::ADH1-AtTIR1-9MYC:URA3 MATa rnh1::HIS3 rnh201::KANMX6 rad30::TRP1 + pFL160.1</i>	This Study
YFL2458	<i>(SY2080) ura3::ADH1-AtTIR1-9MYC:URA3 MATa HPH::MCM4-3XminiAID + pCM185</i>	This Study

## SUPPLEMENTARY FIGURES

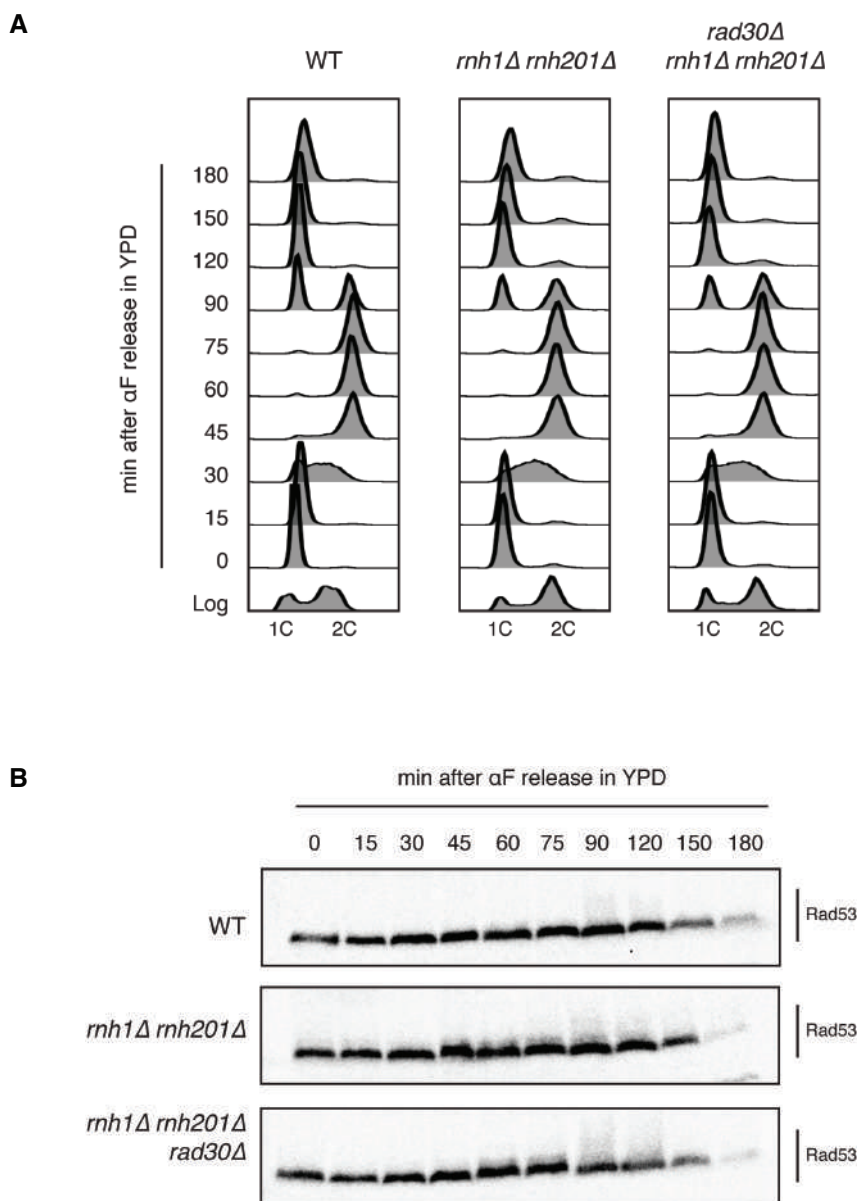


**Figure S1. Cell cycle progression and DDC activation are not compromised in untreated conditions in strains lacking RNase H and Pol  $\eta$ .**

(A-B) Exponentially growing cells were synchronized in G<sub>1</sub> phase by  $\alpha$ -factor addition (4  $\mu$ g/mL) and released in YEPD fresh medium.  $\alpha$ -factor (10  $\mu$ g/mL) was re-added to the medium 90 min after the release to block cells in the next G<sub>1</sub> phase. (A) Cell cycle progression was followed by FACS profiles and (B) Rad53 phosphorylation state was monitored by western blot analysis using anti-Rad53 antibodies.

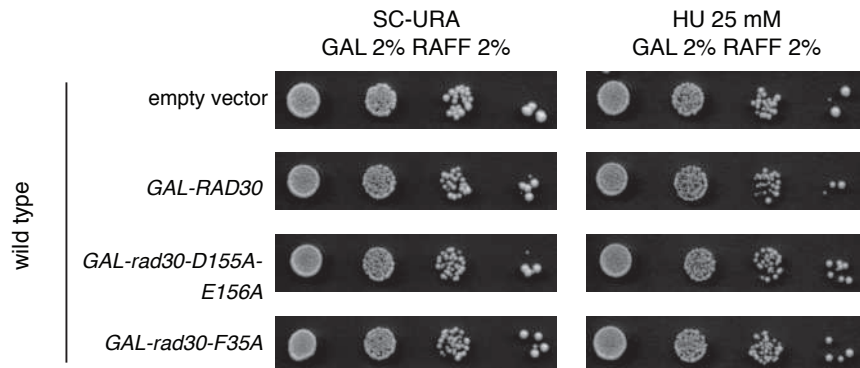


**Figure S2. Wild type cell viability is not affected by the overexpression of Rad30, *rad30-D155A-E156A* and *rad30-F35A*.**

10-fold serial dilutions of the indicated strains were plated on SC-URA and SC-URA + 25 mM HU, supplemented with Raffinose 2% and Glucose 2%. Pictures were taken after 3 days of incubation at 28°C.

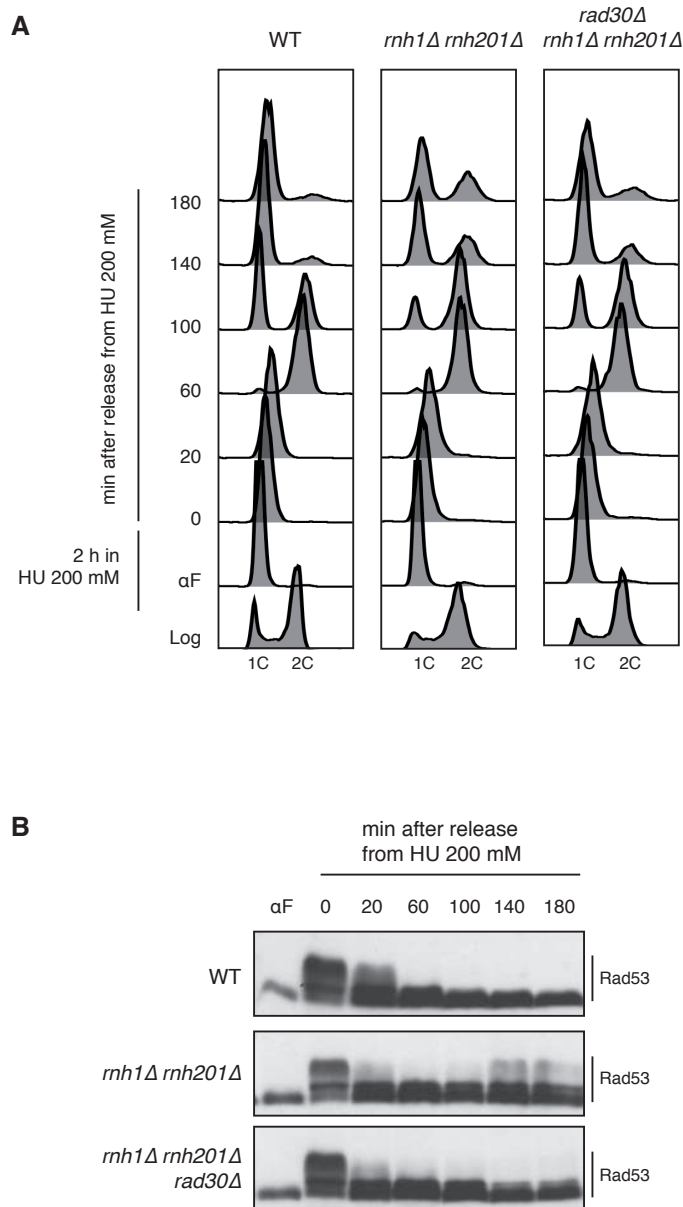


**Figure S3. After acute HU exposure, RNase H deficient cells activate the DCC and arrest in G<sub>2</sub>/M dependently upon Pol  $\eta$ .**

(A-B) Exponentially growing cells were synchronized in G<sub>1</sub> phase by  $\alpha$ -factor addition (4  $\mu$ g/mL) and released from the G<sub>1</sub> arrest in 200 mM HU for 2 hours. HU was then washed out and cells were transferred to fresh medium to allow completion of the cell cycle.  $\alpha$ -factor (10  $\mu$ g/mL) was then re-added 40 min after the HU wash out to block cells in the next G<sub>1</sub> phase. (A) FACS profiles and (B) Rad53 phosphorylation state are shown at the indicated time points.

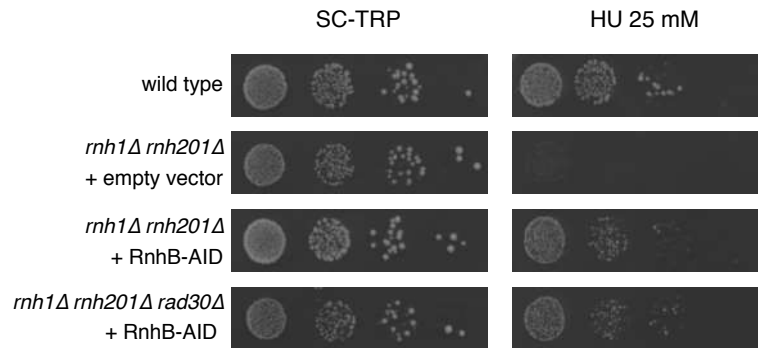


**Figure S4. Expression of a conditional form of RnhB complements the HU sensitivity of cells lacking RNases H.**

10-fold serial dilutions of the indicated strains were plated on SC-TRP and SC-TRP + 25 mM HU, and incubated at 28°C. RnhB-AID is constitutively expressed from the *CYC1* promoter. Pictures were taken after 3 days of incubation.

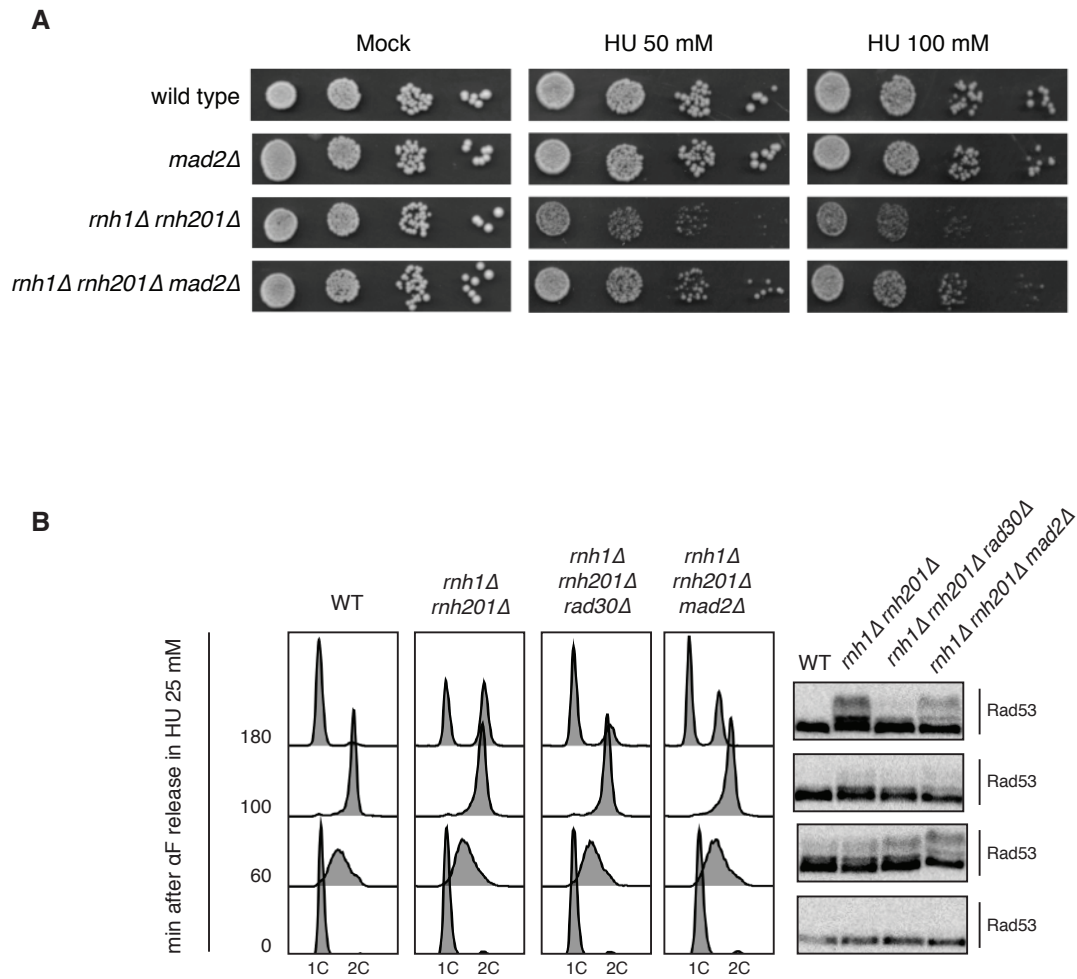


**Figure S5. In absence of RNase H enzymes, Spindle Assembly Checkpoint partially contributes to the HU sensitivity and cell cycle arrest.**

(A) 10-fold serial dilutions of the indicated strains were plated on YEPD and YEPD + 50 mM or 100 mM HU. (B)  $\alpha$ -factor synchronized cells were released in 25 mM HU, after 90 min  $\alpha$ -factor was re-added to block cells in the next G<sub>1</sub> phase. (B) FACS profiles and Rad53 phosphorylation state are shown at the indicated time points.

## REFERENCES

- [1] C.M. Joyce, Choosing the right sugar: how polymerases select a nucleotide substrate., *Proc. Natl. Acad. Sci. U. S. A.* 94 (1997) 1619–22.  
doi:10.1073/pnas.94.5.1619.
- [2] S.A. Nick McElhinny, B.E. Watts, D. Kumar, D.L. Watt, E.-B. Lundström, P.M.J. Burgers, E. Johansson, A. Chabes, T.A. Kunkel, Abundant ribonucleotide incorporation into DNA by yeast replicative polymerases., *Proc. Natl. Acad. Sci. U. S. A.* 107 (2010) 4949–54.  
doi:10.1073/pnas.0914857107.
- [3] J.L. Sparks, H. Chon, S.M. Cerritelli, T.A. Kunkel, E. Johansson, R.J. Crouch, P.M. Burgers, RNase H2-Initiated Ribonucleotide Excision Repair, 2012.  
doi:10.1016/j.molcel.2012.06.035.
- [4] S.M. Cerritelli, R.J. Crouch, Ribonuclease H: the enzymes in eukaryotes., *FEBS J.* 276 (2009) 1494–505. doi:10.1111/j.1742-4658.2009.06908.x.
- [5] J.S. Williams, T.A. Kunkel, Ribonucleotides in DNA: Origins, repair and consequences, *DNA Repair (Amst).* 19 (2014) 27–37.  
doi:10.1016/j.dnarep.2014.03.029.
- [6] S.M. Cerritelli, R.J. Crouch, The Balancing Act of Ribonucleotides in DNA, 2016. doi:10.1016/j.tibs.2016.02.005.
- [7] Y.J. Crow, A. Leitch, B.E. Hayward, A. Garner, R. Parmar, E. Griffith, M. Ali, C. Semple, J. Aicardi, R. Babul-Hirji, C. Baumann, P. Baxter, E. Bertini, K.E. Chandler, D. Chitayat, D. Cau, C. Déry, E. Fazzi, C. Goizet, M.D. King, J. Klepper, D. Lacombe, G. Lanzi, H. Lyall, M.L. Martínez-Frías, M. Mathieu, C. McKeown, A. Monier, Y. Oade, O.W. Quarrell, C.D. Rittey, R.C. Rogers, A. Sanchis, J.B.P. Stephenson, U. Tacke, M. Till, J.L. Tolmie, P. Tomlin, T. Voit, B. Weschke, C.G. Woods, P. Lebon, D.T. Bonthron, C.P. Ponting, A.P. Jackson, Mutations in genes encoding ribonuclease H2 subunits cause Aicardi-Goutières syndrome and mimic congenital viral brain infection, *Nat. Genet.* 38 (2006) 910–916. doi:10.1038/ng1842.
- [8] N. Kim, S.N.S. -y. N. Huang, J.S. Williams, Y.C. Li, A.B. Clark, J.-E.J.-E. Cho, T.A. Kunkel, Y. Pommier, S. Jinks-Robertson, Mutagenic processing of

- ribonucleotides in DNA by yeast topoisomerase I., *Science*. 332 (2011) 1561–4. doi:10.1126/science.1205016.
- [9] P. Yadav, N. Owiti, N. Kim, The role of topoisomerase I in suppressing genome instability associated with a highly transcribed guanine-rich sequence is not restricted to preventing RNA:DNA hybrid accumulation., *Nucleic Acids Res.* (2015) gkv1152-. doi:10.1093/nar/gkv1152.
- [10] S.-Y.N. Huang, J.S. Williams, M.E. Arana, T.A. Kunkel, Y. Pommier, Topoisomerase I-mediated cleavage at unrepaired ribonucleotides generates DNA double-strand breaks., *EMBO J.* (2016) e201592426. doi:10.15252/emj.201592426.
- [11] M. Egli, N. Usman, A. Rich, Conformational influence of the ribose 2'-hydroxyl group: Crystal structures of DNA-RNA chimeric duplexes, *Biochemistry*. 32 (1993) 3221–3237. doi:10.1021/bi00064a004.
- [12] E.F. DeRose, L. Perera, M.S. Murray, T.A. Kunkel, R.E. London, Solution structure of the Dickerson DNA dodecamer containing a single ribonucleotide., *Biochemistry*. 51 (2012) 2407–16. doi:10.1021/bi201710q.
- [13] T.N. Jaishree, G.A. van der Marel, J.H. van Boom, A.H. Wang, Structural influence of RNA incorporation in DNA: quantitative nuclear magnetic resonance refinement of d(CG)r(CG)d(CG) and d(CG)r(C)d(TAGCG)., *Biochemistry*. 32 (1993) 4903–11.
- [14] A. Meroni, E. Mentegari, E. Crespan, M. Muzi-Falconi, F. Lazzaro, A. Podestà, The Incorporation of Ribonucleotides Induces Structural and Conformational Changes in DNA., *Biophys. J.* 113 (2017) 1373–1382. doi:10.1016/j.bpj.2017.07.013.
- [15] M.A.M. Reijns, B. Rabe, R.E. Rigby, P. Mill, K.R. Astell, L.A. Lettice, S. Boyle, A. Leitch, M. Keighren, F. Kilanowski, P.S. Devenney, D. Sexton, G. Grimes, I.J. Holt, R.E. Hill, M.S. Taylor, K.A. Lawson, J.R. Dorin, A.P. Jackson, Enzymatic removal of ribonucleotides from DNA is essential for mammalian genome integrity and development, *Cell*. 149 (2012) 1008–1022. doi:10.1016/j.cell.2012.04.011.
- [16] S. Pizzi, S. Sertic, S. Orcesi, C. Cereda, M. Bianchi, A.P. Jackson, F. Lazzaro, P. Plevani, M. Muzi-Falconi, Reduction of hRNase H2 activity in Aicardi-

- Goutières syndrome cells leads to replication stress and genome instability., *Hum. Mol. Genet.* 24 (2015) 649–58. doi:10.1093/hmg/ddu485.
- [17] F. Lazzaro, D. Novarina, F. Amara, D.L. Watt, J.E. Stone, V. Costanzo, P.M. Burgers, T.A. Kunkel, P. Plevani, M. Muzi-Falconi, RNase H and Postreplication Repair Protect Cells from Ribonucleotides Incorporated in DNA, *Mol. Cell.* 45 (2012) 99–110. doi:10.1016/j.molcel.2011.12.019.
- [18] A.R. Clausen, S. Zhang, P.M. Burgers, M.Y. Lee, T.A. Kunkel, Ribonucleotide incorporation, proofreading and bypass by human DNA polymerase  $\delta$ ., *DNA Repair (Amst)*. 12 (2013) 121–7. doi:10.1016/j.dnarep.2012.11.006.
- [19] J.S. Williams, A.R. Clausen, S.A. Nick McElhinny, B.E. Watts, E. Johansson, T.A. Kunkel, Proofreading of ribonucleotides inserted into DNA by yeast DNA polymerase  $\epsilon$ , *DNA Repair (Amst)*. 11 (2012) 649–656. doi:10.1016/j.dnarep.2012.05.004.
- [20] R.E. Johnson, S. Prakash, L. Prakash, Efficient bypass of a thymine-thymine dimer by yeast DNA polymerase, *Science (80-. )*. 283 (1999) 1001–1004. doi:10.1126/science.283.5404.1001.
- [21] L. Haracska, S. Prakash, L. Prakash, Replication past O(6)-methylguanine by yeast and human DNA polymerase  $\epsilon$ ., *Mol. Cell. Biol.* 20 (2000) 8001–7. doi:10.1128/MCB.20.21.8001-8007.2000.
- [22] S.D. McCulloch, R.J. Kokoska, C. Masutani, S. Iwai, F. Hanaoka, T.A. Kunkel, Preferential cis-syn thymine dimer bypass by DNA polymerase  $\eta$  occurs with biased fidelity, *Nature*. 428 (2004) 97–100. doi:10.1038/nature02352.
- [23] C. Masutani, R. Kusumoto, A. Yamada, N. Dohmae, M. Yokoi, M. Yuasa, M. Araki, S. Iwai, K. Takio, F. Hanaoka, The XPV (xeroderma pigmentosum variant) gene encodes human DNA polymerase  $\epsilon$ ., *Nature*. 399 (1999) 700–4. doi:10.1038/21447.
- [24] A. Gratchev, P. Strein, J. Utikal, G. Sergij, Molecular genetics of Xeroderma pigmentosum variant., *Exp. Dermatol.* 12 (2003) 529–36.
- [25] A. Faili, S. Aoufouchi, S. Weller, F. Vuillier, A. Stary, A. Sarasin, C.-A. Reynaud, J.-C. Weill, DNA Polymerase  $\eta$  Is Involved in Hypermutation

- Occurring during Immunoglobulin Class Switch Recombination, *J. Exp. Med.* 199 (2004) 265–270. doi:10.1084/jem.20031831.
- [26] X. Zeng, D.B. Winter, C. Kasmer, K.H. Kraemer, A.R. Lehmann, P.J. Gearhart, DNA polymerase eta is an A-T mutator in somatic hypermutation of immunoglobulin variable genes., *Nat. Immunol.* 2 (2001) 537–541. doi:10.1038/88740.
- [27] L. Rey, J.M. Sidorova, N. Puget, F. Boudsocq, D.S.F. Biard, R.J. Monnat, C. Cazaux, J.-S.J.-S. Hoffmann, Human DNA polymerase eta is required for common fragile site stability during unperturbed DNA replication., *Mol. Cell. Biol.* 29 (2009) 3344–3354. doi:10.1128/MCB.00115-09.
- [28] V. Bergoglio, A.-S. Boyer, E. Walsh, V. Naim, G. Legube, M.Y.W.T.W.T. Lee, L. Rey, F. Rosselli, C. Cazaux, K.A. Eckert, J.-S. Hoffmann, DNA synthesis by Pol  $\eta$  promotes fragile site stability by preventing under-replicated DNA in mitosis., *J. Cell Biol.* 201 (2013) 395–408. doi:10.1083/jcb.201207066.
- [29] R.P. Barnes, S.E. Hile, M.Y. Lee, K.A. Eckert, DNA polymerases eta and kappa exchange with the polymerase delta holoenzyme to complete common fragile site synthesis, *DNA Repair (Amst).* 57 (2017) 1–11. doi:10.1016/j.dnarep.2017.05.006.
- [30] V.K. Gali, E. Balint, N. Serbyn, O. Frittmann, F. Stutz, I. Unk, Translesion synthesis DNA polymerase  $\eta$  exhibits a specific RNA extension activity and a transcription-associated function., *Sci. Rep.* 7 (2017) 13055. doi:10.1038/s41598-017-12915-1.
- [31] E. Mentegari, E. Crespan, L. Bavagnoli, M. Kissova, F. Bertoletti, S. Sabbioneda, R. Imhof, S.J. Sturla, A. Nilforoushan, U. Hübscher, B. van Loon, G. Maga, Ribonucleotide incorporation by human DNA polymerase  $\eta$  impacts translesion synthesis and RNase H2 activity., *Nucleic Acids Res.* (2016) gkw1275. doi:10.1093/nar/gkw1275.
- [32] E.J. Steele, DNA polymerase- $\eta$  as a reverse transcriptase: implications for mechanisms of hypermutation in innate anti-retroviral defences and antibody SHM systems, *DNA Repair (Amst).* 3 (2004) 687–692. doi:10.1016/j.dnarep.2004.03.040.
- [33] K.A. Donigan, S.M. Cerritelli, J.P. McDonald, A. Vaisman, R.J. Crouch, R.

- Woodgate, Unlocking the steric gate of DNA polymerase  $\eta$  leads to increased genomic instability in *Saccharomyces cerevisiae*, *DNA Repair (Amst)*. 35 (2015) 1–12. doi:10.1016/j.dnarep.2015.07.002.
- [34] R. Stuckey, N. García-Rodríguez, A. Aguilera, R.E. Wellinger, Role for RNA:DNA hybrids in origin-independent replication priming in a eukaryotic system., *Proc. Natl. Acad. Sci. U. S. A.* 112 (2015) 5779–84. doi:10.1073/pnas.1501769112.
- [35] A. Arudchandran, S. Cerritelli, S. Narimatsu, M. Itaya, D.Y. Shin, Y. Shimada, R.J. Crouch, The absence of ribonuclease H1 or H2 alters the sensitivity of *Saccharomyces cerevisiae* to hydroxyurea, caffeine and ethyl methanesulphonate: implications for roles of RNases H in DNA replication and repair., *Genes Cells*. 5 (2000) 789–802.
- [36] A. Pelliccioli, C. Lucca, G. Liberi, F. Marini, M. Lopes, P. Plevani, A. Romano, P.P. Di Fiore, M. Foiani, Activation of Rad53 kinase in response to DNA damage and its effect in modulating phosphorylation of the lagging strand DNA polymerase, *EMBO J.* 18 (1999) 6561–6572. doi:10.1093/emboj/18.22.6561.
- [37] C.M. Kondratyck, M.T. Washington, S. Prakash, L. Prakash, Acidic residues critical for the activity and biological function of yeast DNA polymerase  $\eta$ ., *Mol. Cell. Biol.* 21 (2001) 2018–25. doi:10.1128/MCB.21.6.2018-2025.2001.
- [38] W. Feng, D. Collingwood, M.E. Boeck, L.A. Fox, G.M. Alvino, W.L. Fangman, M.K. Raghuraman, B.J. Brewer, Genomic mapping of single-stranded DNA in hydroxyurea-challenged yeasts identifies origins of replication., *Nat. Cell Biol.* 8 (2006) 148–55. doi:10.1038/ncb1358.
- [39] G.I. Karras, S. Jentsch, The RAD6 DNA Damage Tolerance Pathway Operates Uncoupled from the Replication Fork and Is Functional Beyond S Phase, *Cell*. 141 (2010) 255–267. doi:10.1016/j.cell.2010.02.028.
- [40] Y. Daigaku, A.A. Davies, H.D. Ulrich, Ubiquitin-dependent DNA damage bypass is separable from genome replication., *Nature*. 465 (2010) 951–5. doi:10.1038/nature09097.
- [41] J. Poli, O. Tsaponina, L. Crabbé, A. Keszthelyi, V. Pantesco, A. Chabes, A. Lengronne, P. Pasero, dNTP pools determine fork progression and origin

- usage under replication stress, *EMBO J.* 31 (2012) 883–894.  
doi:10.1038/emboj.2011.470.
- [42] E. Enverald, E. Lindgren, Y. Katou, K. Shirahige, L. Ström, Importance of Pol $\eta$  for Damage-Induced Cohesion Reveals Differential Regulation of Cohesion Establishment at the Break Site and Genome-Wide, *PLoS Genet.* 9 (2013) e1003158. doi:10.1371/journal.pgen.1003158.
- [43] S. de Feraudy, C.L. Limoli, E. Giedzinski, D. Karentz, T.M. Marti, L. Feeney, J.E. Cleaver, Pol  $\eta$  is required for DNA replication during nucleotide deprivation by hydroxyurea., *Oncogene.* 26 (2007) 5713–21.  
doi:10.1038/sj.onc.1210385.
- [44] E. Garí, L. Piedrafita, M. Aldea, E. Herrero, A Set of Vectors with a Tetracycline-Regulatable Promoter System for Modulated Gene Expression in *Saccharomyces cerevisiae*, *Yeast.* 13 (1997) 837–848.  
doi:10.1002/(SICI)1097-0061(199707)13:9<837::AID-YEA145>3.0.CO;2-T.
- [45] K. Nishimura, T. Fukagawa, H. Takisawa, T. Kakimoto, M. Kanemaki, An auxin-based degron system for the rapid depletion of proteins in nonplant cells, *Nat. Methods.* 6 (2009) 917–922. doi:10.1038/nmeth.1401.
- [46] A. Koç, L.J. Wheeler, C.K. Mathews, G.F. Merrill, Hydroxyurea Arrests DNA Replication by a Mechanism that Preserves Basal dNTP Pools, *J. Biol. Chem.* 279 (2004) 223–230. doi:10.1074/jbc.M303952200.
- [47] J.D. Amon, D. Koshland, RNase H enables efficient repair of R-loop induced DNA damage, *Elife.* 5 (2016). doi:10.7554/eLife.20533.
- [48] H. Chon, J.L. Sparks, M. Rychlik, M. Nowotny, P.M. Burgers, R.J. Crouch, S.M. Cerritelli, RNase H2 roles in genome integrity revealed by unlinking its activities, *Nucleic Acids Res.* 41 (2013) 3130–3143. doi:10.1093/nar/gkto27.
- [49] M. Schwartz, E. Zlotorynski, B. Kerem, The molecular basis of common and rare fragile sites, in: *Cancer Lett.*, 2006: pp. 13–26.  
doi:10.1016/j.canlet.2005.07.039.
- [50] E. Ozeri-Galai, R. Lebofsky, A. Rahat, A.C. Bester, A. Bensimon, B. Kerem, Failure of Origin Activation in Response to Fork Stalling Leads to Chromosomal Instability at Fragile Sites, *Mol. Cell.* 43 (2011) 122–131.  
doi:10.1016/j.molcel.2011.05.019.

- [51] M.S. Longtine, A. Mckenzie III, D.J. Demarini, N.G. Shah, A. Wach, A. Brachat, P. Philippsen, J.R. Pringle, Additional modules for versatile and economical PCR-based gene deletion and modification in *Saccharomyces cerevisiae*, *Yeast*. 14 (1998) 953–961. doi:10.1002/(SICI)1097-0061(199807)14:10<953::AID-YEA293>3.0.CO;2-U.
- [52] M. Muzi Falconi, A. Piseri, M. Ferrari, G. Lucchini, P. Plevani, M. Foiani, De novo synthesis of budding yeast DNA polymerase alpha and POL $\gamma$  transcription at the G $_1$ /S boundary are not required for entrance into S phase., *Proc. Natl. Acad. Sci. U. S. A.* 90 (1993) 10519–23.
- [53] M. Giannattasio, C. Follonier, H. Tourrière, F. Puddu, F. Lazzaro, P. Pasero, M. Lopes, P. Plevani, M. Muzi-Falconi, Exo1 competes with repair synthesis, converts NER intermediates to long ssDNA gaps, and promotes checkpoint activation, *Mol. Cell*. 40 (2010) 50–62. doi:10.1016/j.molcel.2010.09.004.